

---


Electronic Theses and Dissertations, 2020-

---

2021

## Topological Changes in the Functional Brain Networks Induced by Isometric Force Exertions Using a Graph Theoretical Approach: An EEG-based Neuroergonomics Study

Lina Ismail  
*University of Central Florida*

 Part of the [Ergonomics Commons](#), [Industrial Engineering Commons](#), and the [Neuroscience and Neurobiology Commons](#)

Find similar works at: <https://stars.library.ucf.edu/etd2020>

University of Central Florida Libraries <http://library.ucf.edu>

This Doctoral Dissertation (Open Access) is brought to you for free and open access by STARS. It has been accepted for inclusion in Electronic Theses and Dissertations, 2020- by an authorized administrator of STARS. For more information, please contact [STARS@ucf.edu](mailto:STARS@ucf.edu).

---

### STARS Citation

Ismail, Lina, "Topological Changes in the Functional Brain Networks Induced by Isometric Force Exertions Using a Graph Theoretical Approach: An EEG-based Neuroergonomics Study" (2021). *Electronic Theses and Dissertations, 2020-*. 956.

<https://stars.library.ucf.edu/etd2020/956>

TOPOLOGICAL CHANGES IN THE FUNCTIONAL BRAIN NETWORKS INDUCED BY  
ISOMETRIC FORCE EXERTIONS USING A GRAPH THEORETICAL APPROACH: AN  
EEG-BASED NEUROERGONOMICS STUDY

by

LINA EL-SHERIF ISMAIL

B.Sc. Arab Academy for Science, Technology and Maritime Transport, Egypt, 2012

M.Sc. Arab Academy for Science, Technology and Maritime Transport, Egypt, 2015

A dissertation submitted in partial fulfillment of the requirements  
for the degree of Doctor of Philosophy  
in the Department of Industrial Engineering and Management Systems  
in the College of Engineering and Computer Science  
at the University of Central Florida  
Orlando, Florida

Spring Term  
2021

Major Professor: Waldemar Karwowski

©2021 LINA EL-SHERIF ISMAIL

## **ABSTRACT**

Neuroergonomics, the application of neuroscience to human factors and ergonomics, is an emerging science focusing on the human brain concerning performance at work and in everyday settings. The advent of portable neurophysiological methods, including electroencephalography (EEG), has enabled measurements of real-time brain activity during physical tasks without restricting body movements. However, the EEG signatures of different physical exertion activity levels that involve the musculoskeletal system in everyday settings remain poorly understood. Furthermore, the assessment of functional connectivity among different brain regions during different force exertion levels remains unclear. One approach to investigating the brain connectome is to model the underlying mechanism of the brain as a complex network. This study applied employed a graph-theoretical approach to characterize the topological properties of the functional brain network induced by predefined force exertion levels, namely extremely light (EL), light (L), somewhat hard (SWH), hard (H), and extremely hard (EH) in two frequency bands, i.e., alpha and beta. Twelve female participants performed an isometric force exertion task and rated their perception of physical comfort at different physical exertion levels. A CGX-Mobile-64 EEG was used for recording spontaneous brain electrical activity. After preprocessing the EEG data, a source localization method was applied to study the functional brain connectivity at the source level. Subsequently, the alpha and beta networks were constructed by calculating the coherence between all pairs of 84 brain regions of

interests that were selected using Brodmann Areas. Graph -theoretical measures were then employed to quantify the topological properties of the functional brain networks at different levels of force exertions at each frequency band. During an ‘extremely hard’ exertion level, a small-world network was observed for the alpha coherence network, whereas an ordered network was observed for the beta coherence network. The results suggest that high-level force exertions are associated with brain networks characterized by a more significant clustering coefficient, more global and local efficiency, and shorter characteristic path length under alpha coherence. The above suggests that brain regions are communicating and cooperating to a more considerable degree when the muscle force exertions increase to meet physically challenging tasks. The exploration of the present study extends the current understanding of the neurophysiological basis of physical efforts with different force levels of human physical exertion to reduce work-related musculoskeletal disorders.

To my beloved father, Essam Ismail

To my lovely mother, Souzan Hegazy

To my beloved sister, Engy Elsherif

To my lovely brother, Mohamed Elsherif

To my lovely Husband, Ahmed Neamatalla

To my lovely son, Suleiman Neamatalla

## ACKNOWLEDGMENTS

First and foremost, praise and thanks to God for his showers of blessings throughout my research work, leading to the successful completion of my Ph.D. dissertation.

I would like to express my deep and sincere gratitude to my advisor, Professor Waldemar Karwowski, for his continuous support and guidance throughout this research. It was a great privilege and honor to work and study under his guidance.

I also would like to thank the members of my committee, Professor Ahmad Elshennawy, Professor Peter Hancock, and Dr. Nichole Lighthall, for their time and valuable comments.

I would also like to thank my laboratory colleagues, especially Dr. Ashraf Alhujaili and Dr. Farzad Farahani, for their extraordinary collaboration, time, effort, and knowledge, which helped me complete this dissertation.

Special thanks to my lovely Husband, Ahmed Neamatalla, for always encouraging, advocating, and supporting me throughout my life. I am grateful for all the sacrifices he made to fulfill my desire for a Ph.D. degree. Thank you!

I am extending my heartfelt thanks to my mother, father, and siblings for their love, enthusiasm, caring, and tolerance, enabling me to complete my degree.

A very special thank my friend Nada Nabil for always listening, supporting, and discussing happy distractions to rest my mind outside of my research.

I would like to express my sincere gratitude to Professor. Khaled S. EL-kilany for always supporting me in my academic journey.

And finally, to my son Suleiman Neamatalla, thank you for being the most beautiful and unpredictable gift during my lonely time.



## TABLE OF CONTENTS

LIST OF FIGURES .....	xvi
LIST OF TABLES .....	xxii
LIST OF ACRONYMS (or) ABBREVIATIONS .....	xxvi
1. CHAPTER ONE: INTRODUCTION .....	1
1.1 Manual Material Handling Task .....	1
1.2 Muscular Strength .....	1
1.3 Perceived Exertion .....	2
1.4 Problem Statement .....	3
1.5 Study Objectives .....	4
1.6 Research Questions .....	5
1.7 Study Hypothesis.....	5
1.8 The Significant of the Study.....	6
1.9 Thesis Organization.....	6
2. CHAPTER TWO: REVIEW OF LITERATURE .....	9

2.1 Human Factors and Ergonomics .....	9
2.2 Neuroergonomics .....	10
2.3 Human Brain .....	11
2.4 Electroencephalography .....	11
2.5 Review of Literature in Physical Neuroergonomics .....	13
2.5.1 Review Standards .....	13
2.5.2 Search Strategy .....	14
2.5.3 Screening Process and Study Selection .....	14
2.5.4 Criteria for Inclusion and Exclusion.....	14
2.5.5 Data Collection and Summary Measures .....	15
2.5.6 Synthesis of Results.....	16
2.5.7 Discussion.....	16
2.5.7.1 Applications of EEG indices in physical work .....	16
2.5.7.1.1 The Effect of Fatigue.....	17
2.5.7.1.2 The Effect of Observation, Imagination, and Execution.....	20
2.5.7.1.3 The Effect of Force and Torque 2.5.7.1.3.1 Power Spectrum Density .....	22
2.5.7.1.4 The Effect of Stress and Emotion Exhaustion .....	23

2.5.7.1.5 The Effect of workload, intensity and exertion.....	24
2.5.7.1.6 The Effect of Motor Learning and practice.....	25
2.5.7.1.7 The Effect of Physical Workload .....	26
2.5.7.2 Applications of EEG Indices in Physical Activity Accompanied by a Mental Task .....	28
2.6. Bibliometric Analysis.....	29
2.6.1 The Categories of the Reviewed Articles .....	29
2.6.2 The Taxonomy of Different Domains in the Reviewed Articles .....	30
2.6.3 The Frequency of the Used EEG Indices in the Reviewed Articles.....	31
2.6.4 Neurophysiological Bases of effect of different force levels .....	32
2.6.5 The Number of the Selected EEG Channels .....	32
2.6.6 Participant’s Demographic Distribution.....	33
2.6.7 Task categorization of the Reviewed Articles.....	34
2.7 Research Gap in Physical activities studies using EEG .....	34
3. CHAPTER THREE FUNCTIONAL CONNECTIVITY AND GRAPH	
THEORETICAL MEASUREMENTS .....	38
3.1 Introduction .....	38
3.2 Functional Connectivity .....	40

3.3 Theoretical Aspects of Graph Theory .....	41
3.4 Pipeline for EEG Functional Brain Network .....	43
3.5 Graph Theoretical Measures and Network Topology Properties.....	50
3.5.1 Global measures .....	50
3.5.2 Nodal measures .....	52
3.5.3 Network Types .....	54
3.6 Application of Graph Theory to EEG .....	55
3.6.1 Connectivity Studies on Movement Execution .....	55
3.6.2 Connectivity Studies on Exertion.....	57
3.6.3 Connectivity Studies on Fatigue.....	57
3.6.4 Connectivity Studies on Physical Workload .....	58
3.7 Results from Graph Theoretical EEG based Studies .....	58
3.8 Limitations and Future Directions for Graph Theory Applications.....	61
<b>4. CHAPTER FOUR: MATERIALS AND METHODS .....</b>	<b>65</b>
4.1 Experiment and Task Description.....	65
4.2 Experimental Design.....	66

4.3 Research Variables .....	68
4.4 Experiment Procedure .....	68
4.5 Apparatus and Instrument .....	69
4.5.1 Electroencephalogram .....	69
4.5.2 Jackson Strength Evaluation System.....	70
4.5.3 TORBAL Force Gauge.....	71
4.5.4 Wireless Trigger .....	71
4.6 Experimental Setup and Paradigm .....	71
4.7 Experiment Environment .....	75
4.8 Anthropometric Measurements .....	75
4.9 Participants Selection and Ethical Code.....	75
4.10 Methodological pipeline.....	76
4.11 EEG Acquisition .....	78
4.12 EEG Data Preprocessing .....	79
4.12.1 EEG Data Pre-Processing.....	80
4.12.2 Data processing .....	82
4.13 Estimation of Functional Connectivity of EEG Cortical Sources.....	86

4.14 Graph Analysis and Measures Computation.....	86
<b>5. CHAPTER FIVE RESULTS AND ANALYSIS .....</b>	<b>88</b>
5.1 Statistical Analysis .....	88
5.1.1 Isometric Force.....	88
5.1.2 Rate of Perceived Physical Comfort.....	88
5.1.3 eLORETA Source Localization .....	89
5.1.4 Source Functional Connectivity Estimations .....	89
5.1.5 Brain Network Analysis .....	90
5.1.6 Correlation Analysis.....	90
5.2 Results .....	91
5.2.1 Anthropometric Characteristics.....	91
5.2.2 Isometric Force.....	91
5.2.3 Rate of Perceived Physical Comfort.....	94
5.2.4 Correlation Analysis for the Exerted Force and RPPC .....	96
5.2.5 Source Localization .....	98

5.2.5.1 eLORETA Source Localization.....	98
5.2.5.2 eLORETA Statistics and Multiple Comparison Corrections.....	101
5.2.6 Functional Connectivity .....	114
5.2.6.1 Functional Connectivity Patterns.....	114
5.2.6.1 Functional Connectivity Multiple Comparison .....	117
5.2.7 Brain Network .....	121
5.2.7.1 Topological differences in global network .....	122
5.2.7.1.1 Alpha coherence brain network.....	122
5.2.7.1.2 Global measures for beta coherence brain network .....	125
5.2.7.2 Topological differences in local network .....	128
5.2.7.2.1 Betweenness centrality .....	128
5.2.7.2.2 Degree centrality analysis .....	131
5.2.7.2.3 Nodal efficiency .....	133
5.2.8 Correlation between Force and Graph theory Measures .....	139
5.2.9 Correlation between RPPC and Graph theory Measures .....	141
<b>6. CHAPTER SIX CONCLUSIONS AND FUTURE WORK.....</b>	<b>144</b>
6.1 Discussion .....	144
6.2 Study Limitations and Future Implications.....	152
6.3 Conclusions.....	153
6.4 Research Contribution.....	153

APPENDIX A REVIEWED PHYSICAL NEUROERGONOMICS ARTICLES .....	155
APPENDIX B SUMMARY OF THE APPLICATIONS OF GRAPH THEORETICAL ANALYSIS .....	165
APPENDIX C ISOMETRIC STRENGTH TEST INSTRUCTIONS .....	174
APPENDIX D BORG'S RPE (6–20) SCALE (BORG, 1982) .....	176
APPENDIX E RATING OF PERCEIVED COMFORT .....	178
APPENDIX F DATA COLLECTION FORM .....	180
APPENDIX G STUDY FLYER .....	182
Appendix H MEDICAL SCREENING .....	184
APPENDIX I IRB APPROVAL OF HUMAN RESEARCH .....	186
APPENDIX J ANTHROPOMETRIC MEASUREMENTS .....	188
APPENDIX K REGIONS OF INTEREST .....	190
LIST OF REFERENCES .....	194



## LIST OF FIGURES

Figure 2-1: Flow chart of the methodology and process selection according to PRISMA .....	17
Figure 2-2: The categories of the reviewed articles.....	29
Figure 2-3: Taxonomy of different domains in the reviewed articles for physical activities .....	30
Figure 2-4: The frequency of the used EEG indices (Event-related potentials [ERP])....	31
Figure 2-5: EEG indices used to characterize brain signals during perceived exertion ...	32
Figure 2-6: Percentage of participants gender distribution in literature .....	33
Figure 2-7: The taxonomy of the reviewed article's tasks.....	34
Figure 3-1: Schematic illustration of the pipeline for constructing a functional brain network based on EEG data using graph theory.....	49
Figure 3-2: Four types of networks (in the scale-free network, the white and striped nodes represent network hubs) (Stam and Reijneveld, 2007; Stam, 2010).....	55
Figure 3-3: Scatter plot of the publications of graph theory studies based on EEG data per year.....	59
Figure 3-4: Pareto chart of methods for estimating functional connectivity (Phase Locking Value [PLV], Partial Directed Coherence [PDC], Phase Lag Index [Phase Lag Index],	

Directed Transfer Function [DTF], Mutual information [MI], Minimum connected component [MCC])..... 60

Figure 3-5: Frequency of graph theory measures (clustering coefficient [CC], path length [PL], global efficiency [Eglobal], local efficiency [Elocal]) ..... 61

Figure 4-1: Isometric Strength test as recommended by Chaffin et al. (1978)..... 66

Figure 4-2: The study protocol for arm force exertion ..... 67

Figure 4-3: Experiment Procedure ..... 69

Figure 4-4: EEG Mobile-64 headset ..... 70

Figure 4-5: Jackson Strength Evaluation System ..... 70

Figure 4-6: Methodological pipeline ..... 77

Figure 4-7: The data processing workflow ..... 79

Figure 4-8: Dipoles for 64 electrodes ..... 82

Figure 4-9: IC label classifier for a single participant for a single channel ..... 83

Figure 4-10: 2D channel location plot (i.e., scalp level) converted to 84 ROI (i.e., source level) ..... 85

Figure 5-1: pairwise comparison between isometric forces at different levels of physical exertion to extremely light [EL], light[L], somewhat hard [SWH], hard [H], and extremely hard [EH] ..... 94

Figure 5-2: pairwise comparison between isometric forces at different levels of physical exertion to extremely light [EL], light[L], somewhat hard [SWH], hard [H], and extremely hard [EH] ..... 96

Figure 5-3: Correlation of RPPC and force exerted, (r: Spearman’s rank correlation coefficient, CI: confidence interval). ..... 97

Figure 5-4: Arm forces and RPPC scores bar plot at different levels of physical exertion across all subjects (N=12)..... 97

Figure 5-5: Current source density for each exertion level for alpha frequency band ..... 98

Figure 5-6: CSD localization for each exertion level for beta frequency band ..... 101

Figure 5-7: Three-dimensional statistical mapping for alpha frequency band in extremely hard vs extremely light exertion levels ..... 102

Figure 5-8: eLORETA statistical maps for beta frequency band in extremely hard vs extremely light exertion levels..... 102

Figure 5-9: eLORETA statistical maps for alpha frequency band in extremely hard vs hard exertion levels ..... 103

Figure 5-10: eLORETA statistical maps for beta frequency band in extremely hard vs hard exertion levels ..... 104

Figure 5-11: eLORETA statistical maps for alpha frequency band in extremely hard vs somewhat hard exertion levels..... 104

Figure 5-12: eLORETA statistical maps for beta frequency band in extremely hard vs somewhat hard exertion levels..... 105

Figure 5-13: eLORETA statistical maps for alpha frequency band in extremely hard vs light exertion levels..... 106

Figure 5-14: eLORETA statistical maps for beta frequency band in extremely hard vs light exertion levels ..... 106

Figure 5-15: eLORETA statistical maps for alpha frequency band in hard vs somewhat hard ..... 107

Figure 5-16: eLORETA statistical maps for beta frequency band in hard vs somewhat hard ..... 108

Figure 5-17: eLORETA statistical maps for alpha frequency band in hard vs light ..... 108

Figure 5-18: eLORETA statistical maps for beta frequency band in hard vs light ..... 109

Figure 5-19: eLORETA statistical maps for alpha frequency band in hard vs extremely light ..... 109

Figure 5-20: eLORETA statistical maps for beta frequency band in hard vs extremely light ..... 110

Figure 5-21: eLORETA statistical maps for alpha frequency band in somewhat hard vs light ..... 111

Figure 5-22: eLORETA statistical maps for beta frequency band in somewhat hard vs light ..... 111

Figure 5-23: eLORETA statistical maps for alpha frequency band in light vs extremely light ..... 112

Figure 5-24: eLORETA statistical maps for beta frequency band in light vs extremely light ..... 113

Figure 5-25: Visualization of the alpha and beta functional brain networks for all exertion levels using coherence method. .... 115

Figure 5-26: The coherence coefficient for each exertion level for alpha and beta ..... 116

Figure 5-27: eLORETA wire diagram comparing extremely hard exertion with other exertion levels for each frequency band (extremely light [EL], light[L], somewhat hard [SWH], hard [H], and extremely hard [EH]). ..... 118

Figure 5-28: eLORETA wire diagram comparing hard exertion with other exertion levels for each frequency band (extremely light [EL], light[L], somewhat hard [SWH], hard [H], and extremely hard [EH]) ..... 119

Figure 5-29: eLORETA wire diagram comparing somewhat hard exertion with other exertion levels for each frequency band (extremely light [EL], light[L], somewhat hard [SWH], hard [H], and extremely hard [EH]). ..... 119

Figure 5-30: eLORETA wire diagram comparing light with extremely light level for each frequency band..... 120

Figure 5-31: Graph theoretical network metrics showing main effects of different exertion levels (a) Characteristic path length (b) Clustering coefficient (c) Global efficiency (d)

Local efficiency for alpha coherence (where extremely hard [EL], hard [H], somewhat hard [SWH], light [L], and extremely light [EL])..... 124

Figure 5-32: Graph theoretical network metrics showing main effects of different exertion levels (a) Characteristic path length (b) Clustering coefficient (c) Global efficiency (d) Local efficiency for beta coherence (where extremely hard [EL], hard [H], somewhat hard [SWH], light [L], and extremely light [EL])..... 127

Figure 5-33: Results for degree centrality for alpha coherence network for all exertion levels ..... 131

Figure 5-34: Degree centrality for beta coherence network for all exertion levels ..... 132

Figure 5-35: Scatterplot reporting the trend of extremely hard force over global efficiency for alpha network. .... 140

Figure 5-36: Scatterplot reporting the trend of light force over path length for beta network. .... 141

Figure 5-37: Scatter plots reporting the correlations between the RPPC at extremely hard exertion level and the Global efficiency for alpha coherence..... 142

Figure 5-38: Scatter plots reporting the correlations between the exertion levels and the graph theory measures ..... 143

## LIST OF TABLES

Table 2-1: The classification of EEG signals by frequency range with description, psychological and behavioral condition and location in the brain.....	12
Table 3-1 Functional connectivity measurements .....	41
Table 5-1: Descriptive statistics of anthropometric measurements and MVC for all subjects .....	91
Table 5-2: Isometric arm exertion forces means, standard deviation (Sd), range and percentage of maximum voluntary contraction (MVC) at different levels of physical exertion levels .....	92
Table 5-3: ANOVA table for the effect of exertion level on the exerted arm forces (N).	92
Table 5-4: Tukey simultaneous Tests for differences of means for forces exerted at different physical exertion levels.....	93
Table 5-5: Summary statistics for arm forces exerted at different levels of physical exertion (Tukey pairwise comparison at 95% confidence level).....	93
Table 5-6: The mean and standard deviation for the rate of perceived physical comfort (RPPC) at each exertion level .....	94
Table 5-7: ANOVA table for the effect of exertion level on RPPC scores .....	95
Table 5-8: Tukey simultaneous Tests for differences of RPPC scores at different levels of physical exertion .....	95

Table 5-9: Summary statistics for RPPC scores at different levels of physical exertion (Tukey pairwise comparison at 95% confidence level).....	95
Table 5-10: CSD localization for each frequency band for each exertion levels .....	99
Table 5-11: CSD localization for each frequency band for each exertion levels .....	100
Table 5-12: The statistical comparisons of eLORETA estimated current source density for pairwise exertion levels for alpha frequency. ....	113
Table 5-13: The statistical comparisons of eLORETA estimated current source density for pairwise exertion levels for beta frequency. ....	113
Table 5-14: Summery of the significant difference in functional connectivity between the exertion levels for each frequency band .....	120
Table 5-15: Mean, standard deviation (sd) and significant statement from permutation test between exertion levels for smalll-world, characteristic path length, clustering coefficient, global efficiency, local efficiency, and modularity in alpha coherence network. ....	122
Table 5-16: Mean, standard deviation (sd) and significant statement from permutation test between exertion levels for smalll-world, characteristic path length, clustering coefficient, global efficiency, local efficiency, and modularity in beta coherence network. ....	126
Table 5-17: Permutation test P-values for betweenness centrality between extremely hard (EH) versus hard (H), somewhat hard (SWH), light(L), and extremely light (EL) for alpha .....	129



Table 5-18: Permutation test P-values for betweenness centrality between hard (H) versus somewhat hard (SWH), light(L), and extremely light (EL) for alpha ..... 129

Table 5-19: Permutation test P-values for betweenness centrality between somewhat hard (SWH) versus light(L), and extremely light (EL), and light(L) versus extremely light (EL) for alpha ..... 130

Table 5-20: List of brain regions, lobe, brain structure, Brodmann area (BA) and P-value for the statistically significant nodal efficiency between extremely hard (EH) and hard (H), extremely hard (EH) and somewhat hard (SWH), extremely hard (EH) and light (L), and extremely hard (EH) and extremely light (EL) for alpha band..... 133

Table 5-21: List of brain regions, lobe, brain structure, Brodmann area (BA) and P-value for the statistically significant nodal efficiency between hard (H) and somewhat hard (SWH), hard (H) and light (L), and hard (H) and extremely light (EL) for alpha band. 134

Table 5-22: List of brain regions, lobe, brain structure, Brodmann area (BA) and P-value for the statistically significant nodal efficiency between somewhat hard (SWH) and light (L), and somewhat hard (SWH) and extremely light (EL) for alpha band. .... 134

Table 5-23: List of brain regions, lobe, brain structure, Brodmann area (BA) and P-value for the statistically significant nodal efficiency between light (L) and extremely light (EL) for alpha band. .... 135

Table 5-24: List of brain regions, lobe, brain structure, Brodmann area (BA) and P-value for the statistically significant nodal efficiency between extremely hard (EH) and hard (H),

extremely hard (EH) and somewhat hard (SWH), extremely hard (EH) and light (L), and extremely hard (EH) and extremely light (EL) for beta band..... 136

Table 5-25: List of brain regions, lobe, brain structure, Brodmann area (BA) and P-value ..... 137

Table 5-26: List of brain regions, lobe, brain structure, Brodmann area (BA) and P-value ..... 138

Table 5-27: List of brain regions, lobe, brain structure, Brodmann area (BA) and P-value for the statistically significant nodal efficiency between light (L) and extremely light (EL) for beta band. .... 138

Table 5-28: Summary of the highest nodal centrality for alpha and beta for each exertion level..... 139

Table 5-29: Correlation analysis between graph measures and exerted forces (N)..... 140

Table 5-30: Correlations between the RPPC levels at predefined exertion levels and the graph theory measures. .... 142

## **LIST OF ACRONYMS (OR) ABBREVIATIONS**

Adaptive Mixture Independent Component Analysis (AMICA)

Alpha ( $\alpha$ )

Analysis of Variances (ANOVA)

Artifact Subspace Reconstruction method (ASR)

Beta ( $\beta$ )

Bereitschafts Potential (BP)

Brain Connectivity Toolbox (BCT)

Boundary Element Head Model (BEM)

Characteristic Path Length (PL)

Clustering Coefficient (CC)

Common Average Reference (CAR)

Current Source Density (CSD)

Degree Centrality (DC)

Delta ( $\delta$ )

Electroencephalogram (EEG)

Electromyography (EMG)

Electrooculogram (EOG)

Event Related Potentials (ERPs)

Event-Related Synchronization and Desynchronization (ERD/ERS)

Exact Low-Resolution Brain Electromagnetic Tomography (eLORETA)

Fast Fourier Transform (FFT)

Fractional Dimension (FD)

functional Magnetic Resonance Imaging (fMRI)

functional Near-Infrared Spectroscopy (fNIRS)

Gamma ( $\gamma$ )

Global Efficiency (Eglobal)

Hertz (Hz)

Independent Component Analysis (ICA)

Kilo Ohm ( $k\Omega$ )

Largest Lyapunov Exponent (L1)

Local Efficiency (Elocal)

Low Resolution Brain Electromagnetic Tomography (LORETA)

Magnetic Resonance Imaging (MRI)

Manual Material Handling (MMH)

Maximum Voluntary Contraction (MVC)

Magnetoencephalography (MEG)

Microvolt ( $\mu\text{V}$ )

Minimum Norm Estimate (MNE)

Motor Potentials (MP)

Motor-related cortical potential (MRCP)

Movement-Monitoring Potentials (MMP)

Mutual information (MI)

Newton (N)

Partial Directed Coherence (PDC)

Peak Alpha Frequency (PAF)

Phase Lag Index (PLI)

Phase-Locking Value (PLV)

Principal Component Analysis (PCA)

Preferred Reporting Items for Systematic Reviews and Meta-Analyses (PRISMA)

Power spectral density (PSD)

Rate of Perceived Physical Comfort (RPPC)

Rate of Perceived Exertion (RPE)

Readiness Potential (RP)

Region of Interest (ROI)

Root Mean Square (RMS)

Small-worldness ( $\sigma$ )

Standard deviation (Sd)

Standardized Low-Resolution Brain Electromagnetic Tomography (SLORETA)

Theta ( $\theta$ )

Weighted Phase Lag Index (wPLI)

Work-related Musculoskeletal Disorder (WMSD)

# CHAPTER ONE: INTRODUCTION

## 1.1 Manual Material Handling Task

Manual material handling (MMH) task is essential in the workplace. Although the widely developed automated handling system has reduced some of these tasks, numerous occupations jobs still require the application of muscular strength for lifting, carrying, pulling, pushing, holding, moving or restraining an object. Forceful exertions, high task repetition, and sustained awkward postures that occur during MMH are ergonomics risk factors that significantly increase the likelihood of work-related musculoskeletal disorders (WMSDs) (Bernard, 1997), along with the individual-related risk factors (Chaffin et al., 1978; Snook, 1978). The National Institute for Occupational Safety and Health reported that forceful exertions are the most important contributor to the WMSD (Bernard and Putz-Anderson, 1997). When requirements for a physical job exceed the individual physical capability (i.e., muscular strength), then the probability of experiencing WMSDs increases (Chaffin et al., 1978; Nicholson and Legg, 1986; Mital and Kumar, 1998). Therefore, previous studies confirmed that the MMH tasks should not exceed human physical capabilities.

## 1.2 Muscular Strength

Human muscular strength is defined as the maximum force a muscle can generate under prescribed conditions that vary according to gender, sex, weight, and stature (Kamon and Goldfuss, 1978; Chaffin et al., 1999). Muscular strength can be measured by assessing the exerted force associated with perception, external stimuli, and tolerance of pain and discomfort. If the individual strength is not sufficient for the task, then the probability of experiencing exertion-related injuries is high

(Chaffin et al., 1978; Nicholson and Legg, 1986). Human strengths can be assessed under static (i.e., isometric) or dynamic (i.e., isotonic muscle strength or isokinetic muscle strength) conditions (Mital and Kumar, 1998). Static muscle strength reflects the muscle capability to exert a force where the length of the muscle does not change, and the joint movement remains stable. In contrast, dynamic strength reflects the muscle ability to repeatedly exert a force over a period of time where motion is required around joints (Mital et al., 1993).

### 1.3 Perceived Exertion

The perceived muscular exertion, also known as the perception of effort or the sense of effort, is the conscious sensation of physical activity (Borg, 1962; Marcora, 2010), which provides information about the difficulty of the physical task or exercise intensity. The perception of physical exertion is subject to the psychophysical power law (Stevens, 1957), which defines the nonlinear relationship between perceived intensity and the strength of the physical stimulus. Improving our understanding of the underlying mechanisms of generating the perception of effort (Robertson and Noble, 1997), endurance in physical performance (Marcora and Staiano, 2010; Comani et al., 2013), and the relationship between workload and physical fatigue and workload (Pageaux et al., 2015; Guo et al., 2017) is important to prevent work-related musculoskeletal injuries.

The perception of force exertion is influenced by various psychophysical, cognitive, and social factors. Therefore, various subjective and physiological measures have been used in the past to quantify the perceived exertion during physical activity. Specifically, the rate of perceived



exertion (RPE) introduced by Borg (1970, 1982, 1998) was found to be a useful tool for assessing the perceived exertion by subjectively rating how strenuous or difficult is the physical activity.

Although subjective scaling methods have contributed greatly to the assessment of the perceived exertion (Gamberale, 1990; Karwowski, 1991), they are insufficient for decoding the whole perception (Richard, 1980; Hernandez et al., 2002; Alessandro et al., (2014). Subjective scales describe people's opinions indicating "what a worker will do rather than what he can do."

Hernandez et al. (2002) and Karwowski et al. (2003) highlighted the importance of studying the human brain function at physical activities combined with perceptual, cognitive, and affective processes, an umbrella of "physical neuroergonomics". Studying the neural signatures of physical exertions might provide useful information that helps in understanding the integration between physiological and psychological processes involved in physical activities (Shortz et al., 2012). In this regard, it is important to identify brain regions associated with force exertion and assess brain activation patterns associated with different levels of perceived rate of physical exertion.

#### 1.4 Problem Statement

There is no published study that investigated the connectivity among different brain regions during the force exertion task in which the human brain is complex systems that continuously processed and transferred information to other interconnected regions (Sporn, et al. 2000, 2004). Few studies have investigated the effect of the force exertion on brain data using the traditional methods such as component analysis (Freude and Ullsperger, 1987; Shibata et al., 1997; Slobounov et al., 2002; Schillings et al., 2006) and the spectrum of power (Cao et al., 2015). These methods do not involve the connection between regional properties, largely neglecting the brain characteristics from a

global perspective. Furthermore, there are no published studies that investigated the changes in the topological properties of the functional brain network with different force exertions for female participants during arm isometric exertion task. In this regard, there is a great potential for providing a more extensive understanding of the neurophysiological basis of physical exertions with different force levels considering the brain as “connectome”, a large-scale network of interconnected regions.

### 1.5 Study Objectives

Our main objective was to explore the topological changes in the functional brain networks induced by isometric force exertions. To this end, we applied the graph-theoretic framework to characterize the global and local network topological properties in the alpha and beta frequency during an isometric arm exertions task based on the EEG source level in a group of healthy female participants. The main objective is divided into the following segments:

1. Locate changes in cortical source related to different force exertion levels at each frequency band.
2. Investigate the different connectivity patterns related to different force exertion levels at each frequency band.
3. Investigate the different network properties related to different force exertion levels at each frequency band.

4. Investigate the correlations between network the brain characteristic for both frequency bands with human performance (i.e., different levels of force exertion and rate of perceiving physical comfort).

### 1.6 Research Questions

Different research questions (RQ) were addressed to achieve the aforementioned research objectives. These questions include:

RQ#1: How can different force exertion levels affect the maximum current source density?

RQ#2: How can different force exertion levels affect the functional connectivity pattern?

RQ#3: How can different force exertion levels affect the network topological properties?

RQ#4: What is the correlation between the exerted forces and human performance?

### 1.7 Study Hypothesis

The proposed hypothesis includes:

Hypothesis #1: EEG source localization changes with different force exertion level.

Hypothesis #2: Connectivity patterns change with different force exertion levels.

Hypothesis #3: : Graph-theoretic properties (global and local) change with different force exertion levels.

Hypothesis #4 : Graph-theoretic properties are correlated with human performance (i.e.: different levels of force exertion and rate of perceiving physical comfort).

## 1.8 The Significant of the Study

This study aims to extend our current understanding of the neurophysiological basis of physical exertions with different force levels in human physical effort aiming to reduce work-related musculoskeletal disorder. The study's findings might also help improve the workplace design to maximize the workers' physical and mental well-being.

## 1.9 Thesis Organization

### Chapter Two

Chapter 2 introduces the concept of neuroergonomics, illustrating how limitations in traditional human factors and ergonomics have led researchers to study brain activity at work. We focus on electroencephalography (EEG), demonstrating its advantages and limitations. Then, we provide a systematic literature review of the EEG methods that have been used to characterize human performance at physical activities. Accordingly, we provide a bibliometric analysis, study limitations, research gaps, and future implications.

### Chapter Three

The main content of this chapter is adapted from the systematic review paper by (Ismail and Karwowski, 2020), which has been published in the IEEE Access journal. This chapter introduces the concepts of brain connectivity (i.e., connectome) and provides an overview of the graph theory approach. We propose a pipeline for constructing the unweighted functional brain network from EEG data for both sensor and source levels. We summarize different methods for estimating the

functional connectivity networks and defined the most commonly used graph theory measures. We provided a second systematic literature review discussing the application of the graph theory approach in task-evoked EEG applications for healthy participants only.

#### Chapter Four

This chapter discusses the materials and methodology that were applied in the current study. We further propose an EEG pipeline for constructing the EEG functional brain network at the source level.

#### Chapter Five

This chapter describes the statistical analysis methods and the results. This chapter is organized as follows: force calculations, rate of perceiving the physical comfort calculations, EEG source localization, functional connectivity estimation, graph theory measurements, and finally correlation analysis.

#### Chapter Six

This chapter provides a discussion, conclusion, and recommendation for future work.

### **Appendices**

**Appendix A:** Summary of Reviewed Physical Activity Articles for EEG Task-Based Applications.

**Appendix B:** Summary of the applications of Graph-Theoretical Analysis for EEG Task-Based.

**Appendix C:** Isometric Strength Test Instructions.

**Appendix D:** Borg's RPE 6-20 Scale for Rating the Perceived Exertion.

**Appendix E:** The Scale for Rating the Perceived Comfort Scale.

**Appendix F:** Data Collection Form

**Appendix G:** Study Flyer

**Appendix H:** Medical Screening Questionnaire Form

**Appendix I:** The approval of the Institutional Review Board (IRB) at the University of Central Florida (UCF).

**Appendix J:** Anthropometric Measurements

**Appendix K:** Selected Brain Regions of Interests.

## **CHAPTER TWO: REVIEW OF LITERATURE**

This chapter introduces the concept of neuroergonomics, illustrating how limitations in traditional human factors and ergonomics have led researchers to study brain activity at work. We focused on Electroencephalography (EEG) technique demonstrating its advantages and limitations. Then, we provided a systematic literature review of the EEG methods that have been used to characterize human performance at physical activities. Accordingly, we provided a bibliometric analysis, study limitations, research gaps and future implications.

### 2.1 Human Factors and Ergonomics

The discipline of human factors and ergonomics investigates the interactions between humans, machines, the environment, and technology while considering human capabilities and limitations to assure safe and satisfying working environments (Wilson and Corlett, 1995; IEA, 2000; Karwowski, 2005, 2006). The implementation of human-centered design principles can lead to a reduction in WMSDs, human errors, and fatigue, and diminished stress in the workplace (Lee et al., 2017), as well as enhanced system performance (Neumann et al., 2016). Many traditional techniques and methods evaluate work tasks in a subjective manner, using a variety of qualitative approaches (Stanton et al., 2004; Marras and Karwowski, 2006; Salvendy, 2012). Such approaches do not allow for adequate analysis of the complex interactions between the cognitive, perceptual, and physical aspects of working with modern technology (Karwowski et al., 2003; Parasuraman, 2003; Karwowski, 2005; Hancock, 2019), nor do they allow us to model and quantify the complex relationship between the human mind and technology (Hancock, 2019). Recent advances in

artificial intelligence, autonomous systems, and modern industrial automation, such as digital manufacturing (i.e., Industry 4.0), created the need for human operators nowadays to collaborate with sophisticated and dynamically changing technological environments that require high levels of cognitive, perceptual, and decision-making behavior (Kelvin et al., 2012; Boy, 2017). Monitoring and assessing tasks that require high levels of vigilance, attention, and decision-making ability have created a need for a deeper understanding of human performance by considering the human brain at work. This pioneering concept, known as neuroergonomics, was first introduced by Parasuraman et al. (2003).

## 2.2 Neuroergonomics

Neuroergonomics—the study of the brain and behavior at work— focuses on integrating techniques from neuroscience to measure the human brain signals during work (Parasuraman, 2003; Parasuraman and Matthew, 2008). Neuroergonomics research aims to expand our understanding of the neural mechanisms underlying human cognitive, perceptual, and motor processing with a focus on real-world contexts. Progress in neuroergonomics research up-to-date mainly focused on analyzing the neural behavior in the cognitive domain of human activity, while few studies were conducted in the physical domain (Ismail and Karwowski, 2020). Humans are daily engaged with tasks that require human body or limb movements alongside cognitive processing, integrating both physical and cognitive considerations should be considered in future neuroergonomics studies to better understand the human capabilities and limitations at work (Karwowski et al., 2003; Johnson and Proctor, 2013; Mehta, 2016).



### 2.3 Human Brain

The human brain is the most complex organ in the human body, composed of 100 billion neurons connected by almost 150 trillion synapses (Pakkenberg et al., 2003; Herculano-Houzel, 2009). Communication between neurons flows via electrical signals results in the generation of an electrical current, which subsequently creates wave patterns termed "brain signals" (i.e., brain rhythm, brain oscillation, neural oscillation, brain electrical activity, or brain potential activity). To measure brain signals, several neurophysiological methods have been used, such as functional magnetic resonance imaging (fMRI), functional near-infrared spectroscopy (fNIRS), computed tomography (CT), positron emission tomography (PET), magnetoencephalography (MEG), and electroencephalography (EEG) (Mehta and Parasuraman, 2013).

### 2.4 Electroencephalography

Electroencephalography (EEG), a powerful noninvasive technique, is one of the most commonly used neurophysiological techniques enabling to study of the high temporal dynamics of the functional brain networks (Henry, 2006; Beres, 2017). EEG signals can be classified into five frequency bands according to brain rhythms, including delta (0.5–3.5 Hz), theta (4–8 Hz), alpha (8–13 Hz), beta (13– 30 Hz), and gamma (30-100 Hz) bands (Teplan, 2002; Al-kadi et al., 2013; Cohen, 2014). The knowledge about different types of brain signals according to their frequency ranges with a description concerning the psychological and behavioral conditions and their location in the brain are provided in (Table 2-1).

Table 2-1: The classification of EEG signals by frequency range with description, psychological and behavioral condition and location in the brain

EEG signals	Frequency Range	Description	Psychological and behavioral condition
Delta ( $\delta$ )	0.5 to 4 Hz	-The slowest brain wave concerning frequency. -The highest amplitude. -Dominant in the infant.	- Dominant during deep sleep stage
Theta ( $\theta$ )	4 to 8 Hz	-Known as a slow activity.	-Dominant during deep relaxation and meditation.
Alpha ( $\alpha$ )	8 to 13 Hz	-Represents white matter. -Found in all ages.	-Dominant in wakeful but relaxed states with closed eyes. -Mainly appears in drowsiness condition.
Beta ( $\beta$ )	13 to 30 Hz	-A fast wave but not the fastest.	-Dominant in alert, concertation, attention, anxiety, thinking, and calculating. -Associated with behavior tasks such as problem-solving, task engagement, and decision-making.
Lower Gamma	30 to 80 Hz	-The fastest brain frequency signal.	-Dominant during a high level of cognitive tasks. -Related to perception, learning, and language processing.
Upper Gamma	80 to 150 Hz		

EEG has many advantages in comparison to other neurophysiological measures including (1) the excellent temporal resolution conveying the brain signals without any delay (Nijholt et al., 2008; Parasuraman and Matthew, 2008; Frey et al., 2013; Zhang et al., 2014), (2) portability and mobility for use in real-life environments, (3) affordability (Gramann and Plank, 2019). EEG techniques also exhibit three significant drawbacks: (1) low spatial resolution which results mainly from the volume conduction phenomena (Brunner et al., 2016), (2) the existence of artifacts (Sethi et al., 2006; Al-kadi et al., 2013; Reis et al., 2014; Tandle and Jog, 2015; Islam et al., 2016), and (3) the

long preparation time required for setup and cleaning (Sullivan et al., 2008; Bulea et al., 2013; Frey et al., 2013).

Different EEG analysis methods have been used to characterize human performance based on the time domain, frequency domain, time-frequency domain, and nonlinear methods. Time-domain analysis methods include EEG components analysis known as event-related potential. Frequency domain method is known as spectral analysis, including power spectrum density, event-related synchronization and desynchronization, the ratio of powers, and peak alpha frequency. Time-frequency domain methods rely on wavelet transform and Hilbert-Huang transform. Finally, nonlinear methods includes entropy, fractural dimension, largest Lyapunov exponents, and Lempel-Ziv complexity (Lutzenberger et al., 1995; Gribkov and Gribkova, 2000).

## 2.5 Review of Literature in Physical Neuroergonomics

### 2.5.1 Review Standards

The present study uses a systematic approach to review the applications of EEG indices that have been used to quantify human performance at work either laboratory or real-life settings. This systematic review was conducted based on the Preferred Reporting Items for Systematic Reviews and Meta-Analyses (PRISMA) guidelines (Liberati et al., 2009; Moher et al., 2009, 2010).

### 2.5.2 Search Strategy

Comprehensive literature searches were independently conducted using the following databases and search engines: IEEE Xplore, Google Scholar, Science Direct, and SpringerLink with no limitations on publication year. We applied the following Boolean operators: “EEG” OR “Electroencephalography” AND “physical work” OR “physical task” OR “physical exercise” OR “physical activity” OR “physical movement” OR “movement-related cortical activity.”

### 2.5.3 Screening Process and Study Selection

A total of 830 articles were originally screened for eligibility. Duplicate studies (n=273) were removed, resulting in (n=557) records. Owing to the number of results obtained by the previous search terms, more keywords were applied with no restrictions regarding publication date including neuroergonomics, human factors, human performance, ergonomics, safety, fatigue, workload, effort, vigilance, attention, alertness, drowsiness, emotion, stress, or decision making. These keywords helped to maintain our focus and narrowed the final selection of the studies by excluding an additional (n=289) article. After reviewing all titles and abstracts of the remaining articles, three researchers independently reviewed the full text of 115 articles for inclusion and exclusion criteria.

### 2.5.4 Criteria for Inclusion and Exclusion

Exclusion criteria were applied to limit the final selection of studies. In order to meet the eligibility requirements, we have included published articles with the following criteria: (a) only English

language publications; (b) experimental studies on healthy participants; (c) content from peer-reviewed journals, conference publications, textbooks, and reference books; (d) studies using EEG technique only; and (e) physical activities that represents the biomechanical properties of movements, such as grasping, gripping, finger wrist, elbow, arm, knee and hip movements that may be present during lifting, assembling, carrying, and placement tasks.

Articles with the following features were excluded: (a) studies that were not associated with physical tasks; (b) studies that combined EEG with other neuroimaging technique; (c) physical activities studies on infants or children; (d) physical activities studies on participants with neural disorders or brain diseases; and (e) physical in vigorous exercise. Accordingly, the following studies were excluded due to the subsequent reasons, (n = 21) studies on brain diseases or neural disorders, (n = 15) studies on vigorous exercise, (n = 11) studies that combined EEG with other neuroimaging techniques, and (n = 2) the full text was only available in the Chinese language. To collect all relevant articles during the literature search, the reference lists of the candidate articles (n = 122) were reviewed, resulting in (n = 15) additional articles that adhered to the criteria for inclusion. The findings of the literature search and the selection process are summarized in the PRISMA diagram (Figure 2-1).

### 2.5.5 Data Collection and Summary Measures

Relevant information from the included articles was extracted and summarized in (Appendix A), which displays physiological measurements, the number of EEG electrodes, EEG index, characteristics of participants, domain, experimental task, artifact removal method, and feature extraction method.

### 2.5.6 Synthesis of Results

A total of 88 articles were eligible for the final inclusion in the systematic literature review. The overall search process and the associated quantitative identifications are shown in (Figure 2-2). The reviewed studies confirmed that EEG indices are highly sensitive to fluctuations during physical activity. In general, 64 (80%) of the reviewed articles were addressing brain activity during physical activity only, while 16 articles (20%) reported on the combined physical and mental activities.

### 2.5.7 Discussion

This section discusses the effect of the following domains on the EEG activity including (1) physical or muscular fatigue, (2) movement observation, planning, and execution, (3) biomechanical properties (e.g., force, torque), (4) stressful and emotional exhaustion, (5) physical workload and intensity, (6) physical exertion, and (7) motor training and learning.

#### 2.5.7.1 Applications of EEG indices in physical work

In this section we focused to review physical activities that represents the biomechanical properties of movements, such as grasping, gripping, finger wrist, elbow, arm, knee and hip movements that may be present during lifting, assembling, carrying, and placement tasks. However, vigorous tasks that require high-intensity movements, such as jogging, dancing, running or jumping were excluded.

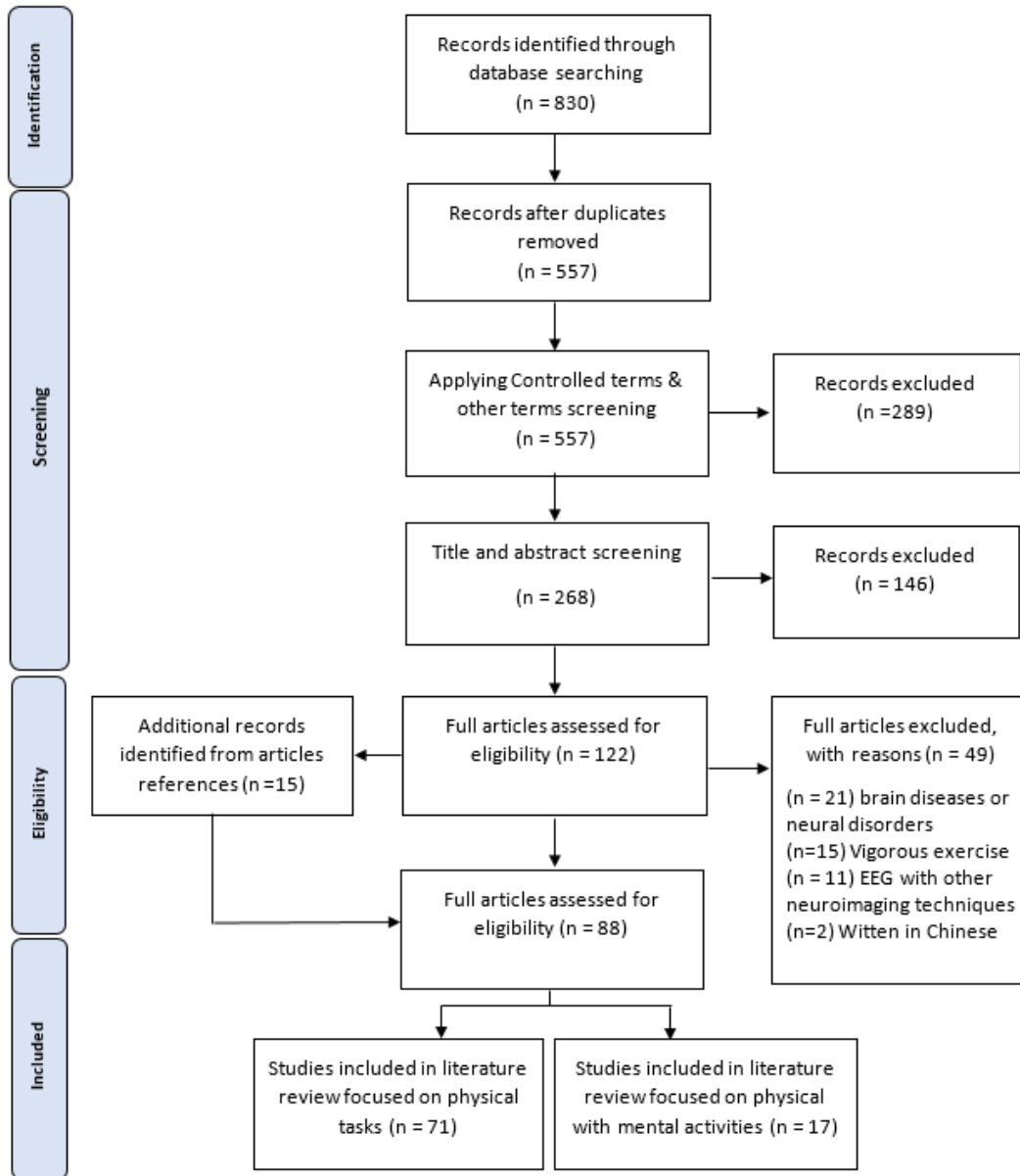


Figure 2-1: Flow chart of the methodology and process selection according to PRISMA

### 2.5.7.1.1 The Effect of Fatigue

Fatigue is a multidimensional concept that combines psychological and physiological aspects (Berchicci et al., 2013; Sengupta et al., 2014a). During a physical task, not only the human muscles

become fatigued, but also the central nervous system resulting in vigilance deterioration, reduces the wellness to exert effort, and declines in physiological capabilities. Consequently, “*If the muscles begin to fatigue, the brain also begins to fatigue*”, as defined by Zadry et al. (2011). Accordingly, understanding the neuromuscular fatigue by analyzing the coherence between EEG signals (i.e., brain) and electromyography (EMG) signal (i.e., muscles) (Kristeva-feige et al., 2002; Gwin and Ferris, 2012; Kim et al., 2017) became an interesting research in sports and exercise neuroscience. Human brain avoids fatigue by shifting the brain activities toward the right anterior and inferior hemispheres, which means the brain requires more resources to complete the task when fatigue occurs (Liu et al., 2007).

#### 2.5.7.1.1.1 Power Spectrum Density

Characteristics of brain activity using EEG Power spectral density (PSD) demonstrated an increase in theta and a reduction in alpha bands after knee joint reproduction task in the frontal cortex (Baumeister et al., 2012). An increase in the ratio of the power of ( $\alpha+\theta/\beta$ ) during a material handling task carried on a construction site was reported (Aryal et al., 2017). The ratio of power of alpha/beta succeeded to reflect the sensation of the core temperature during physical task (Nybo and Nielsen, 2001; Ftaiti et al., 2010). The Root Mean Square (RMS) is a measure of the bio-signal strength, found to increase for alpha, beta, and gamma in the left motor cortex during a hand movement fatigue task (Abdul-latif et al., 2004a). Furthermore, mean rectified amplitude increases in the primary motor and sensory regions during the highest intensity exercise (Flanagan et al., 2012). Other studies established a reduction in the Peak Alpha Frequency (PAF) around motor



cortex region concluding that this might be an indicator of muscular fatigue (Ng and Raveendran, 2007). A reduction in PSD of alpha and beta in frontal and central lobe have been reported during hot exhaustive exercise (Périard et al., 2018).

The PSD of EEG frequencies has been applied as an input parameter for detecting and classifying the physical fatigue (Abdul-latif et al., 2004b; Jain et al., 2016). The application of the advanced algorithm with EEG indices helped in developing smart detection systems (Baumeister et al., 2012; Jain et al., 2016) , and the implementation on adaptive automation systems (Scerbo et al., 2003; Freeman et al., 2004; Parasuraman and Wilson, 2008).

An increase in the current source density (CSD) of beta activity at the left motor cortex was found in a hand gripping task (Ng and Raveendran, 2011), demonstrating that beta activity is associated with motor control.

#### 2.5.7.1.1.2 Event Related Potentials

The motor-related cortical potential (MRCP) is an event related potentials (ERP) component that is locked to the initiation of movement (Hallett, 1994). MRCP has been extensively used to reflect the magnitude of the neural activity before and after physical task through the utilization of three components: (1) *bereitschafts* potential (BP) or readiness potential (RP) (Shibasaki and Hallett, 2006); (2) motor potentials (MP); (3) movement monitoring potentials (MMP). The RP, MP, and MMP potentials are associated with movement planning or preparation, movement execution, and performance control, respectively (Nascimento et al., 2005). An increase in the amplitude of RP values at the supplementary motor area was found with a small level of physiological fatigue

during exertion of highly repetitive forces (Schillings et al., 2006). Studies concluded that muscle fatigue increases the brain activity over the supplementary motor and contralateral sensorimotor areas (Johnston et al., 2001; Dirnberger et al., 2004). Different patterns were observed in a large group of muscles (Spring et al., 2016), emphasizing the importance of the size of the muscle groups when comparing neurophysiological brain responses.

#### 2.5.7.1.1.3 Non-linear Methods

An increase in the fractional dimension (FD) was associated with fatigued handgrip task compared to a resting state (Huang et al., 2003) whereas largest Lyapunov exponents reduced with fatigue (Yao et al., 2009).

#### 2.5.7.1.2 The Effect of Observation, Imagination, and Execution

##### 2.5.7.1.2.1 Power Spectrum Density

Our brain is always active even when we are resting. This attracted researchers to study the brain activity during planning, observation and imaginations, a time where there is no muscle movement (Shakeel et al., 2015). Task observation is activated by the mirror neurons in the motor cortex and the posterior frontal cortex (Cochin, 1999; Rizzolatti and Craighero, 2004). An essential and relevant parameter in this respect is derived from EEG signal power is an event-related synchronization and desynchronization (ERD/ERS). A reduction in power is called event-related desynchronization (ERD), whereas an increase is referred to as event-related synchronization (ERS) (Pfurtscheller, 1992; Pfurtscheller et al., 1998). Mu and beta ERD are sensitive to the

kinematics changes in a hand posture task (Nakayashiki et al., 2014). The sensorimotor cortex is involved in the task observation (Babiloni et al., 1999; Muthukumaraswamy and Johnson, 2004; Storti et al., 2015). Calmels et al. (2006) found a higher power of ERD in alpha and beta for the pre-movement than in post-movement. Different patterns were found in the finger and foot preparation and execution (Cochin, 1999; Pfurtscheller et al., 2000; Zaepffel et al., 2013). Storti found significant changes in the network topological organization by grasping and reaching task (Storti et al., 2015, 2018). An increase in the alpha partially directed coherence in the during the movement preparation reflects the high exchange of information when performing the subsequent movements (Fallani et al., 2008). Compared to motor imagery, the motor execution induced a greater strength coupling between dorsolateral prefrontal cortex to the pre-motor cortex during motor execution than motor imagery. However, the motor imagery induced greater strength coupling between pre-motor cortex to the supplementary motor area and primary motor cortex to the pre-motor cortex (Kim et al., 2018).

#### 2.5.7.1.2.2 Nonlinear Methods

A linearly increase in FD was associated with handgrip force during the holding and the movement, with no significant change during the preparation phase (Liu et al., 2005a). The nonlinear source strength significantly changed patterns during preparation, execution, and sustaining phases of isometric hand exertions (Yang et al., 2011).

### 2.5.7.1.3 The Effect of Force and Torque

#### 2.5.7.1.3.1 Power Spectrum Density

The hand grip force significantly affects the PSD of beta and gamma (Cao et al., 2015). The PSD of beta and gamma are significantly higher at high force levels compared to low force levels in C3, C4, Cz, Pz and Fz electrodes.

#### 2.5.7.1.3.2 Event Related Potentials

There is a direct relationship between the force exerted and the amplitude of MRCP (Shibata et al., 1997). For instance, as the force levels increase the amplitude of BP increases (Freude and Ullsperger, 1987). The negative slope of MRCP is highly correlated with joint forces and the rate of increasing the force mainly in supplementary motor area and contralateral sensorimotor cortex (Siemionow et al., 2000). The amplitude of the RP increases when both the force production and rate of force development torque increase (Nascimento et al., 2005). Slobounov et al. (2004) found an increase in MRCP in frontal, central, and parietal cortical areas associated with the development rate of force. Furthermore, they found that the amplitude of the early MRCP component increased with the perception of effort, while the MMP increases with force level. Other studies explained contradiction results (Slobounov et al., 2002; Schillings et al., 2006).

#### 2.5.7.1.4 The Effect of Stress and Emotion Exhaustion

##### 2.5.7.1.4.1 Power Spectrum Density

Excessive stress significantly deteriorates the human performance and increase the probability of errors. Considering neural mechanism on quantifying human psychosocial conditions can help in early detecting workers' stress for improving workers', health, wellbeing, safety and productivity. The workers emotions significantly altered by working conditions (Jebelli et al., 2018a). For instance the PSD of beta activity was greater in the active versus inactive conditions (Jebelli et al., 2017). Recent studies established the activation of the motor cortex under stressful working conditions (Jebelli et al., 2018b), although it is widely known that the frontal lobe is the emotion control center (Rusinov, 2012). After a stressful physical work, the PSD of the beta band in the right hemisphere was higher than in the left hemisphere (Sulaiman et al., 2009). The difference between the available time and the time required to do the job is known as time pressure, another significant factor that affects the human performance at work (Slobounov et al., 2000). It was evident that the time pressure significantly increases in the frontal midline theta activity and gamma activity in frontal, central, and parietal regions. Another study by Zadry et al. (2009) found an increase in the RMS of alpha band in the frontal and occipital brain regions associated with time-stress. The continues monitoring the brain patterns at work will provide opportunism to avoid excessive stresses to maintain workers' health, wellbeing, safety and productivity.

#### 2.5.7.1.5 The Effect of workload, intensity and exertion

##### 2.5.7.1.5.1 Power Spectrum Density

The perception of physical exertion is associated with cortical activity in especially in the frontal cortex. The PSD of alpha/beta in the F3 electrode found to be an indicator to rate of perceived exertion (2001; Nielsen and Nybo, 2003). Predominant frontal-motor coupling in alpha band and fronto-occipital in beta band was associated with the highest rate of perceiving the exertion (Comani et al., 2013). The prefrontal cortex plays an important role in the initiations of the volitional movement (Hallett, 2007; Berchicci et al., 2013; Robertson and Marino, 2016). Guoa et al (2017) reported an associated between the perceived exertion and cortical activity during movement execution in the prefrontal cortex, supplementary motor area , and primary motor cortex. The premotor cortex, supplementary motor area, and primary motor cortex are associated with the planning and execution of movement and voluntary actions (Lotze et al., 1999; Haggard, 2009; Zaepffel et al., 2013; Kim et al., 2018).

##### 2.5.7.1.5.2 Event Related Potentials

The EEG amplitude of the MRCP at frontal–central electrode sites is a relevant measure to the intensity of perceived exertion associated with different weight levels (de Morree et al., 2012). Desmurget et al. (2009) suggested that not only the frontal cortex but also the parietal cortex mainly the posterior parietal cortex is involved in the experience of conscious intention. De Moree et al. (2012) showed a significant correlation between the amplitude of MRCP and the perception of effort. Two years later, the authors studied the effect of caffeine intake and time spend on the

task over the perception of effort (Morree et al., 2014). Results revealed a reduction in MRCP amplitude and RPE after caffeine intake in the premotor and motor cortex, whereas time spent on task demonstrated an increment in the amplitude of MRCP. According to the general statement of the presented state of research, theoretically the prefrontal cortex, the presupplementary and supplementary motor areas, the premotor cortex, the primary motor cortex, and the posterior parietal cortex might be considered crucial brain regions for the perception of physical effort (de Morree et al., 2012), along with sensory brain areas (Enoka and Stuart, 1992). Although the neural mechanism regarding the perception of physical effort has been clarified to some extent, more neurophysiological studies are needed to precisely understand the brain function and disfunction between different regions forming large-scale networks.

#### 2.5.7.1.6 The Effect of Motor Learning and practice

##### 2.5.7.1.6.1 Power Spectrum Density

Evaluating motor learning based on neural changes has been a challenging area for sports medication, rehabilitation, and kinematic prediction in the neuroergonomics area (Meinel et al., 2016). In general, human performance can be improved through practice and training. Practice reduces the theta ERS in the frontal area, indicating the deterioration in the attention after training. Pitto argued that high synchronization in theta, and desynchronization in both alpha and beta reflects the easiness of the task after training (Pitto et al., 2011). Successful trials were determined by dominant power in alpha band in both frontal midline and right primary sensorimotor areas. Interesting that Babiloni (2008) suggested to train the frontal alpha activity to induce higher ERD

known as “ERD neurofeedback”. Motor learning processes results in a higher gamma band activity in the motor cortex (Amo et al., 2017) and increases the amplitude and latency of the ERP at the premotor cortex (Allami et al., 2014). A significant difference in EEG activity was found when comparing results from single training session with multiple (Jochumsen et al., 2017).

#### 2.5.7.1.7 The Effect of Physical Workload

##### 2.5.7.1.7.1 Power Spectrum Density

Recent evidence suggests that brain cortical function is influenced by different exercise mode, intensity and workload (Weng et al., 2017; Schmitt et al., 2019; Pichardo-Rivas and Gutiérrez, 2021). In a low workload the PSD of alpha was found to be greater than in a high workload task (Zadry et al., 2010, 2011). The PSD for theta, alpha, and beta significantly increased with high intensity at frontal, central and parietal regions (Bailey et al., 2008). Furthermore, an increase in the PSD of beta and gamma activity was found in a weight pressing task (Engchuan et al., 2017). The PSD for most of frequency bands has a positive correlated with exercise workload (Lin et al., 2017). The alpha peak frequency increased after a physical effort task (Gutmann et al., 2015, 2018; di Fronso et al., 2019). Enders et al (2016) speculate that high intensity exercise induced greater brain activity in Brodmann area (BA) 8 followed by BA 6 and BA 7 for alpha and beta bands. Moderate changes in the prefrontal cortex, and higher in the parietal lobe were observed with the elevation of the exercise intensity (Wingfield et al., 2018). Brümmer et al., (2011) found localized brain activity in both primary sensory cortex and prefrontal cortex with elevated exercise intensity. One possible explanation for the aforementioned result is that the high workload requires more



brain activities than low workload task. One study reported a reduction in PSD of alpha during physical activity (Kubitz and Mott, 1996).

#### 2.5.7.1.7.2 Event Related Potentials

The amplitude of contingent negative variation decreased after high-intensity tasks compared to medium intensity, whereas the relative power of theta activity increased after the high intensity exercise compared to medium intensity (Kamijo et al., 2004a). A reduction in amplitude of P300 was observed after high-intensity physical tasks compared to medium intensity (Kamijo et al., 2004b).

#### 2.5.7.1.7.3 Non-Linear Methods

The reduction of fuzzy entropy, an EEG complexity indicator, during high intensity exercise may infer to the increase of the neuronal synchrony (Lin et al., 2017).

#### 2.5.7.1.7.4 Complex network measures

Porter et al. (2019) found an increase in the functional brain network of the frontal region associated with physical and cognitive exertion. Graph theoretical approach were used to characterize the changes of functional network efficiency an endurance performance study (Tamburro et al., 2020). The above-mentioned studies investigated the changes in brain activity caused by cycling. However, the effect of different exertion force levels is still unclear

#### 2.5.7.2 Applications of EEG Indices in Physical Activity Accompanied by a Mental Task

In naturalistic work conditions both cognitive skills and physical abilities are required to perform a task, since “The human action is orchestrated by the mind (brain) and body interactions” as stated by Mehta (2016). Smit et al. (2005) assessed the effect of mental and physical effort on vigilance. Compared to physical effort, an increase in PSD of theta was found in the mental effort. However, an increase in alpha and reduction in beta was found after the physical effort. Therefore, it could be indicated that mental effort deteriorates the alertness level, whereas physical efforts increase of attention level but deteriorate the cognitive processing. Another study demonstrates that attention deteriorate due to physical and mental fatigue, this was quantified by an increase in PSD of theta, alpha, and the ratio of (alpha+theta)/beta activity but a reduction in beta activity (Jagannath and Balasubramanian, 2014). Wascher et al. (2014) analyzed the attention levels with handling boxes and solving cognitive riddles tasks. A significant increase was found in the PSD of theta and alpha activity and the amplitude of N2 during a cognitive task, whereas the amplitude of P300 reduced during the physical task. Two years later, the same authors found an increase in the PSD of alpha activity with time spend on the task, reflecting an increase in mental fatigue and motivation reduction (Wascher et al., 2016). A reduction in the amplitude of P300 during the go condition revealed an increase in the cognitive load due to movement (Yagi et al., 1999; Zink et al., 2016). Physical activity increases the mental fatigue this was quantified by the following: (a) a reduction in the relative energy in beta in most brain regions; (b) a slight rise in the energy ratio of alpha/beta; (c) a reduction in the spectral coherence value beta band; and (d) a reduction in the lempel ziv complexity in frontal, parietal, and temporal (Xu et al., 2018). Another study found that prolonged physical activity deteriorates the attention, this was quantified by a reduction in the amplitude of

P300 while a rise in the P 300 latency. An increase in the brain horizontal visibility graph-based synchronization in parietal and occipital areas with the existence of fatigue was observed (Sengupta et al., 2014a, 2014b). An increasing trend in the network clustering coefficient was found during successful fatigue stages.

## 2.6. Bibliometric Analysis

### 2.6.1 The Categories of the Reviewed Articles

The reviewed studies have confirmed that EEG indices are highly sensitive to fluctuations in the human brain during physical activity. The articles in the current review categorized into physical activities experiment only and physical activity with mental task experiment. In general, (n=72) 82% of the reviewed articles were addressing brain activity during physical activity only, while (n=16) 18 % combined physical and mental activities (Figure 2-2).

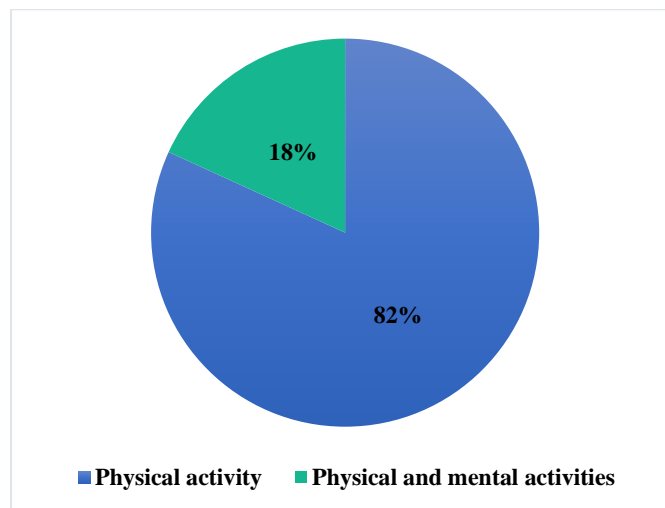


Figure 2-2: The categories of the reviewed articles

### 2.6.2 The Taxonomy of Different Domains in the Reviewed Articles

The taxonomy of the different domains shown in (Figure 2-3) as follows: physical fatigue task (n = 30), followed workload and intensity ( n = 26), observation, imagination, and execution (n= 16), force or torque ( n= 6), stressful and emotional exhaustion (n= 6), motor training and learning (n=4),

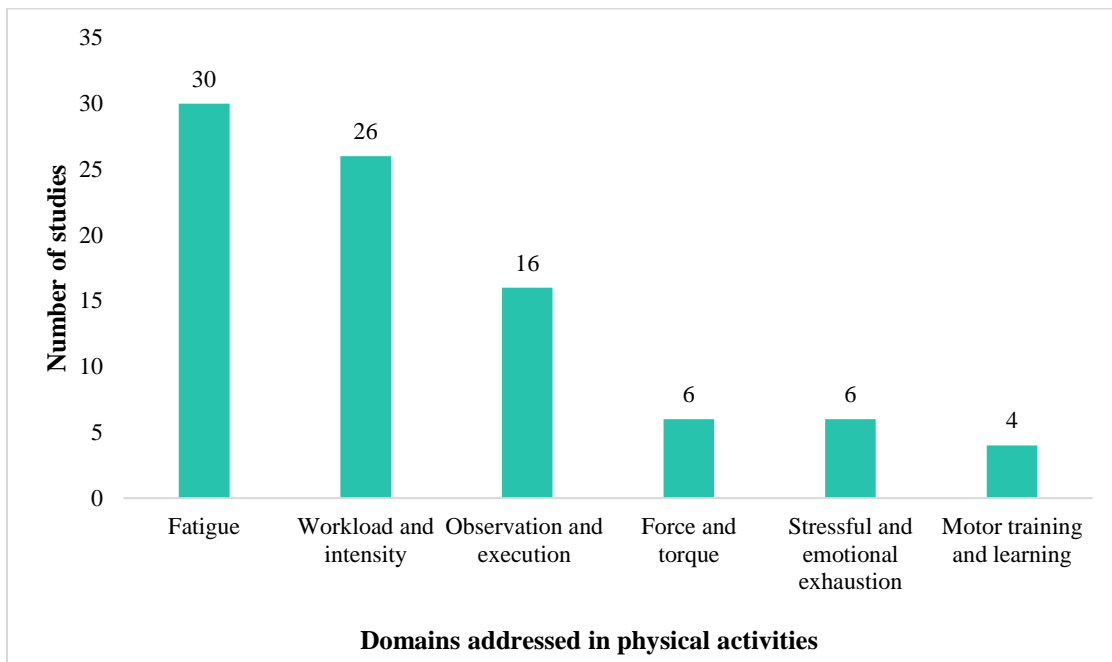


Figure 2-3: Taxonomy of different domains in the reviewed articles for physical activities

### 2.6.3 The Frequency of the Used EEG Indices in the Reviewed Articles

In general, 85% of the reviewed articles applied traditional linear analyses methods to quantify EEG signals in physical activity studies. The majority of studies (n=52) have applied the power of frequency methods (Figure 2-4), followed by the ERP components (n=26). On the contrary, few studies applied nonlinear methods such as entropies, FD and L1 (n= 5). Previous studies have analyzed the EEG for individual electrode site, whereas the connectivity between the pairs of EEG electrodes by applying the network analysis methods to study the brain as a connected complex network were less addressed (n=4). Finally, each of the current source density and the graph theory measures were used in only (n=2).

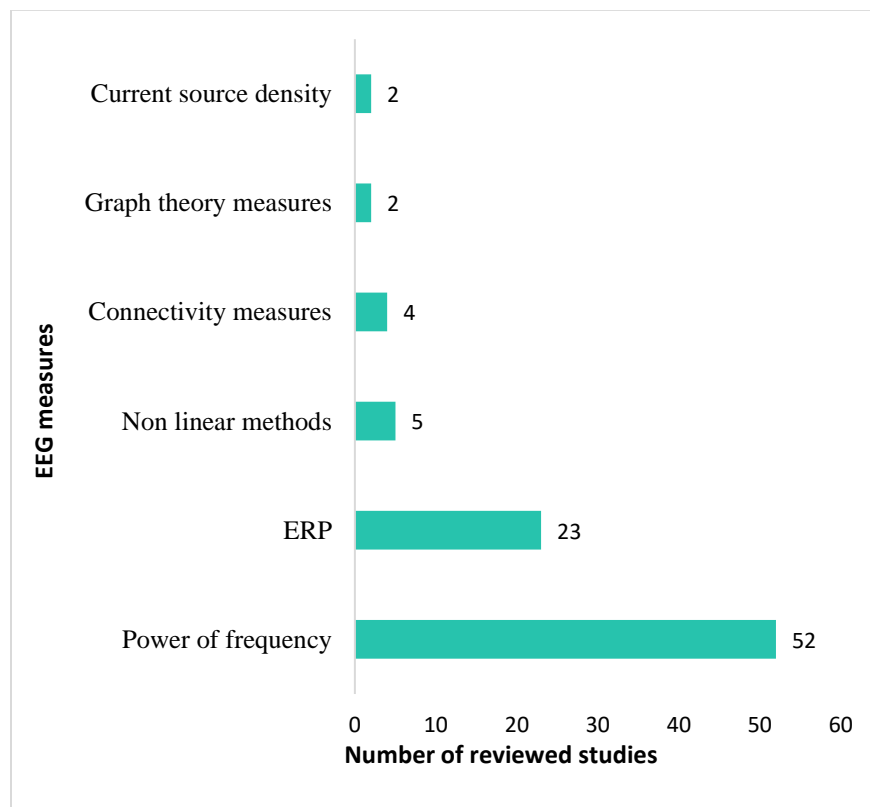


Figure 2-4: The frequency of the used EEG indices (Event-related potentials [ERP])

#### 2.6.4 Neurophysiological Bases of effect of different force levels

Five studies have addressed the effect of different force exertion levels on neural signature of them (n=4) applied the MRCP, and (n=1) applied PSD.

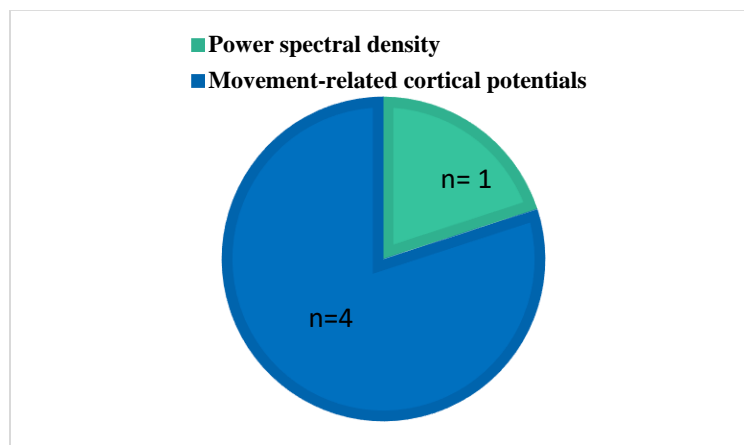


Figure 2-5: EEG indices used to characterize brain signals during perceived exertion

#### 2.6.5 The Number of the Selected EEG Channels

A critical aspect of any EEG study is the selection of the number of recording electrodes. Two recommendations were found in the literature. The first is to reduce the number of electrodes (i.e., <64 channels) to cover the region of interest (Luck, 2014; García-Prieto et al., 2017; Wang et al., 2018b; Li et al., 2019) which provides sufficient analysis especially when using ERPs (Lau et al., 2012). The second is to use a large number of electrodes (i.e.,  $\geq 64$  channels) to help to eliminate the tonic muscle artifacts (Janani et al., 2018; Gramann and Plank, 2019). Moreover, a large number of electrodes are needed for researchers interested in network analysis and EEG

source localization method (Lantz et al., 2003; Fallani et al., 2008; Hassan et al., 2014; Song et al., 2015; Hassan and Wendling, 2018). Our systematic review identified 71 studies that used less than 64 channels, while 16 studies used 64 or more electrodes. One study did not mention the number of electrodes used as summarized in (Appendix A).

### 2.6.6 Participant's Demographic Distribution

The demographic distribution of the studies included healthy male and female participants (Figure 2-6). Of these, 32% of the studies engaged males, and 3% of the studies employed females, and 64% of the studies reported participation of subjects of both genders. The majority of the reviewed studies had a higher number of male participants than females. Only one study did not mention the number of participants (1%).

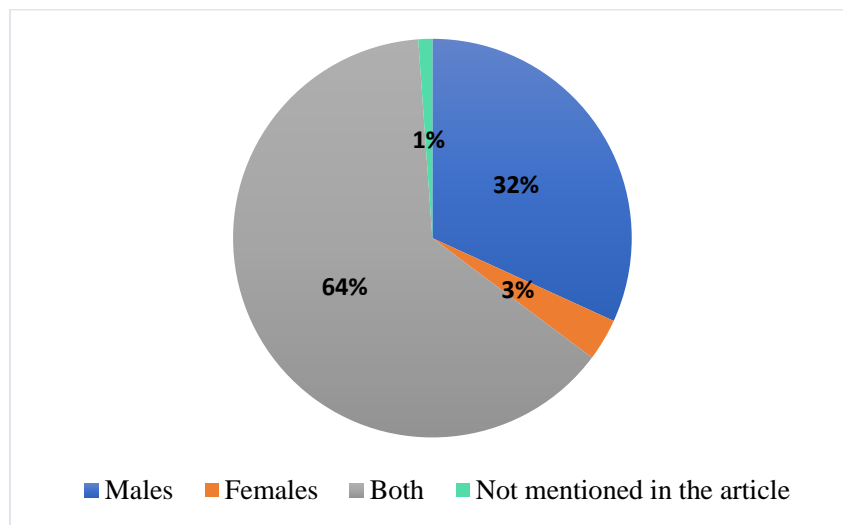


Figure 2-6: Percentage of participants gender distribution in literature

### 2.6.7 Task categorization of the Reviewed Articles

The experimental studies have been categorized into physical tasks only, and studies with physical and mental tasks. Physical tasks were categorized into upper body, lower body, upper and lower body, and stressful and emotional exhaustion. Studies of physical activities associated with mental task are grouped to analyze (1) physical and mental workload on EEG signals, (2) physical and mental fatigue on EEG signals, and (3) physical and mental exertion on EEG signals (Figure 2-7).

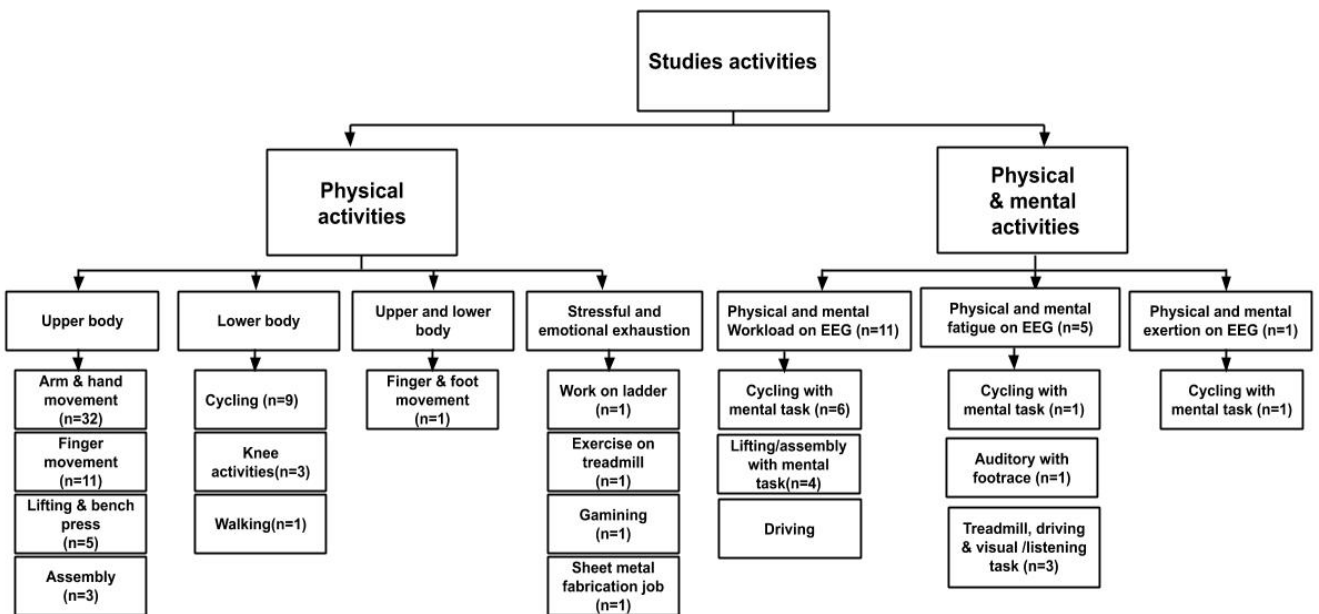


Figure 2-7: The taxonomy of the reviewed article's tasks

### 2.7 Research Gap in Physical activities studies using EEG

This section is addressing some limitations that were found through our review. The research gaps were categorized into (a) methods, (b) tasks, (c) Domains, (d) electrodes, and (e) participants.



## a. Methods

The application of EEG indices has advanced our knowledge in characterizing the brain activity relevant to human physical activities at work. Previous studies focused on traditional linear methods. However, the EEG data are complex and contain dynamic information from different brain regions brain. One method is to study the brain as a complex network using the network science approach (Rubinov and Sporns, 2010). The modern network science, a mixture of dynamic systems theory, graph theory, and statistics, has been applied to study the brain connectivity under various states and conditions.

The application of brain data to advanced mathematical algorithms will help in developing automotive adaptive systems that are capable of monitoring the human physical state to prevent fatigue and excessive workload (Aryal et al., 2017; Qi et al., 2019). Furthermore, it will help in developing smart detective systems, recognition systems, and predictive models (Pitto et al., 2011; Borghetti et al., 2017).

One crucial limitation is the validation of the artifact removal process levitating a research question on to how does clean EEG actually look like? (Daly et al., 2012).

EEG data are spatiotemporal with an excellent temporal resolution but poor spatial resolution. The EEG electrode reference and volume conduction significantly influence spatial resolution. Therefore, localizing the EEG source to correlate the activity of the brain regions might improve the EEG spatial resolution (Cao et al., 2015). The selection of the best reference is still a debate (Ng and Raveendran, 2007; Anastasiadou et al., 2019; Herrera et al., 2019).

The current review includes studies with randomized controlled trials. However, studies considering non-randomized controlled trials were not considered included in the current review. We encourage future systematic reviews to consider both randomized controlled trials and non-randomized controlled trials to assess the methodological quality.

#### b. Tasks

Recent methodological aspects of EEG systems provided the opportunity to apply experiments in real working environments (Reis et al., 2014). However, our review revealed that most of the reported studies were focused on controlled laboratory experiments due to the low signal to noise ratio in controlled laboratory conditions.

Most of the reviewed EEG studies covered the body areas such as upper limbs, mainly finger movement, handgrip, and hand grasping tasks. Tasks that require the activity of the shoulder have been poorly addressed. Moreover, the EEG signatures of tasks that involve the torso, spine, and lumbar area, which are essential for the prevention of WMSD, should also be investigated in the future studies.

#### c. Domains

The number of studies on physical tasks with mental activities is significantly less than the number of studies dealing only with physical tasks. Therefore future research should integrate physical activities and cognitive functions (Mehta, 2016). More attention is required to crucial factors that deteriorate the human performance at work including stress, comfort, discomfort, and excessive muscular strength.

d. EEG channels

The selection of the number of recording electrodes is an open research question. Several studies characterized the EEG information from the individual electrode source point of view, neglecting the integration and segregation between different brain regions.

e. Gender

A considerable gap with respect to the number of female's participants compared to males was found in the reviewed articles. Females have unique needs and responsibilities that must be considered to alleviate the occurrence of WMSD.

## **CHAPTER THREE**

### **FUNCTIONAL CONNECTIVITY AND GRAPH THEORETICAL MEASUREMENTS**

In this chapter, we introduce the concepts of brain connectivity (i.e., connectome) focusing on functional brain connectivity. We provide theoretical background and basic principles for the graph-theoretical approach. We proposed a pipeline for constructing an unweighted functional brain network from EEG data for both sensor source and space source methods. We summarized different methods for estimating the functional connectivity and defined graph theory measures that were used to characterize global and nodal network properties. Besides, we provided another systematic literature review of the functional brain network studies that applied a theoretical graph approach in task-evoked EEG applications for healthy participants only.

#### 3.1 Introduction

*The main content of this chapter is adapted from the systematic review paper by (Ismail and Karwowski, 2020) which has been published in the IEEE access journal.*

A great body of evidence is suggesting to study the brain function as a large-scale network based on “network science” (Bassett and Sporns, 2017). The concept of network science originated from the mathematical field of graph theory (Diestel, 1997) and evolved after the mid-1990s from the increased use of complex integrated systems in a variety of fields (Barabási and Albert, 1999). Modern network science, a mixture of dynamic systems theory, graph theory, and statistics, has been applied to study the functional and structural brain connectivity network under various states and conditions. Over the past couple of decades, mapping the human brain connectivity patterns

have gained considerable attention in the area of neuroscience, and cognitive neuroscience known as “Connectome” (Sporns et al., 2005; Bullmore and Sporns, 2009; Rubinov and Sporns, 2010; Sporns, 2011, 2014). Efforts have been made to study the topological properties of the brain for neurological disorders network (Stam, 2014), brain disease and dysfunction network (Bassett and Bullmore., 2009; Vecchio et al., 2017; Pegg et al., 2020), aging network (Vecchio et al., 2017), resting-state network (Rutter et al., 2013; van Diessen et al., 2015), and high brain functions networks such as perception, problem-solving, memory, and attention (Breckel et al., 2013a; Dai et al., 2017; Taya et al., 2018; Ghaderi et al., 2019).

A considerable amount of connectivity studies were applied using the fMRI data (Raichle, 2009; Farahani et al., 2019; Shou et al., 2020) due to its good spatial resolution. However, the technique has low temporal resolution and provides an indirect measurement of brain activity (van Diessen et al., 2015). To analyze the dynamic processes and the directional of the flow of information (Lopes da Silva, 2013), a high temporal resolution technique is valuable (Teplan, 2002; Stam et al., 2007b; Hassan and Wendling, 2018; O’Neill et al., 2018).

In the last two decades, EEG connectivity studies have gained considerable interest in clinical studies. The first application of graph theory to EEG data was reported by Stam et al. (2007a) comparing the functional brain network of controlled and Alzheimer’s disease patients. Though, little is known regarding the healthy participants in everyday activity.

There are three different types of connectivity that are closely related: structural connectivity, functional connectivity, and effective connectivity (Lee et al., 2003a, 2003b). Structural connectivity encompasses the physical connections among neurons, known as “neuroanatomical”

connections (Iakovidou, 2017), referring to the white matter connectivity in the brain. Functional connectivity is “*the statistical interdependencies between physiological time series recorded from different brain regions*” (Friston et al., 1993b; Friston, 1994). The effective connectivity refers to the causal effect and the direct influence of one neural element on another (Friston et al., 1993a, 1993b; De Vico Fallani et al., 2014). For a review of functional and effective connectivity, we refer the reader to Friston (2011) and Goldenberg and Galván (2015).

### 3.2 Functional Connectivity

Functional connectivity measures the statistical interdependence of physiological time series recorded in different brain regions (Stam et al., 2009). Functional connectivity has been devoted to several studies since it is the best choice for analyzing the functional neuroimaging data and developing computer simulation models (Fingelkurts et al., 2005). Since the calculations of the functional connectivity are highly dependent on brain activities over the time series, a high temporal resolution technique such as EEG ( $<1\text{ms}$ ) is an optimum choice for reflecting the dynamic and rapid neural response (Hassan and Wendling, 2018) and modeling the causal inference (Sakkalis, 2011). The statistical dependencies between pairs of regions are measured through different methods that are summarized in (Table 3-1). The following table provides a variety of the most established estimation methods for functional connectivity; For each measurement we indicate (1) whether it is a univariate or a multivariate connectivity measure; (2) whether it is directed or undirected connectivity methods; (3) whether it is time, frequency domain analysis or cross-frequency phase coupling; (4) whether it is linear, nonlinear or information based

technique; (5) the sensitivity to the volume conduction (Kaminski and Blinowska, 1991; Kamiński et al., 2001; van Diessen et al., 2015; Brunner et al., 2016). For connectivity measurement review articles (see (Blinowska, 2010; Bastos and Schoffelen, 2016; Marzetti et al., 2019)).

Table 3-1 Functional connectivity measurements

(Directed Transfer Function [DTF], Generalized synchronization [GS], Granger causality [GC], Imaginary part of the coherence [IPC], Mutual information [MI], Partial Directed Coherence [PDC], Phase locking value [PLV], Phase synchronization [PS], Weighted Phase Lag Index [wPLI], Synchronization likelihood [SL]).

Functional estimators	Uni-variate	Multi-variate	Direct Causality based	Un-direct	Time-domain	Frequency domain	Phase coupling	Linear	Non-linear	Info-based	Volume conduction sensitivity
Correlation	✓			✓	✓			✓			Highly sensitive
Cross correlation		✓	✓		✓			✓			less sensitive
Coherence	✓			✓		✓		✓			Highly sensitive
PLV	✓			✓		✓	✓		✓		Highly sensitive
Phase lag index	✓			✓		✓			✓		Less sensitive
wPLI	✓			✓		✓			✓		Less sensitive
Partial coherence		✓		✓		✓			✓		Robust
MI	✓			✓	✓					✓	Robust
Transfer entropy	✓		✓		✓				✓		Less sensitive
GS		✓		✓						✓	
SL	✓			✓					✓		Sensitive
PS		✓		✓			✓		✓		Sensitive
GC		✓	✓		✓	✓		✓			Less sensitive
DTF		✓	✓			✓		✓			Sensitive
IPC	✓			✓		✓		✓			Less sensitive
PDC		✓	✓			✓		✓			Less sensitive

### 3.3 Theoretical Aspects of Graph Theory

Graph theory is a powerful mathematical tool that graphically illustrates the architecture of a complex network based on the modern theory of networks (Diestel, 1997). In 1736, the physicist

Leonard Euler solved the problem of crossing the Pregel River, which is known as the “Seven Bridges of Königsberg.” The aim was to cross the seven bridges that connected two small islands in the Pregel river to the city of Königsberg only once and to return to the original location. Euler addressed this problem by reformulating the problem into an abstract representation and eliminating all features except for the landmasses and the bridges connecting them. In modern terms, Euler replaced each landmass with an abstract point (i.e., “vertex” or “node”) and each bridge with an abstract connection (“edge” or “line”), resulting in a mathematical structure called a “graph” or “network.” The contemplation of this problem led to the foundations of “graph theory”—the first true proof in the theory of networks. In 1741, Euler published his paper ‘*Solutio problematis ad geometriam situs pertinentis*,’ describing a hypothetical solution to the Königsberg bridge problem (Euler, 1741).

Since then, graph theory has become a vital method in the field of electrical circuits and chemical structures. The modern era of graph theory began in the late 1990s with the discovery of small-worldness (Watts and Strogatz, 1998) and scale-free network models (Barabasi and Albert, 1999), enabling the quantification of brain connectivity patterns.

Over the last two decades, the application of graph theory to the quantification of neurophysiological data has gained much attention in biology and neuroscience for diagnosing brain disorders such as epilepsy (Dellen et al., 2009; Christodoulakis et al., 2012), schizophrenia (Rutter et al., 2013), Alzheimer’s disease (Stam et al., 2009), rehabilitation after stroke (Westlake and Nagarajan, 2011), and other brain disorders (for a review, see Vecchio et al. (2017) and Farahani et al. (2019)). Whereas several subsequent works aimed to study the topological



configuration of the brain in response to task modulation, the majority of the studies presented herein are primarily focused on cognitive neuroscience. Hence, one of the aims of the current review is to shed light on the functional connectivity of the brain at work and during everyday tasks.

For a better understanding of network properties, the data are presented as a graph ( $G$ ). The graph is a basic topographical representation consisting of a collection of  $V$  vertices (nodes) that are connected by edges ( $E$ ) (links or connectors), where  $G = (V, E)$ . To study the human brain network on a macroscopic scale, the nodes represent brain regions (i.e., EEG electrodes/sensors), whereas the edges represent statistical measures of association, including anatomical, functional, or effective connections (Rubinov and Sporns, 2010; Goldenberg and Galván, 2015). Graph edges include weighted direct, unweighted direct, weighted undirect, and unweighted undirect. A directed edge shows that the information flows in one direction only. The direct edge shows that the activity of one node depends on the other. Whereas an Undirect graph shows that information flows in both directions along edges that connect. The weight between two nodes reflects the connectivity strength of the edge, which allows for discrimination between strong and weak connections. Weak connections can be removed by thresholding.

### 3.4 Pipeline for EEG Functional Brain Network

The following eleven steps present the full pipeline for constructing the unweighted functional brain network using graph theory with EEG data. Here, we briefly describe each step, with the corresponding methodology and brief mathematical descriptions focused on unweighted networks. We have also summarized all steps of the pipeline, starting from the acquisition of EEG brain

signals to the statistical description of the brain network (Figure 3-1). Our aim is to provide a simple stepwise method that can be used by non-expert researchers in the field.

1. Define the nodes of the brain network: The nodes of the brain network represent the brain region. In EEG applications the network nodes are defined by using one of two approaches. The first approach termed “sensor signals” or “individual channel,” which relies on the predefined standard placement of the EEG electrodes (Figure 3-1a) (Jasper, 1958; Chatrian et al., 1985; Oostenveld and Praamstra, 2001). This approach is simple, but the volume conduction may affect the accuracy of the functional connectivity estimates (Brunner et al., 2016; Mierlo et al., 2019). Thus, other researchers have suggested using a second approach based on EEG source space connectivity (Dimitrakopoulos et al., 2017; Hassan and Wendling, 2018) that can be defined by subdividing the brain into different regions to select the regions of interest based on parcellations scheme and individually segregated anatomical regions-of-interest (ROIs) from brain atlases (Tzourio-Mazoyer et al., 2002; Zalesky et al., 2010). The source space is computed after the EEG signals are recorded (Figure 3-1b), preprocessed, and epoched (Figure 3-1c), then the 3D electrode locations are determined via the software acquisition system. To localize the brain source and reconstruct the time course, the inverse problem, which relies on dipole theory, must be solved (Baillet et al., 2001; Michel et al., 2004) by applying the following steps: (a) Obtain a head model by either using simple spherical head models or imaging a realistic head model by MRI (Figure 3-1d). Realistic head models are usually preferable for an accurate calculation for the brain's electric potentials and geometrical characteristics. (b) Estimate the source localization in the head model to determine the location of the dipole source and reconstruct the time course (Figure 3-1e). Several algorithms are used for this purpose, including beamforming, LORETA (Pascual et al.,

1994), standardized LORETA (sLORETA)(Pascual-Marqui, 2002b), exact LORETA (eLORETA), minimum norm estimate (MNE)(Hämäläinen and Ilmoniemi, 1994), and weighted MNE (wMNE) algorithms. Next, the source reconstructed time series is partitioned into an individually ROIs from the brain (Schoffelen and Gross, 2009) (Figure 3-1f) determined from functional atlases (Desikan et al., 2006) to obtain regional time series (Figure 3-1g).

2. Preprocess the EEG data: After high-quality EEG signals are recorded from the scalp surface, the continuous EEG time series data (Figure 3-1b) must be preprocessed for segmentation, filtration, denoising, and artifact removal (Figure 3-1c) (Shamlo et al., 2015). EEG data are contaminated by various types of artifacts, which are categorized as physiological or non-physiological (Ruffini et al., 2006; Sethi et al., 2006; Daly et al., 2012; Bulea et al., 2013). Various methods for data cleaning are discussed in (Reis et al., 2014; Islam et al., 2016). Then specific time-windows are extracted from the cleaned continuous EEG data “epochs”.

3. Define the edges: The edges represent connections between different neurons or brain regions, and exhibit various patterns of connectivity, including structural, functional, and effective connectivity (Kaiser, 2011). In functional connectivity, the edges represent the time-series correlation between two different nodes (Figure 3-1c) or regions (Figure 3-1g). The edge is categorized as either direct or undirect with or without weights. Weights provide more information about the relationship between node pairs.

4. Compute the connectivity matrix (A): The connectivity matrix is known as the adjacency matrix and contains information regarding the associations among connectivity patterns. The connectivity is described by an  $N \times N$  symmetric matrix, in which the rows (i) and columns (j) denote nodes,

and matrix entries ( $a_{ij}$ ) denote edges. There are two types of metrics: one metric is based on channels (Figure 3-1i), whereas the other metric is based on the brain region (current densities for each brain region pair) (Figure 3-1h).

5. Convert the connectivity matrix into a binarized matrix: Matrix binarization is performed to convert the adjacent matrix to an unweighted matrix (Figure 3-1j). For matrix binarization, a threshold value is calculated for each element. If the correlation measures for each pair exceed the threshold, value edges are added between node pairs (otherwise no edge exists). Consequently, a matrix with entry  $a_{ij} = 1$  reflects a connection between nodes  $i$  and  $j$ , while a matrix with entry  $a_{ij} = 0$  reflects no connections between nodes  $i$  and  $j$  (Sporns et al., 2005).

6. Choose a threshold value: The selection of the threshold value is an area of the ongoing research question, and the optimum threshold value is an open question in the literature. Thresholding helps to simplify the complexity of the brain network calculations by eliminating weak, noisy, and insignificant edges in the network (Bullmore and Sporns, 2009; Dellen et al., 2009; Iakovidou, 2017). A careful selection is crucial, some criteria's for appropriate threshold selection are reported in (Bassett et al., 2006; van Wijk et al., 2010a; Toppi et al., 2012).

7. Estimate the functional connectivity measurement: Several methods are available for estimating pairwise associations between electrodes sensors or regions. A comparison between the functional connectivity estimates methods were summarized in (Table 3-1). For a comprehensive review, articles see ((Blinowska, 2011; Sakkalis, 2011; De Vico Fallani et al., 2014)). Unfortunately, there is no such an optimal method to universally assess the functional connectivity (David et al., 2004; Wendling et al., 2009; Sakkalis, 2011). Authors suggested to be careful while choosing the

functional connectivity estimator and proposed some crucial factors to be considered such as (1) define the underlying hypothesis that will be studied (De Vico Fallani et al., 2014); (2) the nature of coupling either linear interdependencies, nonlinear interdependencies or information based technique (David et al., 2004; Imperatori et al., 2019) ; (3) the time-domain or frequency domain dependent of the estimator that is originally based on the neuroimaging technique being selected in the study (De Vico Fallani et al., 2014); (4) the frequency specificity of the interaction (broad vs. narrowband); (5) Direct (i.e., causal interaction) or non-direct type of measurement (Bastos and Schoffelen, 2016); (6) model-based or data-driven techniques (Sakkalis, 2011; Bastos and Schoffelen, 2016); (7) stationary or quasi-stationarity brain signals (De Vico Fallani et al., 2014); (8) bivariate or multivariate modeling consideration(Blinowska, 2011); (9) source or sensor electrode connectivity; (10) the sensitivity to volume conduction phenomena (Brunner et al., 2016; Chella et al., 2016).

In general, the EEG signals are best expressed based on frequency domain characteristics for distinguishing between neural and artifacts signals, thus considering frequency-based functional estimators methods are particularly attractive (Astolfi et al., 2007). Several MATLAB based toolboxes are available for source estimation, estimating the functional connectivity, and analyze the network measurements that are summarized in (Hassan and Wendling, 2018).

8. Construct the network: Mathematically, a network is a matrix (Vecchio et al., 2017). In order to construct a network, the binarized matrix is converted into a sparsely connected graph, represented as a scalp graph (Figure 3-1k) or cortex network (Figure 3-1l) after localizing the source as mentioned in the first step.

9. Analyze the data using graph theory: Different graph theory metrics are used to quantify network by analyzing the topological properties of the network (Figure 3-1m). Different toolkits have been developed for visualizing and analyzing topological properties, as summarized by Xia et al. (2013a) and Hassan et al. (2018). In the following section, we present a detailed description of the measures used to detect aspects of functional integration and segregation for unweighted networks.

10. Apply statistics: Statistical methods are applied to compare the statistical differences between two different states such as exertion (hard vs. light), intensity (high vs. low), conditions (movement vs. rest), populations (healthy vs. diseased), or gender (males vs. females) or by comparing results to a theoretical reference network (network types are described below) (Figure 3-1n). There are several methods for statistical inference, nonparametric statistics, permutational statistics, and bootstrapping are the most appropriate for the nature of EEG data.

11. Classify the conditions: Several methods have been used to classify different brain states (Figure 3-1o). For instance, functional connectivity estimates have been used to classify fatigue and non-fatigue conditions (Sun et al., 2018), whereas hand movements have been classified based on network node strength (Ghosh et al., 2015). Other classification algorithms, such as artificial neural networks (Samima and Sarma, 2019) and support vector machines (Sun et al., 2014b; Chen et al., 2019), have been used to classify mental workload and mental fatigue using connectivity features.

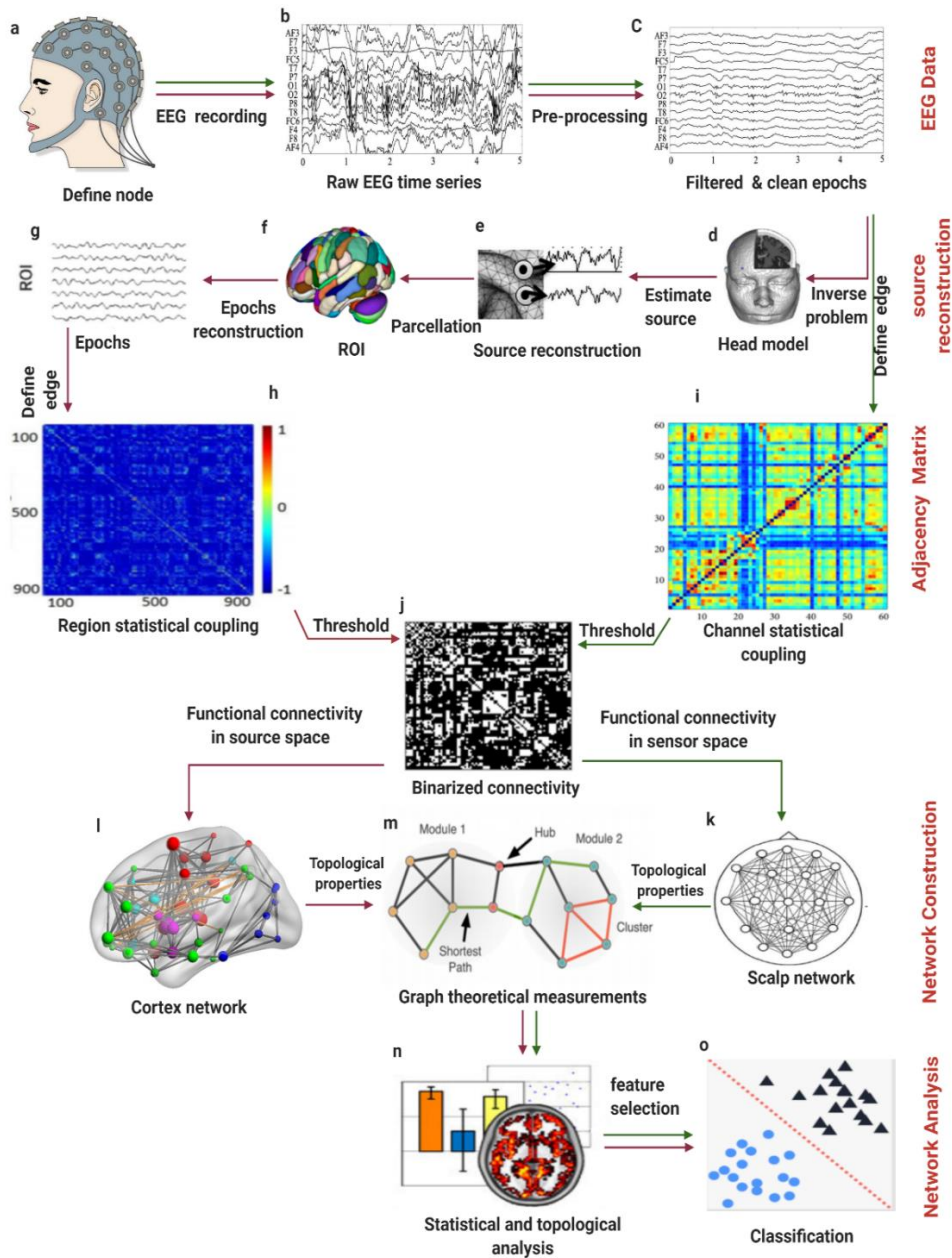


Figure 3-1: Schematic illustration of the pipeline for constructing a functional brain network based on EEG data using graph theory.

The green line defines the first approach, termed the “sensor signal” or “individual channels” method, while the red line defines the second approach, denoted as “EEG source connectivity.” (a) Place the cap with electrodes on the scalp. (b) Record the EEG time series. (c) Preprocess the data by cleaning, filtering, removing artifacts, and epoching. (d) Solve the inverse problem by first

estimating or imaging the head model (method 2). (e) Reconstruct the electrical potential time source (method 2). (f) Parcels the source reconstructed epochs into ROI (method 2). (g) Define the ROI for the epochs. (h) Develop the connectivity matrix for the selected ROI. (i) Develop the connectivity matrix for the selected EEG channels (method 1). (j) Apply the threshold value(s) to binarize the connectivity matrix (methods 1 & 2). (k): Construct the scalp functional brain network between EEG electrodes. (l) Construct the cortex functional brain network within the ROI. (m) Apply network topological properties to calculate graph theory measurements. (n) Apply statistical analysis methods. (o) Classify different states if needed (Hwang et al., 2018; Mierlo et al., 2019).

### 3.5 Graph Theoretical Measures and Network Topology Properties

Network parameters are categorized into global (graph) and local (nodal) properties. Global properties include the characteristic path length, clustering coefficient, small-worldness, global efficiency, local efficiency, and transitivity whereas nodal properties include nodal centrality, betweenness centrality, and nodal efficiency. The following section provides mathematical equations for each network parameter, in which the definitions are limited to unweighted graphs.

#### 3.5.1 Global measures

The path length is the number of edges that must be traversed in order to move from one node to another. The shortest path length (Han et al., 2019), or geodesic path (Newman, 2003), is the minimum number of edges necessary for a node to reach another node. The characteristic path length (PL) is the average of the shortest path lengths over all possible nodes in the network (Latora and Marchiori, 2003; Qi et al., 2019) and represents the speed at which information is transferred between various brain regions, reflecting the global integration of information processing. PL is



defined the distance between two nodes  $i$  and  $j$ , given as the minimum number of edges needed to travel from node  $i$  to node  $j$ .  $N$  is the set of all nodes in the network, and  $n$  is the number of nodes (equation 1). The shorter the length, the better the integration of the graph, resulting in a simpler transfer of information.

$$PL = \frac{1}{n(n-1)} \sum_{i,j \in N, i \neq j} d_{ij} \quad (1)$$

The inverse of the average shortest path length is used to quantify  $E_{global}$  which represents the efficiency of information transfer across the whole network, i.e., global information processing (Li et al., 2016). A higher  $E_{global}$  value indicates a faster parallel transfer of information in a network (Latora and Marchiori, 2001) and a superior integration of information (Ghaderi et al., 2018).

$$E_{global} = \frac{1}{n(n-1)} \sum_{i,j \in N, i \neq j} \frac{1}{d_{i,j}} \quad (2)$$

The local clustering coefficient is the ratio of the number of existing edges between adjacent nodes to all possible connected edges (Kaiser, 2011; Liu et al., 2017) and is a measure of local connectivity or “cliqueness,” as it reflects the local interconnectedness among neighbors of a node in a graph (Kaminski and Blinowska, 2018). A higher clustering coefficient corresponds to more robust and efficient local interactions which is a direct measure to the function segregation. The average of the local clustering coefficient of all nodes is denoted as the global clustering coefficient (CC) (Watts and Strogatz, 1998). where  $k_i$  is the number of edges connected to node  $i$  and  $A_{ij}$  is a binary value indicating the connection status ( $A_{ij} = 1$ , edge exists;  $A_{ij} = 0$ , edge does not exist) (equation 3) (Li et al., 2016).

$$CC = \frac{1}{n} \sum_{i \in N} \frac{\sum_{j, h \in N} m_{ij} m_{ih} m_{jh}}{K_i(K_i-1)} \quad (3)$$

Elocal is the average efficiency of all pairs of nodes, shows whether the communication between nodes is still efficient when a node is removed from the network. A higher Elocal is an indication for the robustness of the network at the local scale.

$$E_{local} = \frac{1}{n} \sum_{i \in G} E_{global} G(i) \quad (4)$$

The small-worldness parameter ( $\sigma$ ) are characterized by a strong local clustering between network nodes with short path length between neighbor nodes (Watts and Strogatz, 1998; Bassett and Bullmore, 2006). Small-world network has a balance between the segregation and integration of the information (Latora and Marchiori, 2001). Meaning that most nodes can be reached from any other node in a small number of steps (Goldenberg and Galván, 2015). The small-worldness is determined as the ratio of the normalized CC (denoted as  $\gamma$ ) to the normalized PL (denoted as  $\lambda$ ) (Humphries et al., 2006; Humphries and Gurney, 2008) (equation 5).

$$\sigma = \frac{CC/CC_{rand}}{PL/PL_{rand}} = \frac{\gamma}{\lambda} \quad (5)$$

### 3.5.2 Nodal measures

Graph theory local measures are commonly used to evaluate the network centrality and detecting network hubs such as betweenness centrality, degree centrality, and eigenvector centrality (Boccaletti et al., 2006; Zuo et al., 2012). The degree centrality (K) is the number of edges that connect one node with all other nodes. A higher degree indicates a more central node (Kaiser,

2011). Mathematically, it is calculated by summing the number of edges connected to each node. In which  $i$  is the source node and  $j$  is the destination node as shown in (equation 6).

$$K_i = \sum_{j \neq i} a_{ij} \quad (6)$$

A node with a high degree of centrality is referred to as a “hub” (Sporns et al., 2007; Iakovidou, 2017). A hub is a node with more edges than any other node (Kaiser, 2011) and indicates the important brain regions that interact with other regions (Iakovidou, 2017). Provincial hubs are hubs that are connected to other nodes in the same module, whereas connector hubs are connected to nodes in other modules (GeethaRamani and Sivaselvi, 2014).

The betweenness centrality of a node measures the proportion of shortest paths between all node pairs in the network that pass through a given index node (Freeman, 1977; Fornito et al., 2016).

The nodal efficiency ( $E_{nodal}$ ) is the inversely proportion of the characteristic path length between node  $i$  and all other nodes in the network. It measures the ability of a node to propagate information with the other nodes in a network. As shown in (equation 7),  $N$  is the number of nodes and  $d_{ij}$  is the shortest path length between node  $i$  and node  $j$ .

$$E_{nodal} = \frac{1}{N(N-1)} \sum_{j \neq i \in G} \frac{1}{d_{i,j}} \quad (7)$$

Detailed descriptions of these network parameters and their interpretations have been provided in several studies (Latora and Marchiori, 2001; Boccaletti et al., 2006; Achard and Bullmore, 2007; Bullmore and Sporns, 2009; Li et al., 2016). Furthermore, reviews on the application of graph theory to neuroscience can be found in several previous works (Stam and Reijneveld, 2007; Wang et al., 2010; Kaiser, 2011).

### 3.5.3 Network Types

There are four types of networks (i.e., regular, well-ordered, or lattice-like networks; random networks; small-world networks; and scale-free networks) (Figure 3-2) (Reijneveld et al., 2007; Stam and Reijneveld, 2007; Stam, 2010). These different networks are distinguished based on the number of local segregation events (i.e., represented through CC) and the global integration between nodes (i.e., represented through PL).

Regular networks have a high CC with a long PL, indicating that the network is robust but inefficient in transferring information. In contrast, random networks have a small CC and a short PL, indicating that the network is efficient in transferring information but is not robust. A small-world network is intermediate between regular and random networks and has a short PL, similar to a random network, with a higher CC than a regular network (Latora and Marchiori, 2003). Small-world networks are robust and efficient in transferring information (Micheloyannis et al., 2006a; Taya et al., 2015). In particular, small-world networks are characterized by high  $E_{local}$  and  $E_{global}$  values, sparse connectivity between nodes, and low wiring costs (Danielle and Bullmore, 2006). Therefore, small-world networks are considered as near-optimal networks in terms of segregation, integration, cost, and performance (Stam and Dijk, 2002; Stam et al., 2009). A scale-free network is unique due to its extremely short path length (Cohen and Havlin, 2003; Stam and Reijneveld, 2007; Broido and Clauset, 2019) and strikes a balance between global and local communications (Taya et al., 2015) with a power-law degree distribution. Other network classifications have been proposed by Kaiser (2011) based on topological and spatial organization.

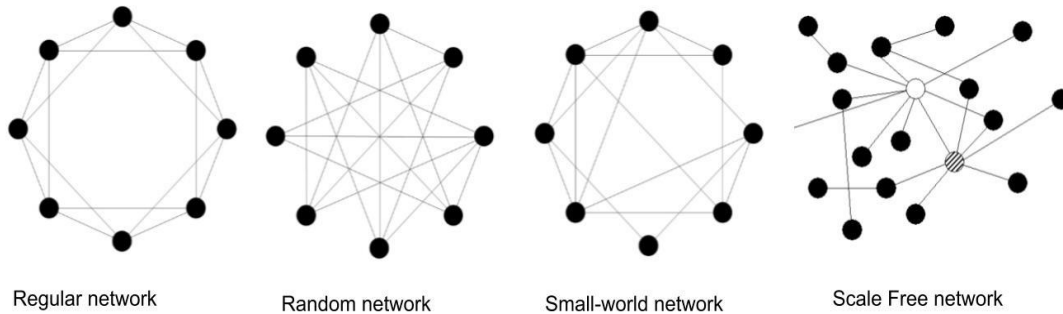


Figure 3-2: Four types of networks (in the scale-free network, the white and striped nodes represent network hubs) (Stam and Reijneveld, 2007; Stam, 2010).

### 3.6 Application of Graph Theory to EEG

#### 3.6.1 Connectivity Studies on Movement Execution

Motion is essential for everyday tasks, as “*human action is orchestrated by mind (and brain) and body interactions*” (Mehta, 2016). The contralateral somatosensory, ipsilateral somatosensory, and motor areas of the brain are strongly related to the function of motor processing. Before movement occurs, there is a transfer of information from the contra-to-ipsilateral hemispheres, whereas the opposite pattern occurs after movement (Nolte et al., 2004). Babiloni et al. (2001) observed a higher degree of activation in the bilateral primary sensorimotor areas during ongoing movement than during the preparation for movement execution. The supplementary motor areas of left and right hemispheres found to have higher strength value (De Vico Fallani et al., 2008). The increase in network edges during the preparation for movement demonstrates the need for a higher degree of information exchange in order to execute movement-related tasks (Fallani et al., 2008). Moreover, decreased accessibility and increased centrality have been observed during the preparation and execution of finger movement tasks.

Different patterns of coupling are observed for different intervention strategies. Particularly, different intensity levels during a cycling task generate different patterns of brain connectivity in the alpha and beta bands of the prefrontal motor and central areas (Comani et al., 2013). Furthermore, an increase in synchronization has been observed in the parietal and occipital lobes after physically and visually fatiguing tasks (Sengupta et al., 2014a). Increased mutual information (MI) values for the beta band have been observed during a finger-tapping task, reflecting an increase in the flow of information (Jin et al., 2012). Lastly, a strong interaction between the sensorimotor and prefrontal areas has been shown to occur during the transition period from the resting state to hand movement (Cheng et al., 2016).

Local network properties have been considered during left- and right-hand movement tasks in order to classify different movements (Filho et al., 2018). Ghosh et al. (2015) showed that the node strength can be applied to classify hand movement without the need for any classifier. The Enodal value of the left sensory and bilateral primary motor cortices increases during motion-related tasks but decreases in posterior parietal areas (Jin et al., 2012). Furthermore, researchers observed an increase in the functional connectivity of the motor region during arm movements, as well as a reduced node accessibility and increased node centrality (Storti et al., 2015, 2016). Two years later, the same research group (Storti et al., 2018) found that arm movement significantly reduced network connectivity, primarily in the alpha and beta bands, and reduced the weighted PL only during movement of the left arm. However, neither the CC nor the small-worldness exhibited any significant changes. Jin et al. (2012) observed the economy of small-worldness in alpha and beta band networks during finger movement and resting tasks. The medial premotor and bilateral prefrontal cortex for the higher frequency bands appear to have greater connectivity and a higher

CC, but a shorter PL during motor tasks (Bassett et al., 2006). Significant changes in the hubs of the lower beta and gamma bands in the superior parietal somatosensory cortex have been shown to characterize visuomotor associations (Nguyen et al., 2019). A comparison between the node degree of spectral coherence and that of imaginary coherence in the beta band during a motor task showed that the spectral coherence network outperformed the imaginary coherence network in the contralateral motor cortex (Cattai et al., 2018).

### 3.6.2 Connectivity Studies on Exertion

A higher perception of effort task revealed strong beta coherence coupling in the prefrontal-motor area (Comani et al., 2013). An increase in partial theta coherence has been observed in the frontal region during working memory tasks associated with physical exertion. An interesting U-shaped pattern was initially observed in the CC, where the CC of the theta band increased during both physical exertion tasks and mental tasks and decreased significantly when the tasks became more difficult (Porter et al., 2019).

### 3.6.3 Connectivity Studies on Fatigue

Fatigue diminishes human performance by slowing the human response time, increasing the error rate, increasing drowsiness, and causing musculoskeletal disorders. Several previous studies have addressed the underlying neural mechanism of mental fatigue in realistic applications (Majumder et al., 2019). Different patterns of connectivity between the right and left hemispheres in sensorimotor areas have also been demonstrated during a state of fatigue (Sun et al., 2014a), similar to the findings of Liu et al. (2010) in different brain regions. Comparing the synchronization

between pre-fatigued and post-fatigued tasks in parietal and occipital lobes indicates that the human brain exhibits stronger coupling during fatigue to maintain information transmission until the required task is accomplished (Kar and Routray, 2013; Sengupta et al., 2014a, 2014b). An increase in CC and K and a reduction in PL is an indication of vigilance reduction as a result of fatigue. The local network topologies of some EEG electrodes were significantly correlated with the degree of fatigue and borg's scale values. Furthermore, the global network topologies were different between adults and children (Wang et al., 2018c).

#### 3.6.4 Connectivity Studies on Physical Workload

The assessment of mental workload based on neuronal data has been of great interest (for a review, see Borghini et al. (Borghini et al., 2014)), while few in physical workload. Activities in the primary motor cortex increased with the incremental of exercise intensity (Brümmer et al., 2011). Sauseng et al. (2007) found an increase in the main local frontal-midline theta activity in conditions requiring the highest level of task demand. The weighted PLI value for the alpha band in all brain regions has been shown to decrease during a high cognitive-motor workload demand, whereas an increase was demonstrated in the coupling of the theta band (Shaw et al., 2019).

#### 3.7 Results from Graph Theoretical EEG based Studies

From 77 articles we have reviewed and summarized in (Appendix B), over than half of the articles selected were published during the four years (70%; n = 52). The results show an increasing trend in brain function studies using brain connectivity techniques and graph theory measures (Figure 3-3). We expect the number of future studies to increase dramatically over the next several years.



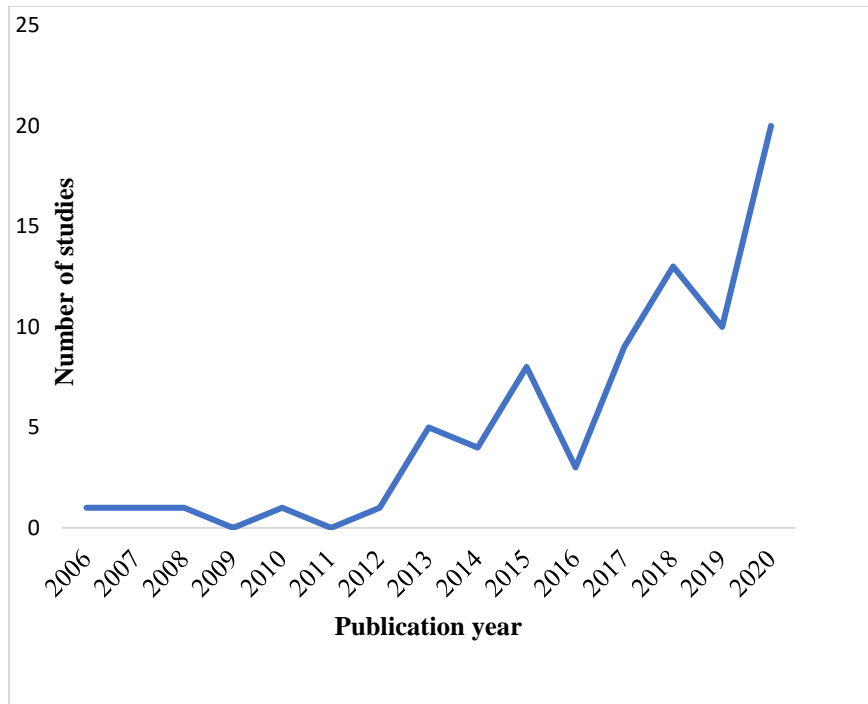


Figure 3-3: Scatter plot of the publications of graph theory studies based on EEG data per year

Overall, the evidence indicates that cognitive functions (80%) are more frequently addressed than motor processing (20%). techniques for estimating functional connectivity, including phase-locking value (PLV) (Lachaux et al., 1999), partial directed coherence (PDC) (Baccalá and Sameshima, 2001), and phase lag index (PLI) (Stam et al., 2007b), exhibited the greatest potential impact (40%) (Figure 3-4). Numerous studies ( $n = 9$ ) used the PLV technique, as it overcomes the limitations involved in using traditional coherence methods and calculates the linear correlation between EEG signals (Lachaux et al., 1999). The PLV technique is followed by the PDC, as this technique allows one to assess the statistical interdependence of EEG signals in the frequency domain (Baccalá and Sameshima, 2001; Baccala et al., 2007).

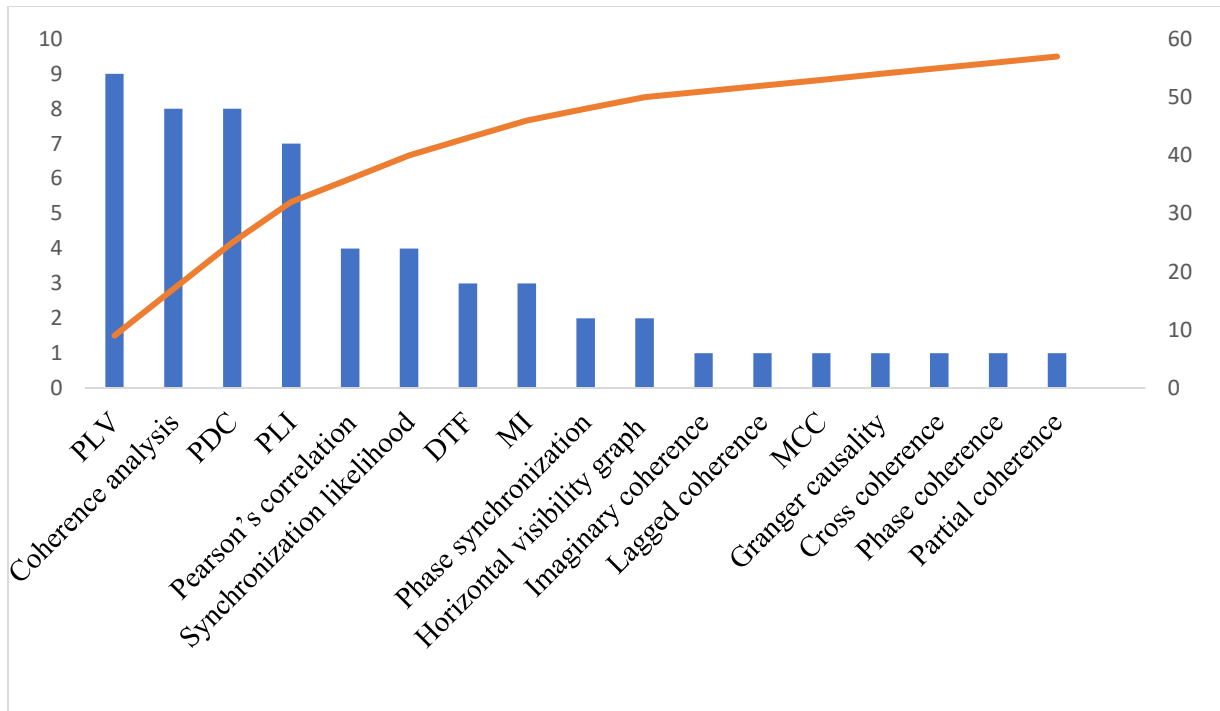


Figure 3-4: Pareto chart of methods for estimating functional connectivity (Phase Locking Value [PLV], Partial Directed Coherence [PDC], Phase Lag Index [Phase Lag Index], Directed Transfer Function [DTF], Mutual information [MI], Minimum connected component [MCC]).

The CC and PL are the most frequently used graph theory metrics to characterize the brain network (average, normalized, or weighted) ( $n = 33$  and  $26$ , respectively) (Figure 3-5).

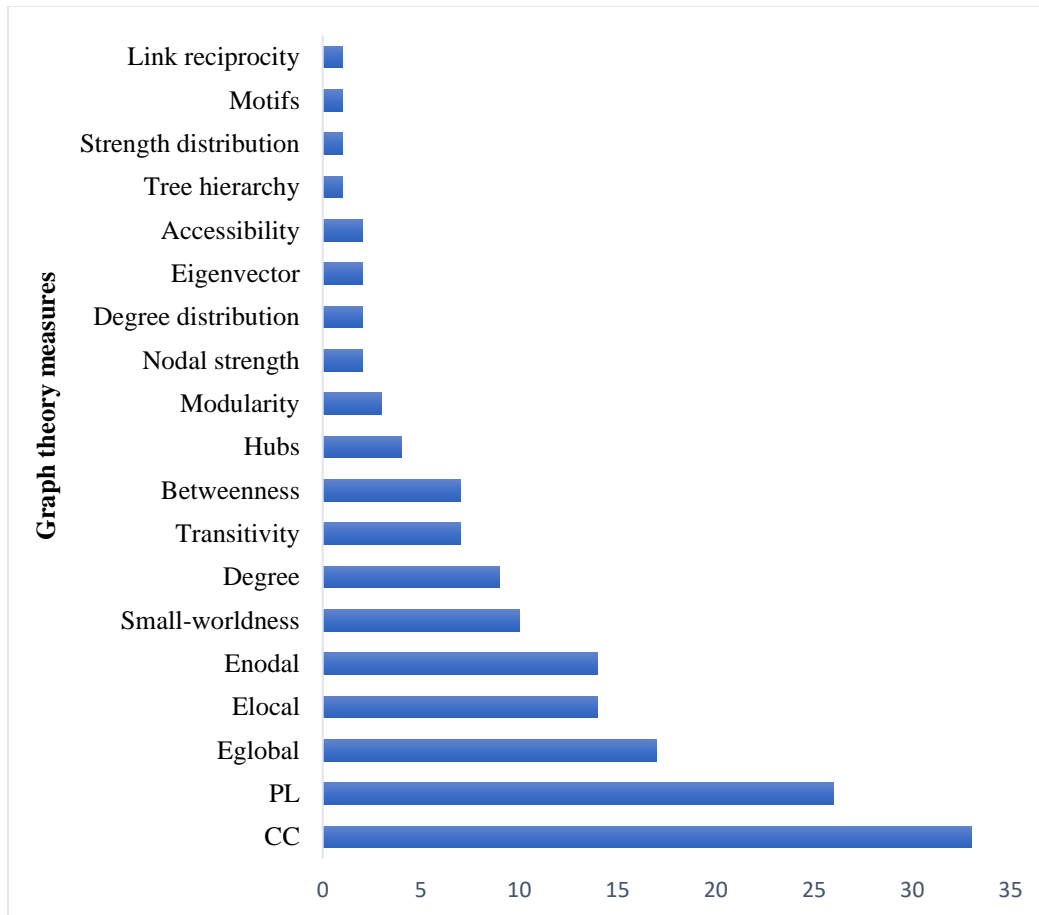


Figure 3-5: Frequency of graph theory measures (clustering coefficient [CC], path length [PL], global efficiency [Eglobal], local efficiency [Elocal])

### 3.8 Limitations and Future Directions for Graph Theory Applications

There is a growing interest in investigating brain connectivity with respect to the execution of specific tasks. The reviewed applications in this chapter indicated that the graph theory measures with EEG data yields reliable and feasible results. Motion tasks were limited to finger movements such as tapping, whereas exertion tasks were limited to cycling activity (Comani et al., 2013; Porter et al., 2019). Regularly performed activities in everyday settings such as handling, lifting, gripping,

grasping, pulling, pushing, assembling, sorting, manual inspection, and lower limb movements have not been well quantified using graph theory measures. Therefore, new exploratory studies are required to address real-world applications.

Methodological choices through EEG recording, pre-processing, and analysis significantly impact the functional connectivity estimations and network topology. These including the choice of reference, artifacts removal, the confounding effect of volume conduction in EEG (in signals space), and inverse problem (in source space) (for a review see (van Diessen et al., 2015)). Hence, future researchers should explore the effects of different types of references on the connectivity measurements, similarly as (Chella et al., 2016; Anastasiadou et al., 2019). For mitigating the volume conduction effect, less sensitive connectivity estimators to volume could be used (Nolte et al., 2004; Stam et al., 2007b; Vinck et al., 2011; Christodoulakis et al., 2015). Other suggestions include the use of spatial filters (Laplacian montage), studying current source density, and implementing the source space method (Bastos and Schoffelen, 2016; Hassan and Wendling, 2018). Although there are several methods were proposed to solve the inverse problem (Anzolin et al., 2019), there is no unique method without assumptions and limitations. Additionally, the source space method is difficult to implement, and the effect of volume conduction can never be completely abolished (Hassan et al., 2014; Hassan and Wendling, 2018).

Many attempts have been proposed to minimize the existence of muscular and ocular artifacts in EEG data (Makeig et al., 1996; Urigüen and Zapirain, 2015; Blum et al., 2019; Pion-Tonachini et al., 2019a). None of the development methods guarantee artifact free data. It is unknown to what extent the reduction of artifacts could influence the connectivity measurements. Filtering is used

to avoid antialiasing and eliminate the effect of direct current. A careful selection of filtering is crucial since filtering affects the phase and amplitude of EEG signals. Thus, a zero-phase filter is highly recommended.

Functional connectivity patterns and graph theory have proven to be powerful tools for characterizing brain signals. However, the ability to use these measurements as an input parameter for developing predictive models, adaptive systems, or monitoring systems has been poorly addressed (Cynthia et al., 2017; Chen et al., 2019; Yuan et al., 2019). One of the most challenging goals in the field of neuroergonomics is to develop smart systems that can accurately monitor and detect an operator's mental state and the intention of movements at work (Samima and Sarma, 2019).

Another limitation is the difficulty of drawing specific conclusions, especially when using different factors, as discrepancies could stem from (a) differences in estimations of functional connectivity (Wendling et al., 2009; Li et al., 2016; Cattai et al., 2018), (b) differences in threshold values (Micheloyannis et al., 2006b; Lithari et al., 2012; Huang et al., 2016; Nguyen et al., 2019), (c) differences in recording reference locations (Nunez et al., 1997; Micheloyannis et al., 2006a; Christodoulakis et al., 2015; Anastasiadou et al., 2019), (d) the numbers of existing edges (De Vico Fallani et al., 2014), (e) sample size bias (Bastos and Schoffelen, 2016), (f) factors related to participant demographics, such as gender and age (Micheloyannis et al., 2009; Wang et al., 2018c) or level of education (Micheloyannis et al., 2006b, 2006a); (g) the brain states of the subjects, such as healthy or pathological (Stam, 2014); or (h) the inclusion of trained or untrained participants (Taya et al., 2015, 2018).

Further research is needed to avoid the arbitrary selection of the threshold value in a binary network and minimize bias. The chance of having a network with a high false-negative value and threshold bias, motivated researchers to propose novel computational methods (Drakesmith et al., 2015).

The unweighted network still dominates the literature, as it simplifies the complexity of brain signals by eliminating the weakest connections (Storti et al., 2016). Although several thresholding approaches are proposed, there is no reliable method that efficiently filters brain information (Vijayalakshmi et al., 2015). Others sustained to implement a weighted network as it is more informative (De Vico Fallani et al., 2014). While In that case, care must be taken since variation in weights affects the network topology (Fornito et al., 2013).

A considerable number of experiments were conducted on males only or both genders. There is a significant gap in investigating the functional brain network on female participants. Studies have demonstrated that there are significant differences between males and females, and therefore, functional brain network studies focused solely on female participants are required to address these differences. Wang et al. (2018c) suggested dividing participants uniformly according to age or gender for more accurate observation. Moreover, the number of participants in future studies should be larger to achieve a higher degree of generalization.

## CHAPTER FOUR: MATERIALS AND METHODS

In this chapter, we describe the study methodology by explain the EEG data acquisition, preprocessing procedures, feature extraction, connectivity estimation and network construction. We proposed an EEG pipeline for constructing functional brain EEG source network.

### 4.1 Experiment and Task Description

The experiment was designed to record the brain signals to investigate the interactions of brain activities in the form of EEG signatures, measures the exerted forces, and collect the perceived comfort with the predefined force exertions levels.

An isometric arm exertion task using the Jackson Strength Evaluation System was performed. The system was developed by Andrew Jackson (1994) to assess the physical ability of workers to perform MMH tasks (Chaffin et al., 1978; Mital and Kumar, 1998). The participant stands straight on a wood plate, in which a metal chain is anchored to the plate. The handle is attached at the top of the metal chain, approximately at the elbow high of the participant and parallel to the floor. The length of the chain is adjusted to match the necessary elongation so the participant's muscles will not contract, which fulfills the definition of isometric. The weight of the handle and chain is 1.5 Kilograms (3.3 lbs).

Participants lift the chain and exert a force by pulling the chain using the handle that matches predefined levels of exertion. Participants must pull the handle upward using their upper arms

approximately 90 degrees without any body movement, as shown in (Figure 4-1). The isometric strength test instructions are provided in (Appendix C).

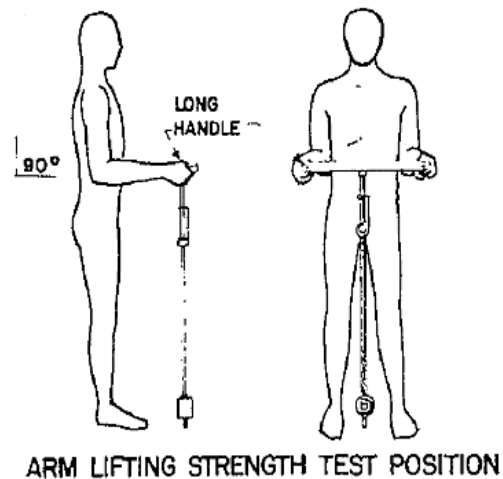


Figure 4-1: Isometric Strength test as recommended by Chaffin et al. (1978)

#### 4.2 Experimental Design

The presented design of the experiment is based on previously established procedures that have been previously conducted in the computational Neuroergonomics laboratory presented by Aljuaid (2016).

The experiment consisted of two tasks: 1) maximum voluntary contraction (MVC), and 2) the isometric force exertion task. In MVC, the participants were asked to apply the maximum force for three seconds for each of three trials separated by 30-second rest periods between each trial. Then, a five-minute rest was provided to avoid muscle fatigue. In the isometric arm flexion task, the participant was asked to exert a force that matched one of five predefined exertion levels, as follows: 1) extremely light, 2) light, 3) somewhat hard, 4) hard, and 5) extremely hard. The utilized



force levels were selected from a 6–20 scale of perceived exertion proposed by Borg (1982) (Appendix D). The participants were asked to maintain steady-state exertion for three seconds for three trials separated by 120-second rest periods between each trial. After each trial, the participants were asked to subjectively assess the level of physical comfort that corresponded to the exerted force [N] using an 11-point scale of perceived physical comfort scale (Appendix E). The order of force exertion levels was determined randomly to prevent potential learning effects. The whole arm experiment for each participant with EEG preparation time lasts for approximately 62 minutes, unless participants asked for more rest. The detailed timeline for the designed experimental is provided in (Figure 4-2).

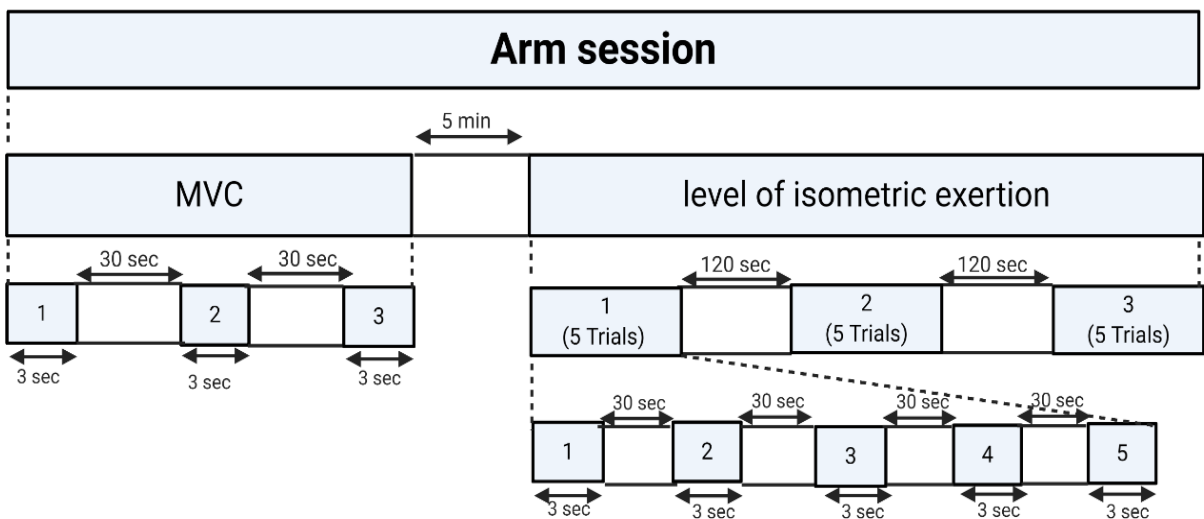


Figure 4-2: The study protocol for arm force exertion

### 4.3 Research Variables

The independent variables of the experiment included MVC, and levels of perceived exertion. While the dependent variables include graph theory measures, exerted force, and rate of perceived physical comfort (RPPC). A sample of the data collection process is shown in (Appendix F).

<b>Independent variables</b>	Maximum voluntary contraction (MVC)		Level of perceived exertion
<b>Dependent variables</b>	Graph theory measures	Exerted force	RPPC

### 4.4 Experiment Procedure

Participants visited the computational neuroergonomics lab in two occasions, for preparation session and for experimental session (Figure 4-3).

The preparation session is crucial to ensure that the assigned participant met all the eligibility criteria mentioned in the flyer (Appendix G). If the participants met all the criteria, we measure the participant's head circumference using a flexible tape measure to prepare a correctly fitted cap size. The available cap sizes include 54, 56, and 58 cm. A detailed description for the experimental session is provided in section (4.6).

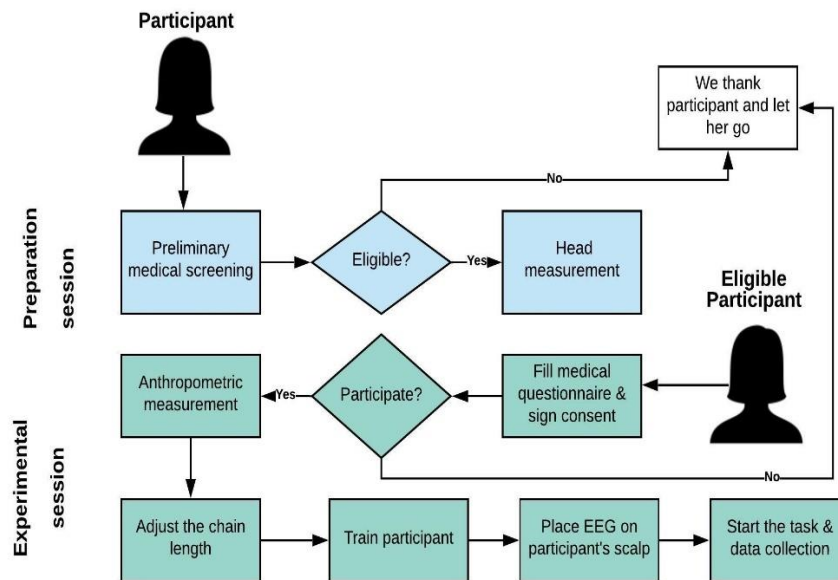


Figure 4-3: Experiment Procedure

## 4.5 Apparatus and Instrument

### 4.5.1 Electroencephalogram

A CGX-Mobile-64 EEG device was used for recording brain activity. The EEG headset is wireless, motion resistant, and easy to use. The system is a wet headset that requires conductive gel to connect the skin of the scalp to the electrodes with Ag/AgCl active electrodes positioned according to the 10–10 international montage system. (Figure 4-4). The EEG signals were acquired using Cognionics acquisition software (CGX software, 2020). A superVisc electrolyte gel was used for active electrodes and connecting impedance was kept below 10 k $\Omega$ . To avoid anti-aliasing, physiological signals were sampled at 500 Hz with a bandpass filter of 0.1–100 Hz.



Figure 4-4:EEG Mobile-64 headset

#### 4.5.2 Jackson Strength Evaluation System

The Jackson Strength Evaluation system is consisting of a wooden platform, a handle, a chain, a hand dynamometer, and a control unit (Figure 4-5). Two types of handles are attached to the device. The short handle for leg strength test, whereas the long handlebar for arm and torso strength test (Chaffin et al., 1978; Mital and Kumar, 1998).



Figure 4-5: Jackson Strength Evaluation System

#### 4.5.3 TORBAL Force Gauge

TORBAL FC5k series force measurement device is be attached to the handle for measuring the exerted force. The device was set to measure force in newton (N) unit. For MVC measurements, the TORBAL FC device was set to multi-peak mode. For exertion force measurements, the TORBAL FC device is set to a standard mode.

#### 4.5.4 Wireless Trigger

A wireless trigger marks the starting and endpoint for each trial using a parallel port. Participants listen to the experiment instructions through E-prime software (E-prime software, 2020), which is the stimulus generation method.

### 4.6 Experimental Setup and Paradigm

For experimental setup, we have followed the recommended procedure addressed in previous studies presented in (Light et al., 2010; Heisz and McIntosh, 2013).

#### **Before the participant arrives, the following were prepared:**

Place all electrodes on the cap. It takes 35-40 minutes to place 64 electrodes on the cap.

Set up the TORBAL force gauge.

Test the stimulus generation software (E-prime software) and ensure that the trigger is sending markers.

Set up the EEG acquisition software for recording.

Fill some syringes with conductive gel.

Prepare consent form, medical screening form, and data collection sheet.

Prepare the cotton swabs, alcohol, tissues, hairbrush (disinfected hard-bristle comb), and tape measurement.

Prepares the supplies for participants to wash their hair after the experiment (i.e., large sink, shampoo, and paper towels).

**When the participant arrives, we followed the following procedures:**

Participants fill a medical screening questionnaire form (Appendix H). If any participant failed to meet the eligibility criteria, a participant would discontinue.

All Participants received a written informed consent which was approved by the Institutional Review Board (IRB) at the University of Central Florida (UCF) (Appendix I). Participants read the informed consent and decide whether they will participate in the experiment or not. If the participant decided to participate in the experiment, we begin to explain the task and demonstrate all the experimental procedures.

Participants received detailed written instruction with enough time to read (Appendix C).

The EEG device was introduced to the participants.

Anthropometric measurements were collected (Appendix J), and the Jackson chain height was adjusted.

Participants were trained to perform the task correctly.

## **Scalp and EEG preparation**

Manual abrasion participants' scalp was conducted with a hard-bristle comb for removing dead skin. Participants were asked to wash their hair without using additives such as hair styling products or conditioners to avoid greasing layer, which is previously mentioned in the experiment flyer (Appendix G).

Measure the distance between the participants' nasion and inion to ensure that Cz electrode is placed at the center of the head. Then measure nasion to Cz, to ensure that the distance is half the distance from nasion to inion.

Mount the cap on the participant's head and tighten the cap with the chinstrap.

Turn on the EEG device and check the wireless connection.

Use a cotton swab with isopropyl alcohol to clean the skin for each electrode opening in the cap.

A second manual abrasion is made before applying the conducting gel using the blunt syringe nose. This is done by gently pushing the participant's hair through the electrode opening to ensure complete visibility of scalp skin.

Fill the electrode cap opening by injecting the superVisc electrolyte gel using a small syringe. Start to fill the reference and ground electrodes.

To lower the electrode impedance, apply more gel and twist the syringe tip on the scalp. This will increase the connectivity between the scalp and electrodes. Applying too much gel may create a bridge between the signals of neighboring electrodes.

Ensure that all electrodes are connected with low impedance.

### **Before collecting the data**

Participants were asked to perform some blinking, head, turning, neck movement, head movement, chowing, and jaw clenching to see the influence of movement on the EEG data quality.

Participants were kindly asked to avoid unnecessary movement and to maintain a stable body position to minimize artifacts during the task (i.e., to collect as much as possible clean data).

Start recording and save the file.

### **During data collection**

Ensure that participants are performing the task correctly.

Ensure that participants are not blinking too much.

Ask participants if they need more break time, water, or snacks.

Ensure that all electrode impedances are low.

After collecting the data

Carefully remove the EEG cap from the participant's head.

Participants were given receive shampoo and paper towels for hair cleaning.

We thank participants and give each a gift card.



We start cleaning the device by first removing all electrodes from the cap then soak the electrodes in warm distilled water for 10 minutes. A toothbrush and alcohol pads were used to remove any excess gel from electrodes. Then electrodes rinsed with distilled water.

We clean the elastic cap by rinsing it with alcohol and water, then lay it to air dry.

#### 4.7 Experiment Environment

This study was conducted in a temperature-controlled laboratory and sound-attenuated environment. This environment helped participants to concentrate on task performance and minimized the non-physiological artifacts as possible (Reis et al., 2014; Islam et al., 2016). To minimize the risk of selection bias, all participants were randomly selected (i.e., selection bias). The participants had no previous knowledge regarding the study purpose (to reduce performance bias) and hypothesized outcomes (to reduce detection bias). All incomplete data outcomes (i.e., reporting bias) and excluded data (i.e., attention bias) were recorded (Higgins et al., 2019).

#### 4.8 Anthropometric Measurements

Anthropometric measurements were collected from all participants, including body weight, shoulder height, hip height, knee height, arm length, knuckle height, and body height (Appendix J).

#### 4.9 Participants Selection and Ethical Code

Twelve healthy adult female participants (mean age  $28 \pm 6$  y) performed an arm isometric exertion task. All participants met the experimental requirements, including absence of history of

cardiovascular problems, neurological disorders, fatigue-related disorders, chronic physical, musculoskeletal disease, back pain, injuries, or mental illness. Pregnant female participants were excluded. Participants were instructed not to take any medication, coffee, or alcohol for a minimum of 24 hours before the experiment, and no exercise for the past 48 hours. All experiments were carried out with the approval of the Institutional Review Board at the University of Central Florida (STUDY00000535) (Appendix I). Written informed consent was obtained from each participant after the explanation of the experimental protocol. To protect the privacy of the participants, and to maintain the ethical standards, we ensured (1) concealment participants' names; (2) confidentiality of anthropometric data; and (3) secure data storage.

Perception is different between males and females (Karwowski, 1991; Wright and Saylor, 1991). A significant difference in muscular strength was observed by gender differences (Chaffin et al., 1978; Delorme et al., 2007). Furthermore, different brain patterns were observed due to gender differences (Dimitrakopoulos et al., 2018; Zhang et al., 2018). A structural brain difference was found between males and females. Thus, gender is a crucial biological variable in brain research (Cahill, 2006; Xin et al., 2019).

#### 4.10 Methodological pipeline

An overview of the methodological pipeline is shown in (Figure 4-6). First, EEG data were collected for all participants using 64 EEG channel locations. Then the collected EEG time-series signals underwent preprocessing processes (shown in detail in section 4.12.1). Fast Fourier Transform (FFT) algorithm using Hanning window was used to calculate cross spectra for each frequency band for each participant at each exertion level for the cleaned and filtered EEG epochs.

Using eLORETA transformation matrix, cross spectra of each subject and for each frequency band were then transformed to eLORETA files (Pascual-Marqui et al., 1994; Pascual-Marqui, 2007) and reconstructed the EEG current source density.

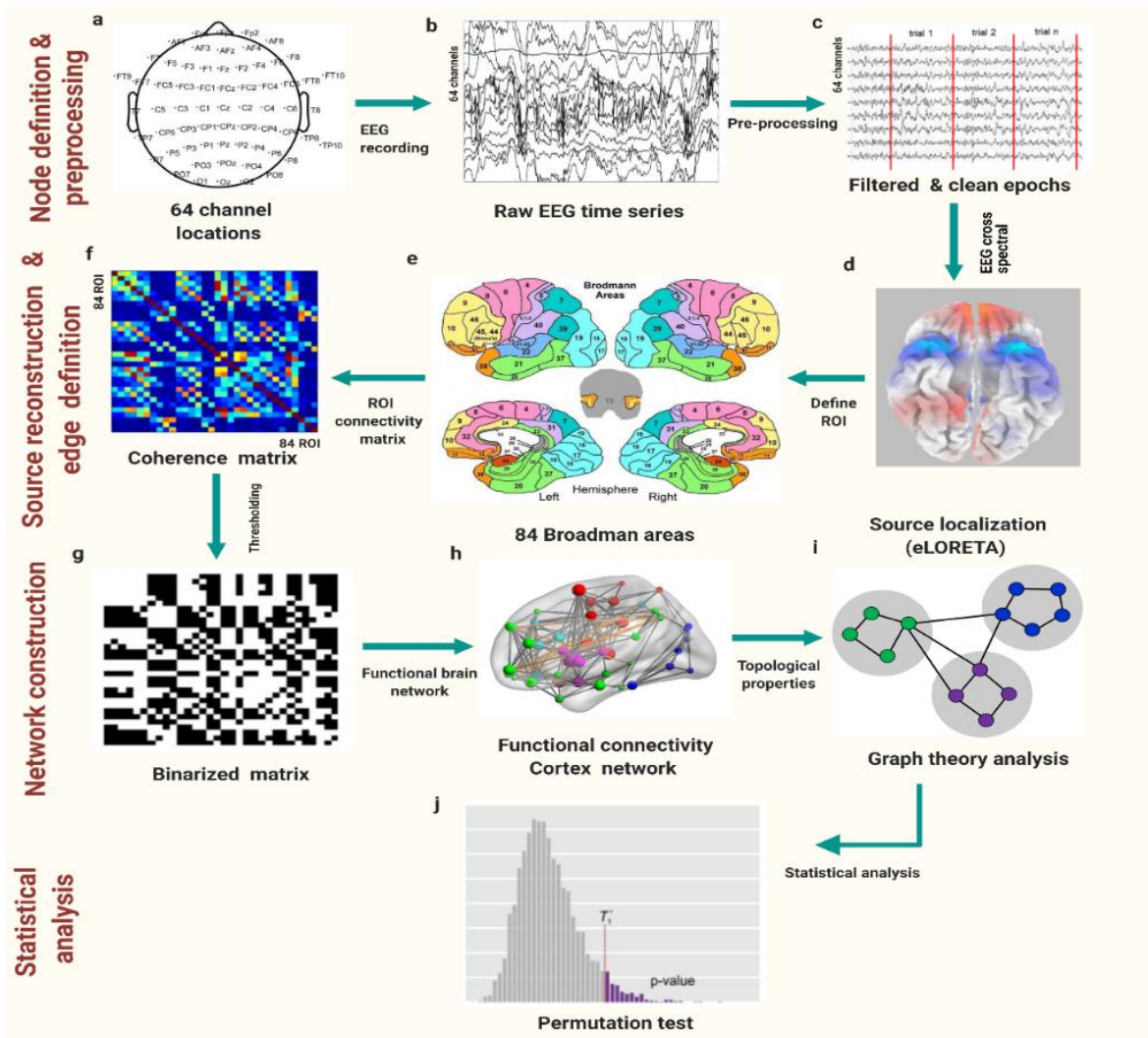


Figure 4-6: Methodological pipeline

(a) Collect the EEG data using 64 channel locations. (b) Record the EEG time series. (c) Filter, clean and epoch the EEG time-series signals. (d) Reconstruct the EEG source from the EEG cross spectral in eLORETA software. (e) Parcellate the cortex according to the Brodmann area (BA) atlas. (f) Construct the adjacent matrix after estimating the connectivity patterns. (g) Binarize the

network using a threshold value. (h) Construct the functional connectivity patterns between Regions of interest (ROI). (i) Calculate the graph theory measures to compute the local and global network properties. (j) Apply a non-parametric permutation tests to assess brain topological changes.

The solution space estimated by source localization was then parcellated into brain anatomical structures according to the Brodmann area (BA) atlas, which was used to define 84 BA regions of interest (i.e., graph nodes) for brain network construction. Functional connectivity was estimated across all pairs of brain regions (i.e., network edges). This step yielded an adjacent matrix (size  $84 \times 84$ ) for each participant for each frequency band at each exertion level that was binarized to remove weak connections (van den Heuvel et al., 2017). Graph theory measures were then used to compute the local and global network properties. Finally, statistical analysis based on non-parametric permutation tests was used to assess brain topological changes in the studied experimental conditions.

#### 4.11 EEG Acquisition

EEGs signals were recorded using a CGX-64 Mobile gel-based system electrode cap with Ag/AgCl active electrodes positioned according to the 10–10 international montage system. The EEG signals were acquired using the Cognionics acquisition software CGX (CGX software, 2020). A superVisc electrolyte gel was used for active electrodes and connecting impedance was kept below 10 k $\Omega$  or less. To avoid anti-aliasing, the physiological signals were sampled at 500 Hz with a bandpass filter of 0.1-100 Hz. The reference electrode is located at the left linked mastoid and the ground at the right linked mastoid.

#### 4.12 EEG Data Preprocessing

The data processing workflow is summarized in (Figure 4-7). The data processing workflow that consisted of ten stages including data curation, cleaning, artifact removal, dipole localization, feature extraction, source reconstruction, defining the regions of interest (ROI), functional connectivity estimation, graph theory calculations and statistical analysis.

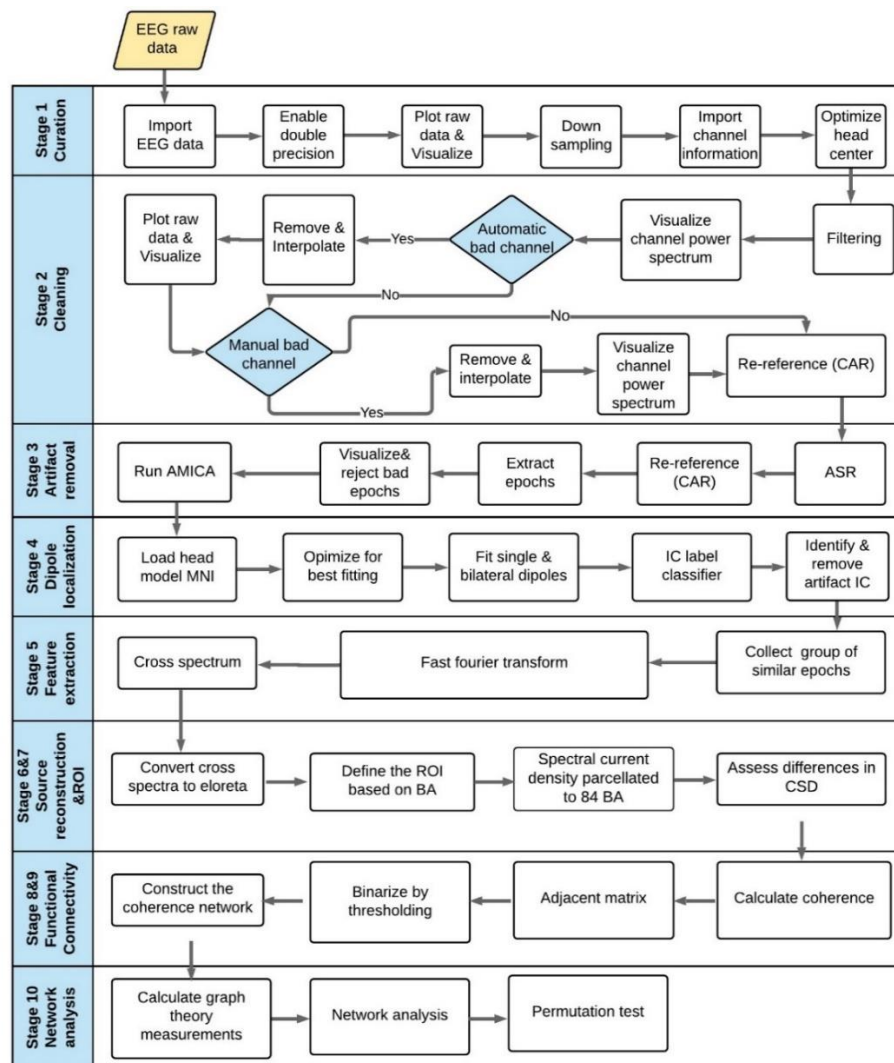


Figure 4-7: The data processing workflow

(artifact substance reconstruction [ASR], adaptive mixture independent component analysis [AMICA], Brodmann areas [BA], current source density [CSD], exact Low Resolution Brain Electromagnetic Tomography [eLORETA], independent component [IC], region of interest [ROI].

#### 4.12.1 EEG Data Pre-Processing

The first four stages were the EEG pre-processing stages. Since raw EEG data is contaminated with artifacts, filtering, denoising, and cleaning are crucial for enhancing the signal to noise ratio (Urigüen and Zapiroain, 2015). EEG pre-processing was performed using EEGLAB (version 14.1.2b; Delorme and Makeig, 2004), an open source toolbox run on Matlab R2019b software (MathWorks, Natick, MA).

**Curation (stage 1):** The raw EEG data was imported ensuring a double-precision option (Shamlo et al., 2015). The data were visually inspected and the sample was reduced from 500 Hz to 250 Hz for easier storage and faster processing. The Montreal Neurological Institute (MNI) coordinates were used for defining the channels location and head center was optimized to fit the head sphere.

**Cleaning (stage 2):** EEG signals were filtered through a 1–50 HZ zero-phase Hamming window known as a finite impulse response bandpass filter (Christiano and Fitzgerald, 2003; Garcés Correa et al., 2007; Winkler et al., 2015; Maess et al., 2016). The spectra for the 64 channels were plotted and manually visualized. Then, an automatic bad channel rejection using the EEGLAB toolbox known as `clean_raw` data (Chang et al., 2018) was applied. This automatic toolbox can detect and separate noisy channels and low-frequency drifts. Then, interpolation was applied after detecting and removing bad channels to alleviate the bias resulting from the unequal number of electrodes between the right and left hemispheres. An offline common average reference (CAR) was applied to reset the data to a zero-sum across channels. Applying all the procedures in stage 2 helped to

obtain more clean data, but most artifacts still exist. Therefore, artifact removal methods are required (stage 3).

**Artifact removal (stage 3):** For artifact removal and correction methods, an artifact substance reconstruction method that subspaces unusually large-amplitude data was first applied. This method does not consider eye-blinking or small-amplitude contamination (Mullen et al., 2013, 2015). Consequently, an independent-component analysis (ICA) decomposition method based on the blind source separation technique was used. Before applying ICA, the continuous EEG data was epoched based on the task structure. For each participant, there were three MVCs and five isometric exertion levels that were repeated three times, resulting in a total of 18 epochs. For 12 participants, there were a total of 216 epochs. An adaptive mixture ICA (AMICA) algorithm was used to decompose EEG signals into independent components (ICs) (Palmer et al., 2011). AMICA proved to outperform all other ICA approaches (Delorme et al., 2012; Hsu et al., 2018). An automated classifier known as IC Label was used to distinguish between the brain and non-brain sources (Pion-Tonachini et al., 2019a, 2019b).

**Dipole localization (Stage 4):** Before rejecting any IC, sources were localized to the separated IC components. An equivalent current dipole and bilateral model were computed for each IC using a boundary element head model (BEM) (Oostendorp and van Oosterom, 1989; Oostenveld and Oostendorp, 2002) based on MNI coordinate (Montreal Neurological Institute). DIPFIT version 3, an EEGLab plugin (Oostenveld and Oostendorp, 2002), was used for calculating the dipole localization. A nonlinear optimization technique using the MATLAB optimizer toolbox was used to locate the best position for a single dipole or bilateral dipole (Piazza et al., 2016)(Figure 4-8).

Residual variances, which measures the variance between original scalp recorded signal locations and models, were kept below 40%. Components that appear to be eye movements and blinking, electrocardiography, motion artifacts, line, and noise channel were manually removed after localizing the dipole. Following Nguyen et al. (2019) protocol, the entire experiment would be rejected if the number of rejected ICs was more than 50% of the total IC. An example of the outcome from IC label classifier is provided in (Figure 4-9).

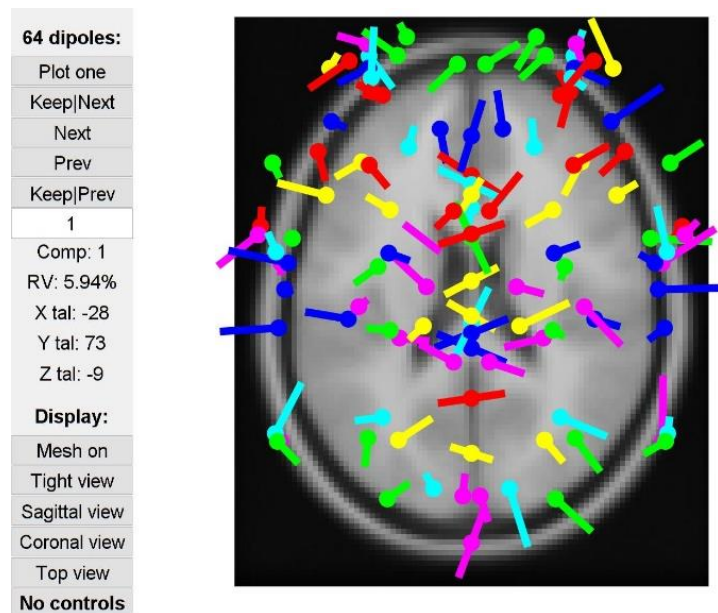


Figure 4-8: Dipoles for 64 electrodes

#### 4.12.2 Data processing

**Feature extraction (stage 5):** EEG cross spectra was extracted based on Fast Fourier Transform using Hanning windows with 10% onset. The cross spectra were averaged across the 50% overlapping windows considering two frequency bands (alpha = 8–13 Hz and beta = 13–30 Hz)



for each participant, using eLORETA software (freely available at <http://www.uzh.ch/keyinst/loreta.htm>).

**Source reconstruction (Stage 6):** Using the eLORETA transformation matrix, cross spectra for each participant and for each frequency band were transformed to eLORETA files. This resulted in three-dimensional intracerebral CSD of the electrical neuronal generators for each participant (Pascual-Marqui et al., 2002). The eLORETA is a genuine inverse solution with exact zero error localization in the presence of measurement and structured biological noise (Pascual-Marqui et al., 1994; Pascual-Marqui, 2002a, 2007).

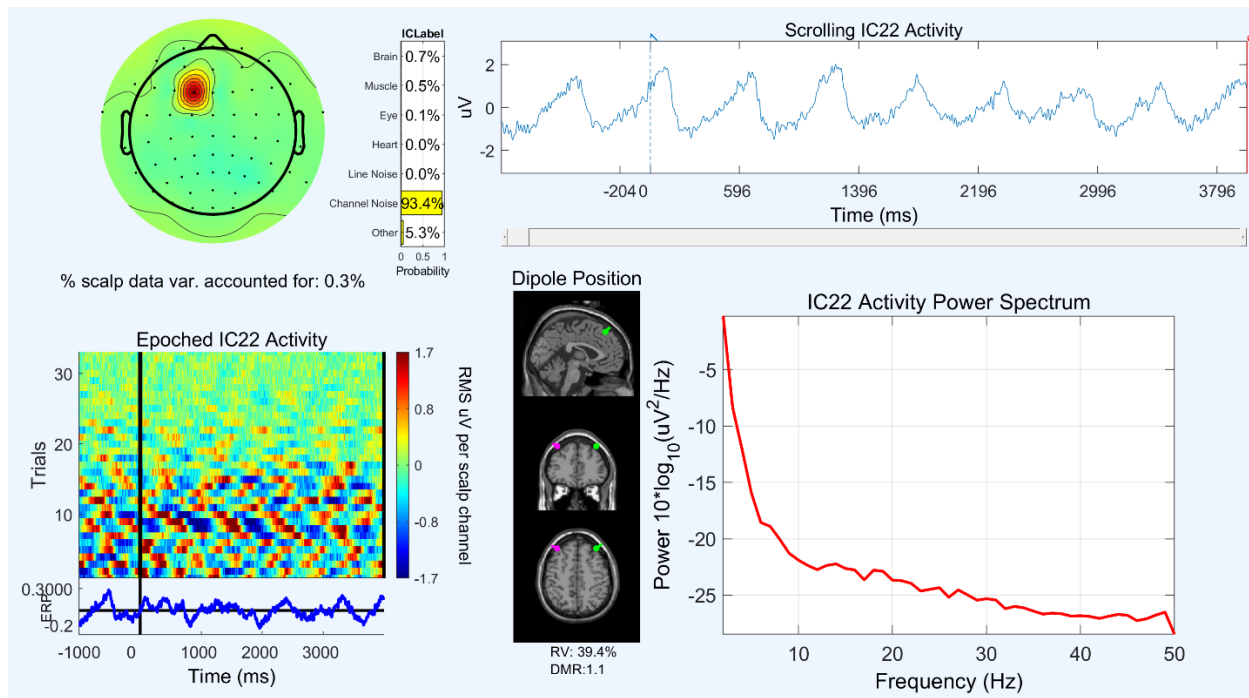


Figure 4-9: IC label classifier for a single participant for a single channel

The software uses a realistic head model (Fuchs et al., 2002) based on the Montreal Neurologic Institute (MNI) 152 template (Mazziotta et al., 2001), with the three-dimensional solution space restricted to the cortical gray matter and hippocampi, as determined by the probabilistic Talairach atlas (Lancaster et al., 2000). The software helps solve the inverse solution by parcellating the spectral current density into 6239 voxels of 5-mm<sup>3</sup> spatial resolution. eLORETA has been used extensively and was validated in several studies using real human data (Canuet et al., 2011, 2012; Olbrich et al., 2013; Di Lorenzo et al., 2015; Hata et al., 2016; Shreekantiah Umesh et al., 2016; Lanzone et al., 2020). eLORETA helps determine the distribution of current density across voxels in the brain (Pascual-Marqui et al., 2011a) and was demonstrated to be more robust and accurate than other source-localization methods (Jatoi et al., 2014; Dai et al., 2017).

**Regions of interests (stage 7):** A voxel-wise approach was used to define the regions of interest (ROI) using a single voxel method in which the ROIs were centered at the given voxel coordinates including all cortical gray matter voxels within 15 mm distance from the center. Anatomical labels corresponding to Brodmann areas (BA) provided by eLORETA software package are based on the Talairach Daemon (<http://www.talairach.org/>) (Appendix K) (Brett et al., 2002). We selected the whole brain 84 ROI ( 42 for each hemisphere) provided by eLORETA software. This step helped in converting the EEG from sensor levels to source level (Figure 4-10). Each brain regions represents the network node.

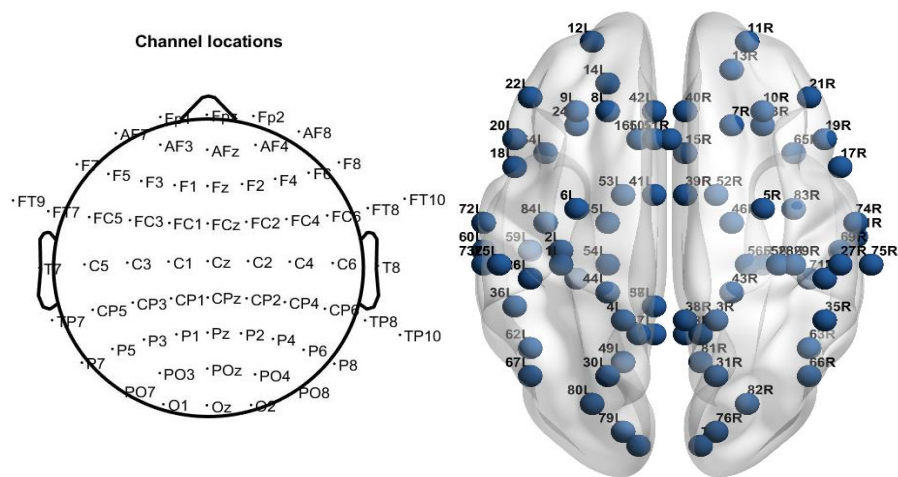


Figure 4-10: 2D channel location plot (i.e., scalp level) converted to 84 ROI (i.e., source level)

**Source Functional connectivity (stage 8):** EEG source-based functional connectivity matrices were computed using eLORETA software using the coherence method to estimate the patterns of statistical dependencies among 84 ROI for two EEG frequency bands (i.e., alpha and beta) for each participant. The  $84 \times 84$  coherence connectivity matrices were converted to a binary matrix using a set of range of sparsity thresholds to maintain strong connections (van den Heuvel et al., 2017). To prevent the formation of a disconnected network and maintain network reachability, wide sparsity values in the range of 5–50% with steps of 5% were used.

**Network analysis (stage 9):** Global and local graph measures were computed for all exertion level for two frequency bands, then we assessed the network properties using nonparametric permutation-based statistical method (Nichols and Holmes, 2002b).

#### 4.13 Estimation of Functional Connectivity of EEG Cortical Sources

Coherence measures the degree of association between two different brain regions. It measures the phase synchrony of EEG signals recorded between pairs of electrodes in the frequency domain as defined by Walter (1968). Mathematically, coherence is defined as the absolute value of the cross spectrum of two signals normalized by spectral power of each of the signals (Nunez et al., 1997), as shown in equation (8). Where  $f$  is the frequency,  $W_x$  is the cross power spectral density of  $x$ ,  $W_y$  is the cross power spectral density of  $y$ , and  $W_{xy}$  is the cross power spectrum density of the two signals.

$$C_{xy}(f) = \frac{|W_{xy}|^2(f)}{W_x(f) * W_y(f)} \quad (8)$$

Coherence is one of the widely used methods to study the functional brain network (Andrew and Pfurtscheller, 1999; Canteroa et al., 1999; Nolte et al., 2004; Sauseng et al., 2005; Comani et al., 2013; Bowyer, 2016; Storti et al., 2016) and represents a reliable method for evaluating the physiological abnormalities (Adler et al., 2003; Wang et al., 2014). In this study, the coherence was computed for 84 ROIs using eLORETA connectivity algorithm (Pascual-Marqui et al., 2011b) for each subject and each EEG frequency band (alpha and beta).

#### 4.14 Graph Analysis and Measures Computation

We calculated the most common global and local graph measures for each exertion level for each frequency band across the network densities, ranging from 0.1 to 0.5, with a step size of 0.05. Global graph measures included average clustering coefficient, characteristic path length, global efficiency, small-worldness (SW), local efficiency, and modularity. The clustering coefficient is a

measure of the degree to which nodes in a graph tend to cluster together. The characteristic path length (PL) is the average of the shortest route between all pairs of nodes in the network and measures the network ability to transfer serial information (Brier et al., 2014). The inverse of PL is global efficiency, which measures the network's ability to transfer parallel information (Berlot et al., 2016). SW is the ratio of the clustering coefficient to PL. An SW index greater than 1 indicates small-world organization of the brain network (Watts and Strogatz, 1998). Local efficiency measures the efficiency of information transfer limited to neighboring nodes. Modularity is the ability of a graph to be subdivided into modules that are maximally connected within a module and sparsely connected between modules (Newman, 2006).

Graph-theoretical local measures provide knowledge of individual nodes' properties. We assessed the importance of various ROIs within the brain network by evaluating nodal properties, including degree centrality, betweenness centrality, and nodal efficiency. Degree centrality counts the number of edges connecting a node with all other nodes. The greater the degree, the more important the node is in the network. Betweenness centrality quantifies the number of times that a node acts as a bridge along the shortest path between two other nodes. Nodal efficiency measures the ability of information propagation between a node and the remaining nodes in the network (Wang et al., 2010).

## **CHAPTER FIVE**

### **RESULTS AND ANALYSIS**

This chapter includes the statistical analysis methods and the results. We started the chapter with the descriptive statistics regarding the anthropometric measures, force measures, and comfort scales. Then we estimated the maximum current source density for each exertion level for each frequency band. We calculated the functional connectivity between the pairs of brain regions and computed the coherence matrices. Finally, we computed the graph theory global and local measures.

#### 5.1 Statistical Analysis

##### 5.1.1 Isometric Force

To assess the effect of predefined levels of physical exertion on generated arm forces, analysis of variance (ANOVA) was used. Tukey's post hoc multiple-comparison test was also performed to identify significant differences in exerted forces.

##### 5.1.2 Rate of Perceived Physical Comfort

ANOVA was also used to assess the effect of predefined levels of physical exertion on the assessed RPPC scores. Tukey's post hoc multiple-comparison test was also performed to identify significant differences in the rate of perceived physical comfort.

### 5.1.3 eLORETA Source Localization

To evaluate the difference in CSD in cortical source-localization between exertion levels in each frequency band, we applied voxel-by-voxel independent sample F-ratio tests, based on eLORETA log-transformed CSD power. To control Type 1 errors, we applied a statistical non-parametric permutation test with 5000 data randomizations to create the permutation distribution and to determine the critical threshold at significance value = 0.05 (Holmes et al., 1996; Nichols and Holmes, 2002b). The critical threshold was then entered to “maximal-statistic” to determine the maximum activation region at the 95th percentile under the null hypothesis (Olbrich et al., 2013). The use of the SnPM has been implemented in many studies due to the advantage of the multiple test correction and controlling type 1 error (Hata et al., 2016; Kitaura et al., 2017). We assessed the difference of the source localization of cortical oscillations between the exertion levels in alpha and beta band using a voxel-by-voxel independent F-ratio-tests, with threshold set at 5% significance level. A total of 5000 data randomizations were used to determine the critical probability threshold values for the actually observed log F-ratio values with correction for multiple comparisons across all voxels and all frequencies, with no need to rely on Gaussianity.

### 5.1.4 Source Functional Connectivity Estimations

For the functional connectivity analysis, we performed a method that applies a single voxel at the centroid of each BA using eLORETA software (Canuet et al., 2012; Hata et al., 2016; Zinn et al., 2016; Ponomareva et al., 2020). A connectivity analysis between pairs of 84 ROIs in two frequency bands in all physical exertion levels was conducted using independent sample t-tests that were

corrected for multiple comparisons using a non-parametric randomization method based on the ‘maximal-statistic’. We applied the same permutation test with 5000 randomizations to identify the critical probability thresholds at significant levels and correct for Type 1 errors.

#### 5.1.5 Brain Network Analysis

For graph theory measures, we applied a non-parametric permutation test (p-values were calculated from 30,000 permutations of group labels) (Nichols and Holmes, 2002a), to examine the topological properties between predefined force exertion levels. Briefly, for each network measure, we first calculated the between-group difference in the mean values. An empirical distribution of the difference was then obtained by randomly reallocating all values into two predefined force exertion levels and recalculating the mean differences between the two randomized groups (30,000 permutations). The 95<sup>th</sup>-percentile points of the empirical distribution were used as critical values in a one-tailed test of whether the observed group differences could occur by chance. For comparisons of nodal measures, Bonferroni correction procedures were used to correct for multiple comparisons (Sture Holm, 1979).

#### 5.1.6 Correlation Analysis

To investigate the interrelationships between the exerted forces and RPPC with global graph theory measures, Spearman correlation coefficients were calculated. Only those graph theoretical measures that showed significance in the correlation analysis were included.



## 5.2 Results

### 5.2.1 Anthropometric Characteristics

displays the summary of anthropometric measurements and static arm flexion strength for all participants.

Table 5-1 displays the summary of anthropometric measurements and static arm flexion strength for all participants.

Table 5-1: Descriptive statistics of anthropometric measurements and MVC for all subjects

<b>Variable</b>	<b>Mean</b>	<b>SD</b>
Age (year)	27.4	6.20
Body Weight (kg)	60.20	11.00
Shoulder Height (cm)	135.84	7.50
Hip Height (cm)	98.04	6.07
Knee Height (cm)	51.65	2.84
Arm Height (cm)	106.26	5.90
Knuckle Height (cm)	73.98	6.28
Body Height (cm)	163.00	7.26
Maximum voluntary contraction (arm flexion, N)	115.00	47.60

### 5.2.2 Isometric Force

Descriptive statistics across all subjects (N=12) for isometric forces exerted at various levels of predefined levels of physical exertion are displayed in (Table 5-2).

Table 5-2: Isometric arm exertion forces means, standard deviation (Sd), range and percentage of maximum voluntary contraction (MVC) at different levels of physical exertion levels

Physical exertion level	Isometric arm exertion force (N)						
	Mean	Sd	Range		%MVC		
			Minimum	Maximum	Mean	Minimum	Maximum
Extremely hard	67.35	35.25	2	18	56.36	3.34	113.8
hard	41.83	18.9	3	28	35.00	5.00	68.60
Somewhat hard	34.58	16.7	3	66	28.9	2.51	55.23
Light	13.61	6.76	6	82	11.39	2.51	23.43
Extremely light	8.04	5.32	4	136	4.455	1.67	15.06

Table 5-3 depicts the results of ANOVA for the effect of exertion level on the generated arm forces (N). Table 4 provides the results of Tukey pairwise comparison of forces for different levels of exertion at 95% confidence level.

Table 5-3: ANOVA table for the effect of exertion level on the exerted arm forces (N)

Source	DF	Adj SS	Adj MS	F-Value	P-Value
Participant	11	11374	1034.0	4.05	0.00
Exertion level	4	27108	6777.08	26.54	0.00
Error	44	11236	255.4		
Total	59	49718			

Pairwise comparison among exertion levels were performed using the post hoc Tukey test and adjusted p-values were computed (Table 5-4). Results revealed no significant difference between ‘hard’ versus ‘somewhat hard’, or ‘light’ versus ‘extremely light’ (Figure 5-1) (Table 5-4 and Table 5-5).

Table 5-4: Tukey simultaneous Tests for differences of means for forces exerted at different physical exertion levels.

Difference of Exertion levels	Difference of mean	SE of Differences	Simultaneous 95% CI	T-Value	Adjusted P-value
EL - EH	-59.31	6.52	(-77.85, -40.76)	-9.09	0.000
H - EH	-25.52	6.52	(-44.06, -6.97)	-3.91	0.003
L - EH	-53.73	6.52	(-72.28, -35.19)	-8.24	0.000
SWH - EH	-32.77	6.52	(-51.32, -14.23)	-5.02	0.000
H - EL	33.79	6.52	(15.25, 52.34)	5.18	0.000
L - EL	5.58	6.52	(-12.97, 24.12)	0.85	NS
SWH - EL	26.53	6.52	(7.99, 45.08)	4.07	0.002
L - H	-28.22	6.52	(-46.76, -9.67)	-4.33	0.001
SWH - H	-7.26	6.52	(-25.80, 11.29)	-1.11	NS
SWH - L	20.96	6.52	(2.41, 39.50)	3.21	0.020

Table 5-5: Summary statistics for arm forces exerted at different levels of physical exertion (Tukey pairwise comparison at 95% confidence level)

Exertion level	Mean force (N)	Grouping
Extremely hard	67.4	<b>A</b>
Hard	41.83	<b>B</b>
Somewhat hard	34.57	<b>B</b>
Light	13.62	<b>C</b>
Extremely light	8.04	<b>C</b>

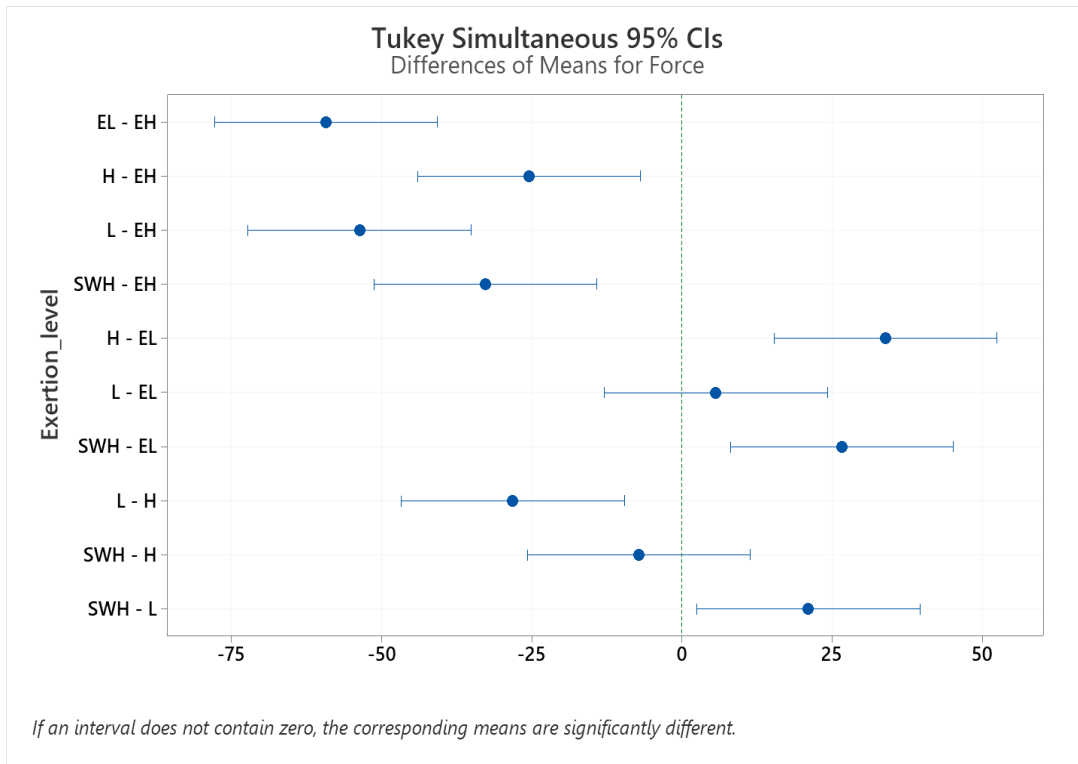


Figure 5-1: pairwise comparison between isometric forces at different levels of physical exertion to extremely light [EL], light[L], somewhat hard [SWH], hard [H], and extremely hard [EH]

### 5.2.3 Rate of Perceived Physical Comfort

Descriptive statistics across all subjects (N=12) for RPPC scores at predefined levels of physical exertion are shown in (Table 5-6).

Table 5-6: The mean and standard deviation for the rate of perceived physical comfort (RPPC) at each exertion level

<b>Exertion level</b>	<b>Mean of RPPC</b>	<b>Standard deviation of RPPC</b>
Extremely light	4.583	1.48
Light	5.375	1.63
Somewhat hard	5.729	1.68
Hard	7.750	2.11
Extremely hard	8.23	2.30

Table 5-7 shows the results of ANOVA for the effect of exertion level on the RPPC scores.

Table 5-7: ANOVA table for the effect of exertion level on RPPC scores

Source	Df	Adj SS	Adj MS	F-Value	P-value
Participants	11	61.71	5.60	7.56	0.000
Exertion levels	4	119.36	29.84	40.23	0.000
Errors	44	32.64	0.7417		
Total	59	213.71			

Table 5-8 provides the results of Tukey pairwise comparison of perceived comfort for various levels of exertion at the 95% confidence level. Results revealed no significant difference between the rating of perceived comfort between ‘hard’ and ‘extremely hard’ levels, between ‘somewhat hard’ and ‘hard’, and between ‘extremely light’ and ‘light’ levels (Figure 5-2)(Table 5-9).

Table 5-8: Tukey simultaneous Tests for differences of RPPC scores at different levels of physical exertion

Difference of Exertion levels	Difference of Means	SE of Difference	Simultaneous 95% CI	T-Value	Adjusted P-Value
EL – EH	3.646	0.352	(2.646, 4.645)	10.37	0.000
H – EH	0.792	0.352	(-0.208, 1.791)	2.25	0.180
L – EH	3.167	0.352	(2.167, 4.166)	9.01	0.000
SWH – EH	1.146	0.352	(0.146, 2.145)	3.26	0.017
H – EL	-2.854	0.352	(-3.854, -1.855)	-8.12	0.000
L – EL	-0.479	0.352	(-1.479, 0.520)	-1.36	0.654
SWH – EL	-2.500	0.352	(-3.499, -1.501)	-7.11	0.000
L – H	2.375	0.352	(1.376, 3.374)	6.75	0.000
SWH – H	0.354	0.352	(-0.645, 1.354)	1.01	0.851
SWH – L	-2.021	0.352	(-3.020, -1.021)	-5.75	0.000

Table 5-9: Summary statistics for RPPC scores at different levels of physical exertion (Tukey pairwise comparison at 95% confidence level)

Exertion level	Mean	Grouping
Extremely hard	4.583	A
Hard	5.375	A B
Somewhat hard	5.729	B
Light	7.750	C

Extremely light	8.23	C
-----------------	------	---

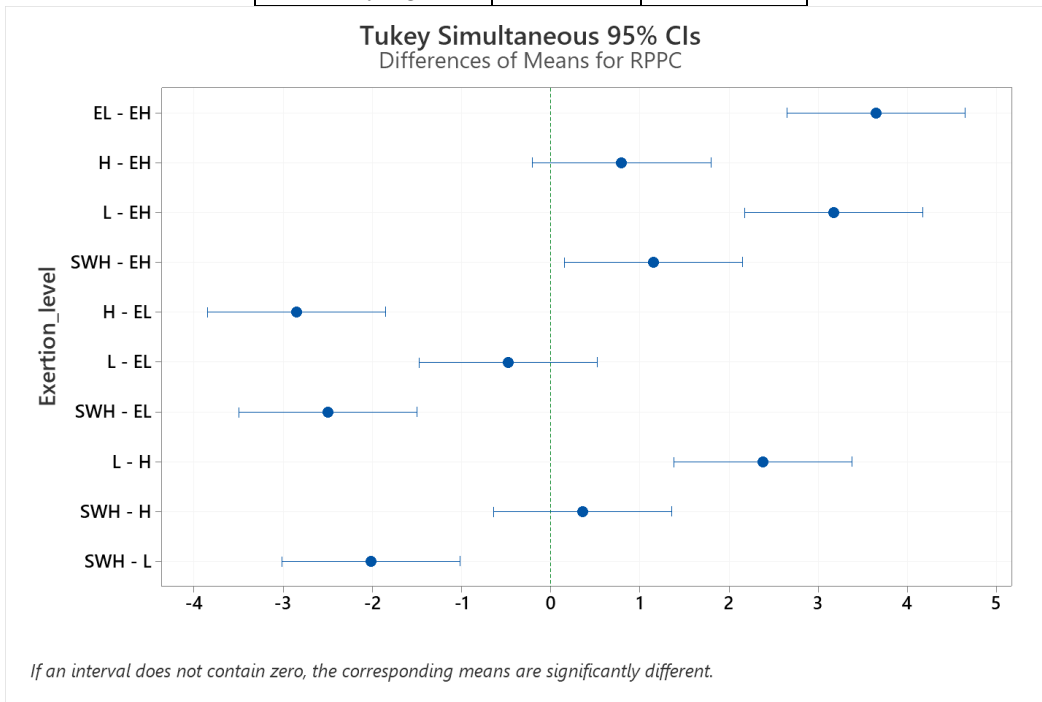


Figure 5-2: pairwise comparison between isometric forces at different levels of physical exertion to extremely light [EL], light[L], somewhat hard [SWH], hard [H], and extremely hard [EH]

#### 5.2.4 Correlation Analysis for the Exerted Force and RPPC

Correlation analysis revealed a significant negative correlation between the RPPC and exerted force ( $r = -0.963$ ;  $p < 0.009$ ) (Figure 5-3). Increasing force exertion correlated with decreasing RPPC score (Figure 5-3). The overall results of forces and RPPC scores at five exertion levels are illustrated in (Figure 5-4).

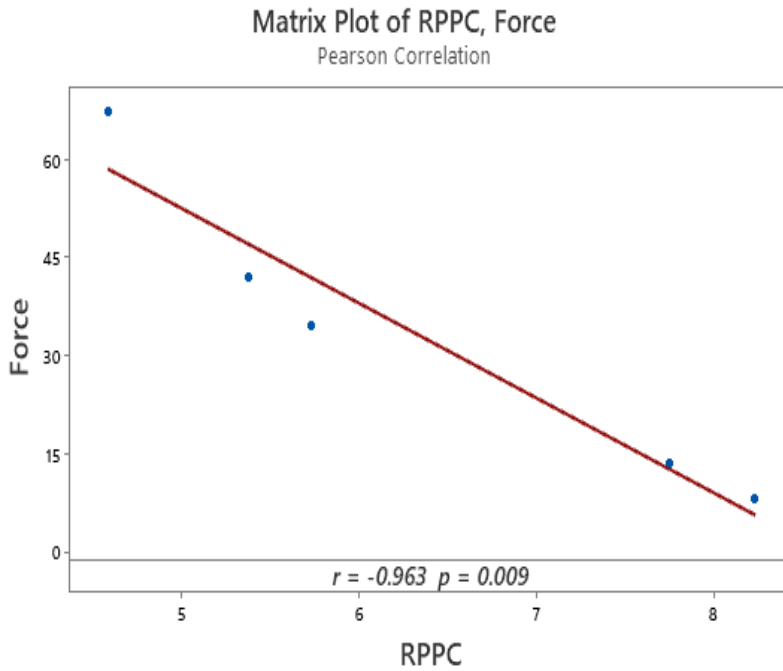


Figure 5-3: Correlation of RPPC and force exerted, (r: Spearman’s rank correlation coefficient, CI: confidence interval).

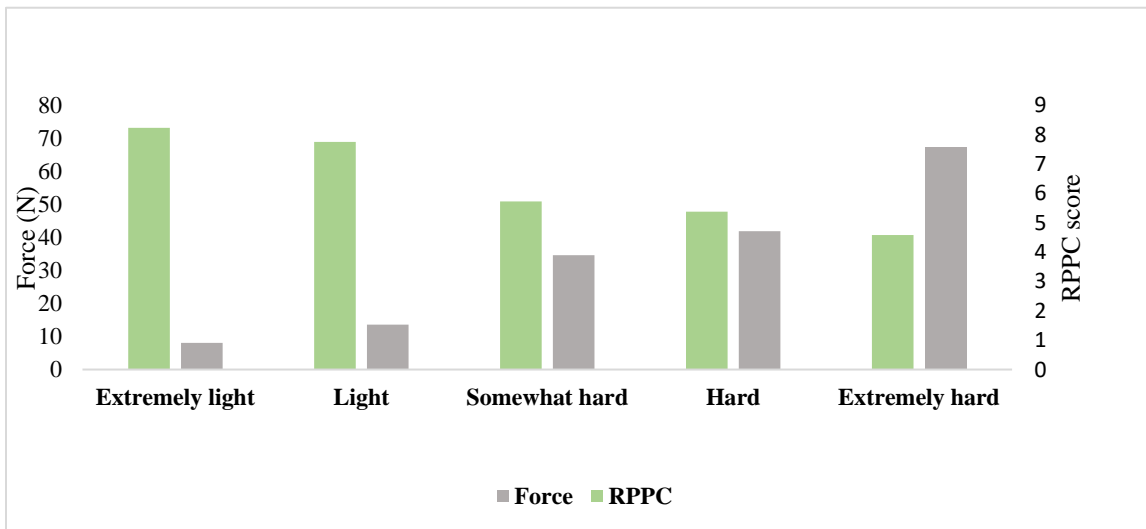


Figure 5-4: Arm forces and RPPC scores bar plot at different levels of physical exertion across all subjects (N=12)

## 5.2.5 Source Localization

### 5.2.5.1 eLORETA Source Localization

The average CSD for each exertion level for each frequency band for 12 female participants were computed (research question 1). For alpha band, the highest CSD was found in the middle frontal gyrus of the frontal lobe corresponding to BA 6 for the “extremely hard exertion” level only. However, for all other exertion levels, the highest CSD was found in the superior frontal gyrus of the frontal lobe, corresponding to BA 8 (Figure 5-5).

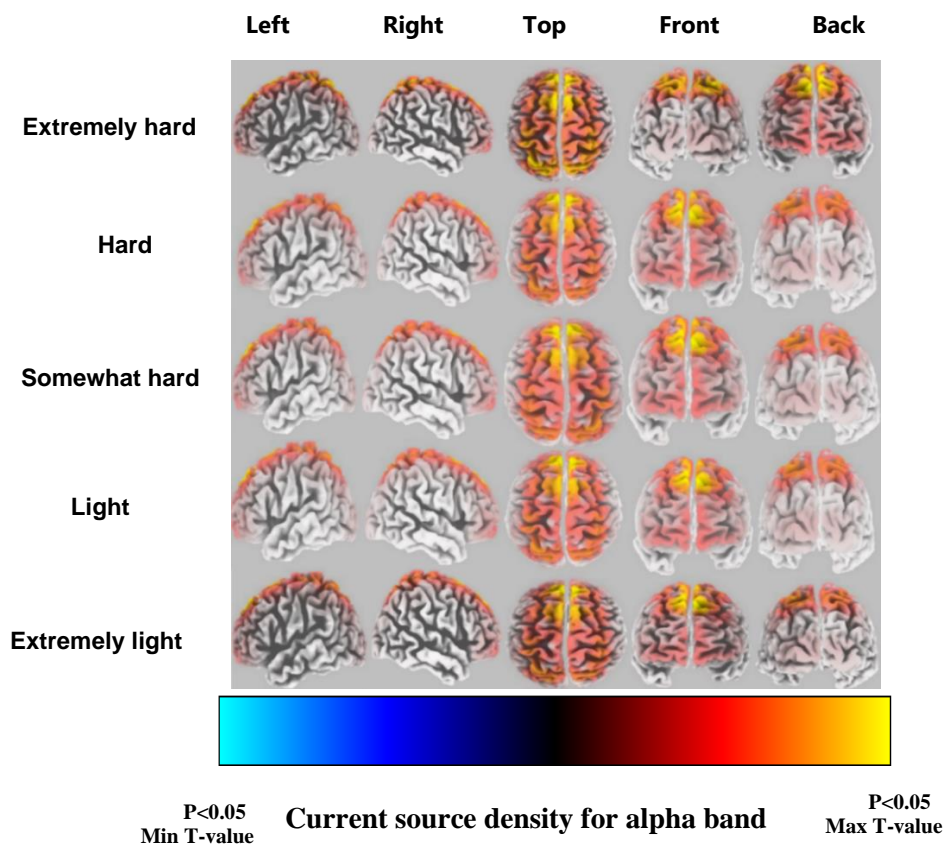


Figure 5-5: Current source density for each exertion level for alpha frequency band (red to yellow is an indication to the source localization strengthening, whereas blue is an indication to the source localization weakness)



Detailed information regarding the brain structure, the maximum activated BA with MNI coordinates, voxel threshold (T-values), for each exertion level for alpha frequency band was reported in (Table 5-10).

Table 5-10: CSD localization for each frequency band for each exertion levels (Brodmann Area [BA]; Montreal Neurological Institute [MNI]; Threshold [T-value]; Middle Frontal Gyrus [MFG], Superior Frontal Gyrus [SFG]).

Exertion levels	Alpha frequency band		
	Brain structure	Maximum activated BA with MNI coordinates	Voxel (T-value)
Extremely hard	MFG	BA 6, MNI (X= 5, Y= 20, Z= 65)	9.49E+4
Hard	SFG	BA 8, MNI (X= 10, Y= 50, Z= 45)	4.78E+4
Somewhat hard	SFG	BA 8, MNI (X= 10, Y= 50, Z= 45)	4.77E+4
Light	SFG	BA 8, MNI (X= 10, Y= 50, Z= 45)	4.79E+4
Extremely light	SFG	BA 8, MNI (X= 10, Y= 50, Z= 45)	4.79E+4

For beta band, the highest CSD was localized in the postcentral gyrus of the parietal lobe corresponding to BA 5 for extremely hard exertion level (Figure 5-6). For all other exertion levels, the highest CSD was highly localized in the precuneus of the parietal lobe corresponding to BA 7. Detailed information regarding the brain structure, the maximum activated BA with MNI coordinates, voxel threshold (T-values), for each exertion level for the beta frequency band was reported in (

Table 5-11).

Table 5-11: CSD localization for each frequency band for each exertion levels (Brodmann Area [BA]; Montreal Neurological Institute [MNI]; Threshold [T-value])

Exertion level	Beta frequency band		
	Brain structure	Maximum activated BA with MNI coordinates	Voxel (T-value)
Extremely hard	Postcentral gyrus	BA 5, MNI (X= 5, Y= -50, Z= 70)	1.75E+5
Hard	Precuneus gyrus	BA 7, MNI (X= 10, Y= -60, Z= 70)	1.31E+5
Somewhat hard	Precuneus gyrus	BA 7, MNI (X= 10, Y= -60, Z=70)	1.31E+5
Light	Precuneus gyrus	BA 7, MNI (X= 10, Y= -60, Z=70)	1.30E+5
Extremely light	Precuneus gyrus	BA 7, MNI (X= 10, Y= -60, Z=70)	1.30E+5

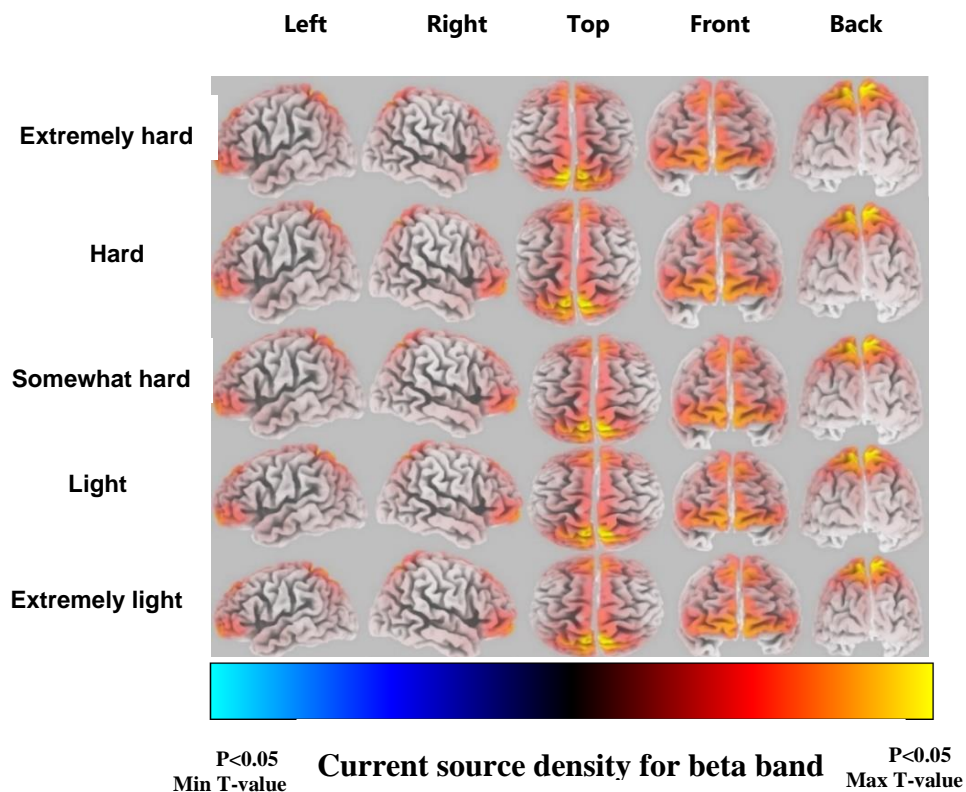
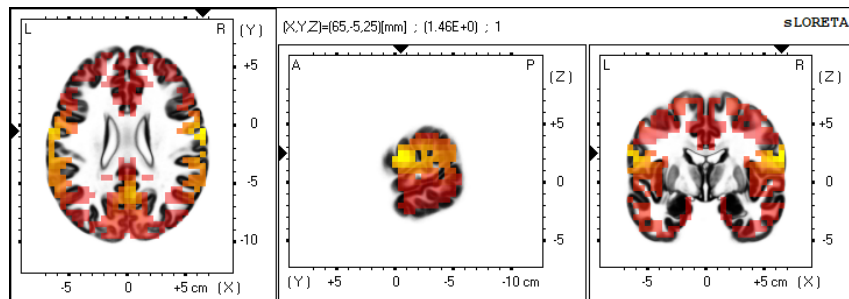
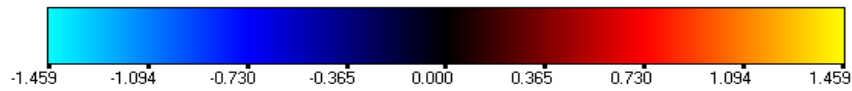


Figure 5-6: CSD localization for each exertion level for beta frequency band  
 (Red to yellow is an indication to the source localization strengthening, whereas blue is an indication to the source localization weakness).

### 5.2.5.2 eLORETA Statistics and Multiple Comparison Corrections

The CSD for pairwise exertion levels resultant from permutation test applied in eLORETA are displayed in Table 5-12 for alpha frequency and in Table 5-13 for beta frequency. For illustration purposes, the three-dimensional statistical mapping figures are also provided, where yellow or red color indicates an increase in the oscillatory activity, and blue color indicates a reduction in the oscillatory activity. Figure 5-7 is a representation of the three-dimensional statistical mapping resulting from the comparison of eLORETA CSD between the ‘extremely hard’ exertion levels for alpha band. The ‘extremely hard’ exertion level generates neurons that oscillate more strongly compared to the ‘extremely light’ exertion level in the frontal lobe (precentral gyrus, BA 4 [X = 65, Y = -5, Z = 20], BA 6, [X = 65, Y = -5, Z = 25]), and the parietal lobe (postcentral gyrus, BA 43 [X = 65, Y = -10, Z = 20]), with log-F-ratio threshold  $T_{\max} = 1.459$ .





**Current source density**

Figure 5-7: Three-dimensional statistical mapping for alpha frequency band in extremely hard vs extremely light exertion levels

Figure 5-8 depicts the three-dimensional statistical mapping resulting from the comparison of eLORETA CSD between the extreme exertion levels for beta band. The “extremely hard” exertions generate neurons that oscillate more strongly than the those at the “extremely light” exertion level in the parietal lobe (inferior parietal lobule, BA 40, [ X= 60 , Y= -35 , Z= 50], and postcentral gyrus, BA 2 [ X= 60 , Y= -30 , Z= 50]) with log-F-ratio threshold T-max = 0.407.

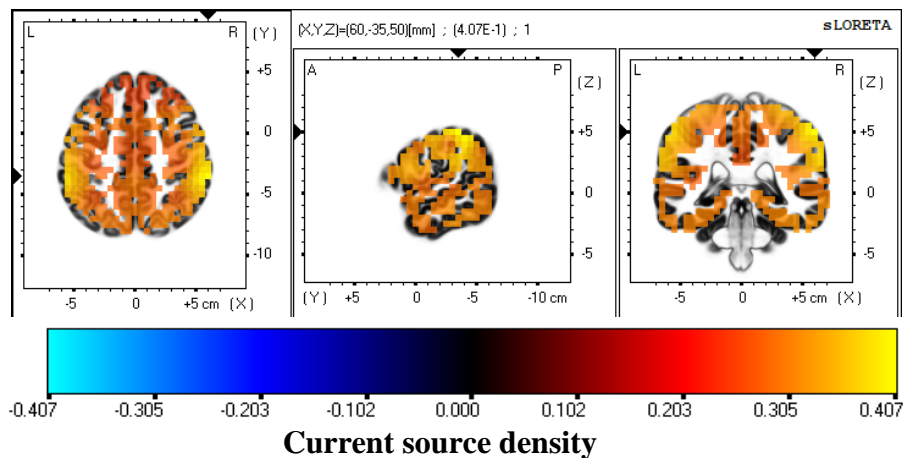


Figure 5-8: eLORETA statistical maps for beta frequency band in extremely hard vs extremely light exertion levels

Figure 5-9 depicts the three-dimensional statistical mapping resulting from the comparison of eLORETA CSD between the “extremely hard” and “hard” exertion levels for alpha band. The “extremely hard” exertions generate neurons that oscillate more strongly than those at the “hard”

exertion level in the frontal lobe (Precentral Gyrus, BA 4 [X= 65 , Y= -5 , Z= 20] with log-F-ratio threshold T-max = 1.46.

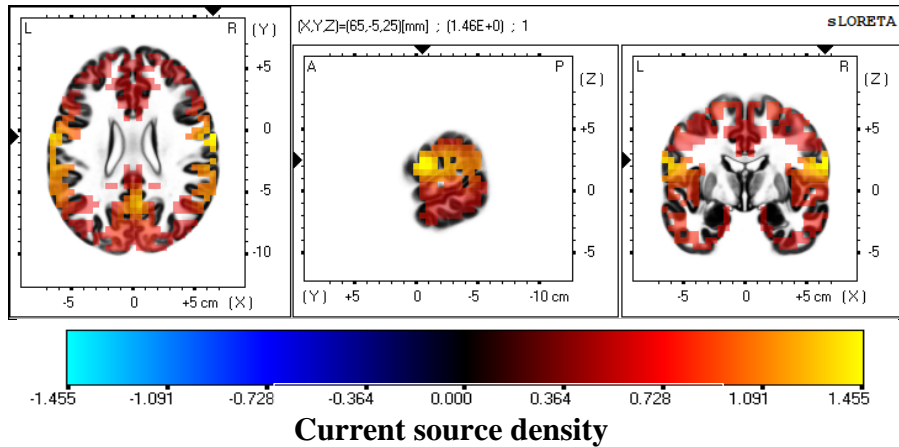
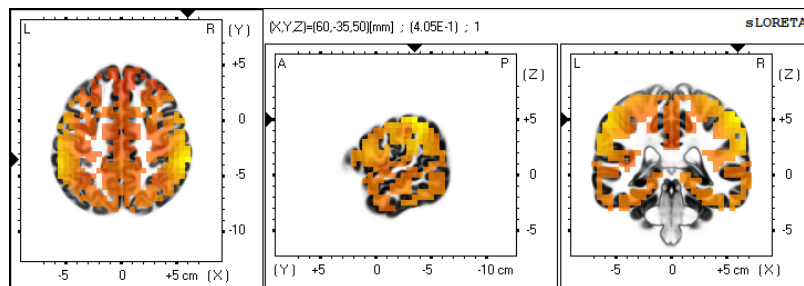
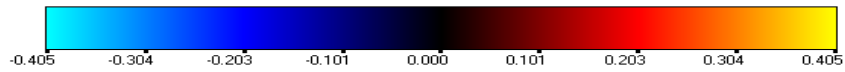


Figure 5-9: eLORETA statistical maps for alpha frequency band in extremely hard vs hard exertion levels

Figure 5-10 depicts the three-dimensional statistical mapping resulting from the comparison of eLORETA CSD between the “extremely hard” and “hard” exertion levels for beta band. The “extremely hard” exertions generate neurons that oscillate more strongly than those at the “hard” exertion level in the parietal lobe (inferior parietal lobule, BA 40, [(X= 60 , Y= -35 , Z= 50 ], with log-F-ratio threshold T-max = 0.405).

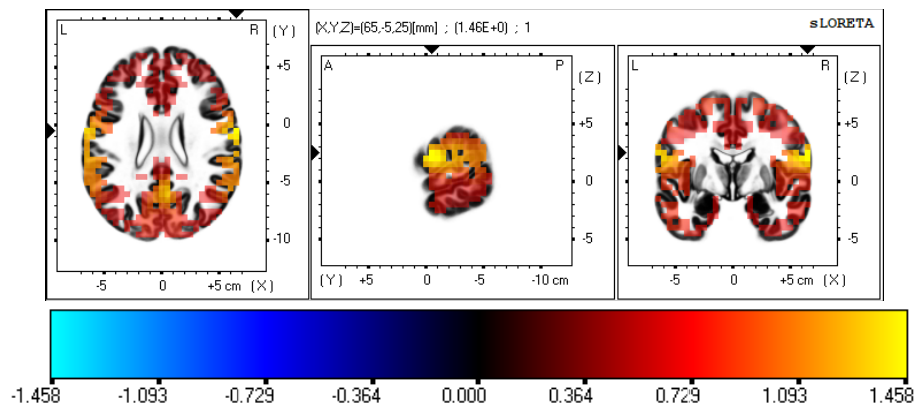




**Current source density**

Figure 5-10: eLORETA statistical maps for beta frequency band in extremely hard vs hard exertion levels

Figure 5-11 depicts the three-dimensional statistical mapping resulting from the comparison of eLORETA CSD between the “extremely hard” and “somewhat hard” exertion levels for alpha band. The “extremely hard” exertions generate neurons that oscillate more strongly than those at the “somewhat hard” exertion level in the frontal lobe (precentral gyrus, BA 4, [X= 65, Y= -5, Z= 25], with log-F-ratio threshold T-max = 1.458).



**Current source density**

Figure 5-11: eLORETA statistical maps for alpha frequency band in extremely hard vs somewhat hard exertion levels

Figure 5-12 depicts the three-dimensional statistical mapping resulting from the comparison of eLORETA CSD between the “extremely hard” and “somewhat hard” exertion levels for beta band. The “extremely hard” exertions generate neurons that oscillate more strongly than those at the

“somewhat hard” exertion level in the parietal lobe (inferior parietal lobule, BA 40, [X= 65 , Y= -35 , Z= 50], with log-F-ratio threshold T-max = 0.406).

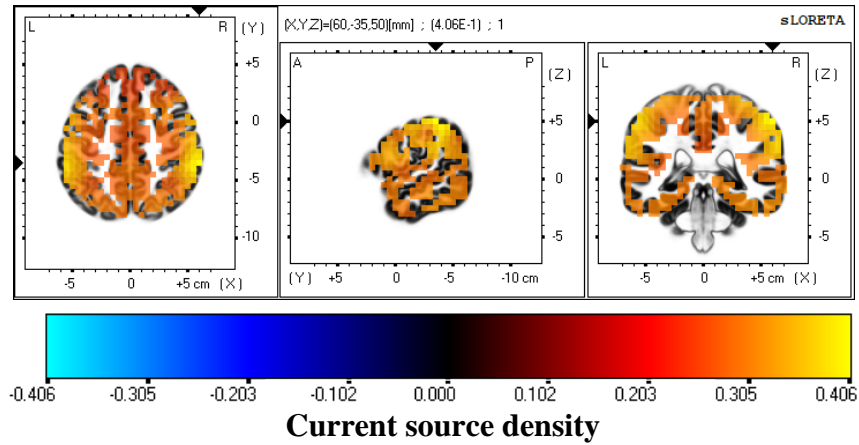


Figure 5-12: eLORETA statistical maps for beta frequency band in extremely hard vs somewhat hard exertion levels

Figure 5-13 depicts the three-dimensional statistical mapping resulting from the comparison of eLORETA CSD between the “extremely hard” and “light exertion” exertion levels for alpha band.

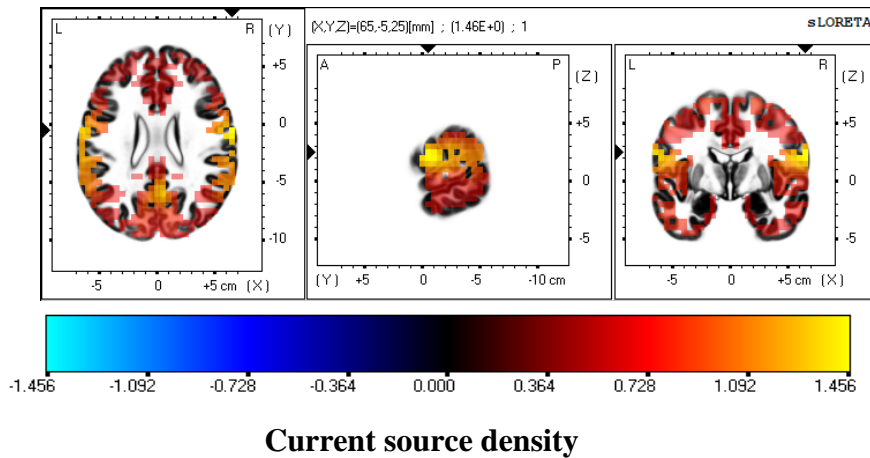


Figure 5-13: eLORETA statistical maps for alpha frequency band in extremely hard vs light exertion levels

The “extremely hard” exertions generate neurons that oscillate more strongly than those at the “light” exertion level in the frontal lobe (precentral gyrus, BA 4, [X= 65, Y= -5 , Z= 25], with log-F-ratio threshold T-max = 1.456).

Figure 5-14 depicts the three-dimensional statistical mapping resulting from the comparison of eLORETA CSD between the “extremely hard” and “light” exertion levels for beta band. The “extremely hard” exertions generate neurons that oscillate more strongly than those at the “light” exertion level parietal lobe (inferior parietal lobule, BA 40 [X= 60 , Y= -35 , Z= 50], with log-F-ratio threshold T-max = 0.407).

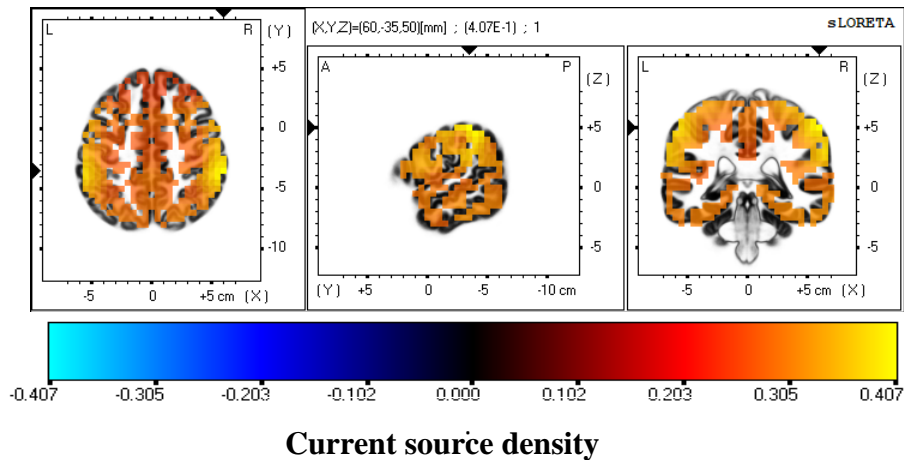


Figure 5-14: eLORETA statistical maps for beta frequency band in extremely hard vs light exertion levels

Figure 5-15 depicts the three-dimensional statistical mapping resulting from the comparison of eLORETA CSD between the “hard” and “somewhat hard” exertion levels for alpha band. The “hard” exertions generate neurons that oscillate more strongly than those at somewhat hard



exertion level in parietal lobe (precentral gyrus, Ba 7, (X= -15, Y= -55, Z= 65), with log-F-ratio threshold T-max =0.009).

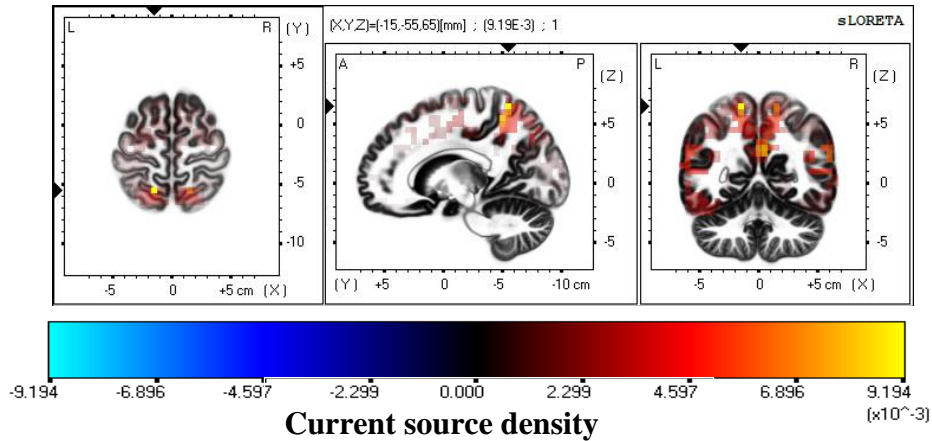
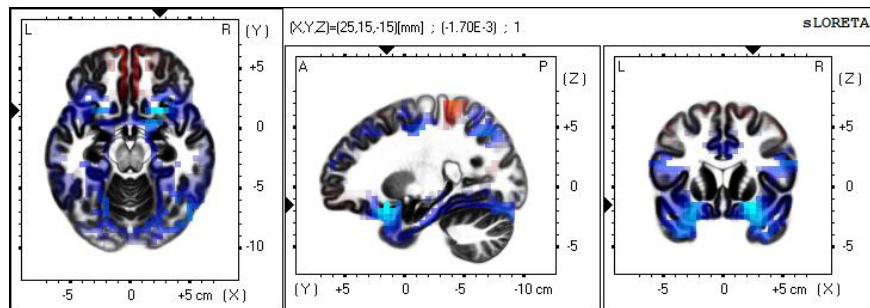


Figure 5-15: eLORETA statistical maps for alpha frequency band in hard vs somewhat hard

Figure 5-16 depicts the three-dimensional statistical mapping resulting from the comparison of eLORETA CSD between the “hard” and “somewhat hard” exertion levels for beta band. The “hard” exertions generate neurons with less oscillation than those at the “somewhat” hard exertion level in frontal lobe (inferior frontal gyrus, Ba 47,  $[X= 25 , Y= 15 , Z= -15]$ , with log-F-ratio threshold T-min = -0.00169).



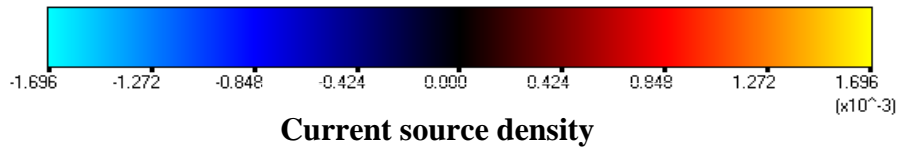


Figure 5-16: eLORETA statistical maps for beta frequency band in hard vs somewhat hard

Figure 5-17 depicts the three-dimensional statistical mapping resulting from the comparison of eLORETA CSD between the “hard” and “light” exertion levels for alpha band. The “hard” exertions generate neurons with less oscillation than those at the “light” exertion level in temporal lobe (superior temporal gyrus, Ba 22, [X= 65 , Y= -25 , Z= 0], with log-F-ratio threshold T-max =-5.40E-3).

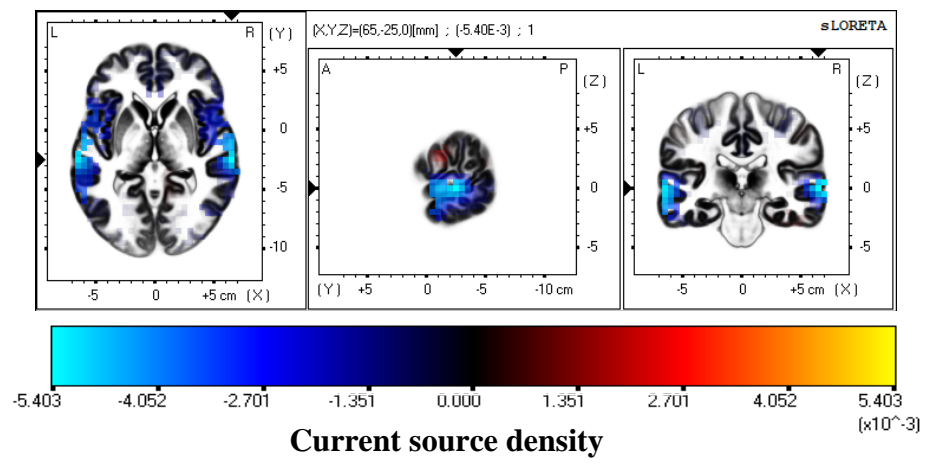


Figure 5-17: eLORETA statistical maps for alpha frequency band in hard vs light

Figure 5-18 depicts the three-dimensional statistical mapping resulting from the comparison of eLORETA CSD between the “hard” and “light” exertion levels for beta band. The “hard” exertions generate neurons that oscillate more strongly than those at the “light” exertion level in frontal lobe (paracentral lobule, BA 5, [X= -15 , Y= -45 , Z= 60], with log-F-ratio threshold T-min =0.00232)

but less oscillation were found in occipital lobe (middle occipital gyrus, BA 19, [X= -55 , Y= -70 , Z= 5], with log-F-ratio threshold T-min = - 0.00231).

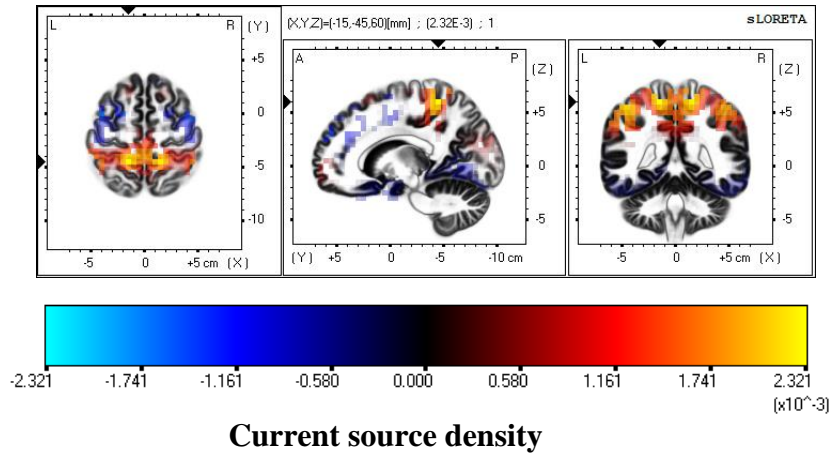


Figure 5-18: eLORETA statistical maps for beta frequency band in hard vs light

Figure 5-19 depicts the three-dimensional statistical mapping resulting from the comparison of eLORETA CSD between the “hard” and “extremely light” exertion levels for alpha band. The “hard” exertions generate neurons that oscillate less strongly than the “extremely light” exertion level in temporal lobe (Superior Temporal Gyrus, BA 22, [X= 65 , Y= -20 , Z= 0], with log-F-ratio threshold T-min =-0.00764).

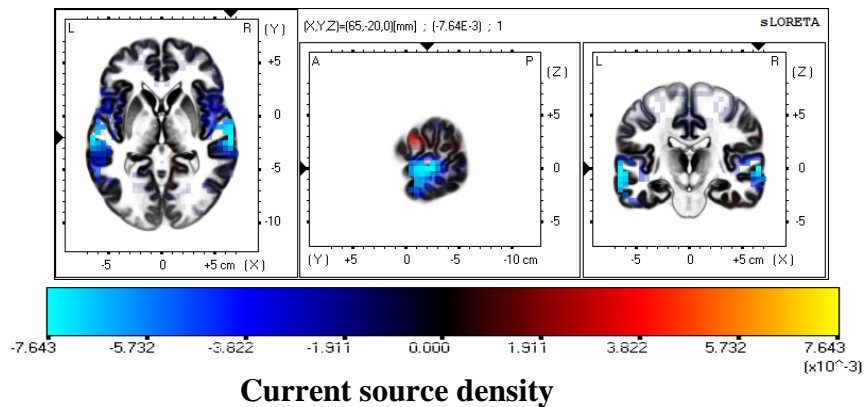


Figure 5-19:eLORETA statistical maps for alpha frequency band in hard vs extremely light

Figure 5-20 depicts the three-dimensional statistical mapping resulted from the comparison of eLORETA CSD between the “hard” and “extremely light” exertion levels for beta band. The “hard” exertions generate neurons that oscillate more strongly than those at the “extremely light” exertion level in frontal lobe (paracentral lobule, BA 4, [X= 0 , Y= -40 , Z= 65], with log-F-ratio threshold T-max= 0.002392).

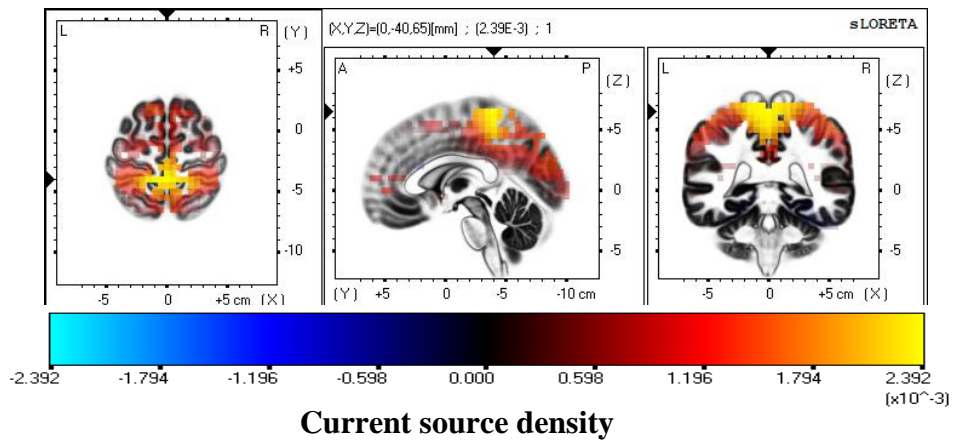
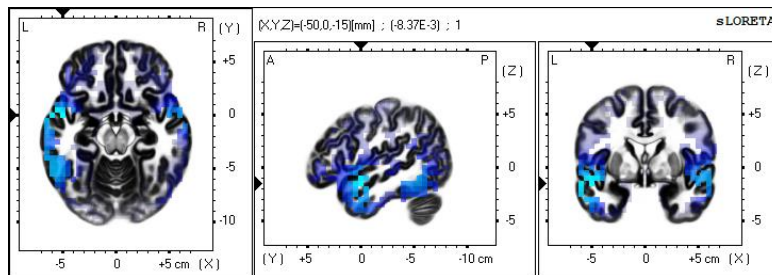


Figure 5-20: eLORETA statistical maps for beta frequency band in hard vs extremely light

Figure 5-21 depicts the three-dimensional statistical mapping resulting from the comparison of eLORETA CSD between the “somewhat hard” and “light” exertion levels for alpha band.



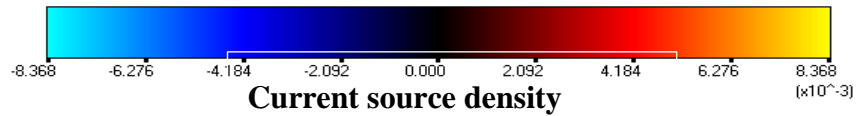


Figure 5-21: eLORETA statistical maps for alpha frequency band in somewhat hard vs light

The “somewhat hard” exertions generate neurons that oscillate less than those at the “light” exertion level in temporal lobe (middle temporal gyrus, BA 21, [X= -50, Y= 0 , Z= -15], with log-F-ratio threshold T-min=-0.00837).

Figure 5-22 depicts the three-dimensional statistical mapping resulting from the comparison of eLORETA CSD between the “somewhat hard” and “light” exertion levels for beta band. The “somewhat hard” exertions generate neurons that oscillate more strongly than those at the light exertion level in frontal lobe (precuneus, BA 31, [X= -15, Y= -45 , Z= 40], with log-F-ratio threshold T-max=-0.001555).

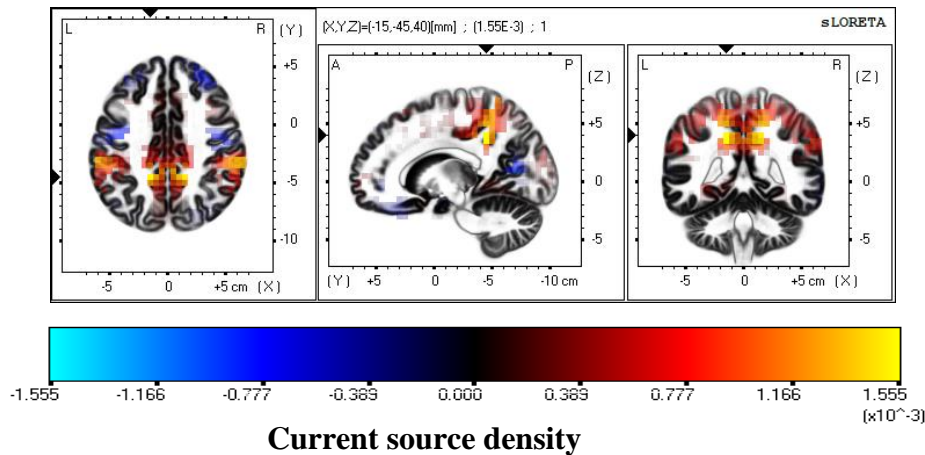


Figure 5-22: eLORETA statistical maps for beta frequency band in somewhat hard vs light

Figure 5-23 depicts the three-dimensional statistical mapping resulting from the comparison of eLORETA CSD between the “light” and “extremely light” exertion levels for alpha band. The “light” exertions generate neurons that oscillate less than those at the “extremely light” exertion

level in parietal lobe (precuneus, BA 7, [X= -10 , Y= -50 , Z= 55], with log-F-ratio threshold  $T_{\min}=-4.42E-3$ ).

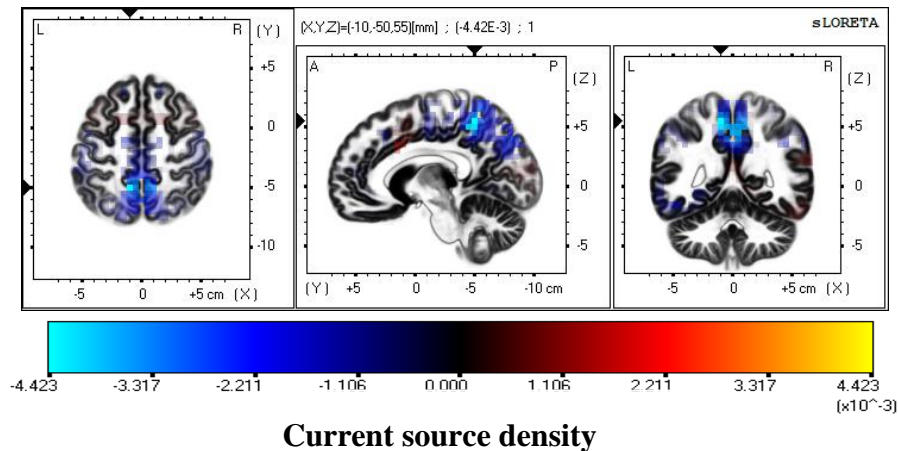
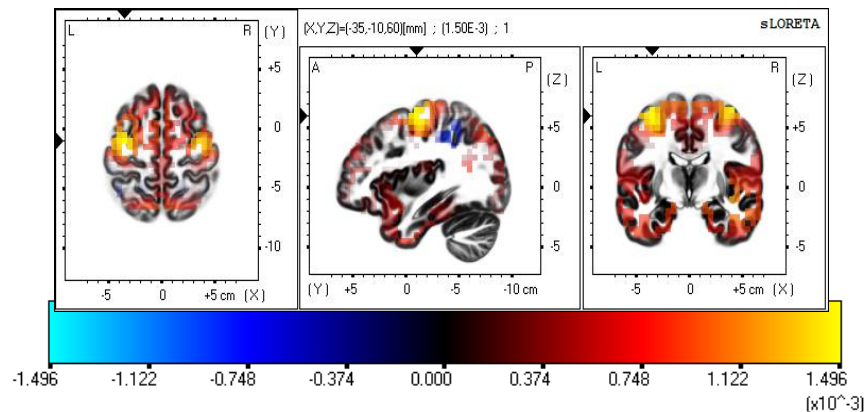


Figure 5-23: eLORETA statistical maps for alpha frequency band in light vs extremely light

Figure 5-24 depicts the three-dimensional statistical mapping resulting from the comparison of eLORETA CSD between the “light” and “extremely light” exertion levels for beta band. The “light” exertions generate neurons that oscillate more strongly than the “extremely light” exertion level in frontal lobe (precentral gyrus, BA 6, [X= -35, Y= -10 , Z= 60], with log-F-ratio threshold  $T_{\max}= 0.001496$ ).



### Current source density

Figure 5-24: eLORETA statistical maps for beta frequency band in light vs extremely light

Table 5-12: The statistical comparisons of eLORETA estimated current source density for pairwise exertion levels for alpha frequency.

<b>Exertion level comparison</b>	<b>Brain structure</b>	<b>Maxi/Min activated BA</b>	<b>Thresholds values (t-value) for p &lt;0.05</b>
Extremely hard vs hard	Precentral gyrus	BA 4	T-max = 1.45
Extremely hard vs somewhat hard	Precentral gyrus	BA 4	T-max = 1.45
Extremely hard vs light	Precentral gyrus	BA 4	T-max = 1.45
Extremely hard vs extremely light	Precentral gyrus	BA 4	T-max = 1.45
Hard vs somewhat hard	Precentral gyrus	BA 7	T-max = 0.009
Hard vs light	Superior temporal gyrus	BA 22	T-max = 0.009
Hard vs extremely light	Superior temporal gyrus	BA 22	T-min = 0.009
Somewhat hard vs light	Middle temporal gyrus	BA 21	T-min = 0.00837
Light vs extremely light	Precuneus	BA 7	T-max = 0.00442

Table 5-13: The statistical comparisons of eLORETA estimated current source density for pairwise exertion levels for beta frequency.

<b>Exertion level comparison</b>	<b>Brain structure</b>	<b>Max/Min activated BA</b>	<b>Thresholds values (t-value) for p &lt;0.05</b>
Extremely hard vs hard	Inferior parietal lobule	BA 40	T-max = 0.405
Extremely hard vs somewhat hard	Inferior parietal lobule	BA 40	T-max = 0.407
Extremely hard vs light	Inferior parietal lobule	BA 40	T-max = 0.407
Extremely hard vs extremely light	Postcentral gyrus	BA 2	T-max = 0.388
Hard vs somewhat hard	Inferior parietal lobule	BA 40	T-min = 0.00153
Hard vs light	Middle occipital gyrus	BA 19	T-min = 0.00231

Hard vs extremely light	Precentral gyrus	BA 4	T-max = 0.003
Somewhat hard vs light	Precuneus gyrus	BA 31	T-max = 0.00155
Light vs extremely light	Precentral gyrus in frontal lobe	BA 4	T-max= 0.003

## 5.2.6 Functional Connectivity

### 5.2.6.1 Functional Connectivity Patterns

Coherence matrices were computed for 84 ROIs using eLORETA connectivity algorithm for each subject and for each frequency band (alpha and beta) (Pascual-Marqui et al., 2011b). Figure 5-25 provides an overview of the functional brain network for the various force exertion levels, using the coherence method in each frequency alpha and beta band (research question 2). The visualization of functional interactions between neighboring and distant brain regions was performed using BrainNet Viewer (<http://www.nitrc.org/projects/bnv/>), a Matlab toolbox (Xia et al., 2013b),



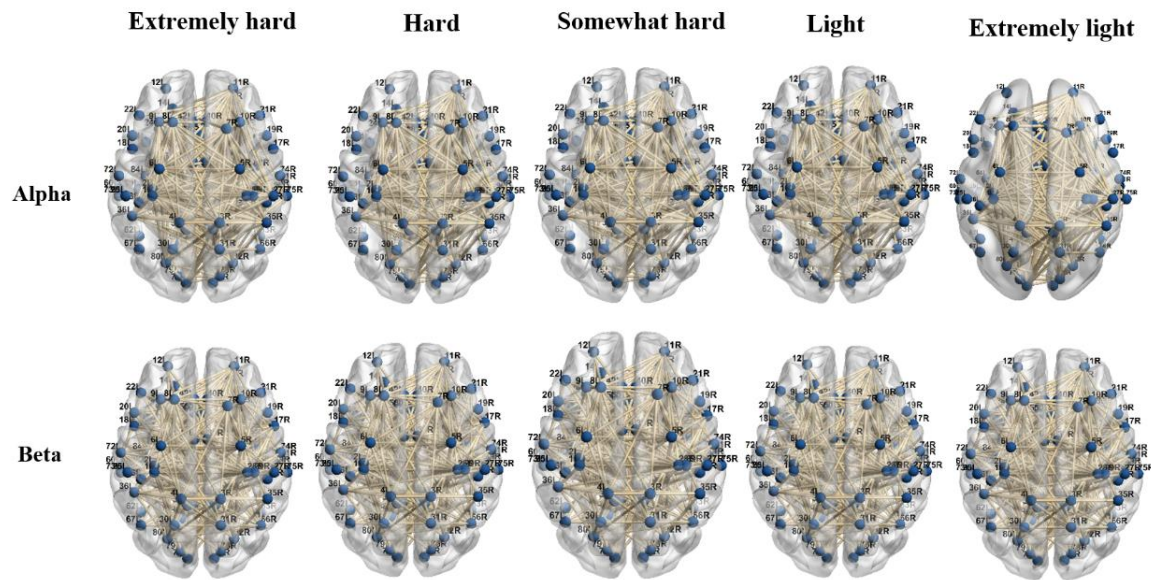


Figure 5-25: Visualization of the alpha and beta functional brain networks for all exertion levels using coherence method.

Overall, we found that beta coherence networks had more connections in the frontal and temporal lobes than the alpha coherence network at all force exertion levels, including the left superior frontal gyrus (BA 10), the left precentral gyrus (BA 44), the right precentral gyrus (BA 44), the left inferior frontal gyrus (BA 45), the middle frontal gyrus (BA 46), the middle temporal gyrus (BAs 21 and 39), the left fusiform gyrus (BA 37), and the left transverse temporal gyrus (BA 42).

When exertion level increases, there is a strong coupling between the left paracentral (BA 5) and the left lingual gyrus (BA 17) in the alpha band. In general, the BA 5 region is involved in somatosensory processing, motor control, and association (Mackenzie et al., 2016), whereas BA 17 is involved in discerning the intensity of the object (i.e., primary visual cortex). This study

identified a strong coupling between the left superior frontal gyrus (BA 10) and the middle frontal gyrus (BA 11). In general, BA 10 is involved in various executive brain functions, whereas BA 11 is involved with planning, decision making, and processing rewards. Disconnections were found between the middle frontal gyrus (BA 14) and the anterior cingulate (BA 33) when exertion level increases. It should be noted that, in general, BA 33 is heavily related to positive emotions (Vogt, 2005).

When exertion level increases, there is strong coupling between the right superior frontal gyrus (BA 10) and the parahippocampal gyrus (BA 34) in the beta band. The coherence coefficient for each exertion level for alpha and beta are shown in (Figure 5-26). The coherence coefficient is a normalized quantity bounded by 0 and 1 (Nunez et al., 1997).

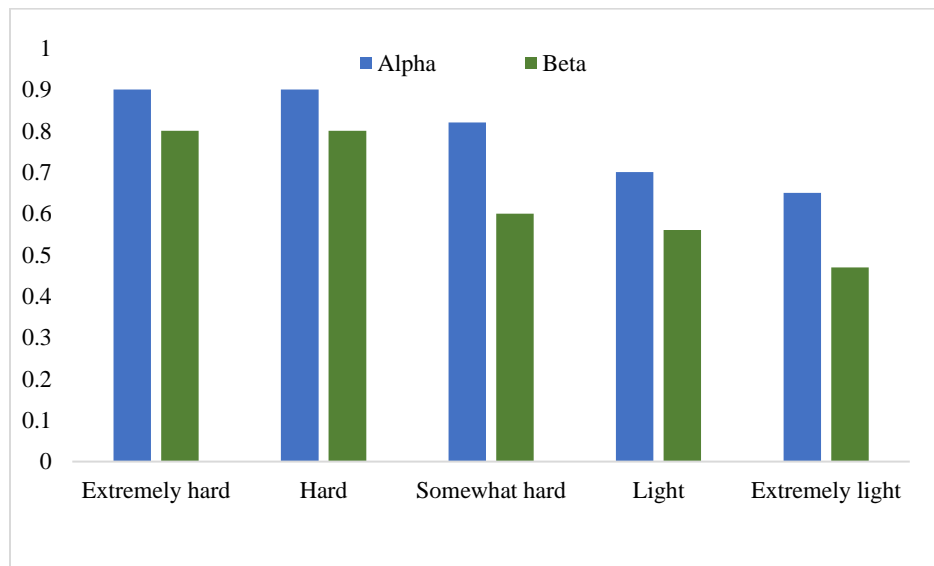


Figure 5-26: The coherence coefficient for each exertion level for alpha and beta

### 5.2.6.1 Functional Connectivity Multiple Comparison

eLORETA wire diagrams were used to graphically demonstrate the significant differences in brain functional connectivity among the force exertion levels. The significant connected regions are mapped in red lines, and the significant disconnected regions are mapped in blue lines. Table 5-14 summarizes the significant differences in the functional connectivity between the exertion levels for each frequency band. The levels of connectivity between extremely hard exertion level versus other exertion levels (hard, somewhat hard, light and extremely light) for each frequency band are shown in Figure 5-27.

Comparing the extremely high exertion to all other exertion levels for alpha network, a significantly increase in the alpha coherence was found. In addition, when comparing extremely high exertion to all other exertion levels for the beta network, a significant increase in the beta coherence was observed. A few disconnections between the left and right hemispheres in the beta network were also present.

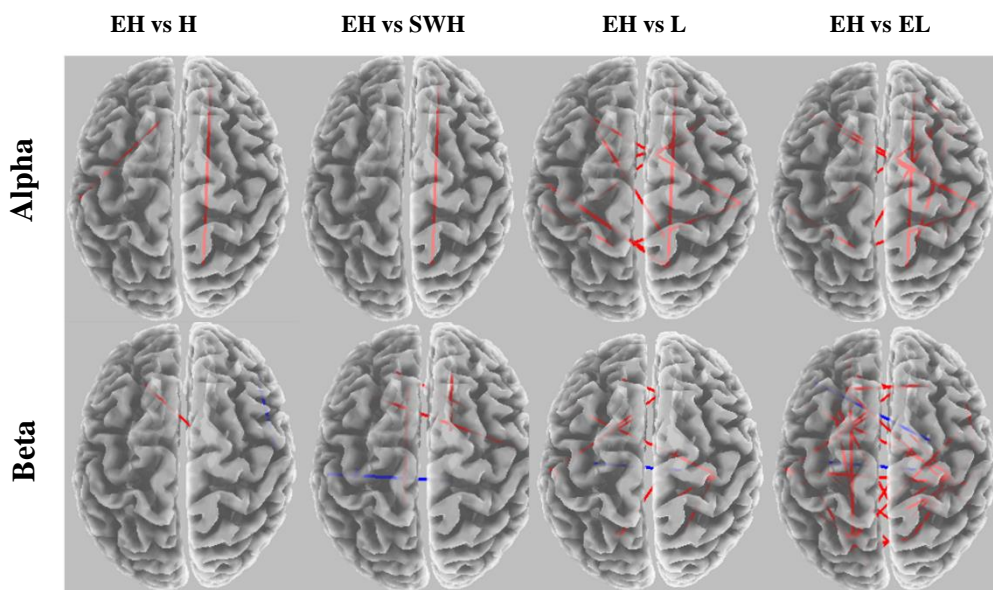


Figure 5-27: eLORETA wire diagram comparing extremely hard exertion with other exertion levels for each frequency band (extremely light [EL], light[L], somewhat hard [SWH], hard [H], and extremely hard [EH]).

Figure 5-28 shows the connectivity between hard exertion level versus somewhat hard, light and extremely light, respectively, for each frequency band. The alpha coherence network was significantly lower for the hard exertion level than the other exertion levels. No significant differences were observed between hard and somewhat hard exertion levels. The beta band network showed a significantly greater functional brain network in hard exertion than the somewhat hard level, whereas significant disconnections were found in comparison to light and extremely light exertion levels.

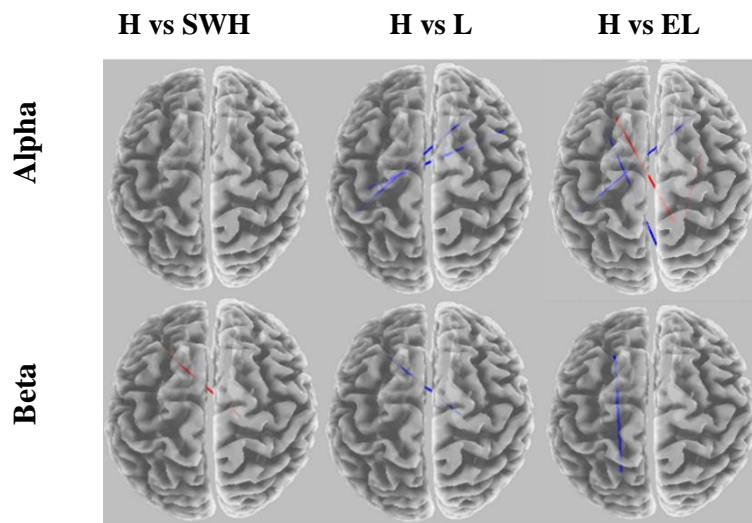


Figure 5-28: eLORETA wire diagram comparing hard exertion with other exertion levels for each frequency band (extremely light [EL], light[L], somewhat hard [SWH], hard [H], and extremely hard [EH])

Figure 5-29 shows the connectivity between somewhat hard exertion level versus other exertion levels including light and extremely light for each frequency band. The alpha network was found to have denser connections in the fronto-central brain region than light and extremely light exertion. No significant alterations were found in the beta coherence network when comparing somewhat hard exertion to extremely light exertion level.

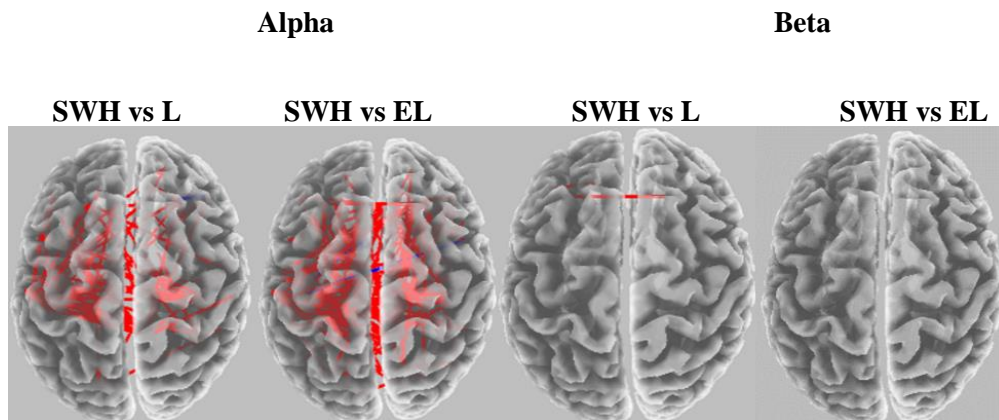


Figure 5-29: eLORETA wire diagram comparing somewhat hard exertion with other exertion levels for each frequency band (extremely light [EL], light[L], somewhat hard [SWH], hard [H], and extremely hard [EH]).

**alpha L vs EL**

**beta L vs EL**

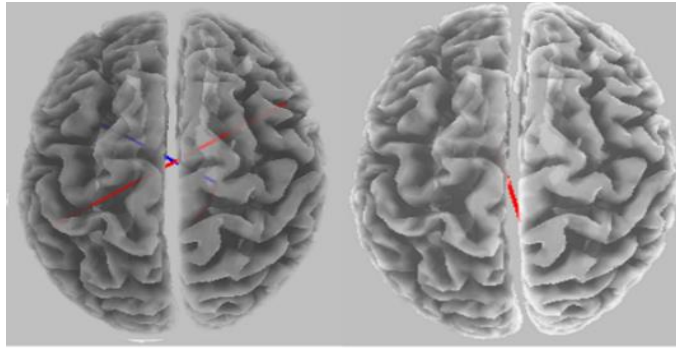


Figure 5-30: eLORETA wire diagram comparing light with extremely light level for each frequency band.

Figure 5-30 shows the connectivity between extremely exertion level versus light, for each frequency band. A significant increase in the coherence connectivity for some cortical regions were found for both alpha and beta networks.

Table 5-14: Summary of the significant difference in functional connectivity between the exertion levels for each frequency band

<b>Exertion level comparison</b>	<b>Frequency band</b>	<b>Connectivity</b>
Extremely hard v hard	Alpha	More connections in frontal-parietal region
Extremely hard vs hard	Beta	More connections in frontal- limbic region
Extremely hard vs somewhat hard	Alpha	More connections in right frontal-parietal region
Extremely hard vs somewhat hard	Beta	More connections in frontal- limbic region and frontal- temporal
Extremely hard vs light	Alpha	More connections in frontal-parietal region and parietal-temporal
Extremely hard vs light	Beta	More connections in frontal- limbic region
Extremely hard vs extremely light	Alpha	More connections in frontal-parietal and parietal-occipital

Extremely hard vs extremely light	Beta	More connections in frontal-parietal and parietal-occipital
Hard vs somewhat hard	Alpha	No significant difference
Hard vs somewhat hard	Beta	More connections in frontal-limbic region
Hard vs light	Alpha	Less connections in central brain regions
Hard vs light	Beta	Less connections in central brain regions
Hard vs extremely light	Alpha	More connections and decreased in some regions
Hard vs extremely light	Beta	Less connections in left frontal-parietal
Somewhat hard vs light	Alpha	More connections in central brain region
Somewhat hard vs light	Beta	More connections in prefrontal cortex
Somewhat hard vs extremely light	Alpha	More connections in central brain region
Somewhat hard vs extremely light	Beta	No significant change was found
Light vs extremely light	Alpha	More connections in central brain region
Light vs extremely light	Beta	More connections parietal-limbic

### 5.2.7 Brain Network

This section discusses the topological differences for global and local network measures (research question 3). Global measures were computed using the Brain Connectivity Toolbox (<http://www.brain-connectivity-toolbox.net>) (Rubinov and Sporns, 2010) whereas local measures were computed based on a developed python code.

### 5.2.7.1 Topological differences in global network

#### 5.2.7.1.1 Alpha coherence brain network

The permutation test for global measures yielded significant differences among the different exertion levels. Table 5-15 displays the mean, the standard deviation (Sd) , the significant P-value observed from permutation test for the all exertion levels in alpha coherence.

A small-worldness network was observed in the extremely hard exertion level for alpha coherence network compared to other exertion levels ( permutation test,  $P < 0.0453$ ). Significant changes in the characteristic path length were found for the different exertion levels as shown in (Figure 5-31A). Significant changes in the characteristic path length were found for the various exertion levels. A significant reduction in the characteristic PL between the following exertion levels was found hard vs somewhat hard (permutation test,  $p < 0.0089$ ), hard vs light (permutation test,  $p < 0.0233$ ), and hard vs extremely light (permutation test,  $p < 0.0179$ ). In general, a reduction in the characteristic PL for high exertion levels indicated strong communication efficiency between brain regions (Figure 5-31C).

Table 5-15: Mean, standard deviation (sd) and significant statement from permutation test between exertion levels for small-world, characteristic path length, clustering coefficient, global efficiency, local efficiency, and modularity in alpha coherence network.

Graph theory measures	Exertion levels	Mean	Sd	P-value from permutation test				
				Extremely hard	Hard	Somewhat hard	Light	Extremely light
	Extremely hard	0.505	0.005	-	-	-	-	0.0453
	hard	0.5038	0.001	-	-	-	-	-



Graph theory measures	Exertion levels	Mean	Sd	P-value from permutation test				
				Extremely hard	Hard	Somewhat hard	Light	Extremely light
Small world	somewhat hard	0.5036	0.001	-	-	-	-	-
	light	0.5037	0.001	-	-	-	-	-
	extremely light	0.5038	0.001	-	-	-	-	-
characteristic path length	Extremely hard	1.436	0.039	-	-	-	-	0.014
	hard	1.4472	0.001	-	-	0.0089	0.023	-
	somewhat hard	1.4476	0.001	-	-	-	-	0.0179
	light	1.4479	0.001	-	-	-	-	-
Clustering coefficient	extremely light	1.4471	0.002	-	-	-	-	-
	Extremely hard	0.2521	0.004	-	0.0123	-	-	-
	hard	0.25098	0.000	-	-	0.0353	-	0.032
	somewhat hard	0.2507	0.001	-	-	-	0.0209	-
Global efficiency	light	0.25093	0.000	-	-	-	-	-
	extremely light	0.2510	0.000	-	-	-	-	-
	Extremely hard	0.1713	0.006	-	-	-	-	-
	hard	0.1698	0.000	-	-	0.0176	0.0203	-
local efficiency	somewhat hard	0.16972	0.000	-	-	-	0.0108	-
	light	0.1697	0.000	-	-	-	-	0.0478
	extremely light	0.16979	0.000	-	-	-	-	-
	Extremely hard	0.278	0.006	-	0.0115	-	-	-
Modularity	hard	0.2767	0.000	-	-	0.0434	-	0.0277
	somewhat hard	0.2763	0.001	-	-	-	0.0247	0.0426
	light	0.2766	0.000	-	-	-	-	-
	extremely light	0.2767	0.000	-	-	-	-	-
Modularity	Extremely hard	0.142	0.084	-	-	-	0.0264	0.0326
	hard	0.138	0.082	-	-	-	0.004	0.0033
	somewhat hard	0.139	0.083	-	-	-	-	-
	light	0.139	0.082	-	-	-	-	-
	extremely light	0.137	0.082	-	-	-	-	-

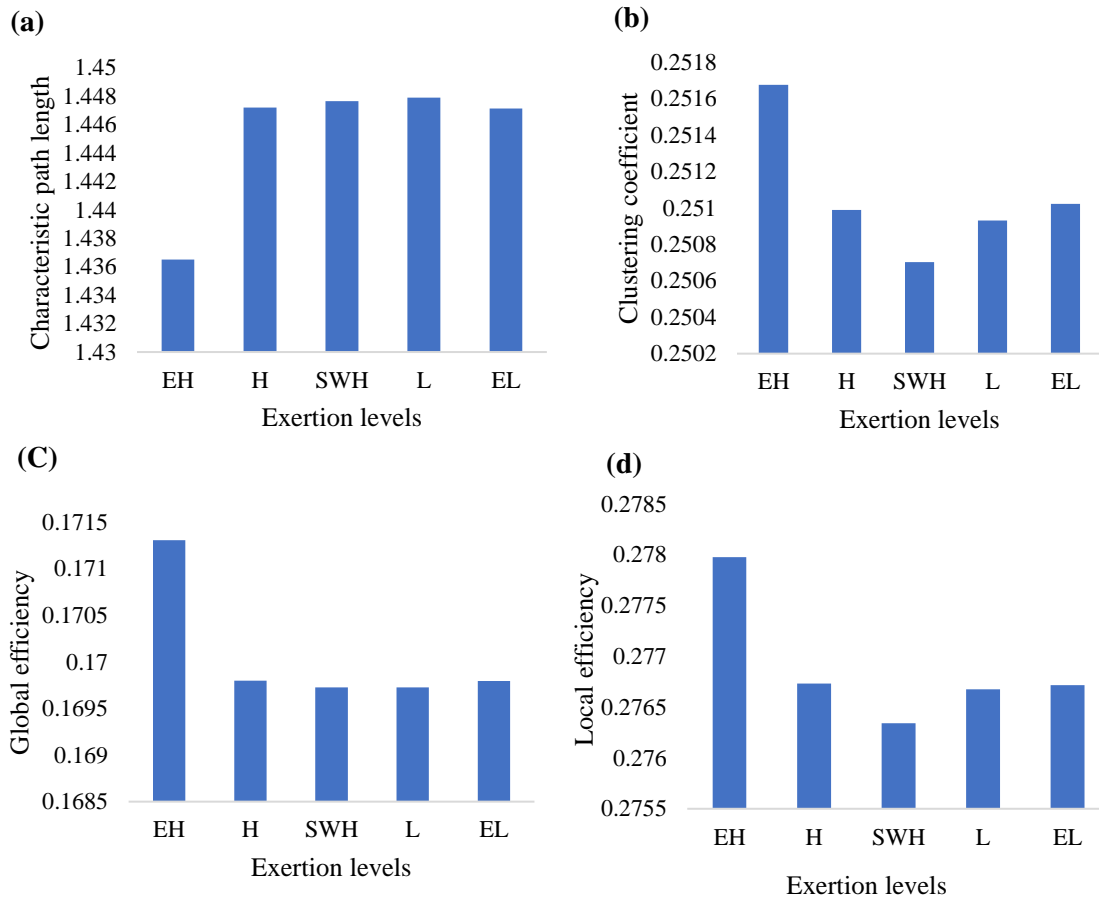


Figure 5-31: Graph theoretical network metrics showing main effects of different exertion levels (a) Characteristic path length (b) Clustering coefficient (c) Global efficiency (d) Local efficiency for alpha coherence (where extremely hard [EH], hard [H], somewhat hard [SWH], light [L], and extremely light [EL]).

A significant increase in the network global efficiency for high exertion levels was also observed (Figure 5-31B). A significant reduction between the the extremely hard exertion versus hard exertion (permutation test,  $P < 0.0123$ ), hard versus some what hard (permutation test,  $P < 0.0353$ ),and hard versus extremely light exertion (permutation test,  $P < 0.032$ ). However a significant increase was observed between and somewhat hard relative to light exertion (permutation test,  $P < 0.0209$ ).

A significant increase in the network local efficiency for extremely hard compared to hard exertion level (permutation test,  $P < 0.0115$ ), hard relative to somewhat hard exertion (permutation test,  $P < 0.0434$ ), hard relative to extremely light exertion (permutation test,  $P < 0.0277$ ), and somewhat hard exertion relative to extremely light (permutation test,  $P < 0.0426$ ) was found. However, significant reduction between somewhat hard and light was also observed (permutation test,  $P < 0.0247$ ). In general, the extremely hard and hard exertion levels provoked dense connected neighboring nodes between the network nodes compared to light and extremely light exertion levels. This was evident from local efficiency and modularity ensuring that the brain is more segregated at the high exertion levels compared to low exertion levels (Figure 5-31D).

#### 5.2.7.1.2 Global measures for beta coherence brain network

The permutation test for global measures yielded significant differences in beta coherence between different exertion levels. Table 5-16 displays the mean, the standard deviation, the significant p-value observed from permutation test for the all exertion levels in beta coherence.

The maximum values for both characteristic path length and clustering coefficient were observed at extremely hard exertion, whereas the minimum values were found at the extremely low exertion level (Figure 5-32A). The reduction in the average characteristic path length and clustering coefficient in the low exertion levels suggests that the brain network might shifted from random network to more organized small world network.

Table 5-16: Mean, standard deviation (sd) and significant statement from permutation test between exertion levels for small-world, characteristic path length, clustering coefficient, global efficiency, local efficiency, and modularity in beta coherence network.

Graph theory measures	Exertion levels	Mean	Sd	P-value from permutation test				
				Extremely hard	Hard	Somewhat hard	Light	Extremely light
Characteristic path length	Extremely hard	0.892059	0.00052	-	0.023	-	0.000	0.0027
	hard	0.891945	0.00032	-	-	0.0171	0.000	0.000
	somewhat hard	0.892022	0.00031	-	-	-	0.000	0.000
	light	0.892034	0.0002	-	-	-	-	0.000
	extremely light	0.891916	0.00029	-	-	-	-	-
Clustering coefficient	Extremely hard	0.244543	0.00178	-	-	-	-	0.0079
	hard	0.243985	0.00019	-	-	-	-	0.0209
	somewhat hard	0.244048	0.00017	-	-	-	-	0.0032
	light	0.244036	0.0002	-	-	-	-	0.0406
	extremely light	0.24393	0.0018	-	-	-	-	-
Global efficiency	Extremely hard	0.252198	0.00042	-	0.018	-	0.000	0.000
	hard	0.252323	0.00005	-	-	0.0174	0.000	0.000
	somewhat hard	0.252307	0.00005	-	-	-	0.021	0.000
	light	0.252303	0.00003	-	-	-	-	0.000
	extremely light	0.252332	0.00005	-	-	-	-	-
Local efficiency	Extremely hard	0.323795	0.00125	-	-	-	-	0.0148
	hard	0.3235	0.00023	-	-	-	-	0.0027
	somewhat hard	0.323527	0.00021	-	-	-	-	0.000
	light	0.323473	0.00018	-	-	-	-	0.0398
	extremely light	0.323458	0.0008	-	-	-	-	-
Modularity	Extremely hard	0.2776	0.1389	-	-	-	-	0.0357
	hard	0.2761	0.1389	-	-	-	0.018	0.0385
	somewhat hard	0.2768	0.1389	-	-	-	-	0.0169
	light	0.2776	0.1380	-	-	-	-	0.0169
	extremely light	0.2768	0.1391	-	-	-	-	-

A significant reduction in the characteristic path length was observed in extremely hard compared to hard exertion level (permutation test,  $P < 0.0239$ ), extremely hard compared to light (permutation test,  $P < 0.00$ ), extremely hard compared to extremely light (permutation test,  $P < 0.0027$ ). Furthermore, a significant decline between hard and light (permutation test,  $P < 0.00$ ), and

light compared to extremely light (permutation test,  $P < 0.00$ ). However, a significant increase in the characteristic path length was found for hard compared to both somewhat hard exertion level (permutation test,  $P < 0.0171$ ) and light (permutation test,  $P < 0.00$ ).

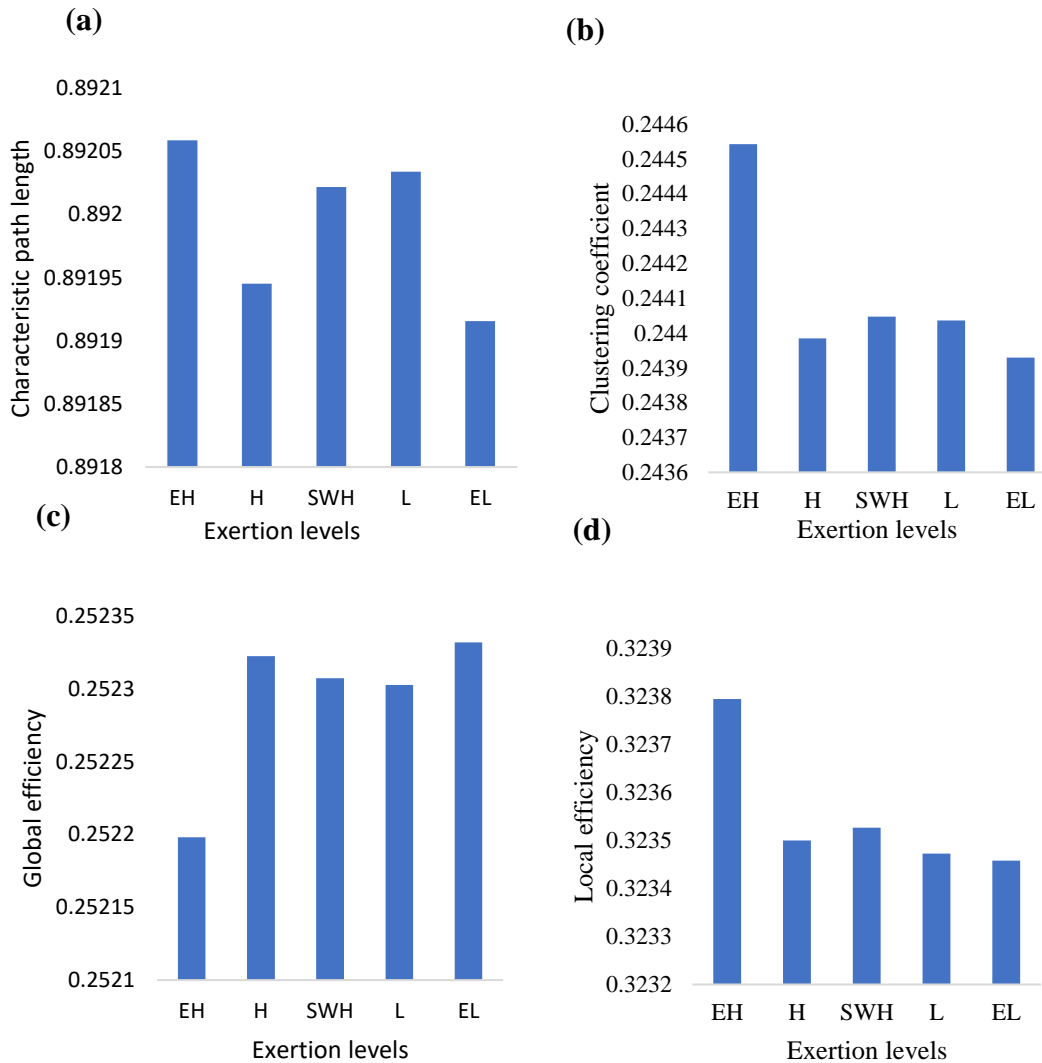


Figure 5-32: Graph theoretical network metrics showing main effects of different exertion levels (a) Characteristic path length (b) Clustering coefficient (c) Global efficiency (d) Local efficiency for beta coherence (where extremely hard [EH], hard [H], somewhat hard [SWH], light [L], and extremely light [EL]).

Over all, a significant increase in the global efficiency for the lower exertion levels compared to higher exertion levels (Figure 5-32C) was observed. The sharp decline of clustering coefficient in the extremely light exertion level compared to the other exertion levels suggest the disconnectivity between brain regions with low exertion levels (Figure 5-32B). Consequently, significant reduction in the local efficiency for the extreme light exertion level was observed compared to other exertion levels (Figure 5-32)

#### 5.2.7.2 Topological differences in local network

Nodal centrality measures that include betweenness centrality, degree centrality and nodal efficiency (Achard and Bullmore, 2007) were used to quantify the relative importance of a node within the overall network.

##### 5.2.7.2.1 Betweenness centrality

Betweenness centrality (BC) measures the centrality of a node which helps in identifying the most central nodes in a network. BC assesses the proportion of shortest paths between all node pairs in the network that pass through a given index node (Freeman, 1977).

Table 5-17 displays the statistically significant betweenness centrality between extremely hard, versus hard, somewhat hard, light, and extremely light for alpha band.

Table 5-17: Permutation test P-values for betweenness centrality between extremely hard (EH) versus hard (H), somewhat hard (SWH), light(L), and extremely light (EL) for alpha

ROI	Lobe	Structure	BA	EH vs H P-value	EH vs SWH P-value	EH vs L P-value	EH vs EL P-value
12	Frontal	Superior Frontal	BA 10	<0.05	<0.05	<0.05	<0.05
19	Frontal	Inferior Frontal	BA 45	<0.05	<0.05	<0.05	<0.05
23	Frontal	Inferior Frontal	BA 47	<0.05	<0.05	<0.05	<0.05
30	Parietal	Precuneus	BA 7	<0.05	<0.05	<0.05	<0.05
32	Parietal	Precuneus	BA 31	<0.05	<0.05	<0.05	<0.05
61	Temporal	Middle Temporal	BA 21	<0.05	<0.05	<0.05	<0.05
62	Temporal	Fusiform gyrus	BA 37	<0.05	<0.05	<0.05	<0.05
70	Temporal	Superior Temporal	BA 41	<0.05	<0.05	<0.05	<0.05
77	Occipital	Lingual Gyrus	BA 17	<0.05	<0.05	<0.05	<0.05

Table 5-18 displays the statistically significant betweenness centrality between hard versus somewhat hard, light, and extremely light for alpha band.

Table 5-18: Permutation test P-values for betweenness centrality between hard (H) versus somewhat hard (SWH), light(L), and extremely light (EL) for alpha

ROI	Lobe	Structure	BA	H vs SWH P-value	H vs L P-value	H vs EL P-value
12	Frontal	Superior Frontal	BA 10	<0.05	<0.05	<0.05
19	Frontal	Inferior Frontal	BA 45	<0.05	<0.05	<0.05
23	Frontal	Inferior Frontal	BA 47	<0.05	<0.05	<0.05
26	Parietal	Postcentral Gyrus	BA 2	<0.05	<0.05	<0.05
30	Parietal	Precuneus	BA 7	<0.05	<0.05	<0.05
32	Parietal	Precuneus	BA 31	<0.05	<0.05	<0.05
61	Temporal	Middle Temporal	BA 21	<0.05	<0.05	<0.05
62	Temporal	Fusiform gyrus	BA 37	<0.05	<0.05	<0.05
70	Temporal	Superior Temporal	BA 41	<0.05	<0.05	<0.05
77	Occipital	Lingual Gyrus	BA 17	<0.05	<0.05	<0.05

Table 5-19 shows the statistically significant betweenness centrality between somewhat hard versus light, and extremely light, and light versus extremely light for alpha band.

Table 5-19: Permutation test P-values for betweenness centrality between somewhat hard (SWH) versus light(L), and extremely light (EL), and light(L) versus extremely light (EL) for alpha

ROI	Lobe	Structure	BA	SWH vs L P-value	SWH vs EL P-value	L vs EL P-value
12	Frontal	Superior Frontal	BA 10	<0.05	<0.05	<0.05
19	Frontal	Inferior Frontal	BA 45	<0.05	<0.05	<0.05
23	Frontal	Inferior Frontal	BA 47	<0.05	<0.05	<0.05
26	Parietal	Postcentral Gyrus	BA 2	<0.05	<0.05	<0.05
30	Parietal	Precuneus	BA 7	<0.05	<0.05	<0.05
32	Parietal	Precuneus	BA 31	<0.05	<0.05	<0.05
61	Temporal	Middle Temporal	BA 21	<0.05	<0.05	<0.05
62	Temporal	fusiform gyrus	BA 37	<0.05	<0.05	<0.05
70	Temporal	Superior Temporal	BA 41	<0.05	<0.05	<0.05
77	Occipital	Lingual Gyrus	BA 17	<0.05	<0.05	<0.05

For all exertion levels, the key nodes were significantly located in the left superior frontal (BA 10), the right inferior frontal (BAs 45 and 47), the left precuneus (BAs 7 and 31), the right middle temporal (BA 21), the left fusiform gyrus (BA 37), the left superior temporal (BA 41), and the right lingual gyrus (BA 17) for the alpha band. For the beta network, significant differences were observed only in the inferior frontal (BA 47) for all force exertion levels.

The nodes with the highest BC are known as highly central or hubs. Such a node might play a controlling role in the passage of information through the network. The key node with highest BC in the extremely hard exertion level for alpha network located in the superior frontal gyrus in the right frontal lobe, corresponding to BA 10. For all other exertion levels, the key node with the highest BC was found in the left superior frontal brain region, corresponding to BA 11. The key node with highest BC in the beta network for all exertion levels was in the left lingual gyrus in the occipital lobe (BA 17). Therefore, we suggest that the aforementioned brain regions are critical for the efficient information processing within the brain network for exertion task.



### 5.2.7.2.2 Degree centrality analysis

The results for degree centrality (DC) for all subjects in all exertion levels for the alpha coherence are shown in ( ).

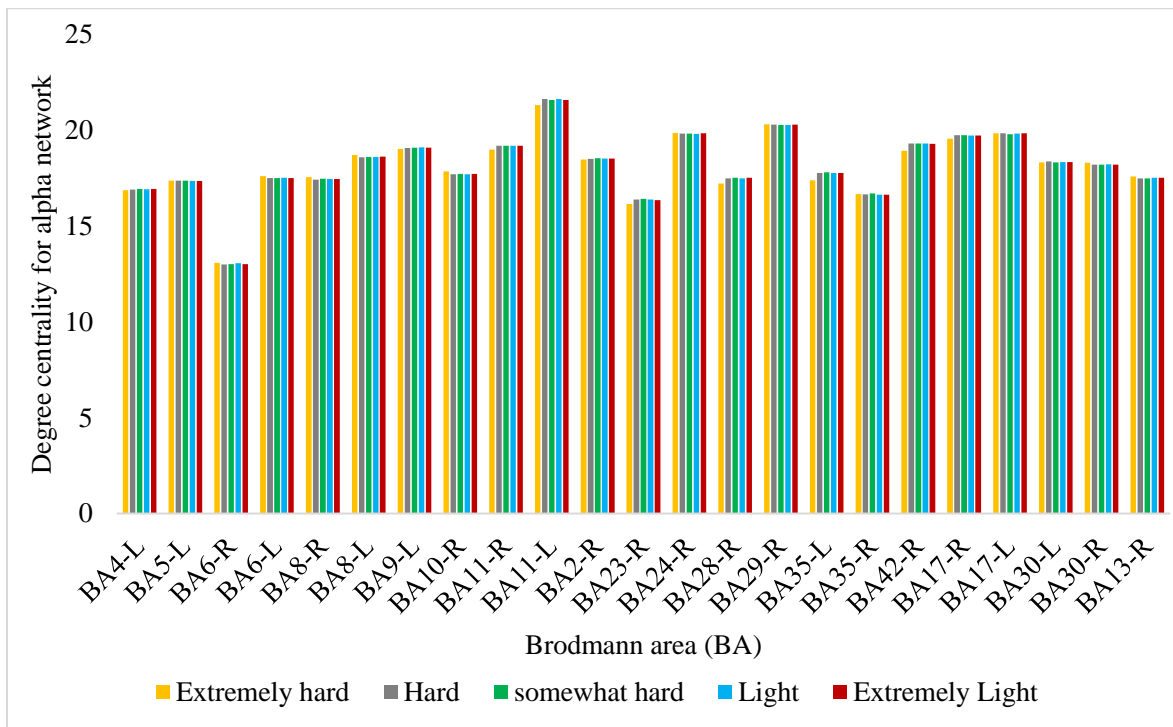


Figure 5-33: Results for degree centrality for alpha coherence network for all exertion levels

The extremely light exertion level exhibited a higher DC in all network nodes compared to other exertion levels. In all the exertion levels superior frontal gyrus in the orbitofrontal part corresponding to (BA 11-Left) was found to be the most important node in the alpha network in terms of the number of edges incident upon a node.

The results for degree centrality for all subjects in all exertion levels for the beta coherence is shown in (Figure 5-34). For all the exertion levels, the precentral gyrus part of the frontal lobe corresponding to (BA 44) was the most important node in the beta network in terms of the number of edges incident upon a node.

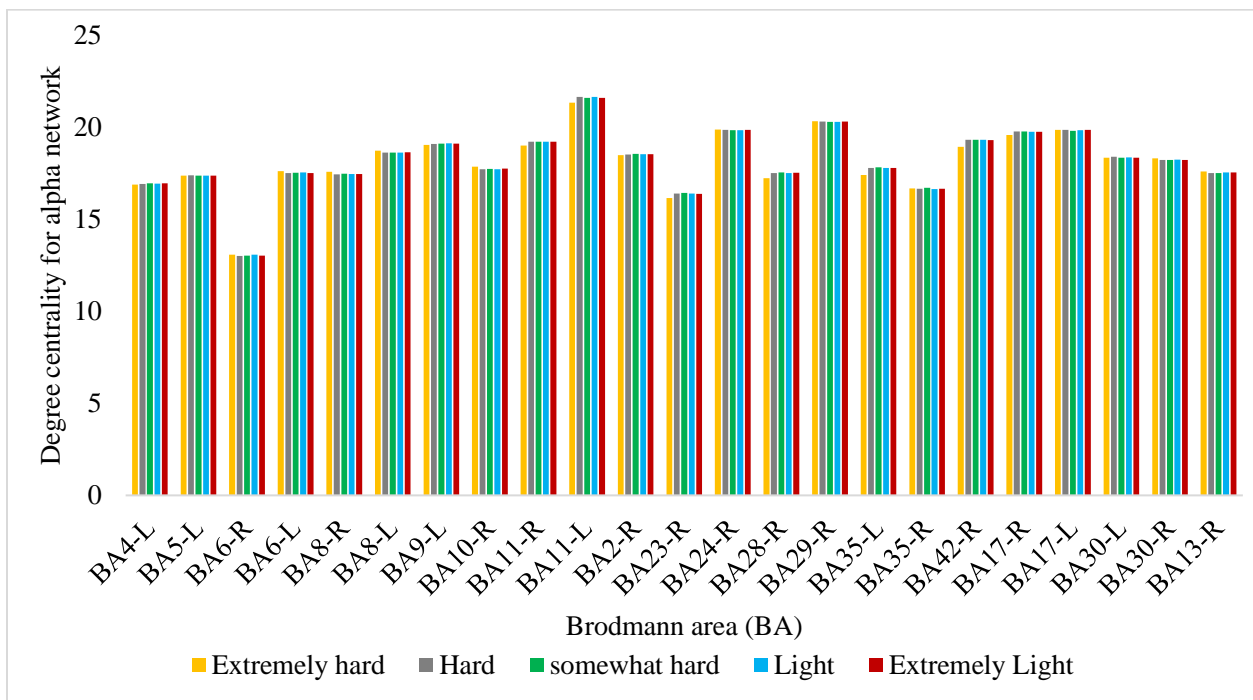


Figure 5-34: Degree centrality for beta coherence network for all exertion levels

### 5.2.7.2.3 Nodal efficiency

Nodal efficiency measures the ability of information exchange between a given node and the other nodes in the network or the ability of a node to propagate information with the other nodes in a network. A node with highest nodal efficiency indicates high capability of information exchange with other nodes and can therefore be categorized as a hub (Ma et al., 2018).

Table 5-20 shows the statistically significant nodal efficiency between extremely hard versus hard, somewhat hard, light, and extremely light exertion levels for alpha band. The significance level was set at  $p < 0.05$ .

Table 5-20: List of brain regions, lobe, brain structure, Brodmann area (BA) and P-value for the statistically significant nodal efficiency between extremely hard (EH) and hard (H), extremely hard (EH) and somewhat hard (SWH), extremely hard (EH) and light (L), and extremely hard (EH) and extremely light (EL) for alpha band.

ROI	Lobe	Brain structure	BA	P-value			
				EH vs H	EH vs SWH	EH vs L	EH vs EL
2	Frontal	Precentral Gyrus	BA4	0.0377	-	-	0.0259
12	Frontal	Superior Frontal	BA 10	0	0	0	0
16	Frontal	Medial Frontal Gyrus	BA25	-	0.0346	0.0235	-
19	Frontal	Inferior Frontal	BA 45	0	0	0	0
23	Frontal	Inferior Frontal	BA 47	0	0	0	0
26	Parietal	Postcentral Gyrus	BA 2	0	0	0	0
30	Parietal	Precuneus	BA 7	0	0	0	0
32	Parietal	Precuneus	BA 31	0	0	0	0
39	Limbic	Cingulate Gyrus	BA24	-	0.0219	-	-
58	Limbic	Posterior Cingulate	BA23	-	-	-	0.0385
61	Temporal	Middle Temporal	BA 21	0	0	0	0
62	Temporal	Fusiform gyrus	BA 37	0	0	0	0
64	Temporal	Superior Temporal	BA38	-	-	-	0
70	Temporal	Superior Temporal	BA 41	0	0	0	0
74	Temporal	Transverse Temporal	BA42	0.0021	-	-	-
77	Occipital	Lingual Gyrus	BA 17	0	0	0	-

Table 5-21 shows the statistically significant nodal efficiency between hard versus somewhat hard, light, and extremely light exertion levels for alpha band. The significance level was set at  $p < 0.05$ .

Table 5-21: List of brain regions, lobe, brain structure, Brodmann area (BA) and P-value for the statistically significant nodal efficiency between hard (H) and somewhat hard (SWH), hard (H) and light (L), and hard (H) and extremely light (EL) for alpha band.

ROI	Lobe	Brain structure	BA	P-value		
				H vs SWH	H vs L	H vs EL
5	Frontal	Middle Frontal Gyrus	BA 6	-	0.0338	-
12	Frontal	Superior Frontal	BA 10	0	0	0
14	Frontal	Middle Frontal Gyrus	BA 11	0.0216	-	-
19	Frontal	Inferior Frontal	BA 45	0	0	0
23	Frontal	Inferior Frontal	BA 47	0	0	0
25	Parietal	Postcentral Gyrus	BA 2	0	0	0
26	Parietal	Postcentral Gyrus	BA 2	0	0	0
30	Parietal	Precuneus	BA 7	0	0	0
32	Parietal	Precuneus	BA 31	0	0	0
37	Limbic	Posterior Cingulate	BA23	-	-	0
53	Limbic	Parahippocampal	BA34	0.017	-	0.0152
57	Limbic	Parahippocampal	BA36	-	-	0.05
61	Temporal	Middle Temporal	BA 21	0	0	0
62	Temporal	Fusiform gyrus	BA 37	0	0	0
70	Temporal	Superior Temporal	BA 41	0	0	0
77	Occipital	Lingual Gyrus	BA 17	0	0	0
78	Occipital	Lingual Gyrus	BA17	0.0311	-	-

Table 5-22 shows the statistically significant nodal efficiency between somewhat hard versus light, and extremely light exertion levels for alpha band. The significance level was set at  $p < 0.05$ .

Table 5-22: List of brain regions, lobe, brain structure, Brodmann area (BA) and P-value for the statistically significant nodal efficiency between somewhat hard (SWH) and light (L), and somewhat hard (SWH) and extremely light (EL) for alpha band.

ROI	Lobe	Brain structure	BA	P-value	
				SWH vs L	SWH vs EL
5	Frontal	Middle Frontal Gyrus	BA 6	0.0373	-

ROI	Lobe	Brain structure	BA	P-value	
				SWH vs L	SWH vs EL
12	Frontal	Superior Frontal	BA 10	0	0
13	Frontal	Superior Frontal	BA 11	-	0.0331
14	Frontal	Middle Frontal Gyrus	BA 11	0.011	-
19	Frontal	Inferior Frontal	BA 45	0	0
23	Frontal	Inferior Frontal	BA 47	0	0
25	Parietal	Postcentral Gyrus	BA 2	0	0
26	Parietal	Postcentral Gyrus	BA 2	0	0
30	Parietal	Precuneus	BA 7	0	0
32	Parietal	Precuneus	BA 31	0	0
33	Parietal	Precuneus	BA 31	-	0.0347
35	Parietal	Inferior Parietal	BA40	0.0203	0.0142
38	Parietal	Posterior Cingulate	BA 23	-	0.0286
53	Limbic	Parahippocampal	BA34	0.0163	0.014
61	Temporal	Middle Temporal	BA 21	0	0
62	Temporal	fusiform gyrus	BA 37	0	0
64	Temporal	Superior Temporal	BA38	-	0
70	Temporal	Superior Temporal	BA 41	0	0
77	Occipital	Lingual Gyrus	BA 17	0	0
78	Occipital	Lingual Gyrus	BA17	-	0.0257

Table 5-23 shows the statistically significant nodal efficiency between light versus extremely light exertion level for alpha band. The significance level was set at  $p < 0.05$ .

Table 5-23: List of brain regions, lobe, brain structure, Brodmann area (BA) and P-value for the statistically significant nodal efficiency between light (L) and extremely light (EL) for alpha band.

ROI	Lobe	Brain structure	BA	P-value
				L vs EL
12	Frontal	Superior Frontal	BA 10	0
13	Frontal	Superior Frontal	BA 11	0.0405
19	Frontal	Inferior Frontal	BA 45	0
23	Frontal	Inferior Frontal	BA 47	0
25	Parietal	Postcentral Gyrus	BA 2	0
26	Parietal	Postcentral Gyrus	BA 2	0
30	Parietal	Precuneus	BA 7	0
32	Parietal	Precuneus	BA 31	0
33	Parietal	Precuneus	BA 31	0.0114
61	Temporal	Middle Temporal	BA 21	0
62	Temporal	fusiform gyrus	BA 37	0

64	Temporal	Superior Temporal	BA38	0
70	Temporal	Superior Temporal	BA 41	0
77	Occipital	Lingual Gyrus	BA 17	0

For all exertion levels in the alpha band, the highest regional efficiencies were found in the middle frontal gyrus of frontal lobe corresponding to BA 11 and the posterior cingulate of limbic lobe corresponding to BA 29. The lowest regional efficiencies were found in the superior frontal of the frontal lobe corresponding to BA 10, the inferior frontal in frontal lobe corresponding to BAs 45 and 47, the precuneus in the parietal lobe corresponding to BAs 7 and 31, the middle temporal gyrus in the temporal lobe corresponding to BA 21, the fusiform gyrus in the temporal lobe corresponding to BA 37, and the lingual gyrus in the occipital lobe corresponding to BA 17.

shows the statistically significant nodal efficiency between extremely hard, versus hard, somewhat hard, light, and extremely light exertion levels for beta band. The significance level was set at  $p < 0.05$ .

Table 5-24 shows the statistically significant nodal efficiency between extremely hard, versus hard, somewhat hard, light, and extremely light exertion levels for beta band. The significance level was set at  $p < 0.05$ .

Table 5-24: List of brain regions, lobe, brain structure, Brodmann area (BA) and P-value for the statistically significant nodal efficiency between extremely hard (EH) and hard (H), extremely hard (EH) and somewhat hard (SWH), extremely hard (EH) and light (L), and extremely hard (EH) and extremely light (EL) for beta band.

ROI	Lobe	Brain structure	BA	P-value			
				EH vs H	EH vs SWH	EH vs L	EH vs EL
23	Frontal	Inferior Frontal	BA 47	0	0	0	0

ROI	Lobe	Brain structure	BA	P-value			
				EH vs H	EH vs SWH	EH vs L	EH vs EL
29	Parietal Lobe	Postcentral Gyrus	BA 3	0.046	-	-	-
33	Parietal Lobe	Precuneus	BA 31	-	0.0408	-	0.0414
34	Parietal Lobe	Inferior Parietal	BA 40	-	0.0125	0.0142	0.0264
36	Parietal Lobe	Inferior Parietal	BA 40	0.0296	-	-	0.0336
49	Limbic Lobe	Posterior Cingulate	BA 30	-	0.0425	-	-
52	Limbic Lobe	Parahippocampal	BA 34	0.035	-	0.027	-
56	Limbic Lobe	Parahippocampal	BA 35	-	-	0.0162	-
58	Limbic Lobe	Posterior Cingulate	BA23	-	-	-	-
61	Temporal	Middle Temporal	BA 21	-	0.0161	-	-
66	Temporal	Middle Temporal	BA 39	-	-	-	0.0101
76	Occipital Lobe	Lingual Gyrus	BA 17	-	0.0211	-	0.0263

Table 5-25 shows the statistically significant nodal efficiency between hard versus somewhat hard, light, and extremely light exertion levels for beta band. The significance level was set at  $p < 0.05$ .

Table 5-25: List of brain regions, lobe, brain structure, Brodmann area (BA) and P-value for the statistically significant nodal efficiency between hard (H) and somewhat hard (SWH), hard (H) and light (L), and hard (H) and extremely light (EL) for beta band.

ROI	Lobe	Brain structure	BA	P-value		
				H vs SWH	H vs L	H vs EL
3	Frontal	Paracentral Lobule	BA 5	0.0077	-	0.0199
23	Frontal	Inferior Frontal	BA 47	0	0	0
29	Parietal	Postcentral Gyrus	BA 3	0.0465	-	-
36	Parietal	Inferior Parietal	BA 40	-	-	0.0274
57	Limbic	Parahippocampal	BA36	-	0.031	-
78	Occipital	Lingual Gyrus	BA17	0.0274	-	-
81	Occipital	Cuneus	BA 30	-	-	0.0233

Table 5-26 shows the statistically significant nodal efficiency between somewhat hard versus light, and extremely light exertion levels for beta band. The significance level was set at  $p < 0.05$ .

Table 5-26: List of brain regions, lobe, brain structure, Brodmann area (BA) and P-value for the statistically significant nodal efficiency between somewhat hard (SWH) and light (L), and somewhat hard (SWH) and extremely light (EL) for beta band.

ROI	Lobe	Brain structure	BA	P-value	
				SWH vs L	SWH vs EL
4	Frontal	Paracentral Lobule	BA 5	-	0.019
16	Frontal	Medial Frontal	BA 25	0.021	-
23	Frontal	Inferior Frontal	BA 47	0	0
38	Limbic	Posterior Cingulate	BA 23	-	0.026
57	Limbic	Parahippocampal	BA36	0.0028	-
76	Limbic	Lingual Gyrus	BA17	0.0174	-

Table 5-27 shows the statistically significant nodal efficiency between light versus extremely light for beta band. The significance level was set at  $p < 0.05$ .

Table 5-27: List of brain regions, lobe, brain structure, Brodmann area (BA) and P-value for the statistically significant nodal efficiency between light (L) and extremely light (EL) for beta band.

ROI	Lobe	Brain structure	BA	P-value
				L vs EL
21	Frontal	Middle Frontal Gyrus	BA 46	0.0315
23	Frontal	Inferior Frontal	BA 47	0.000
26	Parietal	Postcentral Gyrus	BA 2	0.0315
57	Limbic	Parahippocampal	BA36	0.0165
76	Limbic Lobe	Lingual Gyrus	BA17	0.0218

Interesting, for beta network the highest network efficiency was found in precentral gyrus of frontal lobe corresponding to BA44 and lingual gyrus in occipital lobe, corresponding to BA 17.



The minimum network efficiency was present in inferior frontal gyrus of frontal lobe corresponding to BA 47 and middle temporal gyrus in temporal lobe corresponding to BA 21.

A summary for the highest nodal centrality for alpha and beta for each exertion level is shown in (Table 5-28).

Table 5-28: Summary of the highest nodal centrality for alpha and beta for each exertion level

<b>Nodal centrality</b>	<b>Frequency band</b>	<b>Extremely hard</b>	<b>Hard</b>	<b>Somewhat hard</b>	<b>Light</b>	<b>Extremely light</b>
Betweenness centrality	Alpha	BA 10	BA 11	BA 11	BA 11	BA 11
Betweenness centrality	Beta	BA 17	BA 17	BA 17	BA 17	BA 17
Degree centrality	Alpha	BA 11	BA 11	BA 11	BA 11	BA 11
Degree centrality	Beta	BA44	BA44	BA44	BA44	BA44
Nodal efficiency	Alpha	BA 11 & 29	BA 11 & 29	BA 11 & 29	BA 11 & 29	BA 11 & 29
Nodal efficiency	Beta	BA44	BA44	BA44	BA44	BA44

### 5.2.8 Correlation between Force and Graph theory Measures

To investigate a possible relationship of exerted forces (N) and global graph theory measure, correlation analysis was performed to address (research question 4). Spearman rank correlation coefficients were calculated to determine the relationship between the exertion force effect and obtained global graph theory measure. The significant results are displayed in (Table 5-29). The extremely hard level of exertion force was positively correlated with the global efficiency for alpha coherence ( $r=0.629$ ,  $p=0.028$ ) (Figure 5-35), but not correlated with any other network measure. The light force exertion level was negatively correlated with path length for beta coherence ( $r=-$

0.643,  $p=0.024$ ) (Figure 5-36). No significant correlations were found between graph measures and other exertions including somewhat hard, hard, and extremely light exertion levels.

Table 5-29: Correlation analysis between graph measures and exerted forces (N)

Exertion level	Extremely hard	Light
Graph theory measure	Global efficiency for alpha coherence network	Path length for beta coherence network
P- value	0.031	0.024
Correlation coefficient	0.622	-0.643

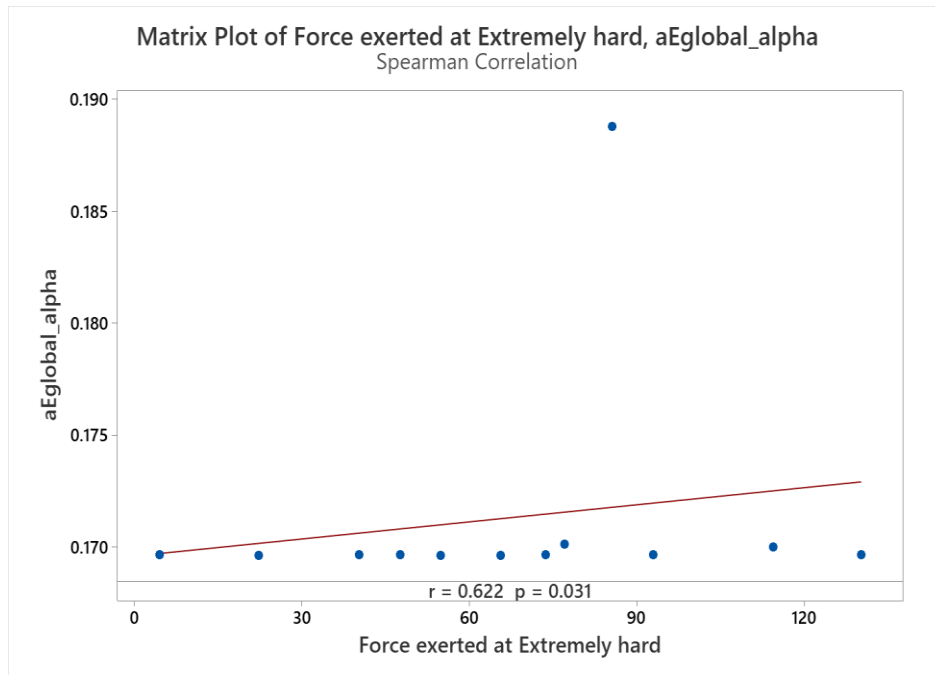


Figure 5-35: Scatterplot reporting the trend of extremely hard force over global efficiency for alpha network.

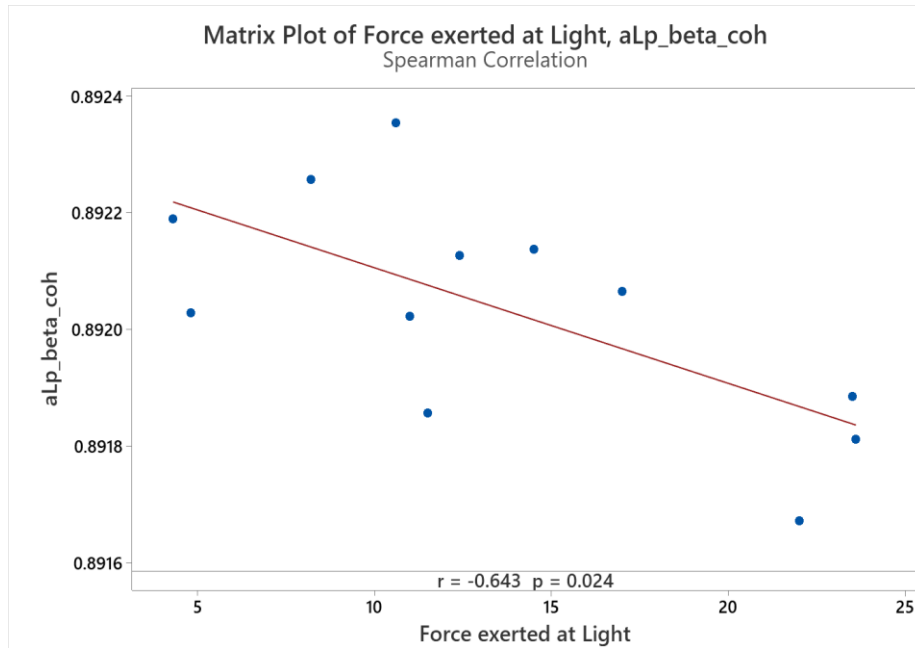


Figure 5-36: Scatterplot reporting the trend of light force over path length for beta network.

### 5.2.9 Correlation between RPPC and Graph theory Measures

The correlation between global measures and RPPC scores at predefined force exertion levels were computed using Spearman rank correlation for both frequency bands. The significant results are displayed in (Table 5-30). For RPPC ratings at the extremely hard exertion level, we found negative correlation between comfort scores and global efficiency for alpha coherence (Figure 5-37). For RPPC ratings at somewhat hard exertion level, we found positive correlation between comfort scores and local efficiency for beta coherence (Figure 5-38). No significant correlations were found between graph measures and the other exertion levels including hard, light and extremely light exertion level.

Table 5-30: Correlations between the RPPC levels at predefined exertion levels and the graph theory measures.

Exertion level	Extremely hard	Somewhat hard
Graph theory measure	Global efficiency for alpha coherence network	Local efficiency for beta coherence network
P- value	0.007	0.041
Correlation coefficient	-0.728	0.596

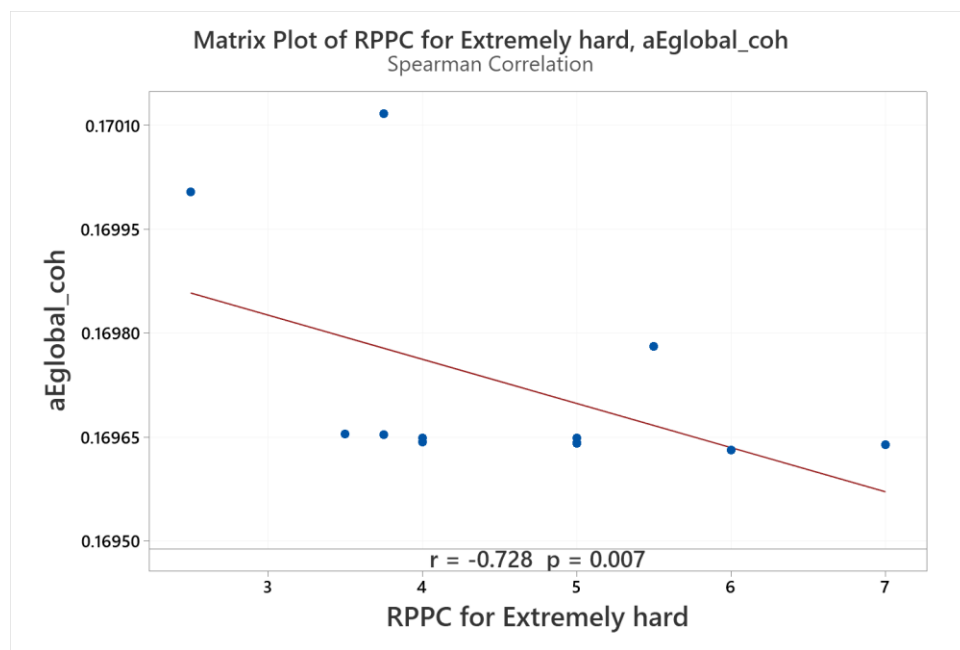


Figure 5-37: Scatter plots reporting the correlations between the RPPC at extremely hard exertion level and the Global efficiency for alpha coherence.

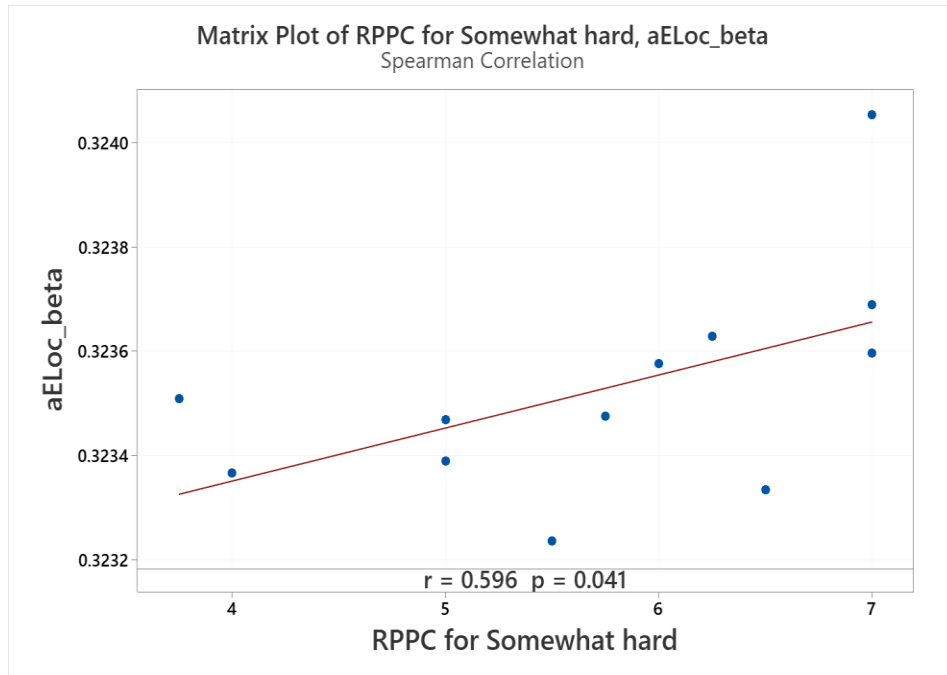


Figure 5-38: Scatter plots reporting the correlations between the exertion levels and the graph theory measures

## CHAPTER SIX CONCLUSIONS AND FUTURE WORK

This chapter provides the discussion, study limitations, recommendations for future work, and the study conclusions.

### 6.1 Discussion

To the best of our knowledge, this research is considered to be the first task-based EEG study to investigate the effect of induced force exertion on the EEG functional brain network at source level for healthy female participants using a graph-theoretical approach. We demonstrated that graph-theoretical measures applied to source EEG data could be used to identify brain network topological properties induced by different force exertion levels.

First, we have established an EEG preprocessing flow process chart to construct the EEG functional brain network at the source level. Second, we localized the current source density and obtained the maximum or minimum activated brain regions at each exertion level at each frequency band. Then, we computed the functional connectivity patterns induced by different force exertion levels and frequency bands using the coherence method. Finally, we computed the global and local graph theoretical measures to characterize the functional brain network at each exertion level and each frequency band. Our study revealed many findings concerning (a) force measures and RPPC scores, (b) source localization, (c) functional brain patterns, (d) global and local graph theory measures, and (e) the correlation between the RPPC, force, and global graph theory.

Results from pairwise comparison revealed no significant difference between hard versus somewhat hard, and light versus extremely light force levels.

#### 6.1.1 Force Measures and RPPC Scores

As expected, a negative correlation between the RPPC and exerted force was found. These results indicate that as the level of exerted forces in physical tasks increases, the participants' feeling of task comfort declines. This observation shed light on investigating the effect of the perception of physical comfort on neural activity in future work.

#### 6.1.2 Source Localization

The source localization method was applied to determine the activated brain regions at different predefined physical exertion levels for alpha and beta bands. For the alpha band, the maximum CSD was found in the middle frontal gyrus of the frontal lobe corresponding to BA 6 under extremely hard exertion level only. Findings from the current study are in line with previous results reported by Schneider et al. (2009b), concluding that high-intensity physical exercise was associated with an increase in the CSD of alpha in frontal brain areas to BA 6 and BA 9, respectively. For all other exertion levels, the maximum CSD was localized in the superior frontal gyrus of the frontal lobe corresponding to BA 8 in the prefrontal cortex. Therefore, when force exertion r

diminishes, the brain recruits more prefrontal neurons. A study by Thomas et al. (2008) found an increase in the prefrontal cortex at the beginning of physical exercise then reduced at the high workload. Greater neural activity in the prefrontal cortex (BA 9) and premotor cortex (BA6) is crucial for motor planning and sensory integration (Schneider et al., 2009b). In general, changes

in the brain activity in the frontal brain regions are involved in emotional processing (Faw, 2003; Coan and Allen, 2004; Umeda, 2012; Palmiero and Piccardi, 2017). Therefore, future research should consider the fact that tasks with forceful exertions might affect participant's mood and workers' general wellbeing (Ekkekakis and Petruzzello, 1999; Schneider et al., 2009a; Mikkelsen et al., 2017).

For beta activity, the maximum CSD was found in the postcentral gyrus of the parietal lobe corresponding to BA 5 under extremely hard exertion level only. For all other exertion levels, the maximum CSD was localized in the precuneus of the parietal lobe corresponding to BA 7, which is believed to be predominate to motor behavior in general (Hyvarinen et al., 1979; Schneider et al., 2009a), somatosensory perception (Heim et al., 2012), and conscious awareness (Vogt and Laureys, 2005). Our results are consistent with those by Fontes et al. (2015), who reported a high activation to the posterior cingulate gyrus and precuneus as the "hard" rate of

perceived exertion and hypothesized that "posterior region and precuneus might integrate physiological afferent signals from the periphery to promote emotional and conscious control during exercise through perceived exertion."

Pairwise comparison of CSD for the "extremely hard" exertion generates stronger oscillations than those for all the other exertion levels in the frontal lobe corresponding to BA 4, BA 6, and BA 43 for alpha band. The oscillations for the beta band were more strongly localized in the parietal lobe, corresponding to BA 2 and BA 40. Our results are similar to previous studies that reported the predominant role of CSD in the prefrontal cortex corresponding to BA 10&46 (Abeln et al., 2015) and in both the primary sensory cortex and prefrontal cortex (Brümmer et al., 2011b) with elevated



exercise intensity. Finally, the comparison of the hard exertion level with other exertion levels revealed many other different significant findings, as discussed below.

For the alpha band, the hard force exertion level, neural oscillated more strongly than at somewhat hard exertion level in precuneus of the parietal lobe corresponding to BA 7. This is consistent with Fontes et al. (2015), who reported an association between higher levels of perceived exertion and both posterior cingulate cortex and precuneus.

For the beta band, more frontal activations also were found at hard exertion level compared to both light and extremely light exertion levels for only BA 5 and BA 4.

An unexpected reduction in brain activity was observed when comparing hard with somewhat hard exertion levels in the frontal region for alpha in BA 47. A comparison of hard exertion with light exertion for the alpha band also revealed less activated brain regions in the temporal lobe corresponding to BA 22. Finally, a less activated occipital region was observed at hard exertion compared to light for the alpha band corresponding to BA 19.

Comparing somewhat hard with light showed a highly activated frontal lobe BA 31 for beta but less for alpha in the temporal lobe (BA 21.) Comparing light with extremely light exertion levels demonstrated a highly activated frontal lobe (BA 6) for the beta band but less parietal lobe (BA 7) for the alpha band.

### 6.1.3 Functional Brain Patterns

Functional connectivity estimators were computed using the coherence method that was proved sufficient to capture the amount of shared activity between brain regions at frequency domain

(Andrew and Pfurtscheller, 1999; Canteroa et al., 1999; Nolte et al., 2004; Sauseng et al., 2005; Comani et al., 2013; Bowyer, 2016; Storti et al., 2016). Comparing the extremely hard with all other exertion levels, the alpha network demonstrated a strong coupling in frontoparietal brain regions. The frontoparietal alpha network reflects attention modulation and perceptual regulation (Misselhorn et al., 2019). Furthermore, increments of functional connectivity over the frontoparietal may indicate the progression of muscular fatigue (Johnston et al., 2001). We found functional disconnections between the middle frontal gyrus and anterior cingulate when exertion level increases in beta frequency. Anterior cingulate plays an important role in cognitive control, emotions working memory processing and decision making. Such disconnections might indicate an impairment in cognitive performance leading to deterioration in task response time (Carter, 1998; Vogt, 2009; Etkin et al., 2011; Tops and Boksem, 2011).

#### 6.1.4 Brain Network

##### 6.1.4.1 Global measures

Using the graph theory measures, we investigated the global and local alterations of the cortical functional connectivity network in alpha and beta bands at predefined force exertion levels.

##### 6.1.4.1.1 Clustering coefficient

An increase in the clustering coefficient and local efficiency for alpha and beta coherence was observed at the extremely hard exertion level compared to the extremely low exertion. This observation suggests an increase in the functional segregation of the brain network during high force exertions. Storti et al. (2018) found an increase in the clustering coefficient during the isometric finger movement task indicating a strong connection of neighbor nodes among the

network during the voluntary arm movement task. However, high mental workload tasks were found to diminish the local clustered connectivity (Sciaraffa et al., 2017). Others suggested that an increase of clustering coefficient is associated with better performance of working memory (Dai et al., 2017).

#### 6.1.4.1.2 Path length and global efficiency

The reduction of characteristic path length at high exertion levels reflects a higher global efficiency for transferring the parallel information. Therefore, we suggest that the brain is more efficient for processing and transferring information when the physical task requires more exertion. Our results are in line with previous studies (see Kar et al., 2011; Chua et al., 2017; Han et al., 2019). The exhibition of small-worldness organization for alpha coherence network indicates the optimal functional segregation and integration under the extremely hard exertions compared to extremely low exertion levels. These results are also consistent with a previous study by Ren et al. (2015) that found an increase in small-worldness, especially in the alpha band during the performance of a task with a high workload level compared to an easy task.

We found that the brain functional network has shifted to a more ordered network configuration for the beta network. Similar phenomena were observed in brain activity after performing a sustained attention task (Breckel et al., 2013). In the present study, the global efficiency was enhanced under hard exertion conditions for the alpha band but not for the beta band. The above results might indicate an enhanced performance during the hard exertion task with more integration of processing in the brain network. The higher global structure in the alpha band might be attributed to the importance of the alpha network in the information processing and the need for a

particular type of attention required for coping with the high force exertion tasks (Klimesch, 2012). In comparison, the lower global structure in the beta band under hard exertion levels might indicate the reduction in processing the sensory information and cognitive functioning during high demanding force tasks.

#### 6.1.4.1.3 Local efficiency and modularity

Greater cognitive efforts induce the presence of the human functional brain networks that are more efficient but also exhibit less economical network configurations (Kitzbichler et al., 2011). Furthermore, mentally fatiguing tasks have been associated with the human functional brain networks that are more economical but also less efficient (Zhao et al., 2017; Li et al., 2019). In this study, an increase of local efficiency for both frequency bands was associated with elevated force exertion levels. In accordance with previous findings (Huang et al., 2016; Dai et al., 2017; Kakkos et al., 2019), the increment of local efficiency suggests that brain regions are communicating and cooperating to a larger degree as the physical force exertion level increases. Modularity has been a good estimator for network robustness (Kim and Cho, 2016) and has been used to predict changes in the working memory capacity (Stevens et al., 2012). The results of the present study suggest that high force exertion.

tasks provoke alpha coherence networks with a more modular network configuration, contrary to the reported results regarding cognitive effort effects (Kitzbichler et al., 2011).

#### 6.1.4.2 Local measures

To investigate the effects of force exertion levels on the nodal properties, three centrality measures were calculated, such as betweenness centrality (BC), degree centrality (DC), and nodal efficiency (NE). For the alpha network, the key node with the highest BC in the extremely hard exertion level was located in the superior frontal gyrus of the right frontal lobe corresponding to (BA 10). For all other exertion levels, the key node with the highest BC was located in the left superior frontal corresponding to (BA11). For the beta network, the key node with the highest BC for all exertion levels was located in the left lingual gyrus of the occipital lobe (BA 17). Therefore, we suggest that the aforementioned brain regions play a vital role in the flow of information and the global information integration between different brain regions during the force exertion task.

Another centrality measure is the degree centrality. We did not find much difference between the different exertion levels. Particularly, for all exertion levels, the region with the highest degree centrality for the alpha network was found in the superior frontal gyrus corresponding to (BA 11), whereas the region with the highest degree centrality for the beta network was found in the precentral gyrus corresponding to (BA 44). Therefore, these regions play an essential role in the connectivity of the whole network during force exertion tasks and also facilitate functional integration.

The last centrality measure is the nodal efficiency which measures the ability of information propagation between a node and the remaining nodes in the network. We did not find much difference between the different exertion levels in nodal efficiency. Particularly, for all exertion

levels in the alpha network, two nodes were found to have the highest nodal efficiency. These are the middle frontal gyrus and posterior cingulate corresponding to B11 and 29, respectively.

Whereas for the beta network for all exertion levels, the highest nodal efficiency was found in the precentral gyrus corresponding to BA 44. Therefore, these nodes have the highest capability of information transmission with all other nodes during the force exertion task.

## 6.2 Study Limitations and Future Implications

The present study results demonstrate that graph-theoretical measures can be used to quantify the changes in the brain network topological properties induced by various physical force exertions. However, many challenges must still be addressed to achieve further progress. Although the existing literature suggests that the sample size of 12 participants is not too small, the participant sample size needs to increase further. Future research is needed to study the perception of both static and dynamic force exertions in other body parts such as legs and torso. We may consider theta and gamma frequency bands in future perceived exertion studies. Future studies may also pay more attention to connectivity estimators' methods to investigate the difference in the network topological properties.

Although the majority of previous work have binarized the brain network to remove weak, noisy, and insignificant connections in the network, other studies reported that the weighted graphs may contain more information and might ensure greater sensitivity in response to distractors effect than unweighted (Bola and Sabel, 2015; Storti et al., 2016). In particular, the choice of the thresholding

value is crucial since it significantly affects the network topology properties. None of them are free from bias, requiring future investigation (van Wijk et al., 2010; Toppi et al., 2012). The superior temporal resolution of EEG helps to capture dynamic changes in brain activity. Consequently, the implementation of the dynamic functional connectivity method is very promising for future neuroergonomics studies.

### 6.3 Conclusions

The study findings, based on graph-theoretic measures, underline the changes in the functional human connectome and show how brain network topological changes at different force exertion levels. The use of the graph-theoretical approach may represent a clear methodological advancement to extend the current understanding of the neurophysiological basis of physical exertions with varying levels of force and can help improve the workplace design to maximize the workers' physical and mental well-being.

### 6.4 Research Contribution

The results of this study provide the following contributions: (1) Investigation of the effects of different levels of force on whole-brain functional connectivity at the source level (2) Combination of the functional connectivity and graph theoretical measurements to quantify the functional brain network topological properties during an isometric force exertions task performed by female

participants. (3) Assessment of the correlations between the brain network characteristics for alpha and beta bands and human performance, i.e., different levels of force exertion and RPPC.



**APPENDIX A**  
**REVIEWED PHYSICAL NEUROERGONOMICS ARTICLES**

A summary of the relevant information from the included articles which displays physiological measurements, the number of EEG electrodes, EEG index, characteristics of participants, domain, experimental task, artifact removal method, and feature extraction method.

(alpha [ $\alpha$ ], beta [ $\beta$ ], Bereitschaftspotential [BP], contingent negative variation [CNV], delta [ $\delta$ ], electroencephalography [EEG], Electromyography [EMG], electrooculography [EOG], energy ratio of alpha to beta [ $E\alpha/\beta$ ], event related potentials [ERP], females [f], finite impulse response filter [FIR], fast Fourier transform [FFT], gamma [ $\gamma$ ], independent component analysis [ICA], Lempel-Ziv complexity [LZC], males [M], movement-monitoring potential (MMP), motor potential (MP), movement-related cortical potential (MRCP), maximum voluntary contraction [MVC], mutual information [MI], power spectrum density [PSD], readiness potential (RP), short time Fourier transform [STFT], spectral coherence value [SCV], theta [ $\theta$ ]).

#	Author	Physiological measurement	Reference	EEG index	Domains	physical activity	Subject gender & number	Artifact removal method	Features Extraction method
1	(Freude and Ullsperger, 1987)	14 channels EEG, EOG & EMG	Linked earlobes	BP	MVC force	Handgrip	M=9	Not mentioned	Averaging signals
2	(Shibata et al., 1997)	3 channels EEG & EMG	Not mentioned	MP & grand mean MRCP	MVC force	Elbow flexions	M=10	Bandpass filter	Epochs from -200 to about -50 milliseconds
3	(Siemionow et al., 2000)	2 channels EEG & EMG	Cz & C3 referred linked earlobes	Magnitude of MRCP	MVC force	Elbow flexion	M=6 F=2	visually check	Averaging signals
4	(Johnston et al., 2001)	30 channels EEG & EMG	Linked earlobes & average reference	Average of BP, MP, & MMP	Muscle fatigue	Hand grasping	6 unknown	visually check & band pass filter	BP:1500 ms before and 5500 ms after trigger MP: the mean from 250 to100 MMP:from 2000 to 4000 ms after
5	(Slobounov et al., 2002)	17 channels EEG	Linked earlobes	Average of BP, MP, & amplitude of MMP	MVC force	Multi-finger isometric force	6 unknown	visually check & NeuroScan's software for ocular artifact	Averaging signals Epochs between 600 &500
6	(Dirnberger et al., 2004)	9 channels EEG	Linked earlobes	MRCP Amplitude of MMP	Muscle fatigue	Index finger movement	Group 1 M=16 F=17	Unknown	Averaging signals

#	Author	Physiological measurement	Reference	EEG index	Domains	physical activity	Subject gender & number	Artifact removal method	Features Extraction method
7	(Slobounov et al., 2004)	17 channels EEG	Linked earlobes	Average of BP, MP & MMP	Perception of effort	Isometric finger movement	6 unknown	visually check	Averaging signals
8	(Nascimento et al., 2005)	40 channels EEG & EOG	Earlobes	Average of RP, MP & MMP	Torque	Isometric plantar flexion tasks	M=6 F=3	visually check & band-pass filter	Averaging signals
9	(Schillings et al., 2006)	32 channels EEG, EOG & EMG	Linked mastoids	Average of RP	Muscle fatigue	Isometric Hand gripping	F=14	visually check, band-pass filter & automatic EOG removal	Averaging signals
10	(Liu et al., 2007)	64 channels EEG	linked earlobes	MRCP negative potential	Muscular fatigue	Hand gripping	M=7	Visual check, bandpass filter, & PCA	Averaging signals
11	(Flanagan et al., 2012)	12 channels EEG	Linked ears	Mean rectified amplitude	Muscular fatigue	Repetition squat exercise	M=7	FIR, spatial filters & visually check	Averaging signals
12	(de Morree et al., 2012)	62 channels EEG & EMG	CZ	Amplitude of MRCP	Perception of effort	Unilateral weightlifting with the elbow flexors	16 unknown	visually check & band-pass filter	Averaging signals
13	(Berchicci et al., 2013)	64 channels EEG & EMG	left mastoid then re-reference to average mastoids	Amplitude of MRCP	Muscular fatigue	Isometric knee extensions	M=10 F=8	visually check	Averaging signals
14	(Morree et al., 2014)	59 channels EEG & EMG	CZ then re-referenced to the average reference	Amplitude of MRCP	Perception of effort	Isometric knee extension	F=12	bandpass filter & ICA	Averaging signals
15	(Spring et al., 2016)	64 channels EEG	Average reference	Amplitude of the MRCP	Muscular fatigue	Cycling with knee extension	M=20	visually check, band pass filters, & low pass filter	Averaging signals
16	(Guo et al., 2017)	64 channels EEG, EMG & EOG	Re-reference to average	Amplitude of MP	Perceived of effort	Hand gripping	28 unknown	visually check, & low pass filter	Averaging signals
17	(Kamijo et al., 2004b)	3 channels EEG	Linked earlobes	P300	The effect of physical workload & mental task on information processing	Cycling	M=12	High cut filters	positive peaks that appeared in a post-S2 window of 250–500 ms.
18	(Mijović et al., 2016)	24 channels EEG	FCz then re-reference to the average of the mastoid channels	P300	The effect of physical & mental task on attention	Manual assembly task with or without instructions	M=14	Bandpass & ICA (EEGLAB)	Averaging signals
19	(Zink et al., 2016)	24 channels EEG & EMG	re-referenced offline to the mean of TP9 & TP10	P300	The effect of physical workload & cognitive task on attention	Cycling with auditory	M=11 F=4	Bandpass & ICA	Averaging signals

#	Author	Physiologic al measur ement	Reference	EEG index	Domains	physical activity	Subject gender & number	Artifact removal method	Features Extraction method
2 0	(Allami et al., 2014)	32 channels EEG	Average reference	N2 component	Motor training	Hand grasping	M=7 F=4	Band-pass filtered	Averaging signals
2 1	(Breitling et al., 1986)	16 channels EEG & EMG	Average reference	PSD for $\delta$ , $\theta$ , $\alpha$ , lower $\beta$ & upper $\beta$	workload	Finger movement	14 un known	visually check, & band-pass filtered	FFT
2 2	(Kubitz and Mott, 1996)	4 channels EEG	referenced to the vertex	PSD of $\alpha$ & $\beta$	Effect of physical or mental workload on information processing	Cycling and/or watching a videotape	M= 20 F=14	Low pass filter	Unknown
2 3	(Cochin, 1999)	14 channels EEG& EOG	common average	PSD for $\theta_1$ , $\theta_2$ , $\alpha_1$ , $\alpha_2$ , $\beta_1$ , $\beta_2$ & $\beta_3$	Observation & execution	Finger movement	M=10 F=10	visually check & automatic EOG correction	FFT
2 4	(Slobounov et al., 2000)	15 channels EEG& EOG	Linked mastoid	PSD for $\theta$ & $\gamma$	Stress & emotion exhaustion	visuomotor task (computer game)	M=6 F=2	visually check, & band-pass filter	FFT
2 5	(Nybo and Nielsen, 2001)	3 channels EEG	Paired mastoid	PSD $\alpha$ , $\beta$ & $\alpha/\beta$	Perception of effort	Cycling	14 unknow n	band-pass filter	FFT
2 6	(Nielsen et al., 2001)	2 channels EEG	Paired mastoid	PSD $\alpha$ , $\beta$ & $\alpha/\beta$	Muscular fatigue	Cycle ergometer	M=7	Not mentioned	FFT
2 7	(Abdul-latif et al., 2004b)	2 channels EEG & EMG	Ipsilateral ear	RMS for an $\alpha$ , $\beta$ , & $\gamma$	Muscle fatigue	Hand movement	M=15 W=10	Low pass filter, high pass filter, notch filter, & visually check	An algorithm written in MATLAB
2 8	(Smit et al., 2005)	3 channels EEG & EOG	Left mastoid	PSD of $\delta$ , $\theta$ , $\alpha$ , $\beta_1$ & $\beta_2$	The effect of physical & mental effort on attention	Cycling with mental task	M=8 F=36	Visually check & bandpass filtered	FFT
2 9	(Ng and Raveendran, 2007)	55 channels EEG & EOG	Linked earlobes	PAF	Physical fatigue	Hand gripping	M=8	Regression coefficient	FFT for PSD The center of gravity method for PAF
3 0	(Bailey et al., 2008)	8 channels EEG	Linked earlobes	PSD of $\theta$ , $\alpha_1$ , $\alpha_2$ , $\beta_1$ & $\beta_2$	Workload (Exercise intensity)	Cycle ergometer	M=20	High & low pass filtered	FFT
3 1	(Zadry, H. R. et al., 2009)	4 channels EEG & EMG	Piciform bone	RMS for $\alpha$	Stress & emotion exhaustion	Light assembly task	M=3 F=3	Bandpass filters	Not mentioned
3 2	(Sulaiman et al., 2009)	2 channels EEG	Ear lobe	PSD of $\beta$	Stressful & emotional exhaustion	Stress exercise on treadmill	M=3 F=2	Butterworth & Bandpass Filter	STFT
3 3	(Ftaiti et al., 2010)	1 channel EEG	Not mentioned	PSD $\alpha$ , $\beta$ & $\alpha/\beta$	Muscular fatigue	cycling exercises	F=7	Not mentioned	FFT
3 4	(Zadry and Dawal, 2010)	4 channels EEG, EOG &EMG	Bipolar	Mean PSD of $\alpha$	The effect of mental &physical workload on fatigue	Assembly with mental task	M=10 F=10	bandpass filter	FFT
3 5	(Zadry, H. R. et al., 2010)	8 channels EEG, EOG & EMG	Bipolar	PSD of $\alpha$ bands	Workload	Light assembly	M=5 F=3	band-pass filter	FFT

#	Author	Physiological measurement	Reference	EEG index	Domains	physical activity	Subject gender & number	Artifact removal method	Features Extraction method
3 6	(Ng and Raveendran, 2011)	64 channels EEG	Average reference	Normalized PSD of $\theta$ , $\alpha$ & $\beta$	Muscular fatigue	Hand gripping	M=10	Blind Source Separation method with the Wavelet method & ICA	Fourier Transform
3 7	(Zadry et al., 2011)	4 channels EEG, EOG & EMG	Piciform bone	Mean PSD of $\alpha$	The effect of mental & physical workload on fatigue	Assembly with mental task	M=5 F=5	Visually check & bandpass filtered	FFT
3 8	(Baumeister et al., 2012).	22 channels EEG	Linked earlobes	Log PSD of $\theta$ & $\alpha$	Muscular fatigue	knee joint reproduction	M=12	Visually check & bandpass filtered	FFT
3 9	(Ma et al., 2013)	2 channels EEG & EMG	Not mentioned	PSD of $\theta$ & SMR	The effect of physical activity on mental workload	Occupational jobs in production line	M= 1	Bio Trace was used to filter the data	Not mentioned
4 0	(Nakayashiki et al., 2014)	8 channels EEG	A1 & A2 (i.e., left & right mastoids)	$\mu$ & $\beta$ ERD	Observation & execution	Hand grasping	11 unknown	Bandpass Filters	STFT
4 1	(Jagannath and Balasubramanian, 2014)	25 channels EEG & EMG	Not mentioned	PSD of $\theta$ , $\alpha$ , $\beta$ & ratio $\frac{\alpha+\theta}{\beta}$ .	The effect of physical & mental task on fatigue	Monotonous driving	M=20	Bandpass Filters	Wavelet packet decomposition
4 2	(Cao et al., 2015)	28 channels EEG & EMG	Apex nasi	PSD of $\alpha$ , $\beta$ & $\gamma$	MVC force & Physical fatigue	Handgrip	M=11	Band-pass filter & linear regression algorithm for ocular artifact	PSD by averaged periodograms.
4 3	(Aljuaid and Karwowski, 2016)	64 channels EEG	Ear lobe	PSD of $\theta$ , $\alpha$ , $\beta$ & $\gamma$	Strength capability	Manual lifting task	M=10 F=2	Band pass filter & ASR	FFT
4 4	(Jain et al., 2016)	8 channels EEG	Ear lobe	PSD of $\theta$ , $\alpha$ & $\beta$	Muscular fatigue	Manual lifting task	M=10 F=4	Bandpass filtered & IIR filter	Not mentioned
4 5	(Amo et al., 2017)	9 channels EEG EMG & EOG	FPz	PSD of $\gamma$	Motor training & learning	wrist extension	M=10 F=6	Bandpass, low pass, notch & Butterworth filters	FFT
4 6	(Aryal et al., 2017)	4 channels EEG	Not mentioned	$(\alpha+\theta) / \beta$	Physical fatigue	Manual lifting task	M=12	Moving average filters & visual check	Neuro Experiment er software
4 7	(Engchuan et al., 2017)	2 channels EEG	Not mentioned	PSD of $\delta$ , $\theta$ , $\alpha$ , $\beta$ & $\gamma$	Workload	bench press	M=9	Not mentioned	FFT
4 8	(Hwang et al., 2018)	4 channels EEG	Linked mastoid	PSD of $\delta$ , $\theta$ , $\alpha$ , $\beta$ & $\gamma$	Stress & emotion exhaustion	Manual lifting task	M= 10	band-pass filter, notch filter & ICA	Not mentioned
4 9	(Kim et al., 2018)	32 channels EEG	right earlobe	Mu ERD	Execution & imaginary	Finger tapping trials	M=10 F=4	EEGLAB	Not mentioned

#	Author	Physiologic al measurement	Reference	EEG index	Domains	physical activity	Subject gender & number	Artifact removal method	Features Extraction method
50	(Jebelli et al., 2018)	14 channels EEG	Linked mastoid	Valence & arousal ratio of $\alpha$ / $\beta$ , &	Stress & emotion exhaustion	Work on ladder vs work on confined space	M=11	ICA, low pass filter, high pass filter & notch filter.	correlation-based methods
51	(Jebelli et al., 2018b)	14 channels EEG	Linked mastoid	PSD of $\beta$	Stress & emotion exhaustion	sheet metal fabrication job	M=8	Low, high, notch Filter & ICA	Fourier transform
52	(Périard et al., 2018)	61 channels EEG	re-referenced to an average reference	PSD $\alpha$ , & $\beta$	Muscular fatigue	Cycling	11	Visually check & ICA	FFT
53	(Porter et al., 2019)	32 EEG channels	common average reference was positioned between Fpz & Fz	PSD for $\theta$ & Partial correlation (graph theory)	The effect of perceived physical & mental exertion on attention	Cycling & working memory	M= 8 F= 5	Band pass filter & ICA	FFT
54	(Pfurtscheller et al., 1998)	23 channels EEG, EOG& EMG	Right mastoid	ERD/ERS for $\alpha$ , $\beta$ & Mu rhythm ERD	Observation & execution	wrist, finger & thumb	11 unknown	Visual check & Bandpass filter	Not mentioned
55	(Pfurtscheller et al., 2000)	34 channels EEG, EOG& EMG	Left mastoid	Mu rhythm ERD	Observation & execution actions	finger & foot movement	M=8 F=4	Visual check & Bandpass filter	Not mentioned
56	(Muthukumaraswamy and Johnson, 2004)	128 channels EEG	Cz reference & re-referenced to average Mastoids	Mu rhythm ERD	Observation & execution	Gripping	M=9 W=7	visual inspection	FFT by hanning window
57	(Calmels et al., 2006)	19 EEG electrode	Mastoids	ERD/ERS for (7–10 Hz; 10–13 Hz; 13–20 Hz; & 20–30 Hz)	Observation & execution	Index finger movement	8 unknown	Visual check & Bandpass filter	ERD/ ERS using Neuroscan 4.1 software
58	(Pitto et al., 2011)	13 channels EEG	Linked ears	ERS ERD $\theta$ , $\alpha$ & $\beta$	Motor learning	Putting	M=5 F=2	band-pass filter & ICA	Not mentioned
59	(Zaepffel et al., 2013)	62 channel EEG	Average reference	ERD/ERS for $\beta$	Observation, preparation & execution	Hand grasping	M= 5 F=9	Visual check, low pass filter, Butterworth & band-pass filter	Continuous wavelet transform
60	(Storti et al., 2015)	21 channels EEG	Fz	PSD, ERD & Spectral coherence for $\alpha$ & $\beta$ (graph theory)	Execution	Arm movement	M = 7 F=3	Band pass filter & ICA	FFT
61	(Storti et al., 2016)	19 EEG channels	Fz	PSD, ERD & Spectral coherence for $\alpha$ & $\beta$ (graph theory)	Execution	Left/right arm movements	M= 7 F = 3	Band pass filter & ICA	FFT
62	(Storti et al., 2018)	64 channels EEG	Fz	PSD, ERD & lagged coherence for $\delta$ , $\theta$ , $\alpha$ & $\beta$	Execution	Reaching & grasping	10 unknown	Band pass filter & ICA	FFT

#	Author	Physiological measurement	Reference	EEG index	Domains	physical activity	Subject gender & number	Artifact removal method	Features Extraction method
6 3	(Babiloni et al., 1999)	128 channels EEG	Not mentioned	(graph theory) BP,RP,MP & $\alpha$ ERD	Observation, preparation & execution	Index finger movement	M=4	Bandpass filter	Averaging signals for ERP. Welch technique for power spectra Averaging signals
6 4	(Kamijo et al., 2004a)	3 channel EEG, EMG & EOG	Linked earlobes	Amplitude of CNV & PSD $\alpha$	Effect of workload on attention	Bicycle ergometer with reaction time task	M=12	High cut filters	Averaging signals
6 5	(Jochumsen et al., 2017)	4 channels EEG & EOG	Right ear lobe	MRCP, ERS/ERD for $\alpha/\mu$ & $\beta$	Motor training	Grasping	M=17 F=21	Bandpass & Butterworth filter	Averaging signals
6 6	(Liu et al., 2005b)	64 channels EEG & EMG	Linked mastoids	PSD of $\delta$ , $\theta$ , $\alpha$ & $\beta$ , MRCP for negative potential	Muscle fatigue	Hand gripping	M=7 F=1	visually check & bandpass filters	FFT for PSD by Hanning window Trigger averaged for MRCP Averaging signals
6 7	(Doppelmayr et al., 2007)	3 channels EEG	Mastoids	P300, N200, & ERS/ERD	Effect of physical task on attention	Auditory oddball paradigm with a footrace	M=1	Visually inspected & bandpass filtered	Averaging signals
6 8	(Wascher et al., 2014)	28 EEG channels & EOG	Linked mastoids	individual $\theta$ , $\alpha$ & the amplitude of P3&N2	Effect of physical & mental activity on attention	Handling & solving cognitive riddles	M=3 F=7	Visually check & regression-based method	Averages for a continuous Wavelet transform FFT
6 9	(Wascher et al., 2016)	2 channels EEG & EOG	Averaged mastoids	Gravity frequency for $\theta$ & $\alpha$ , ERD/ERS for $\theta$ & $\alpha$	Effect of physical task on mental fatigue on motivation	Handling some boxes with Simon task	25 Unknown	ICA	FFT
7 0	(Wang et al., 2017)	32 channels EEG	Average reference	PSD of $\alpha$ , $\beta$ & $\gamma$ , & sample entropy	Muscular fatigue	Hand gripping	M=18	ICA	Periodograms for PSD

#	Author	Physiological measurement	Reference	EEG index	Domains	physical activity	Subject gender & number	Artifact removal method	Features Extraction method
7 1	(Albuquerque et al., 2018)	8 channels EEG	Fpz & Nz	PSD of $\delta$ , $\theta$ , $\alpha$ , $\beta$ , $\delta$ to $\beta$ , $\theta$ to $\beta$ , & low $\gamma$ ; the amplitude modulation rate of change, & the magnitude & phase coherence between power spectra	Effect of physical task on mental workload	cycling with Multi-Attribute Task Battery II	M=24 F=23	band-pass filter	Hilbert transform
7 2	(Xu et al., 2018)	20 channels EEG	Reference bilateral mastoids	$E\beta$ , $E\alpha/\beta$ , SCV of $\beta$ & LZC	Effect of the physical activity on mental fatigue	cycling with N-back task	M= 5 F=9	Band pass filters, Butterworth & ICA (EEGLAB)	WPD using Daubechies
7 3	(Lin et al., 2017)	5 channels EEG & ECG	Left mastoid Re-reference common average	PSD & entropies	Workload	Cycling exercise	M=25 F=19	Bandpass filter	Morlet wavelet transform & Higuchi's fractal dimension
7 4	(Huang et al., 2003)	EEG & EMG	Not mentioned	FD	Muscle fatigue	Hand gripping	unknown	Unknown	Length of signal & k using the least square fit
7 5	(Liu et al., 2005a)	5 channels EEG	Linked mastoid	FD	MVC force	Handgrip	M=6 F=2	Visual check	Katz's algorithm, evcik's method, & Higuchi's method
7 6	(Yao et al., 2009)	64 channels EEG	Linked Mastoids	L1	Muscle fatigue	Handgrip	M=6 F=2	visual check & band-pass filtered	Mean exponential divergence or convergence of nearby trajectories in phase space
7 7	(Brümmer et al., 2011)	32 channels EEG	A triangle of FP1, FP2 & FZ	Magnitude current density	Workload	Rest & Cycling	M=15 F=11	Butterworth, notch-filter, automatic artifact correction algorithm & visually check	LORETA current density
7 8	(Yang et al., 2011)	64 channels EEG	linked earlobes	Nonlinear source strength	Preparation & execution	Isometric hand Handgrip contraction	M=4 F=4	visual check, low pass filter & ICA	LORETA current density estimation were performed



#	Author	Physiological measurement	Reference	EEG index	Domains	physical activity	Subject gender & number	Artifact removal method	Features Extraction method
79	(Fallani et al., 2008) GT	96 channels EEG (16 ROI)	Not mentioned	Alpha partial direct coherence	Observation & execution	Finger movement	M = 5	Low pass filters	using Curry software package Time-frequency
80	(Jin et al., 2012)	58 EEG channels	Right earlobe	MI	Imagination	Sequential finger-tapping task	Males = 12	Visual check	FFT for PSD Morlet wavelet transformation for MI cross spectrum
81	(Comani et al., 2013) FC	32 EEG channels	Common electrical reference	Alpha Coherence	Perception of effort and attention	Road-cycling athlete	n = 1 (gender is unknown)	Band pass filter	
82	(Kar and Routray, 2013)	19 EEG channels	forehead	Synchronization likelihood	Physical, mental, and visual fatigue	Walking, driving, and listening	Males = 12	FIR	Empirical mode decomposition
83	(Sengupta et al., 2014a) GT	19 channels EEG	Not mentioned	Horizontal visibility graph synchronization	Mental, physical & visual fatigue	Driving, treadmill, & visual tasks	M = 12	Band pass filter & power line removal	Time series
84	(Sengupta et al., 2014b)	19 channels EEG	Not mentioned	Weighted visibility graph similarity for 0.5 Hz to 30 HZ	Mental, physical & visual fatigue	Simulated computer driving game	M = 12	Band pass filter & power line removal	Time series
85	(Wang et al., 2018c)	32 EEG channels	NM	Phase synchronization	Physical fatigue	Repetitive forearm task	Adults: Males = 5 Females = 5 Children : Males = 4 Females = 6	Bandpass filter and ICA	FFT
86	(Cattai et al., 2018)	74 EEG channels	NM	Spectral coherence and imaginary coherence for $\theta$ , $\alpha$ , $\beta$ , $\gamma$	Execution	Grasping	Males and females = 10	ICA	Welch method for power spectrum
87	(Filho et al., 2018)	64 EEG channels	CAR	PSD & Pearson's correlation	Execution	Hand imaginary task	M = 7 F = 1	FIR and CAR filtering	Welch method for power spectrum motifs synchronization method

#	Author	Physiological measurement	Reference	EEG index	Domains	physical activity	Subject gender & number	Artifact removal method	Features Extraction method
88	(Shaw et al., 2019)	64 EEG channels	left earlobe	wPLI	Physical workload	Seated and walking	Males and females = 15	band pass, notch, butterworth filters, and ICA	Phase analysis cross-spectrum b

**APPENDIX B**  
**SUMMARY OF THE APPLICATIONS OF GRAPH THEORETICAL**  
**ANALYSIS**

Relevant information from the included articles, including the node definition, edge definition, graph theory metrics, number of participants with gender, domain, experiment, and primary findings.

Study #	Article	Node definition	Edge definition and direction	Graph theory metrics	Number of participants	Domain	Experiment	Primary findings
1	(Michelyannis et al., 2006b)	28 EEG channels	Synchronization likelihood Undirect	CC, PL, and $\sigma$	Group 1: Males = 14 Females = 6 Group 2: Males = 15 Females = 5	Working memory	Two-back working memory tests	Less-educated individuals exhibited more organized small-world network topologies in comparison with more highly educated individuals.
2	(Sauseng et al., 2007)	32 EEG channels	PLV Undirect	FC	Males = 5 Females = 7	Working memory	Finger movement	Greater phase coherence of the theta band was evident in the frontal and posterior parietal regions.
3	(Fallani et al., 2008)	96 EEG channels	PDC Direct	Density, node strength, strength distribution, link reciprocity, motifs, Eglobal, and Elocal	Males = 5	Motion	Dorsal flexion	The observed increase in network edges during the movement preparation phase demonstrates the need for greater information exchange in the execution of movement tasks. Decreased accessibility and increased centrality were observed during the preparation and execution of finger movement tasks.
4	(Liu et al., 2010)	32 EEG channels	DTF Direct	FC	Males = 50	Mental fatigue	Vigilance, arithmetic tasks, and switching tasks	The FC of the alpha band in the parietal to frontal lobes was weakened, whereas the FC in central area and the middle-to-left region of the beta and alpha bands increased during mental fatigue. The middle-to-right FC of the beta bands increased after the task.
5	(Jin et al., 2012)	58 EEG channels	MI Undirect	Enodal	Males = 12	Motion	Sequential finger-tapping task	An economical small-worldness was observed in the alpha and beta bands. The Eglobal value in the alpha band did not change, whereas an increase was observed in the beta band. An increased Enodal was evident in the bilateral primary motor and left sensory areas, whereas contrasting results were found in the posterior parietal areas. The MI increased in the beta band during the task, but not in the alpha band.
6	(Comani et al., 2013)	32 EEG channels	Coherence Undirect	FC	n = 1 (gender unknown)	Motion	Road-cycling athlete	During sustained movement, a strong FC was observed for the beta band in the frontal-motor area.

7	(Dimitriadis et al., 2013)	64 EEG channels	PLV Undirect	Elocal	Males = 1		Mental workload	Arithmetic tasks	The PLV of the alpha frequency was higher in the parietal occipital than in the prefrontal regions, and the task difficulty was best reflected in the parieto-occipital functional connections.
8	(Hassan et al., 2013)	256 EEG channels	PLV Undirect	Degree, number of edges, density, and betweenness	Males and females = 9		Cognitive workload	Spelling tasks	Asymmetric results from the left and right hemispheres were demonstrated by a higher density, betweenness, and node degree for the left hemisphere.
9	(Kar and Routray, 2013)	19 EEG channels	Synchronization likelihood Undirect	Degree, CC, and PL	Males = 12		Physical, mental, and visual fatigue	Walking, driving, and listening	An increase in the degree of connectivity and CC and a decrease in PL were observed during fatigue.
10	(Klados et al., 2013)	32 EEG channels	Magnitude square coherence Undirect	Node strength, Eglobal, Elocal, CC, PL, and $\sigma$	Males = 12 Females = 12		Working memory	Difficult calculations	During difficult mathematics, a denser alpha FC was observed in the fronto-parietal regions. The local and global alpha bands were efficient; however, the beta and gamma bands exhibited no differences in Eglobal, Elocal, or $\sigma$ .
11	(Sengupta et al., 2014a)	19 EEG channels	Horizontal visibility graph Undirect	CC and PL	Males = 12		Mental, physical, and visual fatigue	Driving, treadmill, and visual tasks	A strong FC was observed in the parietal and occipital lobes after fatigue tasks, with an increase in the CC.
12	(Sengupta et al., 2014b)	19 EEG channels	Weighted visibility graph similarity Undirect	CC and PL	Males = 12		Mental, physical, and visual fatigue	Simulated computer driving game	An increased CC in the parietal and occipital lobes demonstrated the occurrence of fatigue.
13	(Sun et al., 2014a)	64 EEG channels	PDC directed	CC, PL, and $\sigma$	Males = 15 Females = 17		Mental fatigue	PVT	Significant increases in weighted PL under a fatigued state and in functional connectivity in the left fronto-parietal brain region were observed.
14	(Sun et al., 2014b)	64 EEG channels	PDC Directed	FC	Males = 12 Females = 14		Mental fatigue	PVT	Different patterns were observed in the right and left sensorimotor regions during a state of fatigue. The middle frontal gyrus and several motor areas were crucial for sustained attention.
15	(Bola and Sabel, 2015)	128 EEG channels	PLV Undirect	CC, PL, modularity, and network hubs	Males = 10 Females = 8		Visual perception	Visual discrimination	A strong CC, interactions between hub nodes, and low modularity were observed in cognitive networks.
16	(Dimitriadis et al., 2013)	64 EEG channels	PLV Undirect	FC	Males = 9 Females = 7		Workload	Mental arithmetic task	The PLV of the theta and alpha bands in the frontal and parieto-occipital brain reflected the cognitive load.

	al., 2015)									
17	(Ghosh et al., 2015)	32 EEG channels	DFT Directed	Network density and node strength	Males = 3 and females = 3	Motion	Motor imagery tasks		The node strength for electrode C3 was observed to be high during right-hand movements.	
18	(Kong et al., 2015)	16 EEG channels	Granger causality Directed	CC, PL, Eglobal, and percentage of unconnected nodes	Males = 12 and females = 12	Mental fatigue	Simulated driving		A reduction in the ability of the human brain to integrate information was reflected by a decrease in Eglobal.	
19	(Ren et al., 2015)	32 EEG channels	PLV Undirect	$\Sigma$	Males = 8	Cognitive workload	Piloting with MATB		A small-world network topology was observed for the alpha bands during a high cognitive workload.	
20	(Storti et al., 2015)	21 EEG channels	Spectral coherence Undirect	Node strength, accessibility, betweenness, and eigenvector	Males = 7 Females = 3	Motion	Arm movements		The FC was found to be strong in the motor regions but weak in other regions. Less accessibility was reported in the central and motor areas during movement.	
21	(Vijayalakshmi et al., 2015)	40 EEG channels	MCC Undirect	Degree, CC, PL, Elocal, and Eglobal	Males = 9 Females = 1	Cognitive workload	Driving simulator		MCC was capable of detecting cognitive impairment. A high degree of connectivity during cognitive tasks indicated strong connections, high functional segregation, and global integration.	
22	(Wang et al., 2015)	19 EEG channels	Synchronization likelihood Undirect	FC	Males = 20	Fatigue	Driving		A weak FC was observed after long driving tasks.	
23	(Huang et al., 2016)	16 EEG channels	PDC Direct	Degree, Elocal, Eglobal, and degree distribution	Males = 19	Mental Workload	Playing and resting tasks		During play, Elocal was observed to be higher for the beta bands and lower for the theta bands in comparison to those for resting tasks.	
24	(Li et al., 2016)	11 EEG channels	PLI Undirect	CC, PL, $\sigma$ , Eglobal, and Elocal	Males = 8 Females = 12	Mental fatigue	Attention task		During fatigue, an increased betweenness centrality was observed in the frontal cortex. The CC and PL increased over time, indicating that the brain regions were more segregated and communicated with each other less efficiently. A reduced Eglobal and enhanced Elocal implied that brain resources might be reorganized and that the concerted activities within regions were more active, whereas interactions between regions were inhibited.	

25	(Storti et al., 2016)	19 EEG channels	Spectral coherence Undirect	Node strength, accessibility, betweenness, CC, centrality, and eigenvector	Males = 7 Females = 3	Motion	Left/right arm movements	The FC increased in the motor region during arm movements, and the node accessibility decreased with increases in node centrality during arm movements.
26	(Chua et al., 2017)	64 EEG channels	PLI Undirect	CC, PL, and Eglobal	Males = 18	Mental fatigue	Driving simulation	An increased CC and decreased PL were observed with mental fatigue.
27	(Cynthia et al., 2017)	16 EEG channels	PLV Undirect	CC, PL, Eglobal, and Elocal	Males = 10 Females = 10	Mental fatigue	Driving	The PLV was found to be able to measure changes in neuronal function.
28	(Dai et al., 2017)	64 EEG channels	Cross-coherence Undirect	Eglobal, CC, PL, Elocal, and betweenness	Males = 11 Females = 17	Working memory	N-back tasks	Memory load resulted in a higher functional integration in the theta bands and a lower functional segregation in the alpha bands. The theta PL and alpha CC were negatively correlated with reaction time, whereas the node betweenness of the theta bands was positively correlated with the reaction time.
29	(Dimitrakopoulos et al., 2017)	64 EEG channels	Pearson correlation Undirect	FC	Males = 11 Females = 17	Mental workload	N-back and mental arithmetic	Changes related to cognitive task difficulty were found to occur in the frontal theta and beta bands based on the features obtained from the functional connectivity.
30	(Li et al., 2017)	19 EEG channels	MI Undirect	Maximum eigenvalue and degree centrality	Males and females = 18	Mental fatigue	Mental arithmetic problems	The maximum eigenvalue increased as mental fatigue increased. The weighted degree centrality exhibited substantial changes during mental fatigue
31	(Ren et al., 2017)	64 EEG channels	Phase synchronization Undirect	$\sigma$	Males = 10	Mental workload	Flight simulation task with MATB	A more globally efficient but less clustered network was observed for a high-difficulty cognitive workload.
32	(Sciaraffa et al., 2017)	30 EEG channels	PDC direct	Nodal strength and CC	Males = 10	Mental workload	Piloting with MATB	The strength changed significantly with task difficulty. A higher workload corresponded to a lower CC in the central and parietal regions.
33	(Zhang et al., 2017)	64 EEG channels	PLI undirect	Eglobal, Elocal, and Enodal	Males = 20	Mental workload	Flight simulation	The Eglobal and Elocal values for the alpha and theta bands were higher in 2D tasks than in 3D tasks. The Enodal value decreased for both the alpha and theta bands with increasing mental workload.

34	(Zhao et al., 2017)	32 EEG channels	Coherence undirect	CC and PL	Males = 13 Females = 3	Mental fatigue	Driving fatigue	A significant increase in PL was observed for all EEG bands; however, an increase in CC was observed only for the delta, alpha, and beta bands.
35	(Cattai et al., 2018)	74 EEG channels	Spectral coherence and imaginary coherence undirect	Weighted node degree	Males and females = 10	Motion	Motor imagery	The spectral coherence in the beta activity outperformed the imaginary coherence in the contralateral motor cortex.
36	(Chen et al., 2018a)	40 EEG channels	Phase coherence undirect	FC	Males = 12	Mental fatigue	Driving	The phase coherence for the alpha and theta bands was high after a driving task.
37	(Chen et al., 2018b)	30 EEG channels	PLI undirect	Nodes, link degree, leaf fraction, kappa, diameter, eccentricity, betweenness centrality, tree hierarchy, and degree correlation	Males = 15	Mental fatigue	Driving	The PLI was observed to be high during drowsiness. The degree of delta activity was significantly lower during alertness, whereas the delta values for betweenness centrality and kappa were higher during a state of drowsiness. The degree of theta, BC, and kappa were significantly lower during a state of alertness than during drowsiness. Also, the authors reported a more organized integrated network during drowsiness compared to that during alertness for the theta frequency band.
38	(Dimitrakopoulos et al., 2018)	64 EEG channels	Generalized PDC direct	CC, PL, and $\sigma$	Males = 40	Mental fatigue	PVT with simulation driving	A positive correlation between PL and task duration was observed, and mental fatigue increased both CC and PL. A disruption in global integration was revealed in both fatigue tasks, whereas increased local segregation was observed only for the simulated driving task.
39	(Filho et al., 2018)	64 EEG channels	Pearson's correlation undirect	Degree, CC, PL, betweenness centrality, and eigenvector	Males = 7 Females = 1	Motion	Motion imagery	Graph theoretical metrics were shown to be useful features for classifying different hand movement tasks, especially the local properties of the network.
40	(Ghaderi et al., 2018)	21 EEG channels	Coherence Undirect	Degree, CC, transitivity, and Eglobal	Group 1, Case 1: Males = 11 Females = 6 Group 1, Case 2: Males = 14 Females = 11	Time perception	Mindfulness state task	Segregation of the beta network was found to be crucial for time perception.



					Group 2, Case 1: Males = 5 Females = 3				
					Group 2, Case 2: Males = 5 Females = 4				
41	(Taya et al., 2018)	62 EEG channels	DTF Direct	CC, normalized CC, normalized PL, PL, and $\sigma$	Males = 18	Workload	Piloting task (MATB)	During training, Eglobal initially decreased and subsequently increased, whereas Elocal and small-worldness exhibited opposite patterns. The centrality of nodes changed in the frontal and temporal regions.	
42	(Toppi et al., 2018)	60 EEG channels	PDC Direct	Degree, Eglobal, Elocal, and $\sigma$	Males = 6 Females = 11	Working memory	Sternberg item recognition	A small-world topology was evident in storage and retrieval.	
43	(Storti et al., 2018)	64 EEG channels	Lagged coherence undirect	CC, PL, and $\sigma$	Males and females = 10	Motion	Reaching and grasping movements	Movement was found to reduce the FC. The weighted PL decreased during left-hand movements.	
44	(Sun et al., 2018)	64 EEG channels	PDC Direct	Betweenness, PL, CC, and $\sigma$	Males = 12 Females = 14	Mental fatigue	PVT	During mental fatigue, the PL increased and $\sigma$ decreased, whereas the nodal betweenness decreased in the left frontal and middle central areas and increased in the right parietal areas. A prolonged time spent on the task reduced the local level of interconnectivity.	
45	(Wang et al., 2018a)	14 EEG channels	Synchronization likelihood undirect	Degree, CC, and Eglobal	Males = 10 Females = 2	Mental fatigue	Driving	A lack of awareness due to mental fatigue was demonstrated by an increase in the CC and network Eglobal in a sub-band (36–44 Hz).	
46	(Wang et al., 2018b)	14 EEG channels	Pearson correlation Undirect	CC and Eglobal	Males = 8 Females = 2	Mental fatigue	Driving fatigue	A dense FC was observed during fatigue, with an increase in the CC and PL as the driving time increased. The degree of FC gradually increased with time.	
47	(Wang et al., 2018c)	32 EEG channels	Phase synchronization Undirect	PL, CC, and degree centrality	Adults: Males = 5 Females = 5 Children: Males = 4 Females = 6	Physical fatigue	Repetitive forearm task	Different movement-related EEG potentials were observed in children and adults during physical fatigue.	

48	(Chen et al., 2019)	14 EEG channels	PLI Undirect	CC and PL	Males = 14	Mental fatigue	Real driving	CC and PL were reduced during fatigue, and a weak FC was observed in the frontal-to-parietal alpha and beta bands during drowsiness.
49	(Han et al., 2019)	62 EEG channels	Pearson correlation undirect	Degree centrality, CC, and PL	Males = 12 Females = 4	Mental fatigue	Driving task	As the degree of fatigue increased, the FC and CC increased, whereas PL decreased for the delta band.
50	(Ghaderi et al., 2019)	19 EEG channels	Coherence undirect	CC, PL, transitivity, Eglobal, degree centrality, and modularity	Males = 12 Females = 12	Mental workload	Mathematical task	During problem-solving, the beta band exhibited strong connectivity with high degrees of transitivity, clustering, and modularity. The alpha band exhibited a disrupted FC with a reduction in segregation. The theta band exhibited unaltered brain network function.
51	(Kakkos et al., 2019)	64 EEG channels	PLV undirect	CC, PL, Eglobal, and Elocal	Males = 33	Mental workload	Flight simulation	Increased alpha and beta bands were observed with increasing workload. The Eglobal beta pattern was evidently a unique trend.
52	(Li et al., 2019)	9 EEG channels	MI undirect	$\sigma$ , CC, and PL	Males = 20	Mental fatigue	Arithmetic task	Mental fatigue was reflected by a strong coupling connection and a reduction in the small-world network.
53	(Nguyen et al., 2019)	17 ROIs	PLV undirect	Hubs	Males = 4 Females = 8	Motion	Visuomotor	An FC pattern with hubs demonstrated the most central brain regions in a visuomotor task.
54	(Porter et al., 2019)	32 EEG channels	Partial correlation undirect	CC	Males = 8 Females = 5	Perceived physical and mental exertion	Cycling and working memory	The partial correlation of theta bands increased in the frontal region during working memory. Initially, the theta CC increased during both tasks and subsequently decreased significantly when the task became more difficult.
55	(Samima and Sarma, 2019)	64 EEG channels	NM	Nodal strength and CC	Males and females = 20	Mental workload	Working memory test battery	The nodal strength was higher when the workload difficulty was increased. Contrasting results were found for the CC.
56	(Shaw et al., 2019)	64 EEG channels	wPLI Undirect	FC	Males and females = 15	Physical workload	Seated and walking	A strong FC was observed in all brain regions for theta band during walking.
57	(Yuan et al., 2019)	32 EEG channels	PLI Undirect	Degree centrality, modularity, CC, PL,	Males = 5 Females = 5	Mental workload	Security inspection monitoring	During high-workload tasks, the average degree centrality between nodes was high, whereas for a low workload, the connectivity was weak. When the experts could not detect whether the blocked item was dangerous, the characteristic shortest

Eglobal,  
and  $\sigma$

path was the costliest. When there was no block but danger or when there was a block but no danger, the CC and degree of modularity increased. The highest Eglobal and small-worldness values were observed in cases of danger with no block. Thus, the highest coherence occurred for the target stimulus without any block.

**APPENDIX C**  
**ISOMETRIC STRENGTH TEST INSTRUCTIONS**

Before starting your first trial, you will be provided with the following instructions based on the protocol by Chaffin et al. (1978). In this task, the measurement of the isometric strength of your arm will take place using Jackson Strength Evaluation System (Figure C.1). Here you will be requested to exert a force without any movements. You will be requested to lift the chain as depicted in (Figure C.2)



Figure C.1: The Jackson Strength Evaluation System

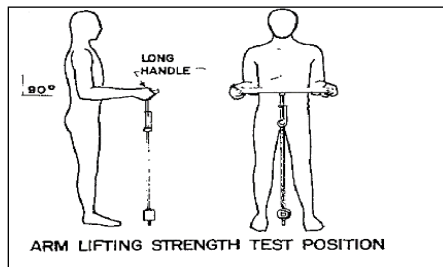


Figure C.2: Arm isometric strength based on Chaffin et al. (1978) protocol

This task will be demonstrated to you. Please ask questions if further clarification is needed. There will be Three attempts, the first attempt is warmup will not be counted. You will be given only almost 50% effort. This will guide you to know what you are going to do. After that, you will have three attempts for each area. You are required to do your best on all of them as your score will be the average among the three trials. During each trial, you will rest for 30 seconds or until you are ready. Once you are ready, wait for the tone from the software and then exert the required force for 3 seconds. You will have a rest for two minutes between each trial. Remember always you are required to stop if you feel pain or discomfort, stop exerting force immediately.

**APPENDIX D**  
**BORG'S RPE (6–20) SCALE (BORG, 1982)**

Borg's RPE (6-20) scale is a linear scale, ranges from 6 to 20, where 6 means "no exertion at all," and 20 means "maximal exertion."

**Question: How might you describe your exertion?**

**Borg's RPE scale**

<b>6</b>	<b>No exertion at all</b>
<b>7</b>	<b>Extremely light</b>
<b>8</b>	
<b>9</b>	<b>Very light</b>
<b>10</b>	
<b>11</b>	<b>Light</b>
<b>12</b>	
<b>13</b>	<b>Somewhat hard</b>
<b>14</b>	
<b>15</b>	<b>Hard</b>
<b>16</b>	
<b>17</b>	<b>Very hard</b>
<b>18</b>	
<b>19</b>	<b>Extremely hard</b>
<b>20</b>	<b>Maximal exertion</b>

**APPENDIX E**  
**RATING OF PERCEIVED COMFORT**



**Question: How you might describe your level of comfort?**

<b>0</b>	<b>No comfort</b>
<b>1</b>	<b>Very low comfort</b>
<b>2</b>	
<b>3</b>	<b>Fair comfort</b>
<b>4</b>	
<b>5</b>	<b>Moderate comfort</b>
<b>6</b>	<b>More than moderate comfort</b>
<b>7</b>	
<b>8</b>	<b>High comfort</b>
<b>9</b>	
<b>10</b>	<b>Very high comfort</b>

**APPENDIX F**  
**DATA COLLECTION FORM**

**Session 1: Maximum voluntary contraction (MVC)**

Exert the maximum force you can by pulling on the bar as hard as you can without jerking.

Force	
1	
2	
3	

**Session 2: Given RPE rate RPC:**

		Trials		
		1	2	3
<b>Somewhat hard</b>	Exert the force level that you believe corresponds to “ <b>somewhat hard.</b> ”			
	<b>Force</b>			
	For this exertion, please rate your comfort level in the scale from 0 to 10			
	<b>RPC-Numerical</b>			

The “Somewhat hard” reference will be changed depending on 5 different levels:

- Extremely light
- Light
- Somewhat hard
- Hard
- Extremely hard.

**APPENDIX G**  
**STUDY FLYER**

Are you interested in participating in a Neuroergonomics study?



**Study title: The Correlation between EEG Signatures and Perceptions Associated with Manual Materials Handling Tasks**

As a participant in this study, you would be asked to perform physically exerting exercises and complete a questionnaire afterwards. Your participation will take approximately two hours including the preparation stage. You will have the option to participate in up to 9 different sessions if enrollment numbers allow it (maximum 400 participants)

**Participants must:**

- Be a healthy female adult with no history of neurological, musculoskeletal, or psychological diseases, free of medication or hormonal treatment.
  - Refrain from caffeine and alcohol for at least 24 hours before the experiment, and from physical exercises for 48 hours before the experiment and not pregnant.
    - Have clean hair that does not prevent access to the head scalp.
- \* Note: The study may cause muscle soreness which is equivalent to soreness after regular exercise. We reserve the right to dismiss participants during pre-screening.

**For your time, you may receive:**

- Monetary compensation, in the form of a \$25 gift card per session
- Class credit according to system policy if you participated via the SONA system.
  - Light refreshment

**To volunteer or for more information, please contact:**

**Raul Fernandez-Sumano**  
Industrial Engineering and Management  
Systems  
Phone: +1 (407) 731-2634  
Email: rsumano@knights.ucf.edu

**Mahjabeen Rahman**  
Industrial Engineering and Management  
Systems  
Phone: +1 (407) 881-8001  
Email: mahjabeen.rahman@knights.ucf.edu

**Lina Ismail**  
Industrial Engineering and Management  
Systems  
Phone: +1 (407) 952-3756  
Email: linaelsherif@knights.ucf.edu

The study has been reviewed and approved by the Institutional Review Board, University of Central Florida

**APPENDIX H**  
**MEDICAL SCREENING**

**Subject** \_\_\_\_\_ **Today's** \_\_\_\_/\_\_\_\_/\_\_\_\_ **Height:** \_\_\_\_

**ID:** \_\_\_\_\_ **Date:** \_\_\_\_\_  
mm dd yy

**DoB:** \_\_\_\_/\_\_\_\_/\_\_\_\_ **Weight:** \_\_\_\_  
mm dd yy

Please circle each of the following medical screening. It will help to determine your eligibility to participate in this experiment. Please be indicated that your participation is voluntary, and you may choose not to answer all questions. Please feel to refer to your copy of the consent form for more details.

Yes   No	Have you ever been diagnosed with any kind of heart disease?
Yes   No	Have you ever been diagnosed with high blood pressure?
Yes   No	Have you had any surgery during the last six months?
Yes   No	Are you currently taking any medications?
Yes   No	Do you have any musculoskeletal diseases?
Yes   No	Do you have any chronic disease?
Yes   No	Have you seen any psychiatric or psychologist before?
Yes   No	Are you at least 24 hours since your last alcoholic drink?
Yes   No	Did you have any known mental or neurological disorders/diseases such as Epilepsy, depression, Attention Deficit Hyperactivity Disorder, etc.?

**APPENDIX I**  
**IRB APPROVAL OF HUMAN RESEARCH**





UNIVERSITY OF CENTRAL FLORIDA

**Institutional Review Board**

FWA00000351  
IRB00001138, IRB00012110  
Office of Research  
12201 Research Parkway  
Orlando, FL 32826-3246

**Memorandum**

To: LINA EL-SHERIF ISMAIL  
From: UCF Institutional Review Board (IRB)  
Date: March 19, 2021  
Re: IRB Coverage

The IRB reviewed the information related to your dissertation *TOPOLOGICAL CHANGES IN THE FUNCTIONAL BRAIN NETWORKS INDUCED BY ISOMETRIC FORCE EXERTIONS USING A GRAPH THEORETICAL APPROACH: AN EEG-BASED NEUROERGONOMICS STUDY*

Your project data is covered under the following protocol previously approved by the IRB. You are listed as a Co-Investigator on the study and your use of the data is consistent with the the protocol. Additionally, this study has been closed and no further IRB requirements are associated with your dissertation

IRB study name	IRB Approval Number
THE CORRELATION BETWEEN EEG SIGNATURES ASSOCIATED WITH PERCEPTIONS WITH MANUAL MATERIALS HANDLING TASKS	STUDY00000535:

If you have any questions, please contact the UCF IRB [irb@ucf.edu](mailto:irb@ucf.edu).

Sincerely,

Renea Carver  
IRB Manager

**APPENDIX J**  
**ANTHROPOMETRIC MEASUREMENTS**



**APPENDIX K**  
**REGIONS OF INTEREST**

Montreal Neurophysiological Institute (MNI) coordinates of the 84 regions of interest (ROIs) used to analyze the electroencephalograph signal of each exertion level.

Hemisphere	MNI			Lobe	Structure	Brodmann area	ROI
	X	Y	Z				
left	-35	-25	55	Frontal Lobe	Precentral Gyrus	BA4	1
left	-35	-20	50	Frontal Lobe	Precentral Gyrus	BA4	2
right	15	-45	60	Frontal Lobe	Paracentral Lobule	BA5	3
left	-15	-45	60	Frontal Lobe	Paracentral Lobule	BA5	4
right	30	-5	55	Frontal Lobe	Middle Frontal Gyrus	BA6	5
left	-30	-5	55	Frontal Lobe	Middle Frontal Gyrus	BA6	6
right	20	25	50	Frontal Lobe	Superior Frontal Gyrus	BA8	7
left	-20	30	50	Frontal Lobe	Superior Frontal Gyrus	BA8	8
left	-30	30	35	Frontal Lobe	Middle Frontal Gyrus	BA9	9
right	30	30	35	Frontal Lobe	Middle Frontal Gyrus	BA9	10
right	25	55	5	Frontal Lobe	Superior Frontal Gyrus	BA10	11
left	-25	55	5	Frontal Lobe	Superior Frontal Gyrus	BA10	12
right	20	45	-20	Frontal Lobe	Superior Frontal Gyrus	BA11	13
left	-20	40	-15	Frontal Lobe	Middle Frontal Gyrus	BA11	14
right	5	15	-15	Frontal Lobe	Subcallosal Gyrus	BA25	15
left	-10	20	-15	Frontal Lobe	Medial Frontal Gyrus	BA25	16
right	55	10	15	Frontal Lobe	Precentral Gyrus	BA44	17
left	-50	10	15	Frontal Lobe	Precentral Gyrus	BA44	18
right	50	20	15	Frontal Lobe	Inferior Frontal Gyrus	BA45	19
left	-50	20	15	Frontal Lobe	Inferior Frontal Gyrus	BA45	20
right	45	35	20	Frontal Lobe	Middle Frontal Gyrus	BA46	21
left	-45	35	20	Frontal Lobe	Middle Frontal Gyrus	BA46	22
right	30	25	-15	Frontal Lobe	Inferior Frontal Gyrus	BA47	23
left	-30	25	-15	Frontal Lobe	Inferior Frontal Gyrus	BA47	24
left	-55	-25	50	Parietal Lobe	Postcentral Gyrus	BA2	25
left	-45	-30	45	Parietal Lobe	Postcentral Gyrus	BA2	26
right	55	-25	50	Parietal Lobe	Postcentral Gyrus	BA2	27
right	35	-25	50	Parietal Lobe	Postcentral Gyrus	BA3	28
right	40	-25	50	Parietal Lobe	Postcentral Gyrus	BA3	29
left	-20	-65	50	Parietal Lobe	Precuneus	BA7	30
right	15	-65	50	Parietal Lobe	Precuneus	BA7	31
left	-10	-50	30	Parietal Lobe	Precuneus	BA31	32
right	10	-50	35	Parietal Lobe	Precuneus	BA31	33
right	50	-30	45	Parietal Lobe	Inferior Parietal Lobule	BA40	34
right	50	-45	45	Parietal Lobe	Inferior Parietal Lobule	BA40	35

Hemisphere	MNI			Lobe	Structure	Brodmann area	ROI
	X	Y	Z				
left	-50	-40	40	Parietal Lobe	Inferior Parietal Lobule	BA40	36
left	-5	-40	25	Limbic Lobe	Posterior Cingulate	BA23	37
right	5	-45	25	Limbic Lobe	Posterior Cingulate	BA23	38
right	5	0	35	Limbic Lobe	Cingulate Gyrus	BA24	39
right	5	30	20	Limbic Lobe	Anterior Cingulate	BA24	40
left	-5	0	35	Limbic Lobe	Cingulate Gyrus	BA24	41
left	-5	30	20	Limbic Lobe	Anterior Cingulate	BA24	42
right	20	-35	-5	Limbic Lobe	Parahippocampal Gyrus	BA27	43
left	-20	-35	-5	Limbic Lobe	Parahippocampal Gyrus	BA27	44
left	-20	-10	-25	Limbic Lobe	Parahippocampal Gyrus	BA28	45
right	20	-10	-25	Limbic Lobe	Parahippocampal Gyrus	BA28	46
left	-5	-50	5	Limbic Lobe	Posterior Cingulate	BA29	47
right	5	-50	5	Limbic Lobe	Posterior Cingulate	BA29	48
left	-15	-60	5	Limbic Lobe	Posterior Cingulate	BA30	49
left	-5	20	20	Limbic Lobe	Anterior Cingulate	BA33	50
right	0	20	20	Limbic Lobe	Anterior Cingulate	BA33	51
right	15	0	-20	Limbic Lobe	Parahippocampal Gyrus	BA34	52
left	-15	0	-20	Limbic Lobe	Parahippocampal Gyrus	BA34	53
left	-20	-25	-20	Limbic Lobe	Parahippocampal Gyrus	BA35	54
right	30	-25	-25	Limbic Lobe	Parahippocampal Gyrus	BA35	55
right	25	-25	-20	Limbic Lobe	Parahippocampal Gyrus	BA35	56
left	-30	-30	-25	Limbic Lobe	Parahippocampal Gyrus	BA36	57
right	-5	-40	25	Limbic Lobe	Posterior Cingulate	BA23	58
left	-45	-20	-30	Temporal Lobe	Fusiform Gyrus	BA20	59
left	-60	-20	-15	Temporal Lobe	Middle Temporal Gyrus	BA21	60
right	60	-15	-15	Temporal Lobe	Middle Temporal Gyrus	BA21	61
left	-45	-55	-15	Temporal Lobe	Fusiform Gyrus	BA37	62
right	45	-55	-15	Temporal Lobe	Fusiform Gyrus	BA37	63
left	-40	15	-30	Temporal Lobe	Superior Temporal Gyrus	BA38	64
right	40	15	-30	Temporal Lobe	Superior Temporal Gyrus	BA38	65
right	45	-65	25	Temporal Lobe	Middle Temporal Gyrus	BA39	66
left	-45	-65	25	Temporal Lobe	Middle Temporal Gyrus	BA39	67
left	-45	-30	10	Temporal Lobe	Transverse Temporal Gyrus	BA41	68
right	55	-20	5	Temporal Lobe	Superior Temporal Gyrus	BA41	69
left	-55	-25	5	Temporal Lobe	Superior Temporal Gyrus	BA41	70
right	45	-30	10	Temporal Lobe	Transverse Temporal Gyrus	BA41	71
left	-60	-10	15	Temporal Lobe	Transverse Temporal Gyrus	BA42	72
left	-60	-25	10	Temporal Lobe	Superior Temporal Gyrus	BA42	73

Hemisphere	MNI			Lobe	Structure	Brodmann area	ROI
	X	Y	Z				
right	60	-10	15	Temporal Lobe	Transverse Temporal Gyrus	BA42	74
right	65	-25	10	Temporal Lobe	Superior Temporal Gyrus	BA42	75
right	15	-85	0	Occipital Lobe	Lingual Gyrus	BA17	76
right	10	-90	0	Occipital Lobe	Lingual Gyrus	BA17	77
left	-10	-90	0	Occipital Lobe	Lingual Gyrus	BA17	78
left	-15	-85	0	Occipital Lobe	Lingual Gyrus	BA17	79
left	-25	-75	10	Occipital Lobe	Cuneus	BA30	80
right	10	-60	5	Occipital Lobe	Cuneus	BA30	81
right	25	-75	10	Occipital Lobe	Cuneus	BA30	82
right	40	-5	10	Sub-lobar	Insula	BA13	83
left	-40	-10	10	Sub-lobar	Insula	BA13	84

## LIST OF REFERENCES

- Abdul-latif, A. A., Cosic, I., Kumar, D. K., Polus, B., Pah, N., and Djuwari, D. (2004a). EEG coherence changes between right and left motor cortical areas during voluntary muscular contraction. *Australas. Phys. Eng. Sci. Med.* 27, 11–15. doi:10.1007/BF03178882.
- Abdul-latif, A., Cosic, I., Kumar, D., Polus, B., and Costa, C. (2004b). Power changes of EEG signals associated with muscle fatigue : The Root Mean Square analysis of EEG bands. *Proc. 2004 Intell. Sensors, Sens. Networks Inf. Process. Conf. IEEE.*, 531–534.
- Achard, S., and Bullmore, E. (2007). Efficiency and cost of economical brain functional networks. *PLoS Comput. Biol.* 3, 0174–0183. doi:10.1371/journal.pcbi.0030017.
- Adler, G., Brassens, S., and Jajcevic, A. (2003). EEG coherence in Alzheimer's dementia. *J. Neural Transm.* 110, 1051–1058. doi:10.1007/s00702-003-0024-8.
- Al-kadi, M. I., Reaz, M., and Ali, M. (2013). Evolution of Electroencephalogram Signal Analysis Techniques during Anesthesia. *Sensors* 13, 6605–6635. doi:10.3390/s130506605.
- Albuquerque, I., Tiwari, A., Gagnon, J., Lafond, D., Parent, M., Tremblay, S., et al. (2018). On the Analysis of EEG Features for Mental Workload Assessment During Physical Activity. *2018 IEEE Int. Conf. Syst. Man, Cybern.*, 538–543. doi:10.1109/SMC.2018.00101.
- Alessandro, N., Nicola, C., Mariarosaria, V., and Rosaria, C. (2014). New trend line of research about comfort evaluation: proposal of a framework for weighing and evaluating contributes coming from cognitive, postural and physiologic comfort perceptions. *Adv. Soc. Organ. Factors* unico, 503–515. doi:10.13140/2.1.3482.7841.
- Aljuaid, A., and Karwowski, W. (2016). A Neuroergonomics Study of Brain EEG ' s Activity During Manual Lifting Tasks.
- Allami, N., Brovelli, A., Hamzaoui, E. M., Regragui, F., Paulignan, Y., and Boussaoud, D. (2014). Neurophysiological correlates of visuo-motor learning through mental and physical practice. *Neuropsychologia* 55, 6–14. doi:10.1016/j.neuropsychologia.2013.12.017.
- Amo, C., Santiago, L. De, Lucianez, D. Z., Alonso- Cortes, J., Alonso-alonso, M., Barea, R., et al. (2017). Induced gamma band activity from EEG as a possible index of training-related brain plasticity in motor tasks. *PLoS One* 12, e0186008.
- Anastasiadou, M., Christodoulakis, M., Papathanasiou, E., Papacostas, S., Hadjipapas, A., and Mitsis, G. (2019). Graph Theoretical Characteristics of EEG-Based Functional Brain Networks in Patients With Epilepsy: The Effect of Reference Choice and Volume



- Conduction. *Front. Neurosci.* 13, 1–18. doi:10.3389/fnins.2019.00221.
- Andrew, C., and Pfurtscheller, G. (1999). Lack of bilateral coherence of post-movement central beta oscillations in the human electroencephalogram. *Neurosci. Lett.* 273, 89–92. doi:10.1016/S0304-3940(99)00632-1.
- Anzolin, A., Presti, P., Van De Steen, F., Astolfi, L., Haufe, S., and Marinazzo, D. (2019). Quantifying the Effect of Demixing Approaches on Directed Connectivity Estimated Between Reconstructed EEG Sources. *Brain Topogr.* 32, 655–674. doi:10.1007/s10548-019-00705-z.
- Aryal, A., Ghahramani, A., and Gerber, B. (2017). Automation in Construction Monitoring fatigue in construction workers using physiological measurements. *Autom. Constr.* 82, 154–165. doi:10.1016/j.autcon.2017.03.003.
- Astolfi, L., Cincotti, F., Mattia, D., Marciani, M. G., Baccala, L. A., Fallani, F. D. V., et al. (2007). Comparison of different cortical connectivity estimators for high-resolution EEG recordings. *Hum. Brain Mapp.* 28, 143–157. doi:10.1002/hbm.20263.
- Babiloni, C., Carducci, F., Cincotti, F., Rossini, P., Neuper, C., Pfurtscheller, G., et al. (1999). Human Movement-Related Potentials vs Desynchronization of EEG Alpha Rhythm : A High-Resolution EEG Study. *Neuroimage* 10, 658–665.
- Babiloni, C., Del Percio, C., Iacoboni, M., Infarinato, F., Lizio, R., Marzano, N., et al. (2008). Golf putt outcomes are predicted by sensorimotor cerebral EEG rhythms. *J. Physiol.* 586, 131–139. doi:10.1113/jphysiol.2007.141630.
- Babiloni, F., Babiloni, C., Carducci, F., Del Gratta, C., Pizzella, V., Romani, G., et al. (2001). Linear Inverse Source Estimate of Combined EEG and MEG Data Related to Voluntary Movements. *Hum. Brain Mapp.* 14, 197–209. doi:10.1055/s-0038-1634217.
- Baccala, L. A., Sameshima, K., and Takahashi, D. Y. (2007). Generalized partial directed coherence. *2007 15th Int. Conf. Digit. Signal Process. DSP 2007*, 163–166. doi:10.1109/ICDSP.2007.4288544.
- Baccalá, L., and Sameshima, K. (2001). Partial directed coherence: A new concept in neural structure determination. *Biol. Cybern.* 84, 463–474. doi:10.1007/PL00007990.
- Bailey, S. P., Hall, E. E., Folger, S. E., and Miller, P. C. (2008). Changes in EEG during graded exercise on a recumbent cycle ergometer. *J. Sport. Sci. Med.* 7, 505–511.
- Baillet, S., Mosher, J. C., and Leahy, R. M. (2001). Electromagnetic brain mapping. *IEEE Signal Process. Mag.* 18, 14–30. doi:10.1109/79.962275.
- Barabasi, A.-L., and Albert, R. (1999). Emergence of Scaling in Random Networks. *Sciencr* 286,

509–513.

- Barabási, A., and Albert, R. (1999). Emergence of Scaling in Random Networks. *Science* (80- ). 286, 509–512.
- Bassett, D. S., and Bullmore., E. T. (2009). Human Brain Networks in Health and Disease. *Curr. Opin. Neurol.* 22, 340–347. doi:10.1097/WCO.0b013e32832d93dd.Human.
- Bassett, D. S., and Bullmore, E. (2006). Small-World Brain Networks. *Neurosci.* 12, 512–523. doi:10.1177/1073858406293182.
- Bassett, D. S., Meyer-lindenberg, A., Achard, S., Duke, T., and Bullmore, E. (2006). Adaptive reconfiguration of fractal small-world human brain functional networks. in *Proceedings of the National Academy of Sciences*, 19518–19523.
- Bassett, D. S., and Sporns, O. (2017). Network neuroscience. *Nat. Neurosci.* 20, 353–364. doi:10.1038/nn.4502.
- Bastos, A. M., and Schoffelen, J. M. (2016). A tutorial review of functional connectivity analysis methods and their interpretational pitfalls. *Front. Syst. Neurosci.* 9, 1–23. doi:10.3389/fnsys.2015.00175.
- Baumeister, J., Reinecke, K., Schubert, M., Schade, J., and Weiss, M. (2012). Effects of induced fatigue on brain activity during sensorimotor control. *Eur J Appl Physiol* 112, 2475–2482. doi:10.1007/s00421-011-2215-6.
- Berchicci, M., Menotti, F., Macaluso, A., and Russo, F. (2013). The neurophysiology of central and peripheral fatigue during sub-maximal lower limb isometric contractions. *Front. Neurosci.* 7, 1–10. doi:10.3389/fnhum.2013.00135.
- Beres, A. M. (2017). Time is of the Essence: A Review of Electroencephalography (EEG) and Event-Related Brain Potentials (ERPs) in Language Research. *Appl. Psychophysiol. Biofeedback* 42, 247–255. doi:10.1007/s10484-017-9371-3.
- Bernard, B. . (1997). Musculoskeletal Disorders and Workplace Factors: A Critical Review of Epidemiological Evidence for Work-Related Musculoskeletal Disorders of the Neck, Upper Extremity, and Low Back. *Cincinnati Natl. Inst. Occup. Saf. Heal.*
- Bernard, B. P., and Putz-Anderson, V. (1997). Musculoskeletal disorders and workplace factors; a critical review of epidemiologic evidence for work-related musculoskeletal disorders of the neck, upper extremity, and low back.
- Blinowska, K. (2011). Review of the methods of determination of directed connectivity from multichannel data. *Med. Biol. Eng. Comput.* 49, 521–529. doi:10.1007/s11517-011-0739-x.

- Blinowska, K. J. (2010). Methods for determination of functional connectivity in brain. *IFMBE Proc.* 28, 195–198. doi:10.1007/978-3-642-12197-5\_43.
- Blum, S., Jacobsen, N. S. J., Bleichner, M. G., and Debener, S. (2019). A riemannian modification of artifact subspace reconstruction for EEG artifact handling. *Front. Hum. Neurosci.* 13, 1–10. doi:10.3389/fnhum.2019.00141.
- Boccaletti, S., Latora, V., Moreno, Y., Chavez, M., and Hwang, D. U. (2006). Complex network: Structure and dynamics. *Phys. Rep.* 424, 175–308. doi:10.1016/j.physrep.2005.10.009.
- Bola, M., and Sabel, B. (2015). Dynamic reorganization of brain functional networks during cognition. *Neuroimage* 114, 398–413. doi:10.1016/j.neuroimage.2015.03.057.
- Borg, G. (1962). *Physical performance and perceived exertion*.
- Borg, G. (1970). PERCEIVED EXERTION AS AN INDICATOR OF SOMATIC STRESS. *Scand. J. Rehabil. Med.* 2, 92–98.
- Borg, G. (1998). *Borg's Perceived Exertion And Pain Scales*. Human Kinetics.
- Borg, G. A. (1982). Psychophysical bases of perceived exertion. *Med. Sci. Sports Exerc.* 14, 377–381.
- Borghetti, B. J., Giametta, J. J., and Rusnock, C. F. (2017). Assessing Continuous Operator Workload With a Hybrid Scaffolded Neuroergonomic Modeling Approach. *Hum. Factors* 59, 134–146. doi:10.1177/0018720816672308.
- Borghini, G., Astolfi, L., Vecchiato, G., Mattia, D., and Babiloni, F. (2014). Measuring neurophysiological signals in aircraft pilots and car drivers for the assessment of mental workload, fatigue and drowsiness. *Neurosci. Biobehav. Rev.* 44, 58–75. doi:10.1016/j.neubiorev.2012.10.003.
- Borghini, G., Vecchiato, G., Toppi, J., Astolfi, L., Maglione, A., Isabella, R., et al. (2012). Assessment of mental fatigue during car driving by using high resolution EEG activity and neurophysiologic indices. *Proc. Annu. Int. Conf. IEEE Eng. Med. Biol. Soc. EMBS* 70, 6442–6445. doi:10.1109/EMBC.2012.6347469.
- Bowyer, S. M. (2016). Coherence a measure of the brain networks: past and present. *Neuropsychiatr. Electrophysiol.* 2, 1–12. doi:10.1186/s40810-015-0015-7.
- Boy, G. (2017). *The handbook of human-machine interaction: a human-centered design approach*. CRC Press.
- Breckel, T. P. K., Thiel, C. M., Bullmore, E. T., Zalesky, A., Patel, A. X., and Giessing, C. (2013a).

- Long-Term Effects of Attentional Performance on Functional Brain Network Topology. *PLoS One* 8, 1–14. doi:10.1371/journal.pone.0074125.
- Breckel, T. P. K., Thiel, C. M., Bullmore, E. T., Zalesky, A., Patel, A. X., and Giessing, C. (2013b). Long-Term Effects of Attentional Performance on Functional Brain Network Topology. *PLoS One* 8, e74125. doi:10.1371/journal.pone.0074125.
- Breitling, D., Guenther, W., and Rondot, P. (1986). Motor Responses Measured by Brain Electrical Activity Mapping. *Behav. Neurosci.* 100, 104–116. doi:10.1037/0735-7044.100.1.104.
- Brett, M., Johnsrude, I. S., and Owen, A. M. (2002). The problem of functional localization in the human brain." *Nat. Rev. Neurosci.* 3, 243–249.
- Broido, A. D., and Clauset, A. (2019). Scale-free networks are rare. *Nat. Commun.* 10, 1–10. doi:10.1038/s41467-019-08746-5.
- Brümmer, V., Schneider, S., Strüder, H., and Askew, C. (2011). Primary motor cortex activity is elevated with incremental exercise intensity. *Neuroscienc* 181, 150–162. doi:10.1016/j.neuroscience.2011.02.006.
- Brunner, C., Billinger, M., Seeber, M., Mullen, T. R., Makeig, S., Lansky, P., et al. (2016). Volume conduction influences scalp-based connectivity estimates. *Front. Comput. Neurosci.* 10, 1–4. doi:10.3389/fncom.2016.00121.
- Bulea, T., Kilicarslan, A., Ozdemir, R., Paloski, W., and Contreras-Vidal, J. (2013). Simultaneous Scalp Electroencephalography (EEG), Electromyography (EMG), and Whole-body Segmental Inertial Recording for Multi-modal Neural Decoding. *J. Vis. Exp.*, 1–13. doi:10.3791/50602.
- Bullmore, E., and Sporns, O. (2009). Complex brain networks : graph theoretical analysis of structural and functional systems. *Nat. Rev. Neurosci.* 10, 186. doi:10.1038/nrn2575.
- Cahill, L. (2006). Why sex matters for neuroscience. *Nat. Rev. Neurosci.* 7, 477–484. doi:10.1038/nrn1909.
- Calmels, C., Holmes, P., Jarry, G., Jean-michel, L., Hars, M., and Stam, C. J. (2006). Cortical Activity Prior to , and During , Observation and Execution of Sequential Finger Movements. *Brain Topogr.* 19, 77–88. doi:10.1007/s10548-006-0014-x.
- Cantero, J. L., Atienza, M., Salasa, R. M., and Gomez, C. M. (1999). Alpha EEG coherence in different brain states: An electrophysiological index of the arousal level in human subjects. *Neurosci. Lett.* 271, 159–162. doi:10.1016/S0304-3940(99)00553-4.
- Canuet, L., Ishii, R., Pascual-Marqui, R. D., Iwase, M., Kurimoto, R., Aoki, Y., et al. (2011). Resting-state EEG source localization and functional connectivity in schizophrenia-like

- psychosis of epilepsy. *PLoS One* 6. doi:10.1371/journal.pone.0027863.
- Canuet, L., Tellado, I., Couceiro, V., Fraile, C., Fernandez-Novoa, L., Ishii, R., et al. (2012). Resting-State Network Disruption and APOE Genotype in Alzheimer's Disease: A lagged Functional Connectivity Study. *PLoS One* 7, 1–12. doi:10.1371/journal.pone.0046289.
- Cao, L., Hao, D., Rong, Y., Zhou, Y., Li, M., and Tian, Y. (2015). Investigating the modulation of brain activity associated with handgrip force and fatigue. *Technol. Heal. Care* 23, S427–S433. doi:10.3233/THC-150979.
- Cattai, T., Colonnese, S., Corsi, M. C., Bassett, D. S., Scarano, G., and De Vico Fallani, F. (2018). Characterization of mental states through node connectivity between brain signals. *Eur. Signal Process. Conf.* 2018-Septe, 1377–1381. doi:10.23919/EUSIPCO.2018.8553000.
- CGX software (2020).
- Chaffin, D., Andersson, G., and Martin, B. (1999). *Occupational biomechanics: Wiley New York*.
- Chaffin, D., Herrin, G., and Keyserling, W. (1978). An Updated Position. *J. Occup. Environ. Med.* 20, 403–408.
- Chang, C.-Y., Hsu, S.-H., Pion-Tonachini, L., and Jung, T.-P. (2018). Evaluation of Artifact Subspace Reconstruction for Automatic EEG Artifact Removal. in *2018 40th Annual International Conference of the IEEE Engineering in Medicine and Biology Society (EMBC)* (IEEE), 1242–1245. doi:10.1109/EMBC.2018.8512547.
- Chatrjian, G., Lettich, E., and Nelson, P. (1985). Ten percent electrode system for topographic studies of spontaneous and evoked EEG activities. *Am. J. EEG Technol.* 25, 83–92.
- Chella, F., Pizzella, V., Zappasodi, F., and Marzetti, L. (2016). Impact of the reference choice on scalp EEG connectivity estimation. *J. Neural Eng.* 13. doi:10.1088/1741-2560/13/3/036016.
- Chen, J., Wang, H., and Hua, C. (2018a). Electroencephalography based fatigue detection using a novel feature fusion and extreme learning machine. *Cogn. Syst. Res.* 52, 715–728. doi:10.1016/j.cogsys.2018.08.018.
- Chen, J., Wang, H., Hua, C., Wang, Q., and Liu, C. (2018b). Graph analysis of functional brain network topology using minimum spanning tree in driver drowsiness. *Cogn. Neurodyn.* 12, 569–581. doi:10.1007/s11571-018-9495-z.
- Chen, J., Wang, H., Wang, Q., and Hua, C. (2019). Exploring the fatigue affecting electroencephalography based functional brain networks during real driving in young males. *Neuropsychologia* 129, 200–211. doi:https://doi.org/10.1016/j.neuropsychologia.2019.04.004.

- Cheng, L., Ayaz, H., Sun, J., Tong, S., and Onaral, B. (2016). Modulation of Functional Connectivity and Activation during Preparation for Hand Movement. *IIE Trans. Occup. Ergon. Hum. Factors* 4, 175–187. doi:10.1080/21577323.2016.1191560.
- Christiano, L., and Fitzgerald, T. (2003). The band pass filter. *Int. Econ. Rev. (Philadelphia)*. 44, 435–465. doi:10.1111/1468-2354.t01-1-00076.
- Christodoulakis, M., Anastasiadou, M., Papacostas, Savvas S Papathana, E., and Mitsis, G. (2012). Investigation of network brain dynamics from EEG measurements in patients with epilepsy using graph-theoretic approaches. *Proc. 12th IEEE Int. Conf. Bioinforma. Bioeng. (BIBE), Larnaca, Cyprus*, 303.
- Christodoulakis, M., Hadjipapas, A., Papathanasiou, E. S., Anastasiadou, M., and Papacostas, Savvas S. Mitsis, G. D. (2015). On the Effect of Volume Conduction on Graph Theoretic Measures of Brain Networks in Epilepsy. *Mod. Electroencephalogr. Assess. Tech.* 91, 103-130 Humana Press, New York, NY. doi:10.1007/7657.
- Chua, B. L., Dai, Z., Thakor, N., Bezerianos, A., and Sun, Y. (2017). Connectome pattern alterations with increment of mental fatigue in one-hour driving simulation. *Proc. Annu. Int. Conf. IEEE Eng. Med. Biol. Soc. EMBS*, 4355–4358. doi:10.1109/EMBC.2017.8037820.
- Coan, J. A., and Allen, J. J. . (2004). Frontal EEG asymmetry as a moderator and mediator of emotion. *Biol. Psychol.* 67, 7–50. doi:10.1016/j.biopsycho.2004.03.002.
- Cochin, S. (1999). Observation and execution of movement: Similarities demonstrated by quantified electroencephalography. *Eur. J. Neurosci.* 11, 1839–1842. doi:10.1046/j.1460-9568.1999.00598.x.
- Cohen, R., and Havlin, S. (2003). Scale-Free Networks Are Ultrasmall. *Phys. Rev. Lett.* 90, 4. doi:10.1103/PhysRevLett.90.058701.
- Comani, S., Fronso, S. Di, Castronovo, A., Schmid, M., Bortoli, L., Conforto, S., et al. (2013). Attentional Focus and Functional Connectivity in Cycling: An EEG Case Study. in *XIII Mediterranean Conference on Medical and Biological Engineering and Computing*, 137-140. Springer, Cham, 2014. doi:10.1007/978-3-319-00846-2.
- Cynthia, A., Patricia, G., Nisrine, J., Mahmoud, H., and Sandy, R. (2017). A new system for detecting fatigue and sleepiness using brain connectivity. *Int. Conf. Adv. Biomed. Eng. ICABME 2017-Octob*, 0–3. doi:10.1109/ICABME.2017.8167573.
- Dai, Z., De Souza, J., Lim, J., Ho, P. M., Chen, Y., Li, J., et al. (2017). Eeg cortical connectivity analysis of working memory reveals topological reorganization in theta and alpha bands. *Front. Hum. Neurosci.* 11, 1–13. doi:10.3389/fnhum.2017.00237.
- Daly, I., Pichiorri, F., Faller, J., and Kaiser, V. (2012). What does clean EEG look like ? What does

- clean EEG look like ? in *Annual International Conference of the IEEE Engineering in Medicine and Biology Society*. doi:10.1109/EMBC.2012.6346834.
- Danielle, S. B., and Bullmore, E. D. (2006). Small-World Brain Networks. *Neuroscientist* 12, 512–523. doi:10.1177/1073858406293182.
- David, O., Cosmelli, D., and Friston, K. J. (2004). Evaluation of different measures of functional connectivity using a neural mass model. *Neuroimage* 21, 659–673. doi:10.1016/j.neuroimage.2003.10.006.
- de Morree, H. M., Klein, C., and Marcora, S. M. (2012). Perception of effort reflects central motor command during movement execution. *Psychophysiology* 49, 1242–1253. doi:10.1111/j.1469-8986.2012.01399.x.
- De Vico Fallani, F., Astolfi, L., Cincotti, F., Mattia, D., Marciani, M. G., Tocci, A., et al. (2008). Cortical network dynamics during foot movements. *Neuroinformatics* 6, 23–34. doi:10.1007/s12021-007-9006-6.
- De Vico Fallani, F., Richiardi, J., Chavez, M., and Achard, S. (2014). Graph analysis of functional brain networks: Practical issues in translational neuroscience. *Philos. Trans. R. Soc. B Biol. Sci.* 369. doi:10.1098/rstb.2013.0521.
- Dellen, E. Van, Douw, L., Baayen, J. C., Heimans, J. J., Ponten, S. C., Vandertopn, P., et al. (2009). Long-Term Effects of Temporal Lobe Epilepsy on Local Neural Networks: A Graph Theoretical Analysis of Corticography Recordings. *PLoS One* 4, e8081. doi:10.1371/journal.pone.0008081.
- Delorme, A., and Makeig, S. (2004). EEGLAB: An open source toolbox for analysis of single-trial EEG dynamics including independent component analysis. *J. Neurosci. Methods* 134, 9–21. doi:10.1016/j.jneumeth.2003.10.009.
- Delorme, A., Palmer, J., Onton, J., Oostenveld, R., and Makeig, S. (2012). Independent EEG sources are dipolar. *PLoS One* 7. doi:10.1371/journal.pone.0030135.
- Delorme, A., Sejnowski, T., and Scott, M. (2007). Enhanced detection of artifacts in EEG data using higher-order statistics and independent component analysis. 34, 1443–1449. doi:10.1016/j.neuroimage.2006.11.004.Enhanced.
- Desikan, R. S., Ségonne, F., Fischl, B., Quinn, B. T., Dickerson, B. C., Blacker, D., et al. (2006). An automated labeling system for subdividing the human cerebral cortex on MRI scans into gyral based regions of interest. *Neuroimage* 31, 968–980. doi:10.1016/j.neuroimage.2006.01.021.
- Desmurget, M., Reilly, K. T., Richard, N., Szathmari, A., Mottolese, C., and Sirigu, A. (2009). Movement Intention After Parietal Cortex Stimulation in Humans. *Science (80-. )*. 324, 811–

813. doi:10.1126/science.1169896.

- di Fronso, S., Fiedler, P., Tamburro, G., Haueisen, J., Bertollo, M., and Comani, S. (2019). Dry EEG in Sports Sciences: A Fast and Reliable Tool to Assess Individual Alpha Peak Frequency Changes Induced by Physical Effort. *Front. Neurosci.* 13, 1–12. doi:10.3389/fnins.2019.00982.
- di Fronso, S., Tamburro, G., Robazza, C., Bortoli, L., Comani, S., and Bertollo, M. (2018). Focusing attention on muscle exertion increases EEG coherence in an endurance cycling task. *Front. Psychol.* 9, 1–12. doi:10.3389/fpsyg.2018.01249.
- Di Lorenzo, G., Daverio, A., Ferrentino, F., Santarnecchi, E., Ciabattini, F., Monaco, L., et al. (2015). Altered resting-state EEG source functional connectivity in schizophrenia: The effect of illness duration. *Front. Hum. Neurosci.* 9, 1–11. doi:10.3389/fnhum.2015.00234.
- Diestel, R. (1997). *Graph Theory*. Springer.
- Dimitrakopoulos, G. N., Kakkos, I., Dai, Z., Lim, J., Desouza, J. J., Bezerianos, A., et al. (2017). Task-Independent Mental Workload Classification Based Upon Common Multiband EEG Cortical Connectivity. *IEEE Trans. Neural Syst. Rehabil. Eng.* 25, 1940–1949. doi:10.1109/TNSRE.2017.2701002.
- Dimitrakopoulos, G. N., Kakkos, I., Dai, Z., Wang, H., Sgarbas, K., and Thakor, N. (2018). Functional Connectivity Analysis of Mental Fatigue Reveals Different Network Topological Alterations Between Driving and Vigilance Tasks. *IEEE Trans. Neural Syst. Rehabil. Eng.* 26, 740–749. doi:10.1109/TNSRE.2018.2791936.
- Dimitriadis, S., Sun, Y., Kwok, K., Laskaris, N. A., Thakor, N., and Bezerianos, A. (2015). Cognitive Workload Assessment Based on the Tensorial Treatment of EEG Estimates of Cross-Frequency Phase Interactions. *Ann. Biomed. Eng.* 43, 977–989. doi:10.1007/s10439-014-1143-0.
- Dimitriadis, S., Sun, Y., Kwok, K., Laskaris, N., and Bezerianos, A. (2013). A tensorial approach to access cognitive workload related to mental arithmetic from EEG functional connectivity estimates. in *Proceedings of the Annual International Conference of the IEEE Engineering in Medicine and Biology Society, EMBS (IEEE)*, 2940–2943. doi:10.1109/EMBC.2013.6610156.
- Dirnberger, G., Duregger, C., Trettl, E., Lindinger, G., and Lang, W. (2004). Fatigue in a simple repetitive motor task : a combined electrophysiological and neuropsychological study. *Brain Res.* 1028, 26–30. doi:10.1016/j.brainres.2004.08.045.
- Doppelmayr, M., Sauseng, P., and Doppelmayr, H. (2007). Modifications in the Human EEG during Extralong Physical Activity. *Neurophysiologie* 39, 76–81.



- Drakesmith, M., Caeyenberghs, K., Dutt, A., Lewis, G., David, A. S., and Jones, D. K. (2015). Overcoming the effects of false positives and threshold bias in graph theoretical analyses of neuroimaging data. *Neuroimage* 118, 313–333. doi:10.1016/j.neuroimage.2015.05.011.
- E-prime software (2020).
- Ekkekakis, P., and Petruzzello, S. J. (1999). Acute Aerobic Exercise and Affect. *Sport. Med.* 28, 337–374. doi:10.2165/00007256-199928050-00005.
- Enders, H., Cortese, F., Maurer, C., Baltich, J., Protzner, A. B., and Nigg, B. M. (2016). Changes in cortical activity measured with EEG during a high-intensity cycling exercise. *J Neurophysiol* 115, 379–388. doi:10.1152/jn.00497.2015.
- Engchuan, P., Wongsuphasawat, K., and Sittiprapaporn, P. (2017). Changes of EEG power spectra in bench press weight training exercise. *ECTI-CON 2017 - 2017 14th Int. Conf. Electr. Eng. Comput. Telecommun. Inf. Technol.*, 13–16. doi:10.1109/ECTICon.2017.8096161.
- Enoka, R. M., and Stuart, D. G. (1992). Neurobiology of muscle fatigue. *J. Appl. Physiol.* 72, 1631–1648. doi:10.1152/jappl.1992.72.5.1631.
- Euler, L. (1741). Solutio problematis ad geometrian situs pertinentis. *Coment. Acad. Sci. Petropolitanae* 8, 128–140. doi:002433.d/232323.
- Fallani, F., Astolfi, L., Cincotti, F., Mattia, D., Tocci, A., Salinari, S., et al. (2008). Brain network analysis from high-resolution EEG recordings by the application of theoretical graph indexes. *IEEE Trans. Neural Syst. Rehabil. Eng.* 16, 442–452. doi:10.1109/TNSRE.2008.2006196.
- Farahani, F. V., Karwowski, W., and Lighthall, N. R. (2019). Application of graph theory for identifying connectivity patterns in human brain networks: A systematic review. *Front. Neurosci.* 13, 1–27. doi:10.3389/fnins.2019.00585.
- Faw, B. (2003). Pre-frontal executive committee for perception, working memory, attention, long-term memory, motor control, and thinking: A tutorial review. *Conscious. Cogn.* 12, 83–139. doi:10.1016/S1053-8100(02)00030-2.
- Filho, C., Attux, R., and Castellano, G. (2018). Can graph metrics be used for EEG-BCIs based on hand motor imagery? *Biomed. Signal Process. Control* 40, 359–365. doi:10.1016/j.bspc.2017.09.026.
- Fingelkurts, A. A., Fingelkurts, A. A., and Ka, S. (2005). Functional connectivity in the brain — is it an elusive concept? *Neurosci. Biobehav. Rev.* 28, 827–836. doi:10.1016/j.neubiorev.2004.10.009.
- Flanagan, S., Dunn-lewis, C., Comstock, B., Maresh, C., Volek, J., Denegar, C., et al. (2012). Cortical Activity during a Highly-Trained Resistance Exercise Movement Emphasizing

- Force, Power or Volume. *Brain Sci.* 2, 649–666. doi:10.3390/brainsci2040649.
- Fontes, E. B., Okano, A. H., De Guio, F., Schabort, E. J., Min, L. L., Basset, F. A., et al. (2015). Brain activity and perceived exertion during cycling exercise: An fMRI study. *Br. J. Sports Med.* 49, 556–560. doi:10.1136/bjsports-2012-091924.
- Fornito, A., Zalesky, A., and Breakspear, M. (2013). Graph analysis of the human connectome: Promise, progress, and pitfalls. *Neuroimage* 80, 426–444. doi:10.1016/j.neuroimage.2013.04.087.
- Fornito, A., Zalesky, A., and Bullmore, E. T. (2016). “Centrality and Hubs,” in *Fundamentals of Brain Network Analysis* (Elsevier), 137–161. doi:10.1016/B978-0-12-407908-3.00005-4.
- Freeman, F. G., Mikulka, P. J., Scerbo, M. W., and Scott, L. (2004). An evaluation of an adaptive automation system using a cognitive vigilance task. *Biol. Psychol.* 67, 283–297. doi:10.1016/j.biopsycho.2004.01.002.
- Freeman, L. (1977). A Set of Measures of Centrality Based on Betweenness. *Sociometry* 40, 35–41. doi:10.1111/j.1468-2494.1993.tb00590.x.
- Freude, G., and Ullsperger, P. (1987). Physiology Changes in Bereitschaftspotential during fatiguing and non-fatiguing hand movements. *Eur. J. Appl. Physiol. Occup. Physiol.* 56, 105–108.
- Frey, J., Mühl, C., Lotte, F., and Hachet, M. (2013). Review of the Use of Electroencephalography as an Evaluation Method for Human-Computer Interaction. in *arXiv preprint arXiv*, 1311.2222.
- Friston, K. (1994). Functional and effective connectivity in neuroimaging: A synthesis. *Hum. Brain Mapp.* 2, 56–78. doi:10.1002/hbm.460020107.
- Friston, K. (2011). Functional and effective connectivity: a review. *Brain Connect.* 1, 13–36.
- Friston, K., Frith, C., and Frackowiak, R. (1993a). Time-dependent changes in effective connectivity measured with PET. *Hum. Brain Mapp.* 1, 69–79. doi:10.1002/hbm.460010108.
- Friston, K., Frith, C., Liddle, P., and Frackowiak, R. (1993b). Functional connectivity: The principal-component analysis of large (PET) data sets. *J. Cereb. Blood Flow Metab.* 13, 5–14. doi:10.1038/jcbfm.1993.4.
- Ftaiti, F., Kacem, A., Jaidane, N., Tabka, Z., and Dogui, M. (2010). Changes in EEG activity before and after exhaustive exercise in sedentary women in neutral and hot environments. *Appl. Ergon.* 41, 806–811. doi:10.1016/j.apergo.2010.01.008.
- Fuchs, M., Kastner, J., Wagner, M., Hawes, S., and Ebersole, J. S. (2002). A standardized

- boundary element method volume conductor model integral equation using analytically integrated elements. *Clin. Neurophysiol.* 113, 702–712. doi:10.1016/S1388-2457(02)00030-5.
- Gamberale, F. (1990). Perception of effort in manual materials handling. *Scand. J. Work. Environ. Heal.* 16, 59–66. doi:10.5271/sjweh.1820.
- Garcés Correa, A., Laciár, E., Patño, H., and Valentinuzzi, M. (2007). Artifact removal from EEG signals using adaptive filters in cascade. *J. Phys. Conf. Ser.* 90. doi:10.1088/1742-6596/90/1/012081.
- García-Prieto, J., Bajo, R., and Pereda, E. (2017). Efficient computation of functional brain networks: Toward real-time functional connectivity. *Front. Neuroinform.* 11, 1–18. doi:10.3389/fninf.2017.00008.
- GeethaRamani, R., and Sivaselvi, K. (2014). Human brain hubs(provincial and connector) identification using centrality measures. in *2014 International Conference on Recent Trends in Information Technology, ICRTIT 2014 (IEEE)*, 1–6. doi:10.1109/ICRTIT.2014.6996144.
- Ghaderi, A., Moradkhani, Haghighatfard, A., Akrami, F., Khayyer, Z., and Balcı, F. (2018). Time estimation and beta segregation: An EEG study and graph theoretical approach. *PLoS One* 13, 1–16. doi:10.1371/journal.pone.0195380.
- Ghaderi, A., Nazari, M., and Darooneh, A. (2019). Functional brain segregation changes during demanding mathematical task. *Int. J. Neurosci.* 129, 904–915. doi:10.1080/00207454.2019.1586688.
- Ghosh, P., Mazumder, A., Bhattacharyya, S., Tibarewala, D. N., and Hayashibe, M. (2015). Functional connectivity analysis of motor imagery EEG signal for brain-computer interfacing application. *Int. IEEE/EMBS Conf. Neural Eng. NER*, 210–213. doi:10.1109/NER.2015.7146597.
- Goldenberg, D., and Galván, A. (2015). The use of functional and effective connectivity techniques to understand the developing brain. *Dev. Cogn. Neurosci.* 12, 155–164. doi:10.1016/j.dcn.2015.01.011.
- Gramann, K., and Plank, M. (2019). *Neuroergonomics: The brain at work and in everyday life.* Elsevier doi:10.1016/C2016-0-02196-4.
- Gribkov, D., and Gribkova, V. (2000). Learning dynamics from nonstationary time series: Analysis of electroencephalograms. *Phys. Rev. E - Stat. Physics, Plasmas, Fluids, Relat. Interdiscip. Top.* 61, 6538–6545. doi:10.1103/PhysRevE.61.6538.
- Guo, F., Sun, Y. J., and Zhang, R. H. (2017). Perceived exertion during muscle fatigue as reflected in movement-related cortical potentials: an event-related potential study. *Neuroreport* 28,

115–122. doi:10.1097/WNR.0000000000000732.

- Guoa, F., Sun, Y.-J., and Zhang, R.-H. (2017). Perceived exertion during muscle fatigue as reflected in movement-related cortical potentials: an event-related potential study. *Neuroreport* 28, 115–122. doi:10.1097/WNR.0000000000000732.
- Gutmann, B., Mierau, A., Hülzdünker, T., Hildebrand, C., Przyklenk, A., Hollmann, W., et al. (2015). Effects of Physical Exercise on Individual Resting State EEG Alpha Peak Frequency. *Neural Plast.* 2015. doi:10.1155/2015/717312.
- Gutmann, B., Zimmer, P., Hülzdünker, T., Lefebvre, J., Binneböbel, S., Oberste, M., et al. (2018). The effects of exercise intensity and post-exercise recovery time on cortical activation as revealed by EEG alpha peak frequency. *Neurosci. Lett.* 668, 159–163. doi:10.1016/j.neulet.2018.01.007.
- Gwin, J., and Ferris, D. (2012). Beta- and gamma-range human lower limb corticomuscular coherence. *Front. Hum. Neurosci.* 6, 258. doi:10.3389/fnhum.2012.00258.
- Haggard, P. (2009). The Sources of Human Volition. *Science* (80-. ). 324, 731–733. doi:10.1126/science.1173827.
- Hallett, M. (1994). Movement-related cortical potentials. *Electromyogr. Clin. Neurophysiol.* 34, 5–13.
- Hallett, M. (2007). Volitional control of movement: The physiology of free will. *Clin. Neurophysiol.* 118, 1179–1192. doi:10.1016/j.clinph.2007.03.019.
- Hämäläinen, M., and Ilmoniemi, R. (1994). Interpreting magnetic fields of the brain: minimum norm estimates. *Med. Biol. Eng. Comput.* 32, 35–42.
- Han, C., Sun, X., Yang, Y., Che, Y., and Qin, Y. (2019). Brain complex network characteristic analysis of fatigue during simulated driving based on electroencephalogram signals. *Entropy* 21. doi:10.3390/e21040353.
- Hancock, P. A. (2019). Neuroergonomics: Where the Cortex Hits the Concrete. *Front. Hum. Neurosci.* 13. doi:10.3389/fnhum.2019.00115.
- Hassan, M., Dufor, O., Merlet, I., Berrou, C., and Wendling, F. (2014). EEG source connectivity analysis: From dense array recordings to brain networks. *PLoS One* 9. doi:10.1371/journal.pone.0105041.
- Hassan, M., Mheich, A., Wendling, F., Dufor, O., and Berrou, C. (2013). Graph-based analysis of brain connectivity during spelling task. in *2nd International Conference on Advances in Biomedical Engineering*, 191–194.

- Hassan, M., and Wendling, F. (2018). Electroencephalography source connectivity: toward high time/space resolution brain networks. *arXiv Prepr. arXiv1801.02549*. Available at: <http://arxiv.org/abs/1801.02549>.
- Hata, M., Kazui, H., Tanaka, T., Ishii, R., Canuet, L., Pascual-Marqui, R. D., et al. (2016). Functional connectivity assessed by resting state EEG correlates with cognitive decline of Alzheimer's disease - An eLORETA study. *Clin. Neurophysiol.* 127, 1269–1278. doi:10.1016/j.clinph.2015.10.030.
- Heim, S., Amunts, K., Hensel, T., Grande, M., Huber, W., Binkofski, F., et al. (2012). The Role of Human Parietal Area 7A as a Link between Sequencing in Hand Actions and in Overt Speech Production. *Front. Psychol.* 3. doi:10.3389/fpsyg.2012.00534.
- Heisz, J. J., and McIntosh, A. R. (2013). Applications of EEG neuroimaging data: event-related potentials, spectral power, and multiscale entropy. *J. Vis. Exp.*, 1–8. doi:10.3791/50131.
- Henry, J. C. (2006). Electroencephalography: Basic Principles, Clinical Applications, and Related Fields, Fifth Edition. *Neurology* 67, 2092–2092. doi:10.1212/01.wnl.0000243257.85592.9a.
- Herculano-Houzel, S. (2009). The human brain in numbers: a linearly scaled-up primate brain. *Front. Hum. Neurosci.* 3, 1–11. doi:10.3389/neuro.09.031.2009.
- Hernandez, L., Alhemood, A., Genaidy, A., and Karwowski, W. (2002). Evaluation of different scales for measurement of perceived physical strain during performance of manual tasks. *Int. J. Occup. Saf. Ergon.* 8, 413–432. doi:10.1080/10803548.2002.11076545.
- Herrera, W., Rodríguez, P., Mena, D., Cabrera, M., Escalona, J., García, A., et al. (2019). The Influence of EEG References on the Analysis of Spatio-Temporal Interrelation Patterns. *Front. Neurosci.* 13, 941. doi:10.3389/fnins.2019.00941.
- Higgins, J. P., Savović, J., Page, M. J., Elbers, R. G., and Sterne, J. A. (2019). “Cochrane Handbook for Systematic Reviews of Interventions,” in.
- Holmes, A. P., Blair, R. C., Watson, J. D. G., and Ford, I. (1996). Nonparametric analysis of statistic images from functional mapping experiments. *J. Cereb. Blood Flow Metab.* 16, 7–22. doi:10.1097/00004647-199601000-00002.
- Hsu, S. H., Pion-Tonachini, L., Palmer, J., Miyakoshi, M., Makeig, S., and Jung, T. P. (2018). Modeling brain dynamic state changes with adaptive mixture independent component analysis. *Neuroimage* 183, 47–61. doi:10.1016/j.neuroimage.2018.08.001.
- Huang, D., Ren, A., Shang, J., Lei, Q., Zhang, Y., Yin, Z., et al. (2016). Combining Partial Directed Coherence and Graph Theory to Analyse Effective Brain Networks of Different Mental Tasks. *Front. Hum. Neurosci.* 10, 1–11. doi:10.3389/fnhum.2016.00235.

- Huang, H., Yao, B., Yue, G., Brown, R., and Jing, L. (2003). Fractal dimension in EEG signals during muscle fatigue. *APS Ohio Sect. Fall Meet. Abstr.*, 25.
- Humphries, M., and Gurney, K. (2008). Network “small-world-ness”: A quantitative method for determining canonical network equivalence. *PLoS One* 3. doi:10.1371/journal.pone.0002051.
- Humphries, M., Gurney, K., and Prescott, T. (2006). The brainstem reticular formation is a small-world, not scale-free, network. *Proc. R. Soc. B Biol. Sci.* 273, 503–511. doi:10.1098/rspb.2005.3354.
- Hwang, S., Jebelli, H., Choi, B., Choi, M., and Lee, S. (2018). Measuring Workers’ Emotional State during Construction Tasks Using Wearable EEG. *J. Constr. Eng. Manag.* 144, 04018050.
- Hyvarinen, J., Laakso, M., Roine, R., and Leinonen, L. (1979). Comparison of effects of pentobarbital and ethanol on the neuronal activity in the posterior parietal association cortex. *Acta Physiol. Scand.* 107, 219–225. doi:10.1111/j.1748-1716.1979.tb06466.x.
- Iakovidou, N. (2017). Graph Theory at the Service of Electroencephalograms. *Brain Connect.* 7, 137–151. doi:10.1089/brain.2016.0426.
- IEA (2000). The Discipline of Ergonomics. International Ergonomics Association.
- Imperator, L. S., Betta, M., Cecchetti, L., Canales-Johnson, A., Ricciardi, E., Siclari, F., et al. (2019). EEG functional connectivity metrics wPLI and wSMI account for distinct types of brain functional interactions. *Sci. Rep.* 9, 1–15. doi:10.1038/s41598-019-45289-7.
- Islam, M., Rastegarnia, A., and Yang, Z. (2016). Methods for artifact detection and removal from scalp EEG: A review. *Neurophysiol. Clin.* 46, 287–305. doi:10.1016/j.neucli.2016.07.002.
- Ismail, L. E., and Karwowski, W. (2020). Applications of EEG indices for the quantification of human cognitive performance: A systematic review and bibliometric analysis. *PLoS One* 15, e0242857. doi:10.1371/journal.pone.0242857.
- Jackson, A. (1994). Preemployment Physical Evaluation. *Exerc. Sport Sci. Rev.* 22, 53–90.
- Jagannath, M., and Balasubramanian, V. (2014). Assessment of early onset of driver fatigue using multimodal fatigue measures in a static simulator. *Appl. Ergon.* 45, 1140–1147. doi:10.1016/j.apergo.2014.02.001.
- Jain, A., Abbas, B., Farooq, O., and Garg, S. K. (2016). Fatigue Detection and Estimation using Auto-Regression analysis in EEG. *2016 Int. Conf. Adv. Comput. Commun. Informatics*, 1092–1095. doi:10.1109/ICACCI.2016.7732190.
- Janani, A., Bakhshayesh, H., Willoughby, J., Grummett, T., Lewis, T., and Pope, K. (2018). How

- many channels are enough? Evaluation of tonic cranial muscle artefact reduction using ICA with different numbers of EEG channels. *Eur. Signal Process. Conf.*, 101–105. doi:10.23919/EUSIPCO.2018.8553261.
- Jasper, H. (1958). The ten-twenty electrode system of the International Federation. *Electroenceph. clin. Neurophysiol* 10, 371–375.
- Jatoi, M. A., Kamel, N., Malik, A. S., and Faye, I. (2014). EEG based brain source localization comparison of sLORETA and eLORETA. *Australas. Phys. Eng. Sci. Med.* 37, 713–721. doi:10.1007/s13246-014-0308-3.
- Jebelli, H., Asce, A. M., Hwang, S., Lee, S., and Asce, M. (2017). An EEG Signal Processing Framework to Obtain High-Quality Brain Waves from EEG Signal-Processing Framework to Obtain High-Quality Brain Waves from an Off-the-Shelf Wearable EEG Device. *J. Comput. Civ. Eng.* doi:10.1061/(ASCE)CP.1943-5487.0000719.
- Jebelli, H., Hwang, S., and Lee, S. (2018a). Automation in Construction EEG-based workers' stress recognition at construction sites. *Autom. Constr.* 93, 315–324. doi:10.1016/j.autcon.2018.05.027.
- Jebelli, H., Hwang, S., and Lee, S. (2018b). EEG Signal-Processing Framework to Obtain High-Quality Brain Waves from an Off-the-Shelf Wearable EEG Device. *J. Comput. Civ. Eng.* 32, 1–12. doi:10.1061/(ASCE)CP.1943-5487.0000719.
- Jensen, O., Kaiser, J., and Lachaux, J.-P. (2007). Human gamma-frequency oscillations associated with attention and memory. *Trends Neurosci.* 30, 317–324. doi:10.1016/j.tins.2007.05.001.
- Jin, S. H., Lin, P., and Hallett, M. (2012). Reorganization of brain functional small-world networks during finger movements. *Hum. Brain Mapp.* 33, 861–872. doi:10.1002/hbm.21253.
- Jochumsen, M., Roving, C., Roving, H., Cremoux, S., Signal, N., Allen, K., et al. (2017). Quantification of movement-related EEG correlates associated with motor training: A study on movement-related cortical potentials and sensorimotor rhythms. *Front. Hum. Neurosci.* 11, 1–12. doi:10.3389/fnhum.2017.00604.
- John, A. T., Wind, J., Horst, F., and Schöllhorn, W. I. (2020). Acute effects of an incremental exercise test on psychophysiological variables and their interaction. *J. Sport. Sci. Med.* 19, 596–612.
- Johnson, A., and Proctor, R. (2013). *Neuroergonomics: A Cognitive Neuroscience Approach to Human Factors and Ergonomics*.
- Johnston, J., Rearick, M., and Slobounov, S. (2001). Movement-related cortical potentials associated with progressive muscle fatigue in a grasping task. *Clin. Neurophysiol.* 112, 68–77. doi:10.1016/S1388-2457(00)00452-1.

- Kaiser, M. (2011). A tutorial in connectome analysis: Topological and spatial features of brain networks. *Neuroimage* 57, 892–907. doi:10.1016/j.neuroimage.2011.05.025.
- Kakkos, I., Dimitrakopoulos, G. N., Gao, L., Zhang, Y., Qi, P., Matsopoulos, G. K., et al. (2019). Mental Workload Drives Different Reorganizations of Functional Cortical Connectivity Between 2D and 3D Simulated Flight Experiments. *IEEE Trans. Neural Syst. Rehabil. Eng.* 27, 1704–1713. doi:10.1109/tnsre.2019.2930082.
- Kamijo, K., Nishihira, Y., Hatta, A., Kaneda, T., Kida, T., Higashiura, T., et al. (2004a). Changes in arousal level by differential exercise intensity. *Clin. Neurophysiol.* 115, 2693–2698. doi:10.1016/j.clinph.2004.06.016.
- Kamijo, K., Nishihira, Y., Hatta, A., Kaneda, T., Wasaka, T., Kida, T., et al. (2004b). Differential influences of exercise intensity on information processing in the central nervous system. *Eur. J. Appl. Physiol.* 92, 305–311. doi:10.1007/s00421-004-1097-2.
- Kaminski, M., and Blinowska, K. J. (2018). Is Graph Theoretical Analysis a Useful Tool for Quantification of Connectivity Obtained by Means of EEG/MEG Techniques? *Front. Neural Circuits* 12, 76. doi:10.3389/fncir.2018.00076.
- Kamiński, M., Ding, M., Truccolo, W. A., and Bressler, S. L. (2001). Evaluating causal relations in neural systems: Granger causality, directed transfer function and statistical assessment of significance. *Biol. Cybern.* 85, 145–157. doi:10.1007/s004220000235.
- Kaminski, M. J., and Blinowska, K. J. (1991). A new method of the description of the information flow in the brain structures. *Biol. Cybern.* 65, 203–210. doi:10.1007/BF00198091.
- Kamon, E., and Goldfuss, A. J. (1978). In-plant evaluation of the muscle strength of workers. *Am. Ind. Hyg. Assoc. J.* 39, 801–807. doi:10.1080/0002889778507859.
- Kar, S., and Routray, A. (2013). Effect of sleep deprivation on functional connectivity of EEG channels. *IEEE Trans. Syst. Man, Cybern. Part A Systems Humans* 43, 666–672. doi:10.1109/TSMCA.2012.2207103.
- Kar, S., Routray, A., and Nayak, B. P. (2011). Functional network changes associated with sleep deprivation and fatigue during simulated driving: Validation using blood biomarkers. *Clin. Neurophysiol.* 122, 966–974. doi:10.1016/j.clinph.2010.08.009.
- Karwowski, W. (1991). Psychophysical acceptability and perception of load heaviness by females. *Ergonomics* 34, 487–496. doi:10.1080/00140139108967331.
- Karwowski, W. (2005). Ergonomics and human factors : the paradigms for science , engineering , design , technology and management of human-compatible systems Ergonomics and human factors : the paradigms for science , engineering , design , technology and. *Ergonomics* 48, 436–463. doi:10.1080/00140130400029167.



- Karwowski, W. (2006). *International Encyclopedia of Ergonomics and Human Factors. 3 Vol. Set.*
- Karwowski, W., Siemionow, W., and Gielo-Perczak, K. (2003). Physical neuroergonomics: The human brain in control of physical work activities. *Theor. Issues Ergon. Sci.* 4, 175–199. doi:10.1080/1463922021000032339.
- Kelvin, S. O., McDowell, K., Metcalfe, J., Hairston, W. D., Kerick, S., Lee, T., et al. (2012). The Cognition and Neuroergonomics (CaN) Collaborative Technology Alliance (CTA): Scientific Vision, Approach, and Translational Paths.
- Kim, B., Kim, L., Kim, Y., and Yoo, S. K. (2017). Cross-association analysis of EEG and EMG signals according to movement intention state. *Cogn. Syst. Res.* 44, 1–9. doi:10.1016/j.cogsys.2017.02.001.
- Kim, J., and Cho, K.-H. (2016). Robustness Analysis of Network Modularity. *IEEE Trans. Control Netw. Syst.* 3, 348–357. doi:10.1109/TCNS.2015.2476197.
- Kim, Y., Park, E., Lee, A., Im, C., and Kim, Y. (2018). Changes in network connectivity during motor imagery and execution. *PLoS One* 13, 1–18. doi:10.1371/journal.pone.0190715.
- Kitaura, Y., Nishida, K., Yoshimura, M., Mii, H., Katsura, K., Ueda, S., et al. (2017). Functional localization and effective connectivity of cortical theta and alpha oscillatory activity during an attention task. *Clin. Neurophysiol. Pract.* 2, 193–200. doi:10.1016/j.cnp.2017.09.002.
- Kitzbichler, M., Henson, R., Smith, M., Nathan, P., and Bullmore, E. (2011). Cognitive Effort Drives Workspace Configuration of Human Brain Functional Networks. *J. Neurosci.* 31, 8259–8270. doi:10.1523/JNEUROSCI.0440-11.2011.
- Klados, M. A., Kanatsouli, K., Antoniou, I., Babiloni, F., Tsirka, V., Bamidis, P. D., et al. (2013). A Graph Theoretical Approach to Study the Organization of the Cortical Networks during Different Mathematical Tasks. *PLoS One* 8, e71800. doi:10.1371/journal.pone.0071800.
- Klimesch, W. (2012). Alpha-band oscillations, attention, and controlled access to stored information. *Trends Cogn. Sci.* 16, 606–617. doi:10.1016/j.tics.2012.10.007.
- Kong, W., Lin, W., Babiloni, F., Hu, S., and Borghini, G. (2015). Investigating driver fatigue versus alertness using the granger causality network. *Sensors (Switzerland)* 15, 19181–19198. doi:10.3390/s150819181.
- Kristeva-feige, R., Fritsch, C., Timmer, J., and Lu, C. (2002). Effects of attention and precision of exerted force on beta range EEG- EMG synchronization during a maintained motor contraction task. *Clin. Neurophysiol.* 113, 124–131.
- Kubitz, K., and Mott, A. (1996). EEG power spectral densities during and after cycle ergometer exercise. *Res. Q. Exerc. Sport* 67, 91–96. doi:10.1080/02701367.1996.10607929.

- Lachaux, J., Rodriguez, E., Martinerie, J., and Varela, F. (1999). Measuring phase synchrony in brain signals. *Hum. Brain Mapp.* 8, 194–208. doi:10.1017/S0007680500048066.
- Lancaster, J. L., Woldorff, M. G., Parsons, L. M., Liotti, M., Freitas, C. S., Rainey, L., et al. (2000). Automated Talairach Atlas labels for functional brain mapping. *Hum. Brain Mapp.* 10, 120–131. doi:10.1002/1097-0193(200007)10:3<120::AID-HBM30>3.0.CO;2-8.
- Lantz, G., Peralta, R., Spinelli, L., Seeck, M., and Michel, C. (2003). Epileptic source localization with high density EEG: How many electrodes are needed? *Clin. Neurophysiol.* 114, 63–69. doi:10.1016/S1388-2457(02)00337-1.
- Lanzone, J., Imperatori, C., Assenza, G., Ricci, L., Farina, B., Di Lazzaro, V., et al. (2020). Power spectral differences between transient epileptic and global amnesia: An eloreta quantitative eeg study. *Brain Sci.* 10, 1–13. doi:10.3390/brainsci10090613.
- Latora, V., and Marchiori, M. (2001). Efficient behavior of small-world networks. *Phys. Rev. Lett.* 87, 198701-1-198701–4. doi:10.1103/PhysRevLett.87.198701.
- Latora, V., and Marchiori, M. (2003). Economic small-world behavior in weighted networks. *Eur. Phys. J. B* 32, 249–263. doi:10.1140/epjb/e2003-00095-5.
- Lau, T. M., Gwin, J. T., and Ferris, D. P. (2012). Phenantrene.Pdf. 2012, 387–393. doi:10.1016/j.jns.2011.09.006.
- Lee, J., Wickens, C., Liu, Y., and Boyle, L. (2017). “Designing for people: an introduction to human factors engineering,” in.
- Lee, L., Harrison, L. M., and Mechelli, A. (2003a). A report of the functional connectivity workshop, Dusseldorf 2002. *Neuroimage* 19, 457–465. doi:10.1016/S1053-8119(03)00062-4.
- Lee, L., Harrison, L. M., and Mechelli, A. (2003b). The Functional Brain Connectivity Workshop: report and commentary. *Netw. Comput. Neural Syst.* 14, R1–R15. doi:10.1088/0954-898X.
- Li, G., Li, B., Wang, G., Zhang, J., and Wang, J. (2017). A New Method for Human Mental Fatigue Detection with Several EEG Channels. *J. Med. Biol. Eng.* 37, 240–247. doi:10.1007/s40846-017-0224-6.
- Li, G., Luo, Y., Zhang, Z., Xu, Y., Jiao, W., Jiang, Y., et al. (2019). Effects of Mental Fatigue on Small-World Brain Functional Network Organization. *Neural Plast.* 2019. doi:10.1155/2019/1716074.
- Li, J., Lim, J., Chen, Y., Wong, K., Thakor, N., Bezerianos, A., et al. (2016). Mid-task break improves global integration of functional connectivity in lower alpha band. *Front. Hum. Neurosci.* 10, 1–12. doi:10.3389/fnhum.2016.00304.

- Liberati, A., Altman, D. G., Tetzlaff, J., Mulrow, C., Gøtzsche, P. C., Ioannidis, J. P. A., et al. (2009). The PRISMA Statement for Reporting Systematic Reviews and Meta-Analyses of Studies That Evaluate Health Care Interventions : Explanation and Elaboration. *PLoS Med.* 6, e1000100. doi:10.1371/journal.pmed.1000100.
- Light, G. A., Williams, L. E., Minow, F., Sprock, J., Rissling, A., Sharp, R., et al. (2010). “Electroencephalography (EEG) and Event-Related Potentials (ERP’s) with Human Participants,” in *Current Protocols in Neuroscience*, 6–25. doi:10.1002/0471142301.ns0625s52.Electroencephalography.
- Lin, S., Jao, C., Wang, P., and Wu, Y. (2017). Analysis of Electroencephalography Alteration During Sustained Cycling Exercise Using Power Spectrum and Fuzzy Entropy. *Int. J. Fuzzy Syst.* 19, 580–590. doi:10.1007/s40815-016-0273-y.
- Lithari, C., Klados, M. A., Papadelis, C., Pappas, C., Albani, M., and Bamidis, P. D. (2012). How does the metric choice affect brain functional connectivity networks? *Biomed. Signal Process. Control* 7, 228–236. doi:10.1016/j.bspc.2011.05.004.
- Liu, J., Lewandowski, B., Karakasis, C., Yao, B., Siemionow, V., Sahgal, V., et al. (2007). Shifting of activation center in the brain during muscle fatigue: An explanation of minimal central fatigue? *Neuroimage* 35, 299–307. doi:10.1016/j.neuroimage.2006.09.050.
- Liu, J., Li, M., Pan, Y., Lan, W., Zheng, R., Wu, F. X., et al. (2017). Complex Brain Network Analysis and Its Applications to Brain Disorders: A Survey. *Complexity* 2017. doi:10.1155/2017/8362741.
- Liu, J., Yang, Q., Brown, R., and Yue, G. (2005a). Linear correlation between fractal dimension of EEG signal and handgrip force. *Biol. Cybern.* 93, 131–140. doi:10.1007/s00422-005-0561-3.
- Liu, J., Yao, B., Siemionow, V., Sahgal, V., Wang, X., Sun, J., et al. (2005b). Fatigue induces greater brain signal reduction during sustained than preparation phase of maximal voluntary contraction. *Brain Res.* 1057, 113–126. doi:10.1016/j.brainres.2005.07.064.
- Liu, J., Zhang, C., and Zheng, C. (2010). Estimation of the cortical functional connectivity by directed transfer function during mental fatigue. *Appl. Ergon.* 42, 114–121. doi:10.1016/j.apergo.2010.05.008.
- Lopes da Silva, F. (2013). EEG and MEG: Relevance to neuroscience. *Neuron* 80, 1112–1128. doi:10.1016/j.neuron.2013.10.017.
- Lotze, M., Montoya, P., Erb, M., Hülsmann, E., Flor, H., Klose, U., et al. (1999). Activation of Cortical and Cerebellar Motor Areas during Executed and Imagined Hand Movements: An fMRI Study. *J. Cogn. Neurosci.* 11, 491–501. doi:10.1162/089892999563553.

- Luck, S. J. (2014). *An Introduction to the Event-Related Potential Technique*. MIT press.
- Lutzenberger, W., Preissl, H., and Pulvermüller, F. (1995). Fractal dimension of electroencephalographic time series and underlying brain processes. *Biol. Cybern.* 482, 477–482.
- Ma, Q., Sun, X., Fu, H., Zhao, D., and Guo, J. (2013). Manufacturing Process Design Based on Mental and Physical Workload Analysis. *Appl. Mech. Mater.* 345, 482–485. doi:10.4028/www.scientific.net/AMM.345.482.
- Ma, X., Jiang, G., Fu, S., Fang, J., Wu, Y., Liu, M., et al. (2018). Enhanced Network Efficiency of Functional Brain Networks in Primary Insomnia Patients. *Front. Psychiatry* 9. doi:10.3389/fpsyt.2018.00046.
- Mackenzie, T. N., Bailey, A. Z., Mi, P. Y., Tsang, P., Jones, C. B., and Nelson, A. J. (2016). Human area 5 modulates corticospinal output during movement preparation. *Neuroreport* 27, 1056–1060. doi:10.1097/WNR.0000000000000655.
- Maess, B., Schröger, E., and Widmann, A. (2016). High-pass filters and baseline correction in M/EEG analysis. Commentary on: “How inappropriate high-pass filters can produce artefacts and incorrect conclusions in ERP studies of language and cognition.” *J. Neurosci. Methods* 266, 164–165. doi:10.1016/j.jneumeth.2015.12.003.
- Majumder, S., Guragain, B., Wang, C., and Wilson, N. (2019). On-board drowsiness detection using EEG: Current status and future prospects. *IEEE Int. Conf. Electro Inf. Technol.* 2019-May, 483–490. doi:10.1109/EIT.2019.8833866.
- Makeig, S., Bell, A. J., Jung, T.-P., and Sejnowski, T. J. (1996). Independent Component Analysis of Electroencephalographic Data. *Adv. Neural Inf. Process. Syst.* 8, 145–151.
- Marcora, S. (2010). *Effort. Perception of.*, ed. I. E. B. Goldstein Thousand Oaks, CA: SAGE In, Publications doi:10.1002/cb.1444/abstract.
- Marcora, S. M., and Staiano, W. (2010). The limit to exercise tolerance in humans: mind over muscle? *Eur. J. Appl. Physiol.* 109, 763–770. doi:10.1007/s00421-010-1418-6.
- Marras, W., and Karwowski, W. (2006). *Fundamentals and Assessment Tools for Occupational Ergonomics*. 1st ed. CRC Press doi:10.1201/9781420003635.
- Marzetti, L., Basti, A., Chella, F., D’Andrea, A., Syrjäälä, J., and Pizzella, V. (2019). Brain Functional Connectivity Through Phase Coupling of Neuronal Oscillations: A Perspective From Magnetoencephalography. *Front. Neurosci.* 13, 1–21. doi:10.3389/fnins.2019.00964.
- Mazziotta, J., Toga, A., Evans, A., Fox, P., Lancaster, J., Zilles, K., et al. (2001). A probabilistic atlas and reference system for the human brain: International Consortium for Brain Mapping

- (ICBM). *Philos. Trans. R. Soc. London. Ser. B Biol. Sci.* 356, 1293–1322. doi:10.1098/rstb.2001.0915.
- Mechau, D., Mücke, S., Liesen, H., and Weiß, M. (1998). Effect of increasing running velocity on electroencephalogram in a field test. *Eur. J. Appl. Physiol. Occup. Physiol.* 78, 340–345.
- Mehta, R. (2016). Integrating Physical and Cognitive Ergonomics Integrating Physical and Cognitive Ergonomics. *Trans. Occup. Ergon. Hum. Factors* 4, 83–87. doi:10.1080/21577323.2016.1207475.
- Mehta, R., and Parasuraman, R. (2013). Neuroergonomics: a review of applications to physical and cognitive work. *Front. Hum. Neurosci.* 7, 1–10. doi:10.3389/fnhum.2013.00889.
- Meinel, A., Castaño-Candamil, S., Reis, J., and Tangermann, M. (2016). Pre-Trial EEG-Based Single-Trial Motor Performance Prediction to Enhance Neuroergonomics for a Hand Force Task. *Front. Hum. Neurosci.* 10, 1–17. doi:10.3389/fnhum.2016.00170.
- Michel, C., Murray, M., Lantz, G., Gonzalez, S., Spinelli, L., and Peralta, R. (2004). EEG source imaging. *Clin. Neurophysiol.* 115, 2195–2222. doi:10.1016/j.clinph.2004.06.001.
- Micheloyannis, S., Pachou, E., Stam, C., Breakspear, M., Bitsios, P., Vourkas, M., et al. (2006a). Small-world networks and disturbed functional connectivity in schizophrenia. *Schizophr. Res.* 87, 60–66. doi:10.1016/j.schres.2006.06.028.
- Micheloyannis, S., Pachou, E., Stam, C., Vourkas, M., Erimaki, S., and Tsirka, V. (2006b). Using graph theoretical analysis of multi channel EEG to evaluate the neural efficiency hypothesis. *Neurosci. Lett.* 402, 273–277. doi:10.1016/j.neulet.2006.04.006.
- Micheloyannis, S., Vourkas, M., Tsirka, V., Karakonstantaki, E., Kanatsouli, K., and Stam, C. J. (2009). The influence of ageing on complex brain networks: A graph theoretical analysis. *Hum. Brain Mapp.* 30, 200–208. doi:10.1002/hbm.20492.
- Mierlo, P., Höller, Y., Focke, N., and Vulliemoz, S. (2019). Network Perspectives on Epilepsy Using EEG / MEG Source Connectivity. *Front. Neurol.* 10, 1–13. doi:doi.org/10.3389/fneur.2019.00721.
- Mijović, P., Ković, V., De Vos, M., Mačuzić, I., Jeremić, B., and Gligorijević, I. (2016). Benefits of Instructed Responding in Manual Assembly Tasks: An ERP Approach. *Front. Hum. Neurosci.* 10, 1–13. doi:10.3389/fnhum.2016.00171.
- Mikkelsen, K., Stojanovska, L., Polenakovic, M., Bosevski, M., and Apostolopoulos, V. (2017). Exercise and mental health. *Maturitas* 106, 48–56. doi:10.1016/j.maturitas.2017.09.003.
- Mital, A., Garg, A., Karwowski, W., Kumar, S., Smith, J., and Ayoub, M. (1993). Status in human strength research and application. *IIE Trans. (Institute Ind. Eng.* 25, 57–69.

doi:10.1080/07408179308964328.

- Mital, A., and Kumar, S. (1998). Human muscle strength definitions , measurement , and usage : Part I — Guidelines for the practitioner. *Int. J. Ind. Ergon.* 22, 101–121.
- Moher, D., Liberati, A., Tetzlaff, J., and Altman, D. (2009). Preferred Reporting Items for Systematic Reviews and Meta-Analyses : The PRISMA Statement. *PLoS Med.* 6, e1000097. doi:https://doi.org/10.1371/journal.pmed.1000097.
- Moher, D., Liberati, A., Tetzlaff, J., and Altman, D. (2010). Preferred reporting items for systematic reviews and meta-analyses: The PRISMA statement. *Int. J. Surg.* 8, 336–341. doi:10.1016/j.ijsu.2010.02.007.
- Morree, H., Klein, C., and Marcora, S. (2014). Cortical substrates of the effects of caffeine and time-on-task on perception of effort. *J. Appl. Physiol.* 117, 1514–1523. doi:10.1152/jappphysiol.00898.2013.
- Mullen, T., Kothe, C., Chi, Y. M., Ojeda, A., Kerth, T., Makeig, S., et al. (2013). Real-Time Modeling and 3D Visualization of Source Dynamics and Connectivity Using Wearable EEG. in *Annual International Conference of the IEEE Engineering in Medicine and Biology Society*, 2184–2187. doi:10.1109/EMBC.2013.6609968.Real-Time.
- Mullen, T. R., Kothe, C. A. E., Chi, Y. M., Ojeda, A., Kerth, T., Makeig, S., et al. (2015). Real-time neuroimaging and cognitive monitoring using wearable dry EEG. *IEEE Trans. Biomed. Eng.* 62, 2553–2567. doi:10.1109/TBME.2015.2481482.
- Muthukumaraswamy, S., and Johnson, B. (2004). Changes in rolandic mu rhythm during observation of a precision grip. *Psychophysiology* 41, 152–156. doi:10.1046/j.1469-8986.2003.00129.x.
- Nakayashiki, K., Saeki, M., Takata, Y., Hayashi, Y., and Kondo, T. (2014). Modulation of event-related desynchronization during kinematic and kinetic hand movements. *J. Neuroeng. Rehabil.* 11, 1–9. doi:10.1186/1743-0003-11-90.
- Nascimento, O., Nielsen, K., and Voigt, M. (2005). Relationship between plantar-flexor torque generation and the magnitude of the movement-related potentials. *Exp. brain Res.* 160, 154–165. doi:10.1007/s00221-004-1996-9.
- Neumann, W. P., Kolus, A., and Wells, R. W. (2016). Human Factors in Production System Design and Quality Performance – A Systematic Review. *IFAC-PapersOnline* 49, 1721–1724. doi:10.1016/j.ifacol.2016.07.830.
- Newman, M. E. J. (2003). The structure and function of complex networks. *SIAM Rev.* 45, 167–256. doi:10.1137/S003614450342480.

- Ng, S., and Raveendran, P. (2007). EEG peak alpha frequency as an indicator for physical fatigue. in *In the 11th Mediterranean Conference on Medical and Biomedical Engineering and Computing*, 517–520. Available at: [http://link.springer.com/chapter/10.1007/978-3-540-73044-6\\_132](http://link.springer.com/chapter/10.1007/978-3-540-73044-6_132).
- Ng, S., and Raveendran, P. (2011). Effects of physical fatigue onto brain rhythms. *IFMBE Proc.* 35 IFMBE, 511–515. doi:10.1007/978-3-642-21729-6\_129.
- Nguyen, P., Li, X., Hayashi, Y., Yano, S., and Kondo, T. (2019). Estimation of Brain Dynamics Under Visuomotor Task using Functional Connectivity Analysis Based on Graph Theory. *2019 IEEE 19th Int. Conf. Bioinforma. Bioeng.*, 577–582. doi:10.1109/BIBE.2019.00110.
- Nichols, T. E., and Holmes, A. P. (2002a). Nonparametric permutation tests for functional neuroimaging: A primer with examples. *Hum. Brain Mapp.* 15, 1–25. doi:<https://doi.org/10.1002/hbm.1058>.
- Nichols, T., and Holmes, A. (2002b). Nonparametric Permutation Tests for Functional Neuroimaging: A Primer with Examples. *Hum. Brain Mapp.* 15, 1–25. doi:10.1016/B978-012264841-0/50048-2.
- Nicholson, L., and Legg, S. (1986). A psychophysical study of the effects of load and frequency upon selection of workload in repetitive lifting. *Ergonomics* 29, 903–911. doi:10.1080/00140138608967202.
- Nielsen, B., Hyldig, T., Bidstrup, F., González-Alonso, J., and Christoffersen, G. R. J. (2001). Brain activity and fatigue during prolonged exercise in the heat. *Pflugers Arch. Eur. J. Physiol.* 442, 41–48. doi:10.1007/s004240100515.
- Nielsen, B., and Nybo, L. (2003). Cerebral changes during exercise in the heat. *Sport. Med* 33, 1–11. doi:10.2165/00007256-200333010-00001.
- Nijholt, A., Tan, D., Pfurtscheller, G., Brunner, C., Millán, J. del R., Allison, B., et al. (2008). Brain-Computer Interfacing for Intelligent Systems. *IEEE Intell. Syst.* 23, 72–79. doi:10.1109/MIS.2008.41.
- Nolte, G., Bai, O., Wheaton, L., Mari, Z., Vorbach, S., and Hallett, M. (2004). Identifying true brain interaction from EEG data using the imaginary part of coherency. *Clin. Neurophysiol.* 115, 2292–2307. doi:10.1016/j.clinph.2004.04.029.
- Nunez, P., Srinivasan, R., Westdorp, A., Wijesinghe, R., Tucker, D., Silberstein, R., et al. (1997). EEG coherency I: Statistics, reference electrode, volume conduction, Laplacians, cortical imaging, and interpretation at multiple scales. *Electroencephalogr. Clin. Neurophysiol.* 103, 499–515. doi:10.1016/S0013-4694(97)00066-7.
- Nybo, L., and Nielsen, B. (2001). Perceived exertion is associated with an altered brain activity

- during exercise with progressive hyperthermia. *J. Appl. Physiol.* 91, 2017–2023. doi:10.1152/jappl.2001.91.5.2017.
- O’Neill, G. C., Tewarie, P., Vidaurre, D., Liuzzi, L., Woolrich, M. W., and Brookes, M. J. (2018). Dynamics of large-scale electrophysiological networks: A technical review. *Neuroimage* 180, 559–576. doi:10.1016/j.neuroimage.2017.10.003.
- Olbrich, S., Olbrich, H., Adamaszek, M., Jahn, I., Hegerl, U., and Stengler, K. (2013). Altered EEG lagged coherence during rest in obsessive-compulsive disorder. *Clin. Neurophysiol.* 124, 2421–2430. doi:10.1016/j.clinph.2013.05.031.
- Oostendorp, T. F., and van Oosterom, A. (1989). Source parameter estimation in inhomogeneous volume conductors of arbitrary shape. *IEEE Trans. Biomed. Eng.* 36, 382–391. doi:10.1109/10.19859.
- Oostenveld, R., and Oostendorp, T. F. (2002). Validating the boundary element method for forward and inverse EEG computations in the presence of a hole in the skull. *Hum. Brain Mapp.* 17, 179–192. doi:10.1002/hbm.10061.
- Oostenveld, R., and Praamstra, P. (2001). The five percent electrode system for high-resolution EEG and ERP measurements. *Clin. Neurophysiol.* 112, 713–719. doi:10.1016/S1388-2457(00)00527-7.
- Pageaux, B., Marcora, S. M., Rozand, V., and Lepers, R. (2015). Mental fatigue induced by prolonged self-regulation does not exacerbate central fatigue during subsequent whole-body endurance exercise. *Front. Hum. Neurosci.* 9. doi:10.3389/fnhum.2015.00067.
- Pakkenberg, B., Pelvig, D., Marner, L., Bundgaard, M. J., Gundersen, H. J. G., Nyengaard, J. R., et al. (2003). Aging and the human neocortex. *Exp. Gerontol.* 38, 95–99. doi:10.1016/S0531-5565(02)00151-1.
- Palmer, J., Kreutz-Delgado, K., and Makeig, S. (2011). AMICA: An Adaptive Mixture of Independent Component Analyzers with Shared Components. *San Diego, CA Tech. report, Swart. Cent. Comput. Neurosci.*, 1–15. Available at: [http://scn.ucsd.edu/~jason/amica\\_a.pdf%5Cnpapers2://publication/uuid/E6296FC1-7F6B-400C-85D0-3A292A27F710](http://scn.ucsd.edu/~jason/amica_a.pdf%5Cnpapers2://publication/uuid/E6296FC1-7F6B-400C-85D0-3A292A27F710).
- Palmiero, M., and Piccardi, L. (2017). Frontal EEG Asymmetry of Mood: A Mini-Review. *Front. Behav. Neurosci.* 11. doi:10.3389/fnbeh.2017.00224.
- Parasuraman, R. (2003). Neuroergonomics: Research and practice. *Theor. Issues Ergon. Sci.* 4, 5–20. doi:10.1080/14639220210199753.
- Parasuraman, R., and Matthew, R. (2008). *Neuroergonomics: The brain at work*. In Oxford University Press.



- Parasuraman, R., and Wilson, G. F. (2008). Putting the Brain to Work: Neuroergonomics Past, Present, and Future. *Hum. Factors J. Hum. Factors Ergon. Soc.* 50, 468–474. doi:10.1518/001872008X288349.
- Pascual-Marqui (2002a). Standardized low-resolution brain electromagnetic tomography (sLORETA): technical details. *Methods Find Exp Clin Pharmacol* 24(Suppl D), 5–12.
- Pascual-Marqui, R. (2002b). Standardized low-resolution brain electromagnetic tomography (sLORETA): technical details. *Methods Find Exp Clin Pharmacol* 24 no. Suppl, 5–12.
- Pascual-Marqui, R. D. (2007). Discrete, 3D distributed, linear imaging methods of electric neuronal activity. Part 1: exact, zero error localization. *larXiv Prepr. arXiv*, 0710.3341. Available at: <http://arxiv.org/abs/0710.3341>.
- Pascual-Marqui, R. D., Biscay, R. J., Valdes-Sosa, P. A., Bosch-Bayard, J., and Riera-Diaz, J. J. (2011a). Cortical current source connectivity by means of partial coherence fields. *arXiv Prepr. arXiv*, 1108.0251. doi:10.5167/uzh-58049.
- Pascual-Marqui, R. D., Esslen, M., Kochi, K., and Lehmann, D. (2002). Functional imaging with low-resolution brain electromagnetic tomography (LORETA): a review. *Methods Find Exp Clin Pharmacol.* 24, 91–95.
- Pascual-Marqui, R. D., Lehmann, D., Koukkou, M., Kochi, K., Anderer, P., Saletu, B., et al. (2011b). Assessing interactions in the brain with exact low-resolution electromagnetic tomography. *Philos. Trans. R. Soc. A Math. Phys. Eng. Sci.* 369, 3768–3784. doi:10.1098/rsta.2011.0081.
- Pascual-Marqui, R. D., Michel, C. M., and Lehmann, D. (1994). Low resolution electromagnetic tomography: a new method for localizing electrical activity in the brain. *Int. J. Psychophysiol.* 18, 49–65. doi:10.1016/0167-8760(84)90014-X.
- Pascual, M., Lehmann, C., and Michel, D. (1994). Low-resolution electromagnetic tomography—a new method for localizing electrical activity in the brain. *Int. J. Psychophysiol.* 18, 49–65.
- Pegg, E. J., Taylor, J. R., Keller, S. S., and Mohanraj, R. (2020). Epilepsy & Behavior Interictal structural and functional connectivity in idiopathic generalized epilepsy : A systematic review of graph theoretical studies. *Epilepsy Behav.* 106, 107013. doi:10.1016/j.yebeh.2020.107013.
- Périard, J., De Pauw, K., Zanow, F., and Racinais, S. (2018). Cerebrocortical activity during self-paced exercise in temperate, hot and hypoxic conditions. *Acta Physiol.* 222, 1–13. doi:10.1111/apha.12916.
- Pfurtscheller, G. (1992). Event-related synchronization (ERS): an electrophysiological correlate of cortical areas at rest. *Electroencephalogr Clin Neurophysiol* 83, 62–9.

- Pfurtscheller, G., Neuper, C., and Krausz, G. (2000). Functional dissociation of lower and upper frequency mu rhythms in relation to voluntary limb movement. *Clin. Neurophysiol.* 111, 1873–1879.
- Pfurtscheller, G., Zalaudek, K., and Neuper, C. (1998). Event-related beta synchronization after wrist, finger and thumb movement. *Electroencephalogr. Clin. Neurophysiol. - Electromyogr. Mot. Control* 109, 154–160. doi:10.1016/S0924-980X(97)00070-2.
- Piazza, C., Miyakoshi, M., Akalin-Acar, Z., Cantiani, C., Reni, G., Bianchi, A. M., et al. (2016). “An Automated Function for Identifying EEG Independent Components Representing Bilateral Source Activity,” in *IFMBE Proceedings*, 105–109. doi:10.1007/978-3-319-32703-7\_22.
- Pichardo-Rivas, K. A., and Gutiérrez, D. (2021). On the functional connectivity between heart, muscle, and frontal brain cortex during exercise fatigability. *Comput. Methods Biomech. Biomed. Engin.*, 1–11. doi:10.1080/10255842.2020.1849154.
- Pion-Tonachini, L., Kreutz-Delgado, K., and Makeig, S. (2019a). ICLabel: An automated electroencephalographic independent component classifier, dataset, and website. *Neuroimage* 198, 181–197. doi:10.1016/j.neuroimage.2019.05.026.
- Pion-Tonachini, L., Kreutz-Delgado, K., and Makeig, S. (2019b). The ICLabel dataset of electroencephalographic (EEG) independent component (IC) features. *Data Br.* 25, 104101. doi:10.1016/j.dib.2019.104101.
- Pitto, L., Novakovic, V., Basteris, A., and Sanguineti, V. (2011). Neural correlates of motor learning and performance in a virtual ball putting task. *IEEE Int. Conf. Rehabil. Robot.*, 1–6. doi:10.1109/ICORR.2011.5975487.
- Ponomareva, N., Andreeva, T., Protasova, M., Konovalov, R., Krotenkova, M., Malina, D., et al. (2020). Genetic Association Between Alzheimer’s Disease Risk Variant of the PICALM Gene and EEG Functional Connectivity in Non-demented Adults. *Front. Neurosci.* 14. doi:10.3389/fnins.2020.00324.
- Porter, S., Silverberg, N., and Virji-Babul, N. (2019). Cortical activity and network organization underlying physical and cognitive exertion in active young adult athletes: Implications for concussion. *J. Sci. Med. Sport* 22, 397–402. doi:10.1016/j.jsams.2018.09.233.
- Qi, P., Ru, H., Gao, L., Zhang, X., Zhou, T., Tian, Y., et al. (2019). Neural Mechanisms of Mental Fatigue Revisited: New Insights from the Brain Connectome. *Engineering* 5, 276–286. doi:10.1016/j.eng.2018.11.025.
- Raichle, M. E. (2009). A Paradigm Shift in Functional Brain Imaging. *J. Neurosci.* 29, 12729–12734. doi:10.1523/JNEUROSCI.4366-09.2009.

- Reijneveld, J. C., Ponten, S. C., Berendse, H. W., and Stam, C. J. (2007). The application of graph theoretical analysis to complex networks in the brain. *Clin. Neurophysiol.* 118, 2317–2331. doi:10.1016/j.clinph.2007.08.010.
- Reis, P., Hebenstreit, F., Gabsteiger, F., Vinzenz, T., and Matthias, L. (2014). Methodological aspects of EEG and body dynamics measurements during motion. *Front. Hum. Neurosci.* 8, 9–27. doi:10.3389/fnhum.2014.00156.
- Ren, S., Li, J., Taya, F., DeSouza, J., Thakor, N. V., and Bezerianos, A. (2017). Dynamic Functional Segregation and Integration in Human Brain Network during Complex Tasks. *IEEE Trans. Neural Syst. Rehabil. Eng.* 25, 547–556. doi:10.1109/TNSRE.2016.2597961.
- Ren, S., Taya, F., Sun, Y., Desouza, J., Thakor, N. V., and Bezerianos, A. (2015). Assessing small-worldness of dynamic functional brain connectivity during complex tasks. *Proc. Annu. Int. Conf. IEEE Eng. Med. Biol. Soc. EMBS 2015-Novem*, 2904–2907. doi:10.1109/EMBC.2015.7318999.
- Richard, L. . (1980). On the psychology of passenger comfort. *Hum. Factors Transp. Res. (London Acad. Press.* 2, 15–23.
- Rizzolatti, G., and Craighero, L. (2004). The Mirror-Neuron System. *Annu. Rev. Neurosci.* 27, 169–192. doi:10.1146/annurev.neuro.27.070203.144230.
- Robertson, R., and Noble, B. (1997). Perception of physical exertion: methods, mediators, and applications. *Exerc Sport Sci Rev.* 25, 407–52.
- Robertson, C. V., and Marino, F. E. (2016). A role for the prefrontal cortex in exercise tolerance and termination. *J. Appl. Physiol.* 120, 464–466. doi:10.1152/jappphysiol.00363.2015.
- Rubinov, M., and Sporns, O. (2010). Complex network measures of brain connectivity: Uses and interpretations. *Neuroimage* 52, 1059–1069. doi:10.1016/j.neuroimage.2009.10.003.
- Ruffini, G., Dunne, S., Farrés, E., Marco-Pallarés, J., Ray, C., Mendoza, E., et al. (2006). A dry electrophysiology electrode using CNT arrays. *Sensors Actuators, A Phys.* 132, 34–41. doi:10.1016/j.sna.2006.06.013.
- Rusinov, V. (2012). “Electrophysiology of the central nervous system,” in, Media, Springer Science & Business.
- Rutter, L., Nadar, S. R., Holroyd, T., Carver, F. W., Apud, J., Weinberger, D. R., et al. (2013). Graph theoretical analysis of resting magnetoencephalographic functional connectivity networks. *Front. Comput. Neurosci.* 7, 1–21. doi:10.3389/fncom.2013.00093.
- Sakkalis, V. (2011). Review of advanced techniques for the estimation of brain connectivity measured with EEG/MEG. *Comput. Biol. Med.* 41, 1110–1117.

doi:10.1016/j.combiomed.2011.06.020.

Salvendy, G. (2012). *Handbook of human factors and ergonomics*. 4th ed. John Wiley & Sons.

Samima, S., and Sarma, M. (2019). EEG-Based Mental Workload Estimation. in *2019 41st Annual International Conference of the IEEE Engineering in Medicine and Biology Society (EMBC)* (IEEE), 5605–5608. doi:10.1109/embc.2019.8857164.

Sauseng, P., Hoppe, J., Klimesch, W., Gerloff, C., and Hummel, F. (2007). Dissociation of sustained attention from central executive functions: Local activity and interregional connectivity in the theta range. *Eur. J. Neurosci.* 25, 587–593. doi:10.1111/j.1460-9568.2006.05286.x.

Sauseng, P., Klimesch, W., Schabus, M., and Doppelmayr, M. (2005). Fronto-parietal EEG coherence in theta and upper alpha reflect central executive functions of working memory. *Int. J. Psychophysiol.* 57, 97–103. doi:10.1016/j.ijpsycho.2005.03.018.

Scerbo, M. W., Freeman, F. G., and Mikulka, P. J. (2003). A brain-based system for adaptive automation. *Theor. Issues Ergon. Sci.* 4, 200–219. doi:10.1080/1463922021000020891.

Schillings, M., Kalkman, J., Werf, S., Bleijenberg, G., van Engelen, B., and Zwarts J., M. (2006). Central adaptations during repetitive contractions assessed by the readiness potential. *Eur. J. Appl. Physiol.*, 521–526. doi:10.1007/s00421-006-0211-z.

Schmitt, A., Upadhyay, N., Martin, J. A., Rojas, S., Strüder, H. K., and Boecker, H. (2019). Modulation of Distinct Intrinsic Resting State Brain Networks by Acute Exercise Bouts of Differing Intensity. *Brain Plast.* 5, 39–55. doi:10.3233/BPL-190081.

Schneider, S., Askew, C. D., Diehl, J., Mierau, A., Kleinert, J., Abel, T., et al. (2009a). EEG activity and mood in health orientated runners after different exercise intensities. *Physiol. Behav.* 96, 709–716. doi:10.1016/j.physbeh.2009.01.007.

Schneider, S., Brümmer, V., Abel, T., Askew, C. D., and Strüder, H. K. (2009b). Changes in brain cortical activity measured by EEG are related to individual exercise preferences. *Physiol. Behav.* 98, 447–452. doi:10.1016/j.physbeh.2009.07.010.

Schoffelen, J. M., and Gross, J. (2009). Source connectivity analysis with MEG and EEG. *Hum. Brain Mapp.* 30, 1857–1865. doi:10.1002/hbm.20745.

Sciaraffa, N., Borghini, G., Aricò, P., Di Flumeri, G., Colosimo, A., Bezerianos, A., et al. (2017). Brain interaction during cooperation: Evaluating local properties of multiple-brain network. *Brain Sci.* 7, 90. doi:10.3390/brainsci7070090.

Sengupta, A., Datta, S., Kar, S., and Routray, A. (2014a). EEG synchronization and brain networks: A case study in Fatigue. in *International Conference on Medical Imaging, m-*

*Health and Emerging Communication Systems (MedCom)*, 278–282.

- Sengupta, A., Routray, A., and Kar, S. (2014b). Estimation of fatigue in drivers by analysis of brain networks. *Proc. - 4th Int. Conf. Emerg. Appl. Inf. Technol. EAIT 2014*, 289–293. doi:10.1109/EAIT.2014.49.
- Sethi, N., Sethi, P., Torgovnick, J., and Arsura, E. (2006). Physiological and non-physiological EEG artifacts. *Internet J. Neuromonitoring* 5, 3–5.
- Shakeel, A., Navid, M., Anwar, M., Mazhar, S., Jochumsen, M., and Niazi, I. K. (2015). A Review of Techniques for Detection of Movement Intention Using Movement-Related Cortical Potentials. *Comput. Math. Methods Med.* 2015.
- Shamlo, N., Mullen, T., Kothe, C., Su, K., and Robbins, K. (2015). The PREP pipeline: Standardized preprocessing for large-scale EEG analysis. *Front. Neuroinform.* 9, 1–19. doi:10.3389/fninf.2015.00016.
- Shaw, E. P., Rietschel, J. C., Shuggi, I. M., Xu, Y., Chen, S., Miller, M. W., et al. (2019). Cerebral cortical networking for mental workload assessment under various demands during dual-task walking. *Exp. Brain Res.* 237, 2279–2295. doi:10.1007/s00221-019-05550-x.
- Shibasaki, H., and Hallett, M. (2006). What is the Bereitschaftspotential? *Clin. Neurophysiol.* 117, 2341–2356. doi:10.1016/j.clinph.2006.04.025.
- Shibata, M., Oda, S., and Moritani, T. (1997). The Relationships Between Movement-related Cortical Potentials and Motor Unit Activity During Muscle Contraction. *J. Electromyogr. Kinesiol.* 7, 79–85.
- Shortz, A., Dyke, S., and Mehta, R. (2012). Neural Correlates of Physical and Mental Fatigue. *Shortz, A. E., Van Dyke, S., Mehta, R. K. (2012, Sept. Neural Correl. Phys. Ment. fatigue. Proc. Hum. Factors Ergon. Soc. Annu. Meet. Sage CA Los Angeles, CA SAGE Publ.* 56, 2172–2176. doi:10.1177/1071181312561459.
- Shou, G., Yuan, H., Li, C., Chen, Y., Chen, Y., and Ding, L. (2020). Whole-brain electrophysiological functional connectivity dynamics in resting-state EEG. *J. Neural Eng.* 17. doi:10.1088/1741-2552/ab7ad3.
- Shreekanth Umesh, D., Tikka, S. K., Goyal, N., Nizamie, S. H., and Sinha, V. K. (2016). Resting state theta band source distribution and functional connectivity in remitted schizophrenia. *Neurosci. Lett.* 630, 199–202. doi:10.1016/j.neulet.2016.07.055.
- Siemionow, V., Yue, G. H., Ranganathan, V., Liu, J., and Sahgal, V. (2000). Relationship between motor activity-related cortical potential and voluntary muscle activation. *Exp. Brain Res.* 133, 303–311.

- Slobounov, S., Fukada, K., Simon, R., Rearick, M., and Ray, W. (2000). Neurophysiological and behavioral indices of time pressure effects on visuomotor task performance. *Cogn. Brain Res.* 9, 287–298.
- Slobounov, S., Hallett, M., and Newell, K. M. (2004). Perceived effort in force production as reflected in motor-related cortical potentials. *Clin. Neurophysiol.* 115, 2391–2402. doi:10.1016/j.clinph.2004.05.021.
- Slobounov, S., Johnston, J., Chiang, H., and Ray, W. (2002). Movement-related EEG potentials are force or end-effector dependent: evidence from a multi-finger experiment. *Clin. Neurophysiol.* 113, 1125–1135.
- Smit, A. S., Eling, P. A. T. M., Hopman, M. T., and Coenen, A. M. L. (2005). Mental and physical effort affect vigilance differently. *Int. J. Psychophysiol.* 57, 211–217. doi:10.1016/j.ijpsycho.2005.02.001.
- Snook, S. H. (1978). THE DESIGN OF MANUAL HANDLING TASKS. *Ergonomics* 21, 963–985. doi:10.1080/00140137808931804.
- Song, J., Davey, C., Poulsen, C., Luu, P., Turovets, S., Anderson, E., et al. (2015). EEG source localization: Sensor density and head surface coverage. *J. Neurosci. Methods* 256, 9–21. doi:10.1016/j.jneumeth.2015.08.015.
- Sporns, O. (2011). The human connectome : a complex network. *Ann. N. Y. Acad. Sci.* 1224, 109–125. doi:10.1111/j.1749-6632.2010.05888.x.
- Sporns, O. (2014). Contributions and challenges for network models in cognitive neuroscience. *Nat. Neurosci.* 17, 652–660. doi:10.1038/nn.3690.
- Sporns, O., Honey, C. J., and Kötter, R. (2007). Identification and Classification of Hubs in Brain Networks. *PLoS One* 2, e1049. doi:10.1371/journal.pone.0001049.
- Sporns, O., Tononi, G., and Kötter, R. (2005). The human connectome: A structural description of the human brain. *PLoS Comput. Biol.* 1, 0245–0251. doi:10.1371/journal.pcbi.0010042.
- Spring, J., Place, N., Borrani, F., Kayser, B., and Barral, J. (2016). Movement-Related Cortical Potential Amplitude Reduction after Cycling Exercise Relates to the Extent of Neuromuscular Fatigue. *Front. Hum. Neurosci.* 10, 1–12. doi:10.3389/fnhum.2016.00257.
- Stam, C. (2010). Characterization of anatomical and functional connectivity in the brain: A complex networks perspective. *Int. J. Psychophysiol.* 77, 186–194. doi:10.1016/j.ijpsycho.2010.06.024.
- Stam, C. (2014). Modern network science of neurological disorders. *Nat. Rev. Neurosci.* 15, 683–695. doi:10.1038/nrn3801.

- Stam, C., De Haan, W., Daffertshofer, A., Jones, B., Manshanden, I., Van Cappellen Van Walsum, A., et al. (2009). Graph theoretical analysis of magnetoencephalographic functional connectivity in Alzheimer's disease. *Brain* 132, 213–224. doi:10.1093/brain/awn262.
- Stam, C., and Dijk, B. (2002). Synchronization likelihood : an unbiased measure of generalized synchronization in multivariate data sets. *Phys. D Nonlinear Phenom.* 163, 236–251.
- Stam, C., Jones, B., Nolte, G., Breakspear, M., and Scheltens, P. (2007a). Small-World Networks and Functional Connectivity in Alzheimer's disease. *Cereb. Cortex* 17, 92–99. doi:10.1093/cercor/bhj127.
- Stam, C., Nolte, G., and Daffertshofer, A. (2007b). Phase Lag Index: Assessment of Functional Connectivity From Multi Channel EEG and MEG With Diminished Bias From Common Sources. *Hum. Brain Mapp.* 1193, 1178–1193. doi:10.1002/hbm.20346.
- Stam, C., and Reijneveld, J. (2007). Graph theoretical analysis of complex networks in the brain. *Nonlinear Biomed. Phys.* 1, 3. doi:10.1186/1753-4631-1-3.
- Stanton, N., Hedge, A., Brookhuis, K., Salas, E., and Hendrick, H. (2004). *Handbook of Human Factors and Ergonomics Methods*. doi:10.1201/9781420055948.ch36.
- Stevens, A. A., Tappon, S. C., Garg, A., and Fair, D. A. (2012). Functional Brain Network Modularity Captures Inter- and Intra-Individual Variation in Working Memory Capacity. *PLoS One* 7, e30468. doi:10.1371/journal.pone.0030468.
- Stevens, S. S. (1957). On the psychophysical law. *Psychol. Rev.* 64, 153–181. doi:10.1037/h0046162.
- Storti, S. F., Galazzo, I. B., Caliandro, P., Iacovelli, C., and Menegaz, G. (2018). Connectivity modulations induced by reaching&grasping movements. *Eur. Signal Process. Conf.* 2018-Septe, 1392–1396. doi:10.23919/EUSIPCO.2018.8553355.
- Storti, S., Formaggio, E., Manganotti, P., and Menegaz, G. (2015). Cortical network modulation during paced arm movements. in *2015 23rd European Signal Processing Conference, EUSIPCO 2015*, 2596–2600. doi:10.1109/EUSIPCO.2015.7362854.
- Storti, S., Formaggio, E., Manganotti, P., and Menegaz, G. (2016). Brain Network Connectivity and Topological Analysis during Voluntary Arm Movements. *Clin. EEG Neurosci.* 47, 276–290. doi:10.1177/1550059415598905.
- Sture Holm (1979). A Simple Sequentially Rejective Multiple Test Procedure. *Scand. J. Stat.* 6, 65–70. doi:10.2307/4615733.
- Sulaiman, N., Hayatee, N., Hamid, A., Murat, Z., and Taib, M. (2009). Initial Investigation of Human Physical Stress Level using Brainwaves. *IEEE Student Conf. Res. Dev.*, 230–233.

doi:10.1109/SCORED.2009.5443088.

- Sullivan, T. J., Deiss, S. R., Tzyy-Ping, J., and Cauwenberghs, G. (2008). A Brain-Machine Interface using Dry-Contact, Low-Noise EEG Sensors. in *IEEE Biomedical Circuits Systems Conf*, 154–157.
- Sun, Y., Bezerianos, A., Thakor, N., and Li, J. (2018). Functional brain network analysis reveals time-on-task related performance decline. in *Proceedings of the Annual International Conference of the IEEE Engineering in Medicine and Biology Society, EMBS*, 271–274. doi:10.1109/EMBC.2018.8512265.
- Sun, Y., Lim, J., Kwok, K., and Bezerianos, A. (2014a). Functional cortical connectivity analysis of mental fatigue unmasks hemispheric asymmetry and changes in small-world networks. *Brain Cogn.* 85, 220–230. doi:10.1016/j.bandc.2013.12.011.
- Sun, Y., Lim, J., Meng, J., Kwok, K., Thakor, N., and Bezerianos, A. (2014b). Discriminative Analysis of Brain Functional Connectivity Patterns for Mental Fatigue Classification. *Ann. Biomed. Eng.* 42, 2084–2094. doi:10.1007/s10439-014-1059-8.
- Tamburro, G., di Fronso, S., Robazza, C., Bertollo, M., and Comani, S. (2020). Modulation of Brain Functional Connectivity and Efficiency During an Endurance Cycling Task: A Source-Level EEG and Graph Theory Approach. *Front. Hum. Neurosci.* 14, 1–10. doi:10.3389/fnhum.2020.00243.
- Tandle, A., and Jog, N. (2015). Classification of Artefacts in EEG Signal Recordings and Overview of Removing Techniques. in *International Journal of Computer Applications*, 8887.
- Taya, F., Sun, Y., Babilioni, F., Thakor, N., and Bezerianos, A. (2015). Brain enhancement through cognitive training: A new insight from brain connectome. *Front. Syst. Neurosci.* 9, 1–19. doi:10.3389/fnsys.2015.00044.
- Taya, F., Sun, Y., Babiloni, F., Thakor, N. V., and Bezerianos, A. (2018). Topological Changes in the Brain Network Induced by the Training on a Piloting Task: An EEG-Based Functional Connectome Approach. *IEEE Trans. Neural Syst. Rehabil. Eng.* 26, 263–271. doi:10.1109/TNSRE.2016.2581809.
- Teplan, M. (2002). Fundamentals of EEG measurement. *Meas. Sci. Rev.* 2, 1–11. doi:10.1021/pr070350l.
- Toppi, J., Astolfi, L., Riseti, M., Anzolin, A., Kober, S. E., Wood, G., et al. (2018). Different topological properties of EEG-derived networks describe working memory phases as revealed by graph theoretical analysis. *Front. Hum. Neurosci.* 11, 1–16. doi:10.3389/fnhum.2017.00637.



- Toppi, J., De Vico Fallani, F., Vecchiato, G., Maglione, A. G., Cincotti, F., Mattia, D., et al. (2012). How the statistical validation of functional connectivity patterns can prevent erroneous definition of small-world properties of a brain connectivity network. *Comput. Math. Methods Med.* 2012. doi:10.1155/2012/130985.
- Tzourio-Mazoyer, N., Landeau, B., Papathanassiou, D., Crivello, F., Etard, O., Delcroix, N., et al. (2002). Automated anatomical labeling of activations in SPM using a macroscopic anatomical parcellation of the MNI MRI single-subject brain. *Neuroimage* 15, 273–289. doi:10.1006/nimg.2001.0978.
- Umeda, S. (2012). “Emotion, Personality, and the Frontal Lobe,” in, 223–241. doi:10.1007/978-4-431-54123-3\_10.
- Urigüen, J., and Zapirain, B. (2015). EEG artifact removal - State-of-the-art and guidelines. *J. Neural Eng.* 12. doi:10.1088/1741-2560/12/3/031001.
- van den Heuvel, M. P., de Lange, S. C., Zalesky, A., Seguin, C., Yeo, B. T. T., and Schmidt, R. (2017). Proportional thresholding in resting-state fMRI functional connectivity networks and consequences for patient-control connectome studies: Issues and recommendations. *Neuroimage* 152, 437–449. doi:10.1016/j.neuroimage.2017.02.005.
- van Diessen, E., Numan, T., van Dellen, E., van der Kooij, A. W., Boersma, M., Hofman, D., et al. (2015). Opportunities and methodological challenges in EEG and MEG resting state functional brain network research. *Clin. Neurophysiol.* 126, 1468–1481. doi:10.1016/j.clinph.2014.11.018.
- van Wijk, B. C. M., Stam, C. J., and Daffertshofer, A. (2010a). Comparing brain networks of different size and connectivity density using graph theory. *PLoS One* 5. doi:10.1371/journal.pone.0013701.
- van Wijk, B. C. M., Stam, C. J., and Daffertshofer, A. (2010b). Comparing Brain Networks of Different Size and Connectivity Density Using Graph Theory. *PLoS One* 5, e13701. doi:10.1371/journal.pone.0013701.
- Vecchio, F., Miraglia, F., and Maria Rossini, P. (2017). Connectome: Graph theory application in functional brain network architecture. *Clin. Neurophysiol. Pract.* 2, 206–213. doi:10.1016/j.cnp.2017.09.003.
- Vecchio, F., Miraglia, F., Marra, C., Quaranta, D., Vita, M. G., Bramanti, P., et al. (2014). Human brain networks in cognitive decline: A graph theoretical analysis of cortical connectivity from EEG data. *J. Alzheimer's Dis.* 41, 113–127. doi:10.3233/JAD-132087.
- Vijayalakshmi, R., Nandagopal, D., Dasari, N., Cocks, B., Dahal, N., and Thilaga, M. (2015). Minimum connected component - A novel approach to detection of cognitive load induced changes in functional brain networks. *Neurocomputing* 170, 15–31.

doi:10.1016/j.neucom.2015.03.092.

- Vinck, M., Oostenveld, R., Van Wingerden, M., Battaglia, F., and Pennartz, C. M. A. (2011). An improved index of phase-synchronization for electrophysiological data in the presence of volume-conduction, noise and sample-size bias. *Neuroimage* 55, 1548–1565. doi:10.1016/j.neuroimage.2011.01.055.
- Vogt, B. A. (2005). Pain and emotion interactions in subregions of the cingulate gyrus. *Nat. Rev. Neurosci.* 6, 533–544. doi:10.1038/nrn1704.
- Vogt, B. A., and Laureys, S. (2005). “Posterior cingulate, precuneal and retrosplenial cortices: cytology and components of the neural network correlates of consciousness,” in, 205–217. doi:10.1016/S0079-6123(05)50015-3.
- Walter, D. (1968). Coherence as a measure of relationship between EEG records. *Electroencephalogr Clin Neurophysiol* 24, 282.
- Wang, F., Wang, H., and Fu, R. (2018a). Real-time ECG-based detection of fatigue driving using sample entropy. *Entropy* 20. doi:10.3390/e20030196.
- Wang, F., Zhang, X., Fu, R., and Sun, G. (2018b). EEG characteristic analysis of coach bus drivers based on brain connectivity as revealed: Via a graph theoretical network. *RSC Adv.* 8, 29745–29755. doi:10.1039/c8ra04846k.
- Wang, H., Zhang, C., Shi, T., Wang, F., and Ma, S. (2015). Real-time EEG-based detection of fatigue driving danger for accident prediction. *Int. J. Neural Syst.* 25. doi:10.1142/S0129065715500021.
- Wang, J., Yang, K., Zhang, J., Zhang, N., and Chen, B. (2018c). Brain function networks reveal movement-related EEG potentials associated with exercise-induced fatigue. *ACM Int. Conf. Proceeding Ser.* 1, 33–40. doi:10.1145/3297067.3297074.
- Wang, J., Zuo, X., and He, Y. (2010). Graph-based network analysis of resting-state functional MRI. *Front. Syst. Neurosci.* 4, 1–14. doi:10.3389/fnsys.2010.00016.
- Wang, R., Wang, J., Yu, H., Wei, X., Yang, C., and Deng, B. (2014). Decreased coherence and functional connectivity of electroencephalograph in Alzheimer’s disease. *Chaos An Interdiscip. J. Nonlinear Sci.* 24, 033136. doi:10.1063/1.4896095.
- Wang, Y., Cao, L., Hao, D., Rong, Y., Yang, L., Zhang, S., et al. (2017). Effects of force load, muscle fatigue and extremely low frequency magnetic stimulation on EEG signals during side arm lateral raise task. *Physiol. Meas.* 38, 745. doi:10.1155/2017/8943850.
- Wascher, E., Heppner, H., and Hoffmann, S. (2014). Towards the measurement of event-related EEG activity in real-life working environments. *Int. J. Psychophysiol.* 91, 3–9.

doi:10.1016/j.ijpsycho.2013.10.006.

- Wascher, E., Heppner, H., Kobald, S. O., Arnau, S., Getzmann, S., and Möckel, T. (2016). Age-Sensitive Effects of Enduring Work with Alternating Cognitive and Physical Load. A Study Applying Mobile EEG in a Real Life Working Scenario. *Front. Hum. Neurosci.* 9, 711. doi:10.3389/fnhum.2015.00711.
- Watts, D., and Strogatz, S. (1998). Collective dynamics of ‘small-world’ networks. *Nature* 393, 440–442. Available at: <https://www.ncbi.nlm.nih.gov/pubmed/9623998>.
- Wendling, F., Ansari-Asl, K., Bartolomei, F., and Senhadji, L. (2009). From EEG signals to brain connectivity: A model-based evaluation of interdependence measures. *J. Neurosci. Methods* 183, 9–18. doi:10.1016/j.jneumeth.2009.04.021.
- Weng, T. B., Pierce, G. L., Darling, W. G., Falk, D., Magnotta, V. A., and Voss, M. W. (2017). The Acute Effects of Aerobic Exercise on the Functional Connectivity of Human Brain Networks. *Brain Plast.* 2, 171–190. doi:10.3233/BPL-160039.
- Westlake, K., and Nagarajan, S. (2011). Functional connectivity in relation to motor performance and recovery after stroke. *Front. Syst. Neurosci.* 5, 1–12. doi:10.3389/fnsys.2011.00008.
- Wilson, J., and Corlett, N. (1995). *Evaluation of human work: a practical ergonomics methodology.*, ed. 2nd Ed. London ; Bristol, PA : Taylor & Francis.
- Wingfield, G., Marino, F., and Skein, M. (2018). The influence of knowledge of performance endpoint on pacing strategies , perception of effort , and neural activity during 30-km cycling time trials. *Physiol. Rep.* 6, e13892. doi:10.14814/phy2.13892.
- Winkler, I., Debener, S., Muller, K.-R., and Tangermann, M. (2015). On the influence of high-pass filtering on ICA-based artifact reduction in EEG-ERP. in *2015 37th Annual International Conference of the IEEE Engineering in Medicine and Biology Society (EMBC)* (IEEE), 4101–4105. doi:10.1109/EMBC.2015.7319296.
- Wright, K. N., and Saylor, W. G. (1991). Male and female employees’ perceptions of prison work: Is there a difference? *Justice Q.* 8, 505–524. doi:10.1080/07418829100091191.
- Xia, M., Wang, J., and He, Y. (2013a). BrainNet Viewer: A Network Visualization Tool for Human Brain Connectomics. *PLoS One* 8. doi:10.1371/journal.pone.0068910.
- Xia, M., Wang, J., and He, Y. (2013b). BrainNet Viewer: A Network Visualization Tool for Human Brain Connectomics. *PLoS One* 8, e68910. doi:10.1371/journal.pone.0068910.
- Xin, J., Zhang, Y., Tang, Y., and Yang, Y. (2019). Brain Differences Between Men and Women: Evidence From Deep Learning. *Front. Neurosci.* 13. doi:10.3389/fnins.2019.00185.

- Xu, R., Zhang, C., He, F., Zhao, X., Qi, H., and Zhou, P. (2018). How Physical Activities Affect Mental Fatigue Based on EEG Energy , Connectivity , and Complexity. *Front. Neurol.* 9, 1–13. doi:10.3389/fneur.2018.00915.
- Yagi, Y., Coburn, K. L., Estes, K. M., and Arruda, J. E. (1999). Effects of aerobic exercise and gender on visual and auditory P300, reaction time, and accuracy. *Eur. J. Appl. Physiol. Occup. Physiol.* 80, 402–408. doi:10.1007/s004210050611.
- Yang, Q., Wang, X., Fang, Y., Siemionow, V., and Yao, W. (2011). Time-Dependent Cortical Activation in Voluntary Muscle Contraction. *Open Neuroimaging* 5, 232–239.
- Yao, B., Liu, J., Brown, R., Sahgal, V., and Yue, G. (2009). Nonlinear features of surface EEG showing systematic brain signal adaptations with muscle force and fatigue. *Brain Res.* 1272, 89–98. doi:10.1016/j.brainres.2009.03.042.Nonlinear.
- Yuan, Y., Wang, H., and Yuan, P. (2019). Experts EEG cognitive analysis and substance classification in security inspection. *Int. J. Pattern Recognit. Artif. Intell.* 33, 1–15. doi:10.1142/S021800141950006X.
- Zadry, H., Dawal, S., and Taha, Z. (2009). Investigation of Upper limb Muscle and Brain Activities on Light Assembly Tasks : A Pilot Study. in *In 2009 International Conference for Technical Postgraduates (TECHPOS)*, 1–4. doi:10.1109/TECHPOS.2009.5412096.
- Zadry, H., Dawal, S., and Taha, Z. (2010). Effect of Load on Upper Limb Muscle and Brain Activity in Light Assembly Task. in *In Proceedings of the International MultiConference of Engineers and Computer Scientists (Vol. 3)*.
- Zadry, H., Dawal, S., and Taha, Z. (2011). The Relation Between Upper Limb Muscle and Brain Activity in Two Precision Levels of Repetitive Light Tasks. *Int. J. Occup. Saf. Ergon.* 17, 373–384.
- Zadry, H. R., and Dawal, S. Z. (2010). Upper Limb Muscle and Brain Activities on Repetitive Light Tasks with Different Level of Pace and Precision. in *The 11th Asia Pacific Industrial Engineering and Management Systems Conference*, 7–10.
- Zaepffel, M., Trachel, R., Kilavik, B. E., and Brochier, T. (2013). Modulations of EEG Beta Power during Planning and Execution of Grasping Movements. *PLoS One* 8. doi:10.1371/journal.pone.0060060.
- Zalesky, A., Fornito, A., and Bullmore, E. T. (2010). Network-based statistic: Identifying differences in brain networks. *Neuroimage* 53, 1197–1207. doi:10.1016/j.neuroimage.2010.06.041.
- Zhang, C., Wang, H., and Fu, R. (2014). Automated Detection of Driver Fatigue Based on Entropy and Complexity Measures. in *IEEE Transactions on Intelligent Transportation Systems*, 168–

177. doi:10.1109/TITS.2013.2275192.

- Zhang, J., Dong, X., Wang, L., Zhao, L., Weng, Z., Zhang, T., et al. (2018). Gender Differences in Global Functional Connectivity During Facial Emotion Processing: A Visual MMN Study. *Front. Behav. Neurosci.* 12. doi:10.3389/fnbeh.2018.00220.
- Zhang, S., Zhang, Y., Sun, Y., Thakor, N., and Bezerianos, A. (2017). Graph theoretical analysis of EEG functional network during multi-workload flight simulation experiment in virtual reality environment. in *In Engineering in Medicine and Biology Society (EMBC), 2017 39th Annual International Conference of the IEEE*, 3957–3960.
- Zhao, C., Zhao, M., Yang, Y., Gao, J., Rao, N., and Lin, P. (2017). The Reorganization of Human Brain Networks Modulated by Driving Mental Fatigue. *IEEE J. Biomed. Heal. Informatics* 21, 743–755. doi:10.1109/JBHI.2016.2544061.
- Zink, R., Hunyadi, B., Huffel, V., and De Vos, M. (2016). Mobile EEG on the bike : disentangling attentional and physical contributions to auditory attention tasks . *J. Neural Eng.* 13, 046017.
- Zinn, M. L., Zinn, M. A., and Jason, L. A. (2016). Intrinsic Functional Hypoconnectivity in Core Neurocognitive Networks Suggests Central Nervous System Pathology in Patients with Myalgic Encephalomyelitis: A Pilot Study. *Appl. Psychophysiol. Biofeedback* 41, 283–300. doi:10.1007/s10484-016-9331-3.
- Zuo, X.-N., Ehmke, R., Mennes, M., Imperati, D., Castellanos, F. X., Sporns, O., et al. (2012). Network Centrality in the Human Functional Connectome. *Cereb. Cortex* 22, 1862–1875. doi:10.1093/cercor/bhr269.